

HIGGS AND RADION PHENOMENOLOGY BEYOND
THE STANDARD MODEL

BESTE KORUTLU

A THESIS
IN
THE DEPARTMENT
OF
PHYSICS

PRESENTED IN PARTIAL FULFILLMENT OF THE REQUIREMENTS
FOR THE DEGREE OF DOCTOR OF PHILOSOPHY
CONCORDIA UNIVERSITY
MONTRÉAL, QUÉBEC, CANADA

SEPTEMBER 2012

© BESTE KORUTLU, 2012

**CONCORDIA UNIVERSITY
SCHOOL OF GRADUATE STUDIES**

This is to certify that the thesis prepared

By: **Ms. Beste Korutlu**
Entitled: **Higgs and Radion Phenomenology Beyond the Standard Model**

and submitted in partial fulfillment of the requirements for the degree of

DOCTOR OF PHILOSOPHY (Physics)

complies with the regulations of the University and meets the accepted standards with respect to originality and quality.

Signed by the final examining committee:

_____	Chair
Dr. S. Shaw	
_____	External Examiner
Dr. M.T. Sher	
_____	External to Program
Dr. G. Vatistas	
_____	Examiner
Dr. T. Ali	
_____	Examiner
Dr. P. Vasilopoulos	
_____	Thesis Supervisor
Dr. M. Frank	

Approved by _____
Dr. L. Kalman, Graduate Program Director

September 11, 2012

Dr. B. Lewis, Dean, Faculty of Arts & Science

Abstract

Higgs and Radion Phenomenology Beyond the Standard Model

Beste Korutlu, Ph.D.

Concordia University, 2012

In this thesis we study models Beyond the Standard Model including Left-Right Supersymmetric Model and Warped Extra Dimensional Models with a Fourth Generation.

First, we revisit the Higgs sector of Left-Right Supersymmetric Model by studying the scalar potential in a version of the model in which the minimum is the charge and R -parity conserving vacuum state, and there are no additional non-renormalizable terms in the Lagrangian. We try to find a parameter space predicting at least one light doubly-charged Higgs boson, light neutral flavor-conserving Higgs bosons. The flavor-violating ones are heavy, and within the limits from $\Delta F = 1, 2$ mixings. The parameter space for such Higgs masses and mixings is very restrictive, thus making the model more predictive.

Subsequently, we study warped extra-dimensional scenarios in the presence of a fourth family of fermions and with the fermion fields lying in the bulk. We concentrate on the flavor structure of the Higgs couplings with fermions in the flavor anarchy ansatz. The occupancy of the fourth family in the model typically enhances the misalignment effects and we show that one should expect them to be highly non-symmetrical in the (34) inter-generational mixing. The radiative corrections from the new fermions and their flavor violating couplings to the Higgs affect negligibly known experimental precision measurements such as the oblique parameters and $Z \rightarrow b\bar{b}$ or $Z \rightarrow \mu^+\mu^-$. On the other hand, $\Delta F = 1, 2$ processes, mediated by tree-level Higgs exchange, as well as radiative corrections to $b \rightarrow s\gamma$ and $\mu \rightarrow e\gamma$ put some pressure on the allowed size of the flavor violating couplings. These couplings produce distinguishable signals in high energy colliders as they alter the Higgs decay patterns as well as those of the new fermions. These signals might become very important indirect signals for these type of models as they would be present even when the Kaluza-Klein mass scale is high and no heavy Kaluza-Klein particle is discovered.

Afterwards, we focus on the radion phenomenology in the same scenario with and without an additional fourth family of fermions. The radion couplings with the fermions are also generically misaligned with respect to the Standard Model fermion mass matrices as in the Higgs case, therefore producing some amount of flavor violating couplings and potentially influencing production and decay rates of the radion. We present simple analytic expressions for the radion-fermion couplings with three or four families. We also update and analyze the current experimental limits on radion couplings and on the model parameters. The modified decay branching ratios of the radion with an emphasis on the new channels involving flavor diagonal and flavor violating decays into fourth generation quarks and leptons are provided.

Finally, we study the Higgs-radion mixing in a warped extra dimensional model in the same scenario. The fourth generation Higgs is now severely constrained by Large Hadron Collider data due to the large enhancement in the Higgs production cross-section in the absence of Higgs-radion mixing. We analyze the production and decay rates of the two physical states emerging from the mixing and confront them with present Large Hadron Collider data. We show that the current signals observed can be compatible with the presence of one, or both, of these Higgs-radion mixed states, although with a severely restricted parameter space. We also present the modified decay branching ratios of the mixed Higgs-radion states, including flavor violating decays into fourth generation quarks and leptons. The windows of allowed parameter space obtained are very sensitive to the increased precision of upcoming Large Hadron Collider data. During the present year, a clear picture of this scenario will emerge, either confirming or further severely constraining this scenario.

to my dear father...

Acknowledgments

I would like to take this opportunity to send my sincere greatfulness to my supervisor Prof. Dr. Mariana Frank not only for her patience and kindness throughout this study, which was a great comfort, but also for exact encouragement during my stay in Concordia University. Without her inspiring discussions, invaluable guidance this accomplishment would have never been fulfilled.

I would like to express my great appreciation to Dr. Manuel Toharia for his contributions, valuable and constructive suggestions during the planning and development of this research work and for his willingness to give his time so generously.

I would like to express my deep gratitude to my loving family, for their endless care and trust in me, especially to the new member of our family, the daughter of my brother Ertan Korutlu and his darling wife Yasemin Sarıgul Korutlu: Ada Korutlu whose innocent, little face gave me motivation to keep going, to my dear Mom for her pure love and for setting me straight, and to my beloved Dad who is my biggest aspiration to fulfill my dreams.

My special thanks go to my dear friends, Serap Yiğen, Tuğba Keskin, Xin Zhao and Nedaa Asbah for their constant moral support and for the charm they brought to my life. I am also thankful to my graduate friends at the Physics Department in Concordia University for providing me with enthusiastic encouragement.

I would like to offer my special thanks to Justin Hakim Muzaula for his being always there by my side while I was going through really tough times and making my life in Montréal a lot more exciting and fun and also to his family for being so gracious.

The Feynman diagrams shown in this thesis have been produced with the help of Jaxodraw [1].

Contents

List of Figures	xi
List of Tables	xvi
1 INTRODUCTION	1
2 THE STANDARD MODEL	9
2.1 Elementary Particles in the Standard Model	10
2.2 Interactions Between the Elementary Particles in the Standard Model	14
2.3 Cabibbo-Kobayashi-Maskawa Matrices	16
2.4 The Standard Model Lagrangian	17
2.5 Higgs Mechanism	21
2.5.1 Mass Generation of Gauge Bosons	22
2.5.2 Mass Generation for Fermions	23
2.6 Experimental Status of the Standard Model	24
2.7 The Shortcomings of the Standard Model	28
3 BEYOND THE STANDARD MODEL	30
3.1 The Left-Right Symmetric Model	30
3.1.1 Elementary Particles in the Left-Right Symmetric Model . . .	32
3.1.2 The Left-Right Symmetric Model Lagrangian	35
3.1.3 Higgs Mechanism in the Left-Right Symmetric Model	36
3.2 The Supersymmetric Standard Model	39
3.2.1 Elementary Particles in the Supersymmetric Standard Model .	42
3.2.2 The Supersymmetric Lagrangians	45
3.3 The Four-Generation Standard Model	49

3.3.1	Experimental Status of the Four-Generation Standard Model .	52
3.3.2	Two-Loop Electroweak Corrections to the Higgs Boson Production	54
3.4	The Warped Extra Dimensions	56
3.4.1	Derivation of the Warp Factor	60
3.4.2	The Higgs Lagrangian	63
3.4.3	The Radion Solution	64
3.4.4	The SM fields propagating in the bulk	67
3.4.5	Flavor Misalignment	73
3.4.6	Radion-Higgs Mixing	77
4	HIGGS BOSONS in a MINIMAL R-PARITY CONSERVING LEFT-RIGHT SUPERSYMMETRIC MODEL	82
4.1	The Particle Content of the Left-Right Supersymmetric Model	83
4.2	R -parity Conserving the Left-Right Supersymmetric Model	87
4.3	Higgs Boson Composition and Masses	89
4.3.1	Doubly Charged Higgs Boson Masses	91
4.3.2	Singly Charged Higgs Boson Masses	92
4.3.3	Neutral Higgs Boson Masses	93
4.4	Constraints on the Higgs sector	94
4.4.1	Flavor Changing Neutral Higgs Bosons	94
4.5	Numerical Results and Discussion	102
4.6	Summary and Conclusion	110
5	HIGGS PHENOMENOLOGY in WARPED EXTRA DIMENSIONS with a 4th GENERATION	112
5.1	Flavor Structure with four families	113
5.1.1	The quark mixing matrix \mathbf{V}_{CKM4}	114
5.1.2	Tree level Higgs FCNC couplings	117
5.1.3	Analytical Estimates of Higgs FCNC Couplings in Flavor Anarchy	118
5.1.4	Numerical Results for Higgs FCNC Couplings	120
5.1.5	Cumulative Effect on Diagonal Yukawa Couplings when $Y_1 = Y_2$	121
5.1.6	Higgs FCNC Couplings in the Lepton Sector	123
5.1.7	Tree Level Z^0 Flavor Violating Couplings	124

5.2	Phenomenology	125
5.2.1	Bounds on Higgs-mediated FCNC Couplings	125
5.3	Conclusions and Outlook	141
6	RADION PHENOMENOLOGY with 3 and 4 GENERATIONS	143
6.1	Flavor-Changing Neutral Couplings of the Radion	144
6.1.1	Radion FCNC's in Flavor Anarchy–Analytical Results	145
6.1.2	Radion FCNC's in Flavor Anarchy–Numerical Results	148
6.1.3	Radion FCNC's in Flavor Anarchy–Leptons	149
6.2	Phenomenology	150
6.2.1	Bounds on Radion Mediated FCNC couplings	150
6.3	Flavor Changing Radion Decays in the 4 Generation Model	154
6.4	Conclusions and Outlook	156
7	SAVING the FOURTH GENERATION HIGGS with RADION MIXING	158
7.1	Production and Decays of a Mixed Higgs-Radion State with Four Generations	159
7.2	Flavor Changing Decays of the Higgs-Radion States in the Four Generation Model	170
7.3	Conclusions and Outlook	174
8	CONCLUSION	176
	Bibliography	180
A	Notations and Conventions	199
A-1	Dirac Matrices and Spinors	200
A-1.1	Pauli-Dirac Representation	200
A-1.2	Chiral Representation	202
B	Gauge Group and Transformations	204
C	Ricci Tensor and Brane Tensions	207
C-1	The Components of the Ricci Tensor	207
C-2	Brane Tensions	214

D	Rotation and CKM4 Matrices in Warped Extra Dimensions with Four Generation	215
D-1	Rotation Matrices	215
D-2	Cabibbo-Kobayashi-Maskawa Matrix for Four Generations in Warped ExtraDimensions	223
E	Feynman Rules in Warped Extra Dimensions with Four Generation	225
E-1	Feynman Rules for the Higgs Field	226
E-2	Feynman Rules for the Radion Field	226
E-3	Feynman Rules for Higgs-Radion Mixed States	228

List of Figures

1	The Higgs potential function for $\mu^2 < 0$ and $\lambda > 0$ on a real-imaginary plane of ϕ	21
2	Standard Model Higgs boson production cross sections at center-of-mass energy of 8 TeV. Figure from [131].	26
3	Standard Model Higgs boson decay branching ratios. Figure from [131].	26
4	The observed (full line) and expected (dashed line) 95% CL combined upper limits on the SM Higgs boson production cross section divided by the SM expectation as a function of m_h in the full mass range. Left panel shows the ATLAS results. Figure from [10]. The dotted curves show the median expected limit in the absence of a signal and the green and yellow bands indicate the corresponding $\pm 1\sigma$ and $\pm 2\sigma$ intervals. Right Panel shows CMS results. Figure from [11]. The green and yellow bands indicate the ranges that are expected to contain 68% and 95% of all observed excursions from the median, respectively. . .	27
5	Extrapolation of the gauge couplings in the SM (on the left), in SUSY (on the right).	40
6	One loop correction to Higgs mass square (m_h^2) due to fermion (f) loop on the left and a scalar (S) on the right.	41
7	The S^1 and S^1/Z_2 Orbifolds.	56
8	Original setup of Randall-Sundrum model.	57
9	Correction to fermion masses and to physical Yukawa couplings (right diagram) of SM fermions using the mass insertion approximation. . .	74
10	Correction to kinetic terms using the insertion approximation.	75
11	Correction to fermion masses and to physical Yukawa couplings (right diagram) of SM fermions using the mass insertion approximation for brane Higgs scenario.	76

12	The variation of the FCNC neutral Higgs H_6^0 mass with the parameters of the LRSUSY model. H_6^0 induces tree-level FCNC in the down-quark sector. Shown are: contour plots in the $M_R - \tan \beta$ plane (the contour values are given in TeV when multiplied by 10^3), the variation of $M_{H_6^0}$ with M_R , and with v_R , for three values of $\tan \delta = \bar{v}_R/v_R$	104
13	The variation of the FCNC neutral Higgs H_2^0 mass with the parameters of the LRSUSY model. H_2^0 induces tree-level FCNC in the up-quark sector. To the left, a contour plot in the $v_R - \bar{v}_R$ plane (the contour values are given in TeV) and, at the right, as a function of v_R for three values of $\tan \delta = \bar{v}_R/v_R$	105
14	The masses of the lightest doubly-charged Higgs boson as a contour plot (the contours values are given in GeV) in the $v_R - m_{L^c}^2$ plane (left) and as a function of v_R plane for three values of $\tan \delta = \bar{v}_R/v_R$ (right).	105
15	Typical geographic location of quarks in RS-4GEN (RS with a fourth family) such that large quark mass hierarchies and small mixing angles are generic. The Higgs boson and the heavier fermions (top and fourth generation quarks and charged leptons) are localized near the TeV brane, whereas light fermions are localized towards the Planck brane.	114
16	Generic loop diagrams enhanced by FCNC couplings between Higgs boson and 4th generation fermions. Here F stand for a 4th generation quark (or lepton), while f_i, f_j are 2nd or 3rd generation quarks (or leptons). The left-hand side graph is the vertex diagram, while the other two are self-energy diagrams.	128

- 17 Decay branching fractions of the Higgs scalar in a warped scenario with four generations of fermions. The bands represent 50% likelihood for the branching ratio, according to our numerical scan, as explained in the text. The light and dark gray regions vertical regions are excluded by both Tevatron and LHC (with varying degree of confidence, see discussion in the text). The flavor anarchy setup (masses and mixings explained through fermion localization, with random 5D Yukawa couplings) predicts generic FV couplings of the Higgs, leading to a few new interesting decay channels such as $h \rightarrow bb'$ and $h \rightarrow \tau\tau'$. The masses chosen for this plot are $m_{b'} = 350$ GeV, $m_{t'} = 400$ GeV, $m_{\tau'} = 160$ GeV and $m_{\nu_{\tau'}} = 250$ GeV ($N_4 \equiv \nu_{\tau'}$), and the KK scale is $(R')^{-1} = 1500$ GeV. (Figure on the curtesy of Dr. Manuel Toharia). 132
- 18 Branching ratios for 2-body t' decays with CKM4 mixing angle $V_{t'b} = 0.1$ and KK scale $R'^{-1}(\equiv M_{KK}) = 1.5$ TeV (left panel), $V_{t'b} = 0.3$, $R'^{-1} = 1.5$ TeV (middle panel) and $V_{t'b} = 0.1$, $R'^{-1} = 3$ TeV (right panel). We take $V_{t's} = V_{t'd} = 0.01$ and $m_h = 500$ GeV throughout. The bands represent 30% likelihood for the branching ratio, according to our numerical scan, as explained in the text. 136
- 19 Branching ratios for 2-body b' decays with CKM4 mixing angle $V_{tb'} = 0.1$ and KK scale $R'^{-1}(\equiv M_{KK}) = 1.5$ TeV (left panel), $V_{tb'} = 0.3$, $R'^{-1} = 1.5$ TeV (middle panel) and $V_{tb'} = 0.1$, $R'^{-1} = 3$ TeV (right panel). We take $V_{cb'} = V_{ub'} = 0.01$ throughout as well as $m_h = 500$ GeV. The bands represent 30% likelihood for the branching ratio, according to our numerical scan, as explained in the text. 138
- 20 Branching ratios for 2-body t' decays with CKM4 mixing angle $V_{t'b} = 0.1$ and KK scale $R'^{-1}(\equiv M_{KK}) = 1.5$ TeV (left panel) and b' decays with CKM4 mixing angle $V_{tb'} = 0.1$ and KK scale $R'^{-1}(\equiv M_{KK}) = 1.5$ TeV (right panel), for $m_h = 120$ GeV. The bands represent 30% likelihood for the branching ratio, according to our numerical scan, as explained in the text. 139

- 21 Contours in the plane (c_i, c_j) of the function $\hat{a}_{ij} = [\mathcal{I}(c_i) - \mathcal{I}(c_j)] \frac{f(c_i)}{f(c_j)}$, which sets the size of radion FCNC couplings with fermions. These are estimated to be $\tilde{a}_{ij} \simeq \sqrt{\frac{m_i}{m_j}} \hat{a}_{ij}$ and so from these contours one can quickly estimate the size of these couplings by knowing the values of the bulk mass parameter c_i of each fermion. (Figure on the curtesy of Dr. Manuel Toharia). 147
- 22 Restrictions in the $m_\phi - \Lambda_\phi$ plane from collider exclusion limits and flavor constraints for ϵ_K (we have defined $a_{ds} = \sqrt{\text{Im}(\tilde{a}_{12}^* \tilde{a}_{21}^*)}$). One sees that for lighter radion ($m_\phi < 160$ GeV) direct bounds are quite weak and flavor physics provide stronger constraints (although less robust). Heavier radions are mostly constrained by the “golden mode” $pp \rightarrow \phi \rightarrow ZZ$ and also $pp \rightarrow \phi \rightarrow WW$ at the LHC, while $p\bar{p} \rightarrow \phi \rightarrow WW$ is used at Tevatron. (Figure on the curtesy of Dr. Manuel Toharia). 152
- 23 Decay branching fractions of the radion in a warped scenario with four generations of fermions. The flavor anarchy setup (masses and mixings explained through fermion localization, with random 5D Yukawa couplings) predicts generic FV couplings of the radion, leading to a few new interesting decay channels such as $\phi \rightarrow bb'$ and $\phi \rightarrow \tau\tau'$. The masses chosen for this plot are $m_{b'} = 350$ GeV, $m_{t'} = 400$ GeV, $m_{\tau'} = 120$ GeV and $m_{\nu_4} = 90$ GeV, and the KK scale is $(R')^{-1} = (\sqrt{6})1500$ GeV (~ 3675 GeV). 155
- 24 Ratio of discovery significances $R(XX) \sim \sigma/\sigma_{SM}$, defined in the text, for $m_h = 125$ GeV, $m_\phi = 60$ GeV and for different values of Λ_ϕ and $m_{\tau'}$, for $m_{\tau'} = 100$ GeV. In the upper panels we show the LO, and in the lower panels the EW corrected branching ratio to $\gamma\gamma$. The light green bands indicate the theoretical uncertainties in the $gg \rightarrow h \rightarrow ZZ^*$ rate, while those for $\gamma\gamma$ are depicted in orange. The dashed purple lines marked by $R_\phi(ZZ)$ indicate the ratio of $\phi Z^* Z^*$ couplings with respect to the $h_{SM} Z^* Z^*$ one. The vertical gray bands indicate the allowed parameter space for ξ 164

25	Ratio of discovery significances $R(XX) \sim \sigma/\sigma_{SM}$, defined in the text, for $m_h = 124$ GeV, $m_\phi = 120$, $m_{\tau'} = 100$ GeV and for different values of Λ_ϕ . In the upper panels we show the LO, and in the lower panel the EW corrected branching ratio to $\gamma\gamma$. The light green bands indicate the theoretical uncertainties in the ZZ^* signal, red for $b\bar{b}$ and orange for $\gamma\gamma$. For ϕ the uncertainties are depicted in pink for ZZ^* , light blue for $b\bar{b}$ and purple for $\gamma\gamma$. The vertical gray bands indicate the allowed parameter space for ξ	166
26	Ratio of discovery significances $R(XX) \sim \sigma/\sigma_{SM}$, defined in the text, for $m_h = 120$ GeV, $m_\phi = 125$ GeV and for different values of Λ_ϕ , for $m_{\tau'} = 100$ GeV. In the upper panels we show the LO, and in the lower panel the EW corrected branching ratio to $\gamma\gamma$. The light green bands indicate the theoretical uncertainties in the ZZ^* signal and the orange the ones are for $\gamma\gamma$. For the ϕ the theoretical uncertainties in ZZ^* are given by pink bands and the ones for $\gamma\gamma$ are in purple. The vertical gray bands indicate the allowed parameter space for ξ	168
27	Ratio of discovery significances $R(XX) \sim \sigma/\sigma_{SM}$, defined in the text, for $m_\phi = 125$ GeV, $\Lambda_\phi = 1.0$ TeV and for different masses of h . The light green bands indicate the theoretical uncertainties in the ZZ signal. There is no change in these graphs if we include the EW corrected branching ratio to $\gamma\gamma$. We took $m_{\tau'} = 150$ GeV, precluding FCNC decays to fourth generation leptons. The vertical gray bands indicate the allowed parameter space for ξ	169
28	Same as Fig. 27, but for $\Lambda_\phi = 1.3$ TeV.	170

List of Tables

1	Quark content of the SM including the corresponding $SU(3)_c \otimes SU(2)_L \otimes U(1)_Y$ gauge quantum numbers together with the PDG values for the rest mass energies of the quarks confined in hadrons.	12
2	Leptons in the SM with their corresponding $SU(3)_c \otimes SU(2)_L \otimes U(1)_Y$ gauge quantum numbers together with the PDG values for their masses.	13
3	Bosonic field content of the SM with their corresponding $SU(3)_c \otimes SU(2)_L \otimes U(1)_Y$ gauge and spin quantum numbers.	14
4	The four fundamental forces in nature.	15
5	First generation of fermions in the LRSM including the corresponding $SU(3)_c \otimes SU(2)_L \otimes SU(2)_R \otimes U(1)_{B-L}$ gauge quantum numbers together with the transformations under parity operator.	33
6	Bosonic field content of the LRSM with their corresponding $SU(3)_c \otimes SU(2)_L \otimes SU(2)_R \otimes U(1)_{B-L}$ gauge quantum numbers.	33
7	Higgs content of the minimal LRSM with their corresponding $SU(3)_c \otimes SU(2)_L \otimes SU(2)_R \otimes U(1)_{B-L}$ gauge quantum numbers and corresponding parity transformations.	34
8	First generation of fermions in the SUSY including the corresponding $SU(3)_c \otimes SU(2)_L \otimes U(1)_Y$ gauge and spin quantum numbers together.	43
9	Gauge Boson content of the SUSY with their corresponding $SU(3)_c \otimes SU(2)_L \otimes U(1)_Y$ gauge and spin quantum numbers.	44
10	Higgs Boson content of the SUSY with their corresponding $SU(3)_c \otimes SU(2)_L \otimes U(1)_Y$ gauge and spin quantum numbers.	44
11	Relative NLO electroweak corrections to the $gg \rightarrow h$ cross sections in SM4, for the mass scenario $m_{t'} = 500$ GeV, $m_{b'} = 450$ GeV, $m_{\nu_{\tau'}} = 375$ GeV, $m_{\tau'} = 450$ GeV. Table is taken courtesy [172].	54

12	NLO electroweak corrections to the $h \rightarrow \gamma\gamma$ decay width and estimate for the missing higher-order corrections δ_{THU} relative to Δ_{LO}^- . Table is taken courtesy [172].	55
13	First generation of fermions and their bosonic superpartners in the LRSUSY including the corresponding $SU(3)_c \otimes SU(2)_L \otimes SU(2)_R \otimes U(1)_{B-L}$ gauge and spin quantum numbers.	84
14	Gauge Bosons and their fermionic partners in the LRSUSY.	85
15	Minimal Higgs sector in the Supersymmetric Left-Right Model	86
16	QCD parameters used for meson mixings.	99
17	Masses and compositions of physical Higgs fields and unphysical Goldstone bosons. Parameters are chosen as follows: $\tan\beta = 10$, $\tan\delta = 1/1.05$, $v_R = 3.5$ TeV, $M_R = 100$ TeV, $\lambda = 1$, $\lambda_{21} = -0.1$, $C_\lambda = 2.5$ TeV, $\langle S \rangle = 1$ TeV, $M_S = 1$ TeV, $m_{L^c}^2 = -20$ TeV ² , $f = 1$. .	107
18	Masses and compositions of physical Higgs fields and unphysical Goldstone bosons. Parameters are chosen as follows: $\tan\beta = 50$, $\tan\delta = 1/1.05$, $v_R = 5$ TeV, $M_R = 100$ TeV, $\lambda = 1$, $\lambda_{21} = -0.1$, $C_\lambda = 2.5$ TeV, $\langle S \rangle = 1$ TeV, $M_S = 1$ TeV, $m_{L^c}^2 = -30$ TeV ² , $f = 1$. .	108
19	The FCNC branching ratios of h and ϕ for allowed points in the parameter space. The fourth generation fermion masses are chosen as $m_{t'} = 400$ GeV, $m_{b'} = 350$ GeV, $m_{\tau'} = 100$ GeV, $m_{\nu_{\tau'}} = 90$ GeV.	172
20	Same as Table 19, but for $m_{\tau'} = 150$ GeV.	172
21	Ratio of significance $R_{h(\phi)}(XX) = S(gg \rightarrow h(\phi) \rightarrow f\bar{f})/S(gg \rightarrow h_{SM} \rightarrow f\bar{f})$ for different parameter space. Last column are the Yukawa couplings for $h(\phi)$ to $t\bar{t}$. The fourth generation fermion masses are chosen as $m_{t'} = 400$ GeV, $m_{b'} = 350$ GeV, $m_{\tau'} = 100$ GeV, $m_{\nu_{\tau'}} = 90$ GeV.	173
22	Same as Table 21, but for $m_{\tau'} = 150$ GeV.	174

Chapter 1

INTRODUCTION

Over the past century remarkable progress has been made to understand the building blocks of matter. It has been identified that all the ordinary matter in the Universe is made from twelve fundamental particles named fermions (six leptons and six quarks which are divided into three generations of four particles each) and they are governed by four fundamental forces (electromagnetic, weak, strong and gravitational forces). The best description of how these twelve particles, their anti-partners and the three out of four forces are related to each other has been encapsulated in the Standard Model (SM) of particle physics by means of global and local gauge symmetries. It is quite elegant and minimalistic in the sense that it has a unified picture of electromagnetic and weak forces, the so called electroweak interactions, which are introduced by Glashow-Weinberg-Salam (GWS) [2–7]. Afterwards, a gauge theory of the strong interactions is also embedded into this framework by Fritzsche and Gell-Mann [8]. The gravitational force on the other hand, cannot be put on the same footing as the other interactions in the SM. In fact, fitting gravity into this scheme has been proved to be a very difficult task. Fortunately, in particle physics at the energy scales available to this generation of experiments the effects of gravity are so weak as to be negligible. The three forces described by the SM result from exchange of induced force carrier particles via local gauge symmetries, known as gauge bosons (photon for electromagnetic, W and Z bosons for weak and eight gluons for strong interactions), between the matter particles. Developed in the early 1970s, the SM has successfully explained a surfeit of experiments at the quantum level and led to the prediction of a wide variety of phenomena and particles prior to their experimental

discovery. However, there is still one essential ingredient of the SM missing, the so called SM Higgs Boson that has yet to be discovered experimentally. In fact, *Conseil Européen pour la Recherche Nucléaire* (CERN) revealed preliminary data from the Large Hadron Collider (LHC) on July the 4th, 2012 consistent with the long-sought Higgs boson [9, 10]. However, further analysis regarding its properties is still important for drawing conclusions concerning whether or not the discovered particle is a SM Higgs boson. The Higgs boson is introduced [11–13] in the SM using the Higgs mechanism to produce mass for the particles by spontaneously breaking (SSB) its gauge symmetry. The problem with its discovery is that the mass of the Higgs boson is an unknown parameter. Therefore, one has to search for it in a mass range which unfortunately was not accessible by the previously built accelerators (Large Electron-Positron Collider (LEP), The Stanford Linear Collider (SLC) and Tevatron), even though they successfully verified many aspects of the SM and were able to introduce the lower mass limit for the Higgs Boson. To fill the knowledge gap, the LHC, the largest and most powerful particle accelerator in the world, has been assembled by CERN within a 27 km circumference and 175 m beneath the Franco-Swiss border near Geneva, Switzerland. Presently, it operates at 7-8 TeV center-of-mass energy (half of its full capacity). It consists of two proton beams which are made to collide at four locations around the accelerator ring, where the particle detectors are situated, namely A Toroidal LHC Apparatus (ATLAS), Compact Muon Solenoid (CMS), A Large Ion Collider Experiment (ALICE) and Large Hadron Collider beauty (LHCb). Detecting the Higgs boson at LHC is a breakthrough for particle physics, although its discovery would not be the whole story because the model leaves too many open questions and suffers from several fine-tuning problems. In the modern way of thinking, the SM is considered as an Effective Field Theory (EFT) by providing a very good description of the physics of fundamental particles and their interactions below the electroweak scale ($M_{EW} \approx 10^2$ GeV), whereas at higher energies it has to be extended into Beyond the Standard Models (BSM) which include natural extensions of the SM such as Grand Unified Theories (GUT) [14–16], Left-Right Symmetric Models (LRSM) [17–19], supersymmetric extensions (SUSY) [20, 21], Left-Right Supersymmetric Model (LRSUSY) [22–27], the Four-Generation Standard Model (SM4) [28, 29], string theory [30] and extra dimensions: large extra dimensions [31–33], universal extra dimensions (UED) [34–37], non-universal extra dimensions

(NUED) [38, 39], Randall-Sundrum model (RS1) [40, 41]. Therefore, LHC does not only search for the Higgs boson but also for some evidence of BSM. In this thesis, we will focus mainly on LRSUSY and warped extra dimensions of RS1-type with a fourth generation.

The SM is a “chiral” gauge theory. This means that different representations of the Lorentz group transform differently not only under the Lorentz group transformations but also with respect to the gauge group of the SM. The chirality of the matter particles, for example, refers to whether they appear in the fundamental or anti-fundamental representation of the Lorentz group. The ones represented in the fundamental representation are called the left-chiral particles. Meanwhile their right-chiral counterparts are represented in the anti-fundamental representation. The symmetry transformation between these two chiral states is named “parity” which is a violated symmetry by the weak interactions of the SM (it favors left-chiral particles and their interactions). The main motivation for considering the left-right symmetric extension of the SM is that it provides a dynamical explanation for the violation of parity. At the fundamental level, parity is an underlying symmetry of the LRSM which is broken spontaneously by the vacuum to yield the results of its low-energy limit, the SM. An additional reason to study LRSM is the experimental evidence [42, 43] supporting non-zero masses for the electrically neutral leptons, the so called neutrinos. The SM with just left-chiral neutrinos and a Higgs doublet is unable to provide masses for the neutrinos. The simplest route to include neutrino masses is to insert the missing right-chiral neutrino states as proposed in LRSM and then utilize the see-saw mechanism [19, 44]. To achieve the see-saw mechanism the underlying gauge symmetry of the LRSM is spontaneously broken by scalar right-chiral triplets, leaving the left-chiral neutrinos much more lighter than the charged leptons of the corresponding family while, keeping the right-chiral ones heavy. Furthermore, everything ever observed with all of our instruments adds up to less than 5% of the Universe, the rest being dark matter and dark energy (energy that is not carried by any matter). The SM does not have a room for dark matter, however, the introduced right-chiral neutrino in LRSM might serve as a dark matter candidate.

In 1974, a symmetry, different from all those defined in the scope of the SM, supersymmetry was introduced by Wess and Zumino [20, 21]. It relates bosonic and fermionic degrees of freedoms of particles simply by introducing a bosonic(fermionic)

partner for each fermion(boson) of the SM. If SUSY was an exact symmetry of nature, the partners would have the same masses as the original particles. We know that in nature this is not the case, otherwise the partners would have been observed by now. Despite the complete absence of experimental evidence that supersymmetry exists in nature as an underlying symmetry, physicists continue to study SUSY, considering the possibility of being spontaneously broken in low energies, because of its undoubted mathematical fascination. It provides an attractive framework for grand unification and the hierarchy problem of the SM. Without supersymmetry, the running coupling constants of the strong, electromagnetic and weak interactions do not meet at a single point, though they come really close at around $\sim 10^{14}$ GeV. If one attempts to include SUSY with its additional radiative corrections, however, the coupling constants meet exactly at one point, at an energy $\sim 10^{16}$ GeV, called as GUT point. Another remarkable achievement of SUSY is that it offers an elegant solution to the SM hierarchy problem. The hierarchy problem is the following: the mass of Higgs boson receives quantum loop corrections from the virtual effect of every particle that couples directly or indirectly to the Higgs field. The SUSY, on the other hand, guarantees the cancellation of those loop corrections by the contributions from the superpartners, leaving the Higgs boson mass relatively light. A supersymmetric partner that does not decay and has the right mass and right interactions might also be a dark matter candidate. The first step towards trying to build a more complete theory as a prototype for SUSY theories is the Minimal Supersymmetric Standard Model (MSSM) which is the smallest and the most basic model of SUSY that includes SM. The SM relies on the conservation of lepton number¹ (L) and the baryon number² (B) in all of its interactions. However, the most general gauge invariant and renormalizable superpotential of MSSM would include B and L violating terms. One could try to impose conservation of B and L as a postulate in the MSSM though it seems like a step-back from the SM where the conservation of these quantum numbers is not assumed, but appears naturally as a consequence of renormalizability of the theory. Therefore, one has to add a new symmetry which has the effect of eliminating the possibility of B and L violating terms in the superpotential. This new symmetry

¹Lepton number is the number of leptons minus the number of anti-leptons. In equation form, $L = n_l - n_{\bar{l}}$ which gives a value of +1 for leptons, -1 for anti-leptons, and 0 for non-leptonic particles.

²Baryon number is one third of the number of quarks minus the number of anti-quarks. In equation form, $B = (n_q - n_{\bar{q}})/3$.

is called “ R -parity” [45] and is assigned for SM particles to be even, while for their superpartners have odd R -parity.

In the domain of flavor physics, including LR symmetry in SUSY resolves several problems of the MSSM, the most important of all being the way R -parity is conserved in the model. In LRSUSY, as opposed to MSSM where R -parity is introduced as an external symmetry, its extended gauge symmetry forbids renormalizable terms that violate B and L . However, this symmetry has to be broken spontaneously since there exists no massless gauge boson observed of the corresponding gauge group. Nevertheless, since the broken symmetry will be due to scalar fields that carry even integer values of $3(B-L)$, R -parity will still survive as an exact symmetry preventing rapid proton decay [46–48] and ensuring the lightest supersymmetric particle (LSP) to be stable designating it as a dark matter candidate. In addition, it offers a solution to the strong Charge-conjugation and Parity (CP) problem of why even though it is possible to write CP violating terms for strong interactions, experiments do not indicate any such violation. In LRSUSY, this is accomplished by insuring that the determinant of the quark mass matrix is real, which is possible due to the fact that the Yukawa couplings are Hermitian and without the need for an axion [49, 50].

Another obvious extension of the SM might be increasing the number of fermion generations. It was considered extensively in the 1980s. However, in 1989 the number of generations (or precisely the number of light neutrinos) were experimentally proven to be equal to three from the Z boson total width, measured to high accuracy in Stanford Linear Accelerator Center (SLAC) [51, 52] and CERN [53–55]. By comparing the invisible width (subtracting from the total width of the Z boson the part from decays to charged leptons and hadrons) with the theoretical predictions for neutrino decays it was established that the number of neutrinos which interact with the Z boson is equal to three [56]. This result is fundamentally important since, by extrapolation, one can assume that there exist only three fermion families. Nonetheless, this is not universally accepted partly because having an additional family of fermions has some desired effects and is not necessarily in conflict with electroweak precision observables such as the constraints from the W boson mass, the effective leptonic mixing angle and the highly accurate measurements of the muon lepton lifetime. As long as the fourth generation contains either very heavy neutrinos ($m_\nu > m_Z/2$), or no neutrinos at all the Z invisible width is satisfied. The simplest

extension of the SM is the Four-Generation Standard Model [28,29]. This might cure certain problems of the SM in flavor physics, such as the CP violation in B_s -mixing [57] and the baryogenesis problem [58,59] (see Section 2.7) by leading to a sizable increase of the measurement of CP violation. In addition, the electroweak symmetry breaking triggered via the fourth generation fermions without a Higgs boson could address the hierarchy problem [60]. It has also been shown that bounds from electroweak precision observables can be softened for the higher values of Higgs mass when the fourth generation is considered [61–63]. Moreover, the gauge couplings can in principle be unified without invoking SUSY [64]. Although none of these reasons are compelling, they provide sufficient grounds to pursue keeping the study of the fourth generation alive.

Warped extra dimensional models were introduced by Lisa Randall and Raman Sundrum [40,41] as an attempt to resolve the hierarchy problem between the Planck scale ($M_{\text{Pl}} \approx 2 \times 10^{18}$ GeV), where quantum effects of gravity become strong, and the M_{EW} , by using an extra-dimensional warp factor to lower the natural scale of the particles masses. In the original scenario, two branes are introduced, one with an energy scale set at M_{Pl} , the other at the TeV scale on which the SM fields are localized, and with gravity allowed to propagate in the space in between, called the bulk. Much research has been done on the possible radius stabilization mechanism to fix the inter-brane distance and on the radion field, emerging from the stabilization as an excitation of the metric tensor [65–72]. At present, it is quite clear that, in an RS-type scenario a realistic electroweak symmetry breaking can only be satisfied by extending the gauge bosons and fermions into the bulk [73–85], which provides a compelling theory of flavor where the hierarchies among the fermion masses and mixings arise naturally [86–90] by assuming all the 5D Yukawa couplings to be $\mathcal{O}(1)$ and with no definite structure. Another interesting feature of these models is the Randall-Sundrum (RS)-Glashow-Iliopoulos-Maiani (GIM) mechanism [75,91,92] which gives rise to suppressed contributions to low-energy phenomena due to the exchange of Kaluza-Klein (KK) modes³. Despite this, $\Delta F = 2$ processes still push the KK excitations to be above ~ 10 TeV [93–97]. These bounds can be relaxed by either introducing additional flavor symmetries [95,96,98] or promoting a bulk Higgs instead of a brane localized one.

³In RS1 the extra dimension is compact and its compactification leads to the appearance of towers of heavy KK modes of particles which propagate in the extra dimension.

While there have been many extensive studies of the SM4, there are few analyzes of BSM scenarios with four generations (see however [99]). The reason is that the fourth generation typically imposes severe restrictions on the models. In particular, there are difficulties in incorporating a chiral fourth family scenario into any Higgs doublet model, such as the MSSM [100]. It was initially shown that, due to large masses for the fourth generation quarks and large Yukawa couplings, there are no values of $\tan \beta = v_u/v_d > 1$ for which the couplings are perturbative to the Grand Unification Scale. (However, this condition does not apply to vector-like quarks [101].) Recently the MSSM with four generations has received some more attention [102], as it was shown that for $\tan \beta \simeq 1$ the model exhibits a strong first order phase transition [103]. The four generation scenario can easily be incorporated in models with warped extra dimensions, as in [104, 105], where it can be argued that the fourth generation arises naturally. In these models the Higgs particle can be thought of as a generic composite state, being a condensate of some of the fourth generation heavy quarks [105–109], thus providing a solution to the hierarchy problem. An additional benefit of a fourth generation extension in warped models, could be the inclusion of the fourth generation neutrino, which may become a novel dark matter candidate [110], typically missing in minimal models (see however [111] for different approaches).

The thesis is divided broadly into three parts. In total there will be eight chapters and five appendices. The first part of the thesis is incorporated in Chapter 2 which is dedicated to a review of SM as a description of physical phenomena at energies below M_{EW} . We describe the model in detail and mention why we consider the SM as an EFT and the requirement for BSM. In Chapter 3, which is the second part of the thesis, we introduce some of the BSM, which closely resemble the SM at the energies that have already been explored. We start with perhaps the simplest extension of the SM, LRSM, which treats the left and right-chiral particles and their interactions on an equal basis. The next section introduces SUSY. Then, another extension of the SM, Four-Generation Standard Model, is introduced, and finally we give an extended treatment of Warped Extra Dimensional models. The final part of the thesis will be on our works on LRSUSY [27] in Chapter 4 and Warped Extra Dimensional models with a fourth generation [107–109] in Chapters 5-7 where each work is presented in a separate chapter. A discussion and conclusion will be presented in the last chapter. In addition, Appendix A presents notations and conventions used

throughout the thesis, Appendix B is about the gauge group and transformations, Appendix C includes the details of the Ricci Tensor and brane tensions calculations, Appendix D covers Rotation and CKM4 Matrices in Warped Extra Dimensions with Four Generation and finally, Appendix E addresses Feynman Rules in Warped Extra Dimensions with Four Generations.

Chapter 2

THE STANDARD MODEL

The Standard Model of particle physics, which combines special relativity and quantum mechanics into a Quantum Field Theory (QFT), is currently accepted as an empirically adequate model describing the known elementary particles, together with the three out of four fundamental interactions among them. It has been tested over the scales from the Hubble radius of 10^{30} cm ($\sim 10^{-45}$ GeV) all the way down to 10^{-16} cm ($\sim 10^2$ GeV) and still being tested by LHC at a center-of-mass energy of 7-8 TeV in proton-proton collisions. The LHC has been able to deliver data sets of several fb^{-1} to both ATLAS [9] and CMS [10] detectors and the SM so far demonstrated an amazing success in (almost) all experimental data, with one of its key prediction, the Higgs Particle, in the process of being confirmed with event excesses measured around the mass window of 125-126 GeV. Previously, the SM had led to many other successful predictions of particles and phenomena prior to their discoveries experimentally, such as the existence of massive W^\pm , Z gauge bosons, the quark model which was introduced by Gell-Mann and Zweig mathematically, the prediction of tau neutrino, charm, top and bottom quarks, and so on. Although, the SM has a remarkable body of experimental support, it suffers from some shortcomings, which we will mention in the last section of this chapter. The SM can be thought as an EFT of a more fundamental theory. This is why there are BSM searches such as SUSY, SM4 or extra dimensions etc., going on at the LHC, besides the searches for the Higgs boson.

According to the SM, the elementary particles are called fermions (i.e., they have spin-1/2 in the units of \hbar), namely quarks and leptons (see Tables 1 and 2), and the

fundamental interactions are the electromagnetic force, the weak force (responsible for radioactive decay) and the strong force (which holds atomic nuclei together) (see Table 4). The remaining force, the so called the gravitational force, is excluded in the SM.

The dynamics of a system in QFT is given by the Lagrangian and gauge symmetry plays a central role in determining this dynamical structure. Based on compelling experimental evidence the gauge group of the SM is given by

$$G_{\text{SM}} = SU(3)_c \otimes SU(2)_L \otimes U(1)_Y. \quad (2.1)$$

The SM Lagrangian exhibits invariance under $SU(3)_c$ gauge transformation for the strong interactions, c indicating the group couples only to the colored particles, and $SU(2)_L \otimes U(1)_Y$ for the electroweak interactions, which is the unified description of electromagnetic and the weak interactions introduced by Glashow-Weinberg-Salam [2–7] (Nobel Prize in Physics in 1979). The subscript, L means that, only the left-chiral particles participate in the interactions of $SU(2)_L$, and Y denotes that the group $U(1)_Y$ couples to the weak hypercharged particles. The weak hypercharge of a particle is obtained from a quasi-Gell-Mann-Nishijima relation [112, 113]

$$Q = I_w^3 + \frac{Y}{2}, \quad (2.2)$$

where I_w^3 , is the third generator of the group $SU(2)_L$ and Q is the electric charge. However, the gauge symmetry of the SM Lagrangian is not an exact symmetry. At low energies, it is spontaneously broken to the subgroup

$$SU(3)_c \otimes U(1)_Q, \quad (2.3)$$

via Higgs mechanism (which will be explained in the Section 2.5). The corresponding gauge bosons (i.e., they have spin-1), introduced by the local gauge invariance for mediating these interactions are the eight gluons for strong interactions, the W^\pm and Z^0 bosons for weak interactions, and the photon for electromagnetic interactions (see Table 3).

2.1 Elementary Particles in the Standard Model

The particle content of the SM is composed of quarks and leptons which are the fundamental fermionic constituents of the matter discovered at the various collider

experiments. They transform according to the fundamental representations of the gauge symmetry group G_{SM} given in eq. (2.1) (Appendix B explains more about gauge transformations). Some of their properties and representations are summarized in the Tables 1 and 2. It is important to note that, in the SM, both quarks and leptons fall into three generations. We will indicate the generation of fermions by a subscript, i (for example, $Q_{i,L}^\alpha$ where $i = 1, 2, 3$). The subscript $L(R)$ stands for the left-chiral(right-chiral) components of the field operator $Q_i^\alpha(U_i^\alpha$ or $D_i^\alpha)$, and they are projected as $Q_{i,L}^\alpha = P_L Q_i^\alpha(U_{i,R}^\alpha = P_R U_i^\alpha$ or $D_{i,R}^\alpha = P_R D_i^\alpha)$, where $P_L(P_R)$ is the projection operator whose the explicit form is given in Appendix A. Table 1 is devoted to quarks which, in addition to the flavor also carry the color charge as another degree of freedom such that, each quark can have three different colors, namely red (R), green (G) and blue (B). The color indices are denoted as a superscript, α (for instance, $Q_{i,L}^\alpha$ where $\alpha = \text{R,G,B}$). We give the approximate rest mass energies of quarks confined in hadrons taken from Particle Data Group [114], since no free quarks have been observed yet. Quarks possess six degrees of freedom (up, down, charm, strange, truth and beauty), called flavor.

Chiral Field	Component Fields	$SU(3)_c \otimes SU(2)_L \otimes U(1)_Y$ Quantum Numbers			Masses (GeV)
$Q_{1,L}^\alpha$	$\begin{pmatrix} u_L^\alpha \\ d_L^\alpha \end{pmatrix}$	3	2	$\frac{1}{3}$	$(2.49_{-0.79}^{+0.81}) \times 10^{-3}$ $(5.05_{-0.95}^{+0.75}) \times 10^{-3}$
$U_{1,R}^\alpha$	u_R^α	3	1	$\frac{4}{3}$	$(2.49_{-0.79}^{+0.81}) \times 10^{-3}$
$D_{1,R}^\alpha$	d_R^α	3	1	$-\frac{2}{3}$	$(5.05_{-0.95}^{+0.75}) \times 10^{-3}$
$Q_{2,L}^\alpha$	$\begin{pmatrix} c_L^\alpha \\ s_L^\alpha \end{pmatrix}$	3	2	$\frac{1}{3}$	$1.270_{-0.09}^{+0.07}$ $0.101_{-0.021}^{+0.029}$
$U_{2,R}^\alpha$	c_R^α	3	1	$\frac{4}{3}$	$1.270_{-0.09}^{+0.07}$
$D_{2,R}^\alpha$	s_R^α	3	1	$-\frac{2}{3}$	$0.101_{-0.021}^{+0.029}$
$Q_{3,L}^\alpha$	$\begin{pmatrix} t_L^\alpha \\ b_L^\alpha \end{pmatrix}$	3	2	$\frac{1}{3}$	$172.0 \pm 0.9 \pm 1.3$ $4.19_{-0.06}^{+0.18}$
$U_{3,R}^\alpha$	t_R^α	3	1	$\frac{4}{3}$	$172.0 \pm 0.9 \pm 1.3$
$D_{3,R}^\alpha$	b_R^α	3	1	$-\frac{2}{3}$	$4.19_{-0.06}^{+0.18}$

Table 1: Quark content of the SM including the corresponding $SU(3)_c \otimes SU(2)_L \otimes U(1)_Y$ gauge quantum numbers together with the PDG values for the rest mass energies of the quarks confined in hadrons.

Leptons, on the other hand, have three different flavors (electron number, muon number and tau number) and they do not carry color. Table 2 summarizes the leptons in the SM. In its original formulation, the right-chiral neutrinos were not included in the SM to keep neutrinos massless. The mass values of the leptons are taken from PDG [114].

Note that for each quark and lepton given in the tables there is a corresponding anti-quark and anti-lepton of the same mass and the spin, but opposite charge and opposite magnetic moment relative to the direction of spin.

Chiral Field	Component Fields	$SU(3)_c \otimes SU(2)_L \otimes U(1)_Y$ Quantum Numbers			Masses (MeV)
$L_{1,L}$	$\begin{pmatrix} \nu_{eL} \\ e_L \end{pmatrix}$	1	2	-1	< 0.225 $0.510998910 \pm 0.000000013$
$E_{1,R}$	e_R	1	1	-2	$0.510998910 \pm 0.000000013$
$L_{2,L}$	$\begin{pmatrix} \nu_{\mu L} \\ \mu_L \end{pmatrix}$	1	2	-1	105.658367 ± 0.000004 < 0.19
$E_{2,R}$	μ_R	1	1	-2	105.658367 ± 0.000004
$L_{3,L}$	$\begin{pmatrix} \nu_{\tau L} \\ \tau_L \end{pmatrix}$	1	2	-1	1776.82 ± 0.16 < 18.2
$E_{3,R}$	τ_R	1	1	-2	1776.82 ± 0.16

Table 2: Leptons in the SM with their corresponding $SU(3)_c \otimes SU(2)_L \otimes U(1)_Y$ gauge quantum numbers together with the PDG values for their masses.

Let us explain how to get the $SU(3)_c \otimes SU(2)_L \otimes U(1)_Y$ gauge quantum numbers for particles. Let us consider the right chiral electron state $E_{1,R}(\mathbf{1}, \mathbf{1}, -2) = e_R$ as an example. Leptons do not carry color charge. Therefore, they do not transform under the group $SU(3)_c$. Thus, we assign $SU(3)_c$ quantum number of $E_{1,R}$ (and also for all the other leptons) as $\mathbf{1}$ to make it into a singlet under this group. Moreover, since only the left-chiral particles participate in the interactions of $SU(2)_L$, the quantum number of $L_{1,R}$ is again $\mathbf{1}$. Finally, we use eq. (2.2) to get quantum number associated with the group $U(1)_Y$.

In addition to the fermions, there are also bosonic particles in the SM introduced in order to keep the kinetic terms of the matter fields invariant under the Local Gauge Transformations (LGT) of the symmetry group given in eq. (2.1) (see Appendix B). Thus, the local gauge invariance under the gauge group G_{SM} , restricts the interactions of the fields mediated by the these gauge bosons which then act as force carriers. Some of the properties of these induced gauge bosons are summarized in the Table 3. We also introduce, the Higgs Boson in the last row.

Chiral Field	Component Fields	$SU(3)_c \otimes SU(2)_L \otimes U(1)_Y$ Quantum Numbers			Spin
B_μ	B_μ	1	1	0	1
W_μ	$W_\mu^+, W_\mu^-, W_\mu^3$	1	3	0	1
G_μ^a	$G_\mu^1, G_\mu^2, \dots, G_\mu^8$	8	1	0	1
Φ	$\begin{pmatrix} \phi^+ \\ \phi^0 \end{pmatrix} = \frac{1}{\sqrt{2}} \begin{pmatrix} \phi_3^+ + i\phi_4^+ \\ \phi_1^0 + i\phi_2^0 \end{pmatrix}$	1	2	1	0

Table 3: Bosonic field content of the SM with their corresponding $SU(3)_c \otimes SU(2)_L \otimes U(1)_Y$ gauge and spin quantum numbers.

The Higgs boson is introduced in the model for generating masses. In local gauge symmetries Spontaneous Symmetry Breaking (SSB) is used to give masses to gauge bosons and fermions (see Section 2.5). Recently, it was announced that there is significant evidence for the Higgs boson gathered at CERN LHC [9, 10], but further data is needed to confirm this signal to be due to the SM Higgs Boson.

2.2 Interactions Between the Elementary Particles in the Standard Model

It is well known that there are four interactions among the elementary particles which are summarized in Table 4. The electromagnetic, weak, and strong forces are all gauge forces and therefore are mediated by the exchange gauge bosons as given in the last column of the Table 4. We include also the coupling strengths for each force which are related to the coupling constants of the corresponding group by

$$\alpha_i(\mu) = \frac{g_i(\mu)^2}{4\pi}, \quad (2.4)$$

where $g_i = g', g$ and g_s are the corresponding coupling constants. These are running coupling constants, as they are subjected to quantum loop corrections. Therefore their values depend on the renormalization scale μ . Note that as the energy scale considered becomes larger, the strong coupling becomes weaker. More specifically,

at low energies such as $\mu = 200 \text{ MeV}$, $\alpha_s(200) \text{ MeV} \gtrsim \mathcal{O}(1)$, which calls for non-perturbative methods; while α_s becomes asymptotically free for high energies.

Force	Coupling Strength	Range	Mediator
Strong	$\alpha_s = \frac{g_s^2}{4\pi} \cong 0.1$	$< 10^{-15}m$	Gluon
Electromagnetic	$\alpha = \frac{e^2}{4\pi} \cong \frac{1}{137}$	∞	Photon
Weak	$G_F \cong 1.16 \times 10^{-5} \text{ GeV}^{-2}$	$< 10^{-18}m$	W^\pm, Z
Gravitational	$G_N \cong 6.71 \times 10^{-39} \text{ GeV}^{-2}$	∞	Graviton

Table 4: The four fundamental forces in nature.

The electromagnetic force is described by Quantum Electrodynamics (QED) which is an Abelian gauge theory with the $U(1)_Q$ symmetry. It is a renormalizable theory and because of the smallness of the coupling constant (α) perturbation works well. The mediator of electromagnetic force is the photon which is massless. Therefore, due to the uncertainty principle, the electromagnetic force has an infinite range.

The theory of weak interactions (responsible for radioactive decay) was originally formulated by Fermi [115], and it works well for low energies. However, the coupling constant G_F has the dimension of $[\text{mass}]^{-2}$, so it is not a renormalizable theory. This is why the Fermi theory is regarded as the effective model for weak processes. In the 1960's there were dedicated studies of weak interactions and Glashow-Weinberg-Salam [2-7] formulated a renormalized theory based on the unified picture of weak and electromagnetic interactions in the framework of the non-Abelian gauge theory with $SU(2)_L \otimes U(1)_Y$ symmetry, which is now called as electroweak theory of the SM. Unlike the photon, weak gauge bosons W^\pm, Z have masses. Thus, the weak interaction has a short range.

The field theory for strong interactions (which hold atomic nuclei together) is formulated with $SU(3)_c$ color symmetry and is called as Quantum Chromodynamics (QCD). The gluons, mediators of strong force, being massless are expected to have infinite ranges, but unlike the electromagnetic field, gluon fields are confining, that is they have a limited range.

Several attempts have been made to fit gravity, the remaining force, into this gauge framework but these attempts have failed. However, the gravity is too weak to change particle physics predictions in the current experimental energy scales.

2.3 Cabibbo-Kobayashi-Maskawa Matrices

In the charged weak interactions of leptons, the coupling of W^\pm takes place strictly within a particular generation in the case of massless neutrinos. In other words, upper members of left-chiral lepton doublets couple to the lower members in the same doublet. That is, only the vertices $e^-\nu_e W^-$, $\mu^-\nu_\mu W^-$, and $\tau^-\nu_\tau W^-$ appear. There is no cross generational vertices such as $e^-\nu_\mu W^-$. However, the coupling of W^\pm to quarks is not so simple, since there exist cross generational vertices as well, such as $\bar{s}u W^-$. The idea is that, the quark generations are rotated for the purposes of weak interactions such that

$$\begin{pmatrix} u_L \\ d'_L \end{pmatrix} ; \quad \begin{pmatrix} c_L \\ s'_L \end{pmatrix} ; \quad \begin{pmatrix} t_L \\ b'_L \end{pmatrix}, \quad (2.5)$$

where (d', s', b') are weak eigenstates not equal to the corresponding mass eigenstates (d, s, b) but rather are linear combinations of them. The Cabibbo-Kobayashi-Maskawa (CKM) matrix describes this mixing between three different families of quark in the SM. Since there are three generations of quarks, the matrix is therefore a unitary 3×3 matrix given as

$$\begin{pmatrix} d' \\ s' \\ b' \end{pmatrix} = \begin{pmatrix} V_{ud} & V_{us} & V_{ub} \\ V_{cd} & V_{cs} & V_{cb} \\ V_{td} & V_{ts} & V_{tb} \end{pmatrix} \begin{pmatrix} d \\ s \\ b \end{pmatrix}, \quad (2.6)$$

where the off-diagonal elements of the CKM matrix allow flavor transitions between different generations.

There are several parametrizations of the CKM matrix, \mathbf{V}_{CKM} . A convenient way, been proposed by Wolfenstein [116], approximates \mathbf{V}_{CKM} by using four independent parameters and expanding each element of V as a power series of the sine of the Cabibbo angle, λ ($\lambda = \sin \theta_C \approx V_{us}$). In the approximation up to order of λ^3 , the CKM matrix is written as

$$\mathbf{V}_{\text{CKM}} = \begin{pmatrix} 1 - \frac{\lambda^2}{2} & \lambda & A\lambda^3(\rho - i\eta) \\ -\lambda & 1 - \frac{\lambda^2}{2} & A\lambda^2 \\ A\lambda^3(1 - \rho - i\eta) & -A\lambda^2 & 1 \end{pmatrix} + \mathcal{O}(\lambda^4), \quad (2.7)$$

with $\lambda = 0.2257$, $A = 0.814$, $\rho = 0.135$, and $\eta = 0.349$ [117, 118]. A 3×3 unitary matrix cannot be forced to have real values. As a result, the couplings for quarks

differ from the corresponding couplings for antiquarks as they have different phases. In mathematical terms $\mathbf{V}_{\text{CKM}} \neq \mathbf{V}_{\text{CKM}}^*$ which implies CP violation in the quark sector in weak interactions. In the Wolfenstein parametrization of the CKM matrix, this is encoded in the η parameter.

2.4 The Standard Model Lagrangian

Before we start writing the SM Lagrangian density (\mathcal{L}_{SM}) I will give some preliminary information about how to sort the Lagrangian according to the mass dimensions of the products of field operators that they contain. In a Four Dimensional (4D) theory, the Lagrangian has to carry a mass dimension $D = 4$ to keep the action dimensionless. If there exist terms that have a mass dimension $D > 4$, then inverse powers of a new physics (NP) mass scale M have to appear. In mathematical terms we can write the most general Lagrangian of a fundamental theory as

$$\mathcal{L} = \mathcal{L}_{\leq 4} + \frac{\mathcal{L}_5}{M} + \frac{\mathcal{L}_6}{M^2} + \dots, \quad (2.8)$$

where the subscripts denote the mass dimension of the corresponding Lagrangian with $\mathcal{L}_{\leq 4}$, including coefficients with positive mass dimensions. The mass scale M can be considered as a cut-off scale for the theory, such that $\mathcal{L}_{\leq 4}$, the low energy part of a more complete theory, will describe Nature at energies $E < M$. Consequently, terms $\mathcal{L}_{i>4}$, will be suppressed by the powers of E/M . They could even be neglected depending on the ratio E/M .

The SM Lagrangian is considered as the EFT of a more fundamental theory. Thus, the part of the Lagrangian \mathcal{L} given in eq. (2.8) with $D \leq 4$ will be the SM Lagrangian, and the rest will be the NP. Now, we will write the most general, gauge invariant, renormalizable SM Lagrangian density based on the observed particle content and symmetries.

It is divided into four parts:

$$\mathcal{L}_{SM} = \mathcal{L}_F^{Kin} + \mathcal{L}_{GB}^{Kin} + \mathcal{L}_\Phi + \mathcal{L}_Y \quad (2.9)$$

The \mathcal{L}_F^{Kin} term corresponds to the kinetic energy Lagrangian of the fermionic sector

in the SM. For the representations of the fields see Tables 1 and 2.

$$\begin{aligned} \mathcal{L}_F^{Kin} &= \sum_{i=1}^3 \left(\bar{L}_{i,L} i\gamma^\mu D_\mu L_{i,L} + \bar{E}_{i,R} i\gamma^\mu D_\mu E_{i,R} + \bar{Q}_{i,L} i\gamma^\mu D_\mu Q_{i,L} + \bar{U}_{i,R} i\gamma^\mu D_\mu U_{i,R} \right. \\ &\quad \left. + \bar{D}_{i,R} i\gamma^\mu D_\mu D_{i,R} \right), \end{aligned} \quad (2.10)$$

where $\bar{\psi}_i \equiv \psi_i^\dagger \gamma^0$, $\psi = Q, U, D, L, E$. The Dirac-gamma matrices are summarized in Appendix A. The normal derivative, ∂_μ , is replaced by the covariant derivative, $D_\mu = \partial_\mu - ig_s t_a G_\mu^a - ig \tau_i W_\mu^i - ig' \frac{Y}{2} B_\mu$ to preserve the gauge invariance in eq. (2.1). Here, g_s , g , and g' are the coupling constants, which are not constants but functions of the renormalization scale (μ), and they determine the strength of the interaction. They are associated with the $SU(3)_c$, $SU(2)_L$ and $U(1)_Y$ gauge groups, respectively. The corresponding generators to each gauge group are $t_a (a = 1, \dots, 8) = \lambda_a/2$ for $SU(3)_c$, $\tau_i (i = 1, \dots, 3) = \sigma_i/2$ for $SU(2)_L$, and Y for $U(1)_Y$ (see Appendix A), and the corresponding gauge vector bosons are $G_\mu^a (a = 1, \dots, 8)$, $W_\mu^i (i = 1, \dots, 3)$ and B_μ . One can write the fermion kinetic term more explicitly by inserting the corresponding covariant derivatives, hypercharge quantum numbers and also indicating the quark color indices as follows

$$\begin{aligned} \mathcal{L}_F^{Kin} &= \sum_{i,j=1}^3 \left(\bar{L}_{i,L} i\gamma^\mu \left[\partial_\mu - i\frac{g}{2} \sigma^j W_\mu^j + i\frac{g'}{2} B_\mu \right] L_{i,L} + \bar{E}_{i,R} i\gamma^\mu \left[\partial_\mu + i\frac{g'}{2} B_\mu \right] E_{i,R} \right. \\ &\quad + \sum_{\alpha,\beta=1}^3 \sum_{a=1}^8 \left(\bar{Q}_{i,L}^\alpha i\gamma^\mu \left[\left\{ \partial_\mu - i\frac{g}{2} \sigma^j W_\mu^j - i\frac{g'}{6} B_\mu \right\} \delta_{\alpha\beta} - i\frac{g_s}{2} \lambda_{\alpha\beta a} G_\mu^a \right] Q_{i,L}^\beta \right. \\ &\quad + \bar{U}_{i,L}^\alpha i\gamma^\mu \left[\left\{ \partial_\mu - i\frac{2g'}{3} B_\mu \right\} \delta_{\alpha\beta} - i\frac{g_s}{2} \lambda_{\alpha\beta a} G_\mu^a \right] U_{i,L}^\beta \\ &\quad \left. \left. + \bar{D}_{i,L}^\alpha i\gamma^\mu \left[\left\{ \partial_\mu + i\frac{g'}{3} B_\mu \right\} \delta_{\alpha\beta} - i\frac{g_s}{2} \lambda_{\alpha\beta a} G_\mu^a \right] D_{i,L}^\beta \right) \right) \end{aligned} \quad (2.11)$$

We can construct further gauge invariant Lorentz scalars using the gauge vector bosons as

$$\mathcal{L}_{GB}^{Kin} = -\frac{1}{4} B^{\mu\nu} B_{\mu\nu} - \frac{1}{4} \sum_{i=1}^3 W^{\mu\nu i} W_{\mu\nu}^i - \frac{1}{4} \sum_{a=1}^8 G^{\mu\nu a} G_{\mu\nu}^a, \quad (2.12)$$

where

$$\begin{aligned} B_{\mu\nu} &= \partial_\mu B_\nu - \partial_\nu B_\mu, \\ W_{\mu\nu}^i &= \partial_\mu W_\nu^i - \partial_\nu W_\mu^i - g\epsilon^{ijk} W_\mu^j W_\nu^k, \quad i, j, k = 1, \dots, 3, \\ G_{\mu\nu}^a &= \partial_\mu G_\nu^a - \partial_\nu G_\mu^a - g_s f^{abc} G_\mu^b G_\nu^c, \quad a, b, c = 1, \dots, 8, \end{aligned} \quad (2.13)$$

are the corresponding field strength tensors of the $U(1)_Y$, $SU(2)_L$ and $SU(3)_c$ gauge groups, respectively. Eq. (2.12) include the gauge boson kinetic energy terms as well as the three and four-point self interactions for W_μ^i and G_μ^a . The $U(1)_Y$ gauge boson has no self interaction. In addition, ϵ^{ijk} and f^{abc} (see Appendix B) are the structure constants of $SU(2)_L$ and $SU(3)_c$, respectively. The generators of the group $SU(2)_L$ obey an algebra of the form

$$[T^i, T^j] = i\epsilon^{ijk}T^k, \quad i, j, k = 1, \dots, 3, \quad (2.14)$$

whereas the generators of $SU(3)_c$ will satisfy

$$[T^a, T^b] = if^{abc}T^c, \quad a, b, c = 1, \dots, 8. \quad (2.15)$$

The masses of the fermions and the gauge bosons do not appear in the SM Lagrangian because it is not possible to write down gauge invariant mass terms for the (non-Abelian) vector bosons and chiral fermions. There is then a conflict between the SM and the observations from particle accelerators that there exist massive particles in nature. Otherwise, all the particles would be traveling with the speed of light making it impossible to form atoms, compounds and so on. Therefore, a spin zero complex scalar doublet under the group $SU(2)_L$, called as the Higgs boson (Φ), is introduced into the model through the Higgs mechanism [11–13] via which electroweak gauge symmetry is broken in vacuum and SM particles receive mass, whereas the fundamental Lagrangian remains gauge invariant. We will talk more about the Higgs particle and describe the Higgs mechanism in the following section. For now, it is sufficient to understand that an additional scalar particle Φ with G_{SM} gauge quantum numbers given in Table 3 has to be introduced to give masses to the SM particles. The third part of the SM Lagrangian are the kinetic and potential terms for the Higgs field, responsible for the interaction of the gauge bosons and Higgs particle. The gauge invariant kinetic and potential terms for the Higgs field can be written as follows

$$\mathcal{L}_\Phi = (D_\mu \Phi)^\dagger (D_\mu \Phi) - V(\Phi^\dagger \Phi), \quad (2.16)$$

with

$$\Phi(x) = \begin{pmatrix} \phi^+(x) \\ \phi^0(x) \end{pmatrix} = \frac{1}{\sqrt{2}} \begin{pmatrix} \phi_3^+(x) + i\phi_4^+(x) \\ \phi_1^0(x) + i\phi_2^0(x) \end{pmatrix} \quad (2.17)$$

and the covariant derivative

$$D_\mu = \partial_\mu - i\frac{g}{2}\sigma^i W_\mu^i - i\frac{g'}{2}B_\mu. \quad (2.18)$$

The Higgs potential term is conventionally written as

$$V(\Phi^\dagger\Phi) = -\frac{\mu^2}{2}(\Phi^\dagger\Phi) - \frac{\lambda}{4}(\Phi^\dagger\Phi)^2, \quad (2.19)$$

where μ^2 (mass term) and λ (Higgs quartic coupling term) are the free parameters and λ should be positive to ensure a stable vacuum.

Now, let us turn our attention to the Yukawa Lagrangian that describes the interactions among the fermions and the Higgs field. The general form can be expressed as¹

$$\mathcal{L}_Y = \sum_{i,j=1}^3 \left(y_{ij}^d \bar{Q}_{i,L} \Phi D_{j,R} + y_{ij}^u (\bar{Q}_{i,L}) \tilde{\Phi} (U_{j,R}) + y_{ij}^e (\bar{L}_{i,L}) \Phi (E_{j,R}) + \text{h.c.} \right), \quad (2.20)$$

where

$$\tilde{\Phi}(x) = i\tau_2 \Phi^*(x) = \begin{pmatrix} \phi^{0*}(x) \\ -\phi^-(x) \end{pmatrix}, \quad (2.21)$$

and $y_{ij}^{u,d,e}$'s are responsible for fermion masses. They are 3×3 completely arbitrary matrices. Most of the free parameters of the SM are embedded in these couplings. Note that the field $\tilde{\Phi}(x)$ has $(1, 2^*, -1)$ as $SU(3)_c \otimes SU(2)_L \otimes U(1)_Y$ quantum numbers, respectively. The Higgs field Φ is responsible for generating masses for the lower components of fermions. The upper components, on the other hand, interact with $\tilde{\Phi}$ to receive their masses.

The Yukawa terms are given with fermion fields in their gauge eigenstates, it will be useful to summarize them

$$\begin{aligned} \mathbf{L}_L^e &= \{e_L^0, \mu_L^0, \tau_L^0\}^T, & \mathbf{L}_L^\nu &= \{\nu_{e_L}^0, \nu_{\mu_L}^0, \nu_{\tau_L}^0\}^T, \\ \mathbf{E}_R^e &= \{e_R^0, \mu_R^0, \tau_R^0\}^T, \\ \mathbf{Q}_L^d &= \{d_L^0, s_L^0, b_L^0\}^T, & \mathbf{Q}_L^u &= \{u_L^0, c_L^0, t_L^0\}^T, \\ \mathbf{D}_R &= \{d_R^0, s_R^0, b_R^0\}^T, & \mathbf{U}_R &= \{u_R^0, c_R^0, t_R^0\}^T. \end{aligned} \quad (2.22)$$

Notice that right-handed neutrinos \mathbf{L}_R^ν does not exist in the framework of the SM to keep neutrinos massless.

¹In the case of massive neutrinos, there is an additional term in the Lagrangian: $\mathcal{L}_Y^{SM} = \eta_{ij}^\nu \bar{L}_{i,L} \tilde{\Phi} \nu_{j,R} + \text{h.c.}$

2.5 Higgs Mechanism

The Higgs mechanism, is introduced by Brout, Englert [11], Higgs [12], Guralnik, Hagen and Kibble [13] in the SM to spontaneously (i.e., in the ground state not in the fundamental level) break the gauge symmetry $SU(3)_c \otimes SU(2)_L \otimes U(1)_Y$ to the subgroup $SU(3)_c \otimes U(1)_Q$. Consecutively, it gives masses to the three electroweak gauge bosons W^\pm, Z but leaves the gluons and the photon, the gauge particles of the unbroken symmetries $SU(3)_c$ and $U(1)_Q$, respectively, massless. This process is called as the electroweak symmetry breaking (EWSB) and it is achieved by introducing a complex scalar doublet under $SU(2)_L$, the Higgs boson. The mechanism works as follows. The Higgs potential term, $V(\Phi^\dagger\Phi)$, given in eq. (2.19) is minimized for $\lambda > 0$ (so that the Higgs potential will be bounded from below) and $\mu^2 < 0$. The minimum of the potential occurs at a nontrivial value of $\Phi^\dagger\Phi$

$$(\Phi^\dagger\Phi)_0 = \frac{1}{2}[(\phi_1^2)_0 + (\phi_2^2)_0 + (\phi_3^2)_0 + (\phi_4^2)_0] = v^2, \quad v = \sqrt{-\mu^2/\lambda}, \quad (2.23)$$

instead of occurring at $(\Phi^\dagger\Phi)_0 = 0$, which gives a local maximum. The subscript zero indicates that, this specific solution produces a minimum value for the Higgs potential. Therefore, the Higgs potential has the so called Mexican hat form as shown in Fig. 1.

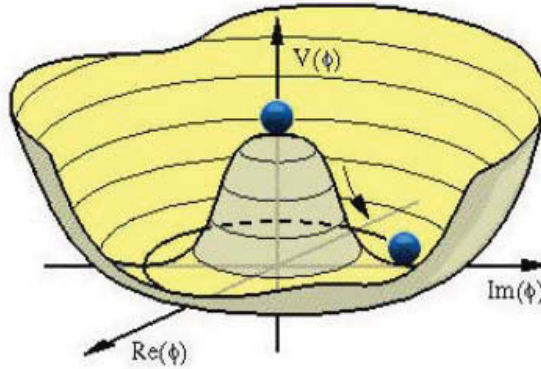


Figure 1: The Higgs potential function for $\mu^2 < 0$ and $\lambda > 0$ on a real-imaginary plane of ϕ .

Above M_{EW} , the Higgs field resides at the local maximum point where $v = 0$ and the gauge symmetry G_{SM} is preserved. However, if the energy falls below the electroweak

scale Higgs field cannot stay on top of the local maximum anymore. It chooses an arbitrary direction and spontaneously breaks the electroweak symmetry $SU(2)_L \otimes U(1)_Y$ into the subgroup $U(1)_Q$. In summary, at the minimum configuration of the potential, the Higgs field develops a vacuum expectation value (VEV)

$$\Phi_0 = \langle 0|\Phi|0\rangle = \begin{pmatrix} 0 \\ v \end{pmatrix}, \quad (2.24)$$

and consequently breaks the gauge symmetry spontaneously. In the minimum configuration one can choose the Higgs parametrization to be

$$(\phi_1)_0 = \sqrt{2}v, \quad (\phi_2)_0 = 0, \quad (\phi_3)_0 = 0, \quad (\phi_4)_0 = 0. \quad (2.25)$$

Experimentally, we know the VEV $v \sim 174$ GeV. Let us show that the generators I_w^3 and Y are broken at the vacuum:

$$\begin{aligned} I_w^3 \Phi_0 &= \frac{1}{2} \begin{pmatrix} 1 & 0 \\ 0 & -1 \end{pmatrix} \begin{pmatrix} 0 \\ v \end{pmatrix} = -\frac{1}{2} \begin{pmatrix} 0 \\ v \end{pmatrix} = -\frac{1}{2} \Phi_0, \\ Y \Phi_0 &= \Phi_0. \end{aligned} \quad (2.26)$$

Therefore, $e^{-i\alpha^3 I_w^3} \Phi_0 \neq \Phi_0$ and $e^{-i\beta \frac{Y}{2}} \Phi_0 \neq \Phi_0$, whereas the electric charge operator Q remains as unbroken generator since

$$Q \Phi_0 = \left(I_w^3 + \frac{Y}{2} \right) \Phi_0 = \begin{pmatrix} 1 & 0 \\ 0 & 0 \end{pmatrix} \begin{pmatrix} 0 \\ v \end{pmatrix} = 0, \quad (2.27)$$

i.e., $e^{-ieQ} \Phi_0 = \Phi_0$. Since the symmetry is local we may perform a different isospin rotation to each point in space so that Φ may be reduced to the form

$$\Phi = \begin{pmatrix} 0 \\ v + \frac{h(x)}{\sqrt{2}} \end{pmatrix}, \quad (2.28)$$

where $h(x)$ is the famous Higgs particle.

2.5.1 Mass Generation of Gauge Bosons

The masses of gauge fields manifest themselves in the kinetic part of the Higgs Lagrangian when the Higgs field receives a VEV. Therefore, the gauge fields acquire

masses by the kinetic interaction with the Higgs field. At the vacuum, the covariant derivative of Φ yields using eq. (2.18) yields

$$\begin{aligned} D_\mu \Phi &= \begin{pmatrix} 0 \\ \frac{1}{\sqrt{2}} \partial_\mu h \end{pmatrix} - \left[i \frac{g}{2} \begin{pmatrix} W_\mu^3 & \sqrt{2} W_\mu^+ \\ \sqrt{2} W_\mu^- & -W_\mu^3 \end{pmatrix} + i \frac{g'}{2} B_\mu \right] \begin{pmatrix} 0 \\ v + \frac{h}{\sqrt{2}} \end{pmatrix} \\ &= -\frac{i}{2} \begin{pmatrix} \sqrt{2} g v W_\mu^+ + g h W_\mu^+ \\ i \sqrt{2} \partial_\mu h + v(-g W_\mu^3 + g' B_\mu) + \frac{1}{\sqrt{2}} h(-g W_\mu^3 + g' B_\mu) \end{pmatrix}, \end{aligned} \quad (2.29)$$

where $W_\mu^\pm = \frac{1}{\sqrt{2}}(W_\mu^1 \mp i W_\mu^2)$. Hence,

$$(D_\mu \Phi)^\dagger (D^\mu \Phi) = \frac{1}{2} (\partial_\mu h)^2 + \frac{g^2 v^2}{2} W_\mu^+ W_\mu^- + \frac{v^2}{4} (g W_\mu^3 - g' B_\mu)^2. \quad (2.30)$$

We define an orthogonal transformation to remove the mixing of neutral fields (W_μ^3 and B_μ) such that

$$\begin{pmatrix} Z_\mu \\ A_\mu \end{pmatrix} = \begin{pmatrix} \cos \theta_W & -\sin \theta_W \\ \sin \theta_W & \cos \theta_W \end{pmatrix} \begin{pmatrix} W_\mu^3 \\ B_\mu \end{pmatrix}, \quad (2.31)$$

with

$$\sin \theta_W = \frac{g'}{\sqrt{g^2 + g'^2}}, \quad \cos \theta_W = \frac{g}{\sqrt{g^2 + g'^2}}, \quad (2.32)$$

where θ_W is the Weinberg angle. Substituting eq. (2.31) in eq. (2.30), the photon, A , becomes massless while the mass eigenstates for W^\pm and Z^0 bosons are obtained as

$$M_{W^\pm} = \frac{g v}{\sqrt{2}}, \quad M_{Z^0} = \sqrt{\frac{g^2 + g'^2}{2}} v. \quad (2.33)$$

2.5.2 Mass Generation for Fermions

The fermions acquire their masses from Yukawa interactions of Higgs field given in eq. (2.20) in the vacuum state. For simplicity, let us show how the up-type quarks receives their masses via Higgs mechanism. In the vacuum, the Yukawa Lagrangian for up-type quarks reads

$$\mathcal{L}_Y^u = \sum_{i,j=1}^3 y_{ij}^u \bar{Q}_{i,L} \tilde{\phi} U_{j,R} + \text{h.c.} = \left(v + \frac{h}{\sqrt{2}} \right) \bar{\mathbf{Q}}_L^u \mathbf{Y}_u \mathbf{U}_R + \text{h.c.} \quad (2.34)$$

Note that on the right-hand side the we have used the the representation of fermions in their gauge eigenstates, introduced in eq. (2.22), and \mathbf{Y}_u is a 3×3 Yukawa coupling matrix for the up-type quarks. We can rewrite eq. (2.34) as follows

$$\mathcal{L}_Y^u = \bar{\mathbf{Q}}_L^u (\mathbf{M}^u + \mathbf{Y}_u h) \mathbf{U}_R + \text{h.c.}, \quad (2.35)$$

where $\mathbf{M}_u = v \mathbf{Y}_u$ is the 3×3 fermion mass matrix for up-type quarks. However, these are not the physical eigenstates since the mass matrix is not diagonal. We can diagonalize \mathbf{M}_u by separate unitary transformations \mathbf{U}_{Q_u} and \mathbf{W}_u on the left- and right- chiral fermion fields, respectively

$$\mathbf{U}_{Q_u}^\dagger \mathbf{Q}_L^u = (u_L \ c_L \ t_L)^T, \quad \mathbf{W}_u^\dagger \mathbf{U}_R = (u_R \ c_R \ t_R)^T, \quad (2.36)$$

which will result in

$$\mathbf{U}_{Q_u}^\dagger \mathbf{M}_u \mathbf{W}_u = \mathbf{M}_u^{\text{diag}} = \begin{pmatrix} m_u & 0 & 0 \\ 0 & m_c & 0 \\ 0 & 0 & m_t \end{pmatrix}, \quad (2.37)$$

where the diagonal entries are real, non-negative eigenvalues corresponding to the physical masses of up-type quarks. The down-type quark and charged lepton matrices are also diagonalized in a similar way by

$$\mathbf{U}_{Q_d}^\dagger \mathbf{M}_d \mathbf{W}_d = \mathbf{M}_d^{\text{diag}}, \quad \mathbf{U}_{L_e}^\dagger \mathbf{M}_l \mathbf{W}_e = \mathbf{M}_l^{\text{diag}}. \quad (2.38)$$

by making use of

$$\begin{aligned} \mathbf{U}_{Q_d}^\dagger \mathbf{Q}_L^d &= (d_L \ s_L \ b_L)^T, & \mathbf{W}_d^\dagger \mathbf{D}_R &= (d_R \ s_R \ b_R)^T, \\ \mathbf{U}_{L_e}^\dagger \mathbf{L}_L^e &= (e_L \ \mu_L \ \tau_L)^T, & \mathbf{W}_e^\dagger \mathbf{E}_R^e &= (e_R \ \mu_R \ \tau_R)^T. \end{aligned} \quad (2.39)$$

2.6 Experimental Status of the Standard Model

There are three assumptions made for constructing SM. Its gauge group is $SU(3)_c \otimes SU(2)_L \otimes U(1)_Y$. There is only one Higgs doublet. Fermion representations compromise left-chiral weak isodoublets and right-chiral singlets.

There are 21 free parameters of which three are coupling constants, twelve fermion masses, four fermion mixing parameters, one Higgs mass and one independent gauge

boson mass. We have briefly introduced these essential ingredients of the SM in the previous sections. We now summarize its successes. The theory is formulated as a renormalizable quantum theory. Therefore, it preserves its predictive power beyond tree-level computations and allows for the probing of quantum effects. In the mid 1980s, the elements of the SM which still awaited experimental confirmation were the discovery of top quark to verify the multiplet structure of fermions, validation of universality, demonstration of asymptotic freedom over a wide range of energy scale, extraction of $\sin\theta_W$ from numerous experiments, discovery of the properties of W and Z bosons (predicted prior to their observation) and finding the Higgs. All those confirmations, except for the Higgs properties, are accomplished at various levels of sensitivity. The existence of the top quark was established in 1995 using 67 pb^{-1} data sample of $\bar{p}p$ collisions at Fermilab [119, 120]. The universality, which is explained as the coupling of the leptons to gauge bosons being flavor independent, has been tested many times for instance, the probability that W^- decay to $l^- \nu_l$ is the same for electron, muon and tau leptons to a very good precision. The weak current which was discovered in 1973 [121–123] together with the W and Z bosons [124, 125] have been the primary predictions of the SM. In short, every feature of the theory is confirmed to a high degree of precision by the experiments over the decades except the missing Higgs boson. In the SM, the Higgs boson mass ($m_h = \sqrt{\lambda/2} v$) is a free parameter since the self coupling constant (λ) is unknown. The SM Higgs production cross sections and its branching fractions has been calculated as a function of Higgs mass. At high-energy hadron colliders the relevant cross sections for Higgs production are presented in Figure 2 as function of the Higgs mass. The main production mechanism for the SM Higgs boson is the gluon fusion through a heavy quark loop over the all mass range of the Higgs which is then followed by vector-boson fusion (VBF) channels contributing significantly to the Higgs production for heavy Higgs where the coupling to longitudinal polarized vector bosons is strong. We do not aim here at a detailed discussion of the importance of each production channel, but only at providing the most accurate and up-to-date theoretical predictions.

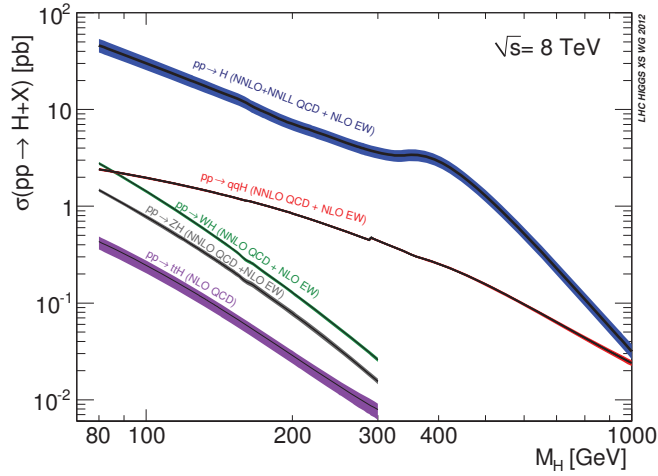


Figure 2: Standard Model Higgs boson production cross sections at center-of-mass energy of 8 TeV. Figure from [131].

Since the Higgs boson decays very rapidly, in order to get a complete and correct vision of Higgs phenomenology, one has to look for its decay modes including both tree level massive and loop level massless particles of the SM. Figure 3 shows the the most relevant decay modes of the SM Higgs boson to the SM particles as functions of its mass.

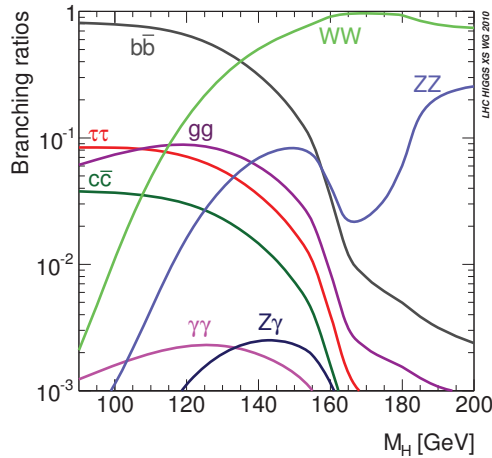


Figure 3: Standard Model Higgs boson decay branching ratios. Figure from [131].

In the high mass region, the SM Higgs decays mainly to the vector bosons, whereas in

the low mass region the decays to fermion pairs dominate. Despite the small expected signal rate, decay of Higgs boson into a pair of photons is particularly relevant for the discovery potential of Higgs boson at the LHC for a low mass Higgs boson since the reconstructed mass resolution provides a way to separate signal from background.

Previously, production of Higgs mass below 114.4 GeV has been excluded by the direct searches at the CERN LEP at 95% Confidence Level (CL) [126] and between 156 GeV and 177 GeV at the Fermilab Tevatron at 95% CL [127]. On July the 4th, 2012 both ATLAS [9] and CMS [10] experiments presented a preview of their updated results on the search for the SM Higgs Boson. It has been announced that they observed a particle consistent with the SM Higgs boson which is the first spin zero fundamental scalar that has ever been discovered with 5σ deviation in the combination of $\gamma\gamma$ and ZZ decay channels. The question is it the SM Higgs or not still remains to be resolved. See Figure 4.

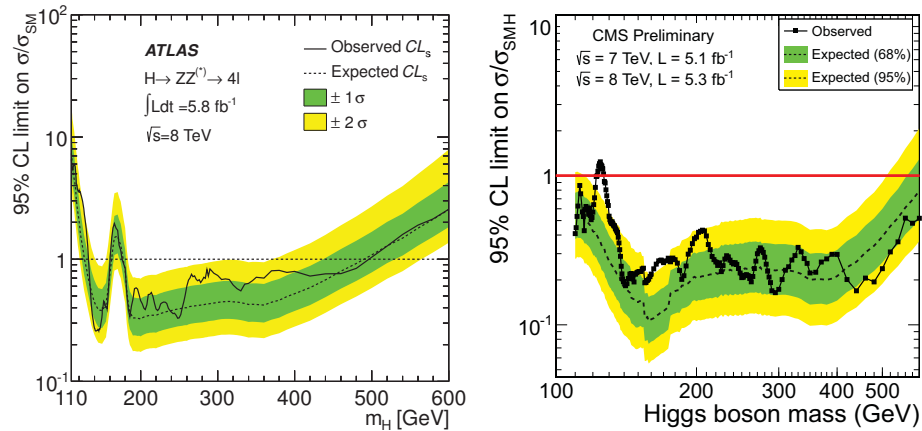


Figure 4: The observed (full line) and expected (dashed line) 95% CL combined upper limits on the SM Higgs boson production cross section divided by the SM expectation as a function of m_h in the full mass range. Left panel shows the ATLAS results. Figure from [10]. The dotted curves show the median expected limit in the absence of a signal and the green and yellow bands indicate the corresponding $\pm 1\sigma$ and $\pm 2\sigma$ intervals. Right Panel shows CMS results. Figure from [11]. The green and yellow bands indicate the ranges that are expected to contain 68% and 95% of all observed excursions from the median, respectively.

2.7 The Shortcomings of the Standard Model

Although the SM has been impressively successful in explaining all observed low-energy phenomena, it is still unsatisfactory since it builds on many assumptions and leaves some fundamental questions unanswered. Below we list the major drawbacks of the SM.

- **The Gauge Symmetry Problem:** The SM is a complicated direct product of three subgroups groups $SU(3)_c \times SU(2)_L \times U(1)_Y$ with their corresponding gauge coupling constants, which are completely arbitrary. In a more satisfactory theory, one should have a way of understanding the origin of the three different gauge couplings. In addition, there is no explanation for electroweak part of the SM being chiral (parity-violating).
- **Fermion Problem:**
 - There are three generations of fermions in the SM. However, we know that all the matter in the Universe can be constructed from the first family only. The second and third generations are heavier copies of the first family with no obvious role in the nature. The SM does not explain the reason of the their existence and leaves the question: “Whether or not there are more families ” without an answer.
 - There is a hierarchical pattern in the masses of the fermions, i.e., $m_t, m_b \gg m_c, m_s \gg m_u, m_d, m_\tau \gg m_\mu \gg m_e$, which varies over 5 orders of magnitude and not understood in the scope of SM.
 - In the SM neutrinos are massless. However, recent neutrino oscillation experiments show that neutrinos have small masses [42, 43].
- **Hierarchy Problem:** The SM introduces Higgs field to generate masses for W , Z bosons and fermions. For the model to be consistent, the Higgs mass should not be too different from that of W . Otherwise, Higgs self-interactions would be excessively strong. However, the Higgs mass receives enormous quantum corrections (quadratically divergent) from virtual effects of every particle that couples directly or indirectly to the Higgs field.
- **Gravity Problem:** SM does not include a quantum theory of gravity. Other than gravity all the other forces follow from the local gauge invariance. However,

gravity remains a mystery which is expected to become important at the Planck scale. The mere fact that $M_{\text{Pl}}/M_{\text{EW}}$ is so huge is a powerful clue that new physics exists in the higher energies.

- **Baryogenesis Problem:** It is a natural assumption that in the early Universe matter and antimatter were created equally, but today we see a baryon² asymmetry of the Universe as there is only protons, neutrons and electrons. Baryogenesis, the elimination of antimatter while leaving behind some matter, is one of the most fundamental problems of the SM.
- **Dark Matter Problem:** In recent years a remarkable concordance of cosmological observations involving the acceleration of Universe has allowed precise determinations of the cosmological parameters such that 74% Dark energy, 21% Dark matter and 4 – 5% ordinary matter are constituents of the Universe. The mysterious Dark energy which leads to the acceleration of the expansion of the Universe is not accounted for in the SM neither is the Dark matter.

This list of unanswered questions provides the primary motivation for the consideration of physics beyond the SM. Numerous theories are studied in the hope that they will address at least one of these issues. However, no single theory exists that successfully addresses all of these questions simultaneously.

²A composite subatomic particle containing three quarks.

Chapter 3

BEYOND THE STANDARD MODEL

A decade of increasingly intense experimental studies has put the SM on strong footing such that it is now firmly believed that the SM describes the nature extremely well in quantum realm up to current collider energies. However, there are some strong theoretical arguments and experimental hints (summarized in Section 2.7) indicating that at higher energy scales the SM has to be extended to BSM. Nevertheless, considering its successful predictions, any extension should reproduce the SM at the energies that have been already explored. In the following sections we will introduce LRSM, SUSY, SM4, and Warped Extra Dimensions.

3.1 The Left-Right Symmetric Model

Prior to 1956 the parity invariance (or mirror symmetry) of physical systems was taken for granted as self-evident. However, that year, Lee and Yang [128] decided to carry out an experiment to test this assumption, which was repeated later by Wu [129] to settle the issue, on radioactive Cobalt 60 nuclei undergoing beta decay. In this famous experiment, the spins of Cobalt 60 nuclei were aligned to be pointing in the same direction and the direction of emitted electrons after the beta decay were recorded. It was observed that the electrons came out in the same direction as the direction of nuclear spin. Examining the mirror image of that same process (i.e., the Cobalt 60 nuclei were aligned to be pointing in the opposite direction to the initial set-up), the

electrons were monitored to be emitted in the direction opposite to the nuclear spin, thus violating the parity. Later, it has been realized that, the parity violation is not only limited to beta decays but is actually typical for the weak interactions where it is violated maximally. In the SM, the parity violation reveals itself most dramatically in the behavior of neutrinos (they interact only weakly). As they are assumed to be massless, there is no room for the right-chiral neutrinos. While chirality is an elegant ingredient of the SM to explain the massless neutrinos, most of the nature is actually left-right symmetric, suggesting the reasonable hypothesis that parity must be a broken symmetry. In addition, the recent measurements in the solar [42] and atmospheric neutrino [43] fluxes seem to indicate that the neutrinos should have small masses, which is considered as a support for BSM. The most straightforward way for including neutrino masses would be to insert the missing right-chiral neutrino states as proposed in LRSM [17–19] extensions of the SM, where the smallness of the neutrino masses is explained by the see-saw mechanism [19, 44].

The main motivation, however, for studying the LRSM is that it provides a dynamical explanation for the parity violation, observed in the low energy weak interactions, on the same footing as the gauge symmetry breaking of the SM. As we have already mentioned in Chapter 2, the SM accommodates the left- and right-chiral fermions in different ways such that under $SU(2)_L$ gauge group transformations, the left-chiral fermions transform as doublets, whereas the right-chiral ones transform as singlets. LRSM, on the other hand, assumes that at the energy scales higher than M_{EW} the underlying symmetry of the nature is parity conserving (i.e., the left- and right-chiral fermions enter into the theory in a symmetrical fashion, both placed in doublets) which requires the gauge symmetry of the SM to be extended to

$$G_{LRSM} = SU(3)_c \otimes SU(2)_L \otimes SU(2)_R \otimes U(1)_{B-L}. \quad (3.1)$$

In the subscript $B - L$, B and L correspond to the baryon and the lepton quantum numbers, respectively. However, we know that at the current accessible energy scales the theory should exhibit the symmetry of the SM. In order to meet this experimental constraint, the LRSM is broken spontaneously. The SSB of the left-right symmetry is accomplished in two stages. At the first stage the right-chiral sector breaks the gauge symmetry $SU(2)_R \otimes U(1)_{B-L}$ down to $U(1)_Y$ at an energy scale v_R and the gauge bosons of $SU(2)_R$ become massive. The resulting symmetry is the SM gauge symmetry given in eq. (2.1). The next step is EWSB which happens in the same

manner as in the SM. Recall that, the SM symmetry is also spontaneously broken to the subgroup $U(1)_Q$ at M_{EW} . The group generator Q is given by the modified Gell-Mann-Nishijima formula

$$Q = I_{w,L}^3 + I_{w,R}^3 + \frac{B - L}{2}, \quad (3.2)$$

where $I_{w,L}^3$ and $I_{w,R}^3$ are the third components of the $SU(2)_L$ and $SU(2)_R$ isospin quantum numbers. We will show explicit calculations of the symmetry breaking process in the Subsection 3.1.3.

3.1.1 Elementary Particles in the Left-Right Symmetric Model

In this Subsection, we will briefly describe the field content of LRSM. Implementation of the left-right symmetry requires the introduction of left-chiral partners of the observed gauge bosons, neutrinos, and a Higgs sector containing at least one bi-doublet, one right-chiral and one left-chiral triplets¹. Table 5, summarizes the representation of the matter fields and the corresponding quantum numbers under the gauge group G_{LRSM} for the first generation of fermions (the subscript $i = 1$). The Q_1 and L_1 are the first generation quark and lepton fields of the SM, respectively and Q_1^c and L_1^c are the equivalent $SU(2)_R$ fields (see Appendix A for the detailed discussion about the notation). As the LRSM treats the left- and right-chiral fermions on an equal footing, right-chiral fermions are also represented as doublets under $SU(2)_R$ group transformations. There are three generation of quarks and leptons as in the case of the SM. The doublet representations of the other generations can be written in a similar fashion by making sure that the charges of the fields satisfy eq. (3.2). Note that the color charge of quarks are indicated by a superscript (α). In the last column of the Table 5, the parity transformations for the corresponding matter fields are stated.

¹Doublets instead of triplets can also be used.

Chiral Field	Component Fields	$SU(3)_c \otimes SU(2)_L \otimes SU(2)_R \otimes U(1)_{B-L}$ Quantum Numbers				Parity Transformations
Q_1^α	$\begin{pmatrix} u^\alpha \\ d^\alpha \end{pmatrix}$	3	2	1	$\frac{1}{3}$	$Q_1 \rightarrow Q_1^{c*}$
$Q_1^{c\alpha}$	$\begin{pmatrix} d^{c\alpha} \\ -u^{c\alpha} \end{pmatrix}$	3*	1	2	$-\frac{1}{3}$	$Q_1^c \rightarrow Q_1^*$
L_1	$\begin{pmatrix} \nu_e \\ e \end{pmatrix}$	1	2	1	-1	$L_1 \rightarrow L_1^{c*}$
L_1^c	$\begin{pmatrix} e^c \\ -\nu_e^c \end{pmatrix}$	1	1	2	1	$L_1^c \rightarrow L_1^*$

Table 5: First generation of fermions in the LRSM including the corresponding $SU(3)_c \otimes SU(2)_L \otimes SU(2)_R \otimes U(1)_{B-L}$ gauge quantum numbers together with the transformations under parity operator.

The addition of a new $SU(2)_R$ to the gauge group requires the existence of three weakly interacting gauge bosons: two charged ($W_{R\mu}^\pm$) and one neutral ($Z_{R\mu}$). While an extra neutral gauge boson is predicted by extensions of the SM with an extra $U(1)$ gauge symmetry group, a charged gauge boson would be a more likely indication of left-right symmetry. The bosonic (spin-1) field content of LRSM is encapsulated in Table 6.

Chiral Field	Component Fields	$SU(3)_c \otimes SU(2)_L \otimes SU(2)_R \otimes U(1)_{B-L}$ Quantum Numbers			
V_μ	V_μ	1	1	1	0
$W_{L\mu}$	$W_{L\mu}^+, W_{L\mu}^-, W_{L\mu}^3$	1	3	1	0
$W_{R\mu}$	$W_{R\mu}^+, W_{R\mu}^-, W_{R\mu}^3$	1	1	3	0
G_μ^a	$G_\mu^1, G_\mu^2, \dots, G_\mu^8$	8	1	1	0

Table 6: Bosonic field content of the LRSM with their corresponding $SU(3)_c \otimes SU(2)_L \otimes SU(2)_R \otimes U(1)_{B-L}$ gauge quantum numbers.

While the SM contains one neutral Higgs boson only, most of the BSM predicts more than one Higgs doublet which means there will be at least one singly-charged Higgs boson. Recently, non-SM Higgs searches are taking place at CMS and ATLAS [130–132]. Discovery of a singly-charged Higgs boson, would raise the question which

fundamental gauge symmetry is responsible for its existence. Hence, the hope of clearer signal rests on more exotic Higgs bosons, such as the ones predicted in the LRSM where two triplets, which contain a doubly-charged, a singly-charged and a neutral Higgs components, are introduced. The doubly-charged Higgs fields, if light, would give distinctive and spectacular signals at the colliders. In Table 7 the Higgs content of the LRSM and their G_{LRSM} quantum numbers together with the corresponding parity transformations are summarized.

Chiral Field	Component Fields	$SU(3)_c \otimes SU(2)_L \otimes SU(2)_R \otimes U(1)_{B-L}$ Quantum Numbers				Parity Transformations
Φ	$\begin{pmatrix} \phi_1^+ & \phi_2^0 \\ \phi_1^0 & \phi_2^- \end{pmatrix}$	1	2	2	0	$\Phi \rightarrow \Phi^\dagger$
Δ	$\begin{pmatrix} \frac{\delta^+}{\sqrt{2}} & \delta^{++} \\ \delta^0 & -\frac{\delta^+}{\sqrt{2}} \end{pmatrix}$	1	3	1	2	$\Delta \rightarrow \Delta^{c*}$
Δ^c	$\begin{pmatrix} \frac{\delta^{c-}}{\sqrt{2}} & \delta^{c0} \\ \delta^{c--} & -\frac{\delta^{c-}}{\sqrt{2}} \end{pmatrix}$	1	1	3	-2	$\Delta^c \rightarrow \Delta^*$

Table 7: Higgs content of the minimal LRSM with their corresponding $SU(3)_c \otimes SU(2)_L \otimes SU(2)_R \otimes U(1)_{B-L}$ gauge quantum numbers and corresponding parity transformations.

We know that left-right symmetry is not an exact symmetry of nature. At low energy scales it has to be broken spontaneously. In the Subsection 3.1.3, the breakdown of the G_{LRSM} will be explained in more details. The Higgs fields which are required to break the underlying symmetry of the LRSM down to $U(1)_Q$ are not unique. The choice with one bi-doublet (Φ) and two triplets Δ and Δ^c is the most common. The latter field is responsible for the first stage of the symmetry breaking while giving masses to the right-chiral weak bosons, and the second stage is accomplished by the bi-doublet acquiring a VEV and giving masses to quarks and charged fermions as well as left-chiral weak bosons. The remaining triplet, Δ is introduced into the theory to maintain the left-right symmetry, does not have any significant role in the dynamics of the theory.

It is important to note that for convenience the representations of triplets in Table 7 are rewritten by 2×2 matrices (fundamental representation) instead of 1×3 (adjoint representation) so that we can use the fundamental representation of the covariant

derivative for all Higgs fields. The procedure is as follows. The adjoint representation of a triplet and its covariant derivative reads

$$\Delta_{\text{adj.rep.}} = \begin{pmatrix} \delta^1 \\ \delta^2 \\ \delta^3 \end{pmatrix}, \quad D_\mu \Delta_{\text{adj.rep.}} = (\partial_\mu - ig\epsilon^{ijk}W_\mu^j)\Delta_{\text{adj.rep.}}^k \quad (3.3)$$

By utilizing the following relation

$$\Delta_{\text{fun.rep.}} \rightarrow \sum_{i=1}^3 \frac{\sigma^i \Delta_{\text{adj.rep.}}^i}{\sqrt{2}}, \quad (3.4)$$

we rewrite them in fundamental representation as

$$\Delta_{\text{fun.rep.}} = \begin{pmatrix} \frac{\delta^+}{\sqrt{2}} & \delta^{++} \\ \delta^0 & -\frac{\delta^+}{\sqrt{2}} \end{pmatrix}, \quad (3.5)$$

where

$$\frac{\delta^1 + i\delta^2}{\sqrt{2}} = \delta^0, \quad \frac{\delta^1 - i\delta^2}{\sqrt{2}} = \delta^{++}, \quad \delta^3 = \delta^+. \quad (3.6)$$

The covariant derivative can be written as

$$D_\mu \Delta = \partial_\mu \Delta - i\frac{g}{2}(\sigma \cdot W)\Delta + i\frac{g}{2}\Delta(\sigma \cdot W). \quad (3.7)$$

3.1.2 The Left-Right Symmetric Model Lagrangian

The Lagrangian density of the LRSM is divided into four parts as follows

$$\mathcal{L}_{LRSM} = \mathcal{L}_F^{Kin} + \mathcal{L}_{GB}^{Kin} + \mathcal{L}_H + \mathcal{L}_Y. \quad (3.8)$$

The first piece of the Lagrangian accommodates the kinetic terms for the matter fields as well as the interactions of the matter fields with the gauge bosons.

$$\begin{aligned} \mathcal{L}_F^{Kin} &= \sum_{i,j=1}^3 \left(\bar{L}_i i\gamma^\mu \left[\partial_\mu - i\frac{g_L}{2}\sigma^j W_{L\mu}^j + i\frac{g_{B-L}}{2}V_\mu \right] L_i \right. \\ &\quad - \bar{L}_i^c i\gamma^\mu \left[\partial_\mu - i\frac{g_R}{2}\sigma^j W_{R\mu}^j + i\frac{g_{B-L}}{2}V_\mu \right] L_i^c \\ &\quad + \sum_{\alpha,\beta=1}^3 \sum_{a=1}^8 \left(\bar{Q}_i^\alpha i\gamma^\mu \left[\left\{ \partial_\mu - i\frac{g_L}{2}\sigma^j W_{L\mu}^j - i\frac{g_{B-L}}{6}V_\mu \right\} \delta_{\alpha\beta} - i\frac{g_s}{2}\lambda_{\alpha\beta a} G_\mu^a \right] Q_i^\beta \right. \\ &\quad \left. - \bar{Q}_i^{c\alpha} i\gamma^\mu \left[\left\{ \partial_\mu - i\frac{g_R}{2}\sigma^j W_{R\mu}^j - i\frac{g_{B-L}}{6}V_\mu \right\} \delta_{\alpha\beta} - i\frac{g_s}{2}\lambda_{\alpha\beta a} G_\mu^a \right] Q_i^{c\beta} \right) \right). \quad (3.9) \end{aligned}$$

The second part of the Lagrangian is devoted to gauge bosons. It contains kinetic and self interaction terms for the vector fields.

$$\mathcal{L}_{GB}^{Kin} = -\frac{1}{4}V^{\mu\nu}V_{\mu\nu} - \frac{1}{4}\sum_{i=1}^3 W_L^{\mu\nu i}W_{L\mu\nu}^i - \frac{1}{4}\sum_{i=1}^3 W_R^{\mu\nu i}W_{R\mu\nu}^i - \frac{1}{4}\sum_{a=1}^8 G^{\mu\nu a}G_{\mu\nu}^a, \quad (3.10)$$

where the field strength tensors are given by

$$\begin{aligned} V^{\mu\nu} &= \partial_\mu V_\nu - \partial_\nu V_\mu, \\ W_{L\mu\nu}^i &= \partial_\mu W_{L\nu}^i - \partial_\nu W_{L\mu}^i - g_L \epsilon^{ijk} W_{L\mu}^j W_{L\nu}^k, \quad i, j, k = 1, \dots, 3, \\ W_{R\mu\nu}^i &= \partial_\mu W_{R\nu}^i - \partial_\nu W_{R\mu}^i - g_R \epsilon^{ijk} W_{R\mu}^j W_{R\nu}^k, \quad i, j, k = 1, \dots, 3, \\ G_{\mu\nu}^a &= \partial_\mu G_\nu^a - \partial_\nu G_\mu^a - g_s f^{abc} G_\mu^b G_\nu^c, \quad a, b, c = 1, \dots, 8. \end{aligned} \quad (3.11)$$

The gauge invariant kinetic term for the Higgs multiplets is

$$\mathcal{L}_H = \sum_i \text{Tr} \left[(D^\mu H_i)^\dagger D_\mu H_i \right] - V_H, \quad (3.12)$$

where $H_i = \Phi, \Delta$ and Δ^c , and the covariant derivatives for each multiplet reads

$$D_\mu \Phi = \partial_\mu \Phi - i\frac{g_L}{2}(\sigma \cdot W_{L\mu})i\sigma_2\Phi + i\frac{g_R}{2}i\sigma_2\Phi(\sigma \cdot W_{R\mu}), \quad (3.13)$$

$$D_\mu \Delta = \partial_\mu \Delta - i\frac{g_L}{2}(\sigma \cdot W_{L\mu})\Delta + i\frac{g_L}{2}\Delta(\sigma \cdot W_{L\mu}) - ig_{B-L}V_\mu\Delta, \quad (3.14)$$

$$D_\mu \Delta^c = \partial_\mu \Delta^c - i\frac{g_R}{2}(\sigma \cdot W_{R\mu})\Delta^c + i\frac{g_R}{2}\Delta^c(\sigma \cdot W_{R\mu}) - ig_{B-L}V_\mu\Delta^c. \quad (3.15)$$

Finally, the Yukawa Lagrangian in LRSM reads

$$\begin{aligned} \mathcal{L}_Y &= \sum_{i,j=1}^3 \left(y_{ij}^Q Q_i^T \sigma_2 \Phi \sigma_2 Q_j^c + \tilde{y}_{ij}^Q Q_i^T \sigma_2 \tilde{\Phi} \sigma_2 Q_j^c + y_{ij}^L L_i^T \sigma_2 \Phi \sigma_2 L_j^c \right. \\ &\quad \left. + \tilde{y}_{ij}^L L_i^T \sigma_2 \tilde{\Phi} \sigma_2 L_j^c + f_{ij} (L_i^T i\sigma_2 \Delta L_j + L_i^{cT} i\sigma_2 \Delta^c L_j) + \text{h.c.} \right), \end{aligned} \quad (3.16)$$

where $\tilde{\Phi}$ is the conjugated Higgs bi-doublet given by

$$\tilde{\Phi} = \sigma_2 \Phi^* \sigma_2 = \begin{pmatrix} \Phi_2^0 & -\Phi_2^+ \\ -\Phi_1^- & \Phi_1^0 \end{pmatrix}. \quad (3.17)$$

3.1.3 Higgs Mechanism in the Left-Right Symmetric Model

In LRSM the SSB via Higgs mechanism arises in two steps. At the first step right-chiral triplet develops a VEV

$$\langle \Delta^c \rangle = \begin{pmatrix} 0 & v_R \\ 0 & 0 \end{pmatrix}, \quad (3.18)$$

and breaks the left-right symmetry as

$$SU(3)_c \otimes SU(2)_R \otimes SU(2)_L \otimes U(1)_{B-L} \rightarrow SU(3)_c \otimes SU(2)_L \otimes U(1)_Y. \quad (3.19)$$

The kinetic energy term of the right-chiral triplet then becomes

$$\text{Tr} \left[(D^\mu \Delta^c)^\dagger D_\mu \Delta^c \right] = g_R^2 v_R^2 W_R^{\mu+} W_{R\mu}^- + v_R^2 \left(g_R W_R^{\mu 3} - g_{B-L} V^\mu \right)^2, \quad (3.20)$$

where $W_{R\mu}^\pm = \frac{1}{\sqrt{2}}(W_{R\mu}^1 \mp W_{R\mu}^2)$. By applying the orthogonal transformation

$$\begin{pmatrix} Z_{R\mu} \\ B_\mu \end{pmatrix} = \begin{pmatrix} \cos \varphi & -\sin \varphi \\ \sin \varphi & \cos \varphi \end{pmatrix} \begin{pmatrix} W_{R\mu}^3 \\ V_\mu \end{pmatrix}, \quad (3.21)$$

to the gauge eigenstates we obtain the physical massive right-chiral neutral gauge boson ($Z_{R\mu}$) and the massless hypercharge field (B_μ) where

$$M_{Z_R} = v_R \sqrt{2(g_R^2 + g_{B-L}^2)}. \quad (3.22)$$

The physical field $Z_{R\mu}$ decouples from further breakdown process. The mixing angle φ is given by

$$\cos \varphi = \frac{g_R}{\sqrt{g_R^2 + g_{B-L}^2}}, \quad \sin \varphi = \frac{g_{B-L}}{\sqrt{g_R^2 + g_{B-L}^2}}. \quad (3.23)$$

The following stage of the symmetry breaking is as follows

$$SU(3)_c \otimes SU(2)_L \otimes U(1)_Y \rightarrow SU(3)_c \otimes U(1)_Q, \quad (3.24)$$

where the bi-doublet Φ and possibly but not necessarily the left-chiral triplet Δ get VEVs which are

$$\langle \Delta \rangle = \begin{pmatrix} 0 & 0 \\ v_L & 0 \end{pmatrix}, \quad \langle \Phi \rangle = \begin{pmatrix} 0 & v_u \\ v_d & 0 \end{pmatrix}, \quad (3.25)$$

and the value $\sqrt{v_u^2 + v_d^2} = v \equiv 174$ GeV. The kinetic term for the left-chiral triplet Δ is

$$\text{Tr} \left[(D^\mu \Delta)^\dagger D_\mu \Delta \right] = g_L^2 v_L^2 W_L^{\mu+} W_{L\mu}^- + v_L^2 \left(g_L W_L^{\mu 3} - g_{B-L} \cos \varphi B_\mu \right)^2, \quad (3.26)$$

and for the bi-doublet we have

$$\begin{aligned} \text{Tr}[(D^\mu \Phi)^\dagger (D_\mu \Phi)] &= \frac{v^2}{4} \left(g_L W_L^{\mu 3} - g_R \sin \varphi B^\mu \right)^2 + \frac{v^2}{2} (g_L^2 W_L^{\mu+} W_{L\mu}^- + g_R^2 W_R^{\mu+} W_{R\mu}^-) \\ &+ g_L g_R v_u v_d (W_L^{\mu+} W_{R\mu}^- + W_R^{\mu+} W_{L\mu}^-), \end{aligned} \quad (3.27)$$

where $W_{L\mu}^\pm = \frac{1}{\sqrt{2}}(W_{L\mu}^1 \mp iW_{L\mu}^2)$ and the compositions of physical gauge bosons at this stage are

$$\begin{pmatrix} Z_{L\mu} \\ A_\mu \end{pmatrix} = \begin{pmatrix} \cos \theta_W & -\sin \theta_W \\ \sin \theta_W & \cos \theta_W \end{pmatrix} \begin{pmatrix} W_{L\mu}^3 \\ B_\mu \end{pmatrix}. \quad (3.28)$$

Here the Weinberg mixing angle is defined as

$$\cos \theta_W = \frac{g_L}{\sqrt{g_L^2 + g_Y^2}}, \quad \sin \theta_W = \frac{g_Y}{\sqrt{g_L^2 + g_Y^2}}, \quad g_Y = \frac{g_R g_{B-L}}{\sqrt{g_R^2 + g_{B-L}^2}}, \quad (3.29)$$

and g_Y is the hypercharge coupling constant. The masses

$$M_{Z_L} = v \sqrt{\frac{g_L^2 + g_Y^2}{2}}, \quad M_A = 0. \quad (3.30)$$

It is apparent from eq. (3.27) that the gauge bosons W_R^\pm and W_L^\pm states are mixed. This is due to the bi-doublet Φ transforming non-trivially under both $SU(2)_L$ and $SU(2)_R$. One can easily write the mass-squared matrix in the basis $\{W_{L\mu}^\pm, W_{R\mu}^\pm\}$ in the following manner

$$M_{W_{L,R}^\pm}^2 = \begin{pmatrix} M_L^2 & M_{LR}^2 \\ M_{LR}^2 & M_R^2 \end{pmatrix} = \frac{1}{2} \begin{pmatrix} g_L^2 (2v_L^2 + v^2) & 2g_L g_R v_u v_d \\ 2g_L g_R v_u v_d & g_R^2 (2v_R^2 + v^2) \end{pmatrix}, \quad (3.31)$$

The mass eigenstates W_1^\pm and W_2^\pm will emerge after applying the following orthogonal transformation on physical W gauge bosons

$$\begin{pmatrix} W_{1\mu}^\pm \\ W_{2\mu}^\pm \end{pmatrix} = \begin{pmatrix} \cos \xi & e^{-i\omega} \sin \xi \\ -\sin \xi & e^{-i\omega} \cos \xi \end{pmatrix} \begin{pmatrix} W_{L\mu}^\pm \\ W_{R\mu}^\pm \end{pmatrix}. \quad (3.32)$$

Here ξ is a mixing angle which is severely bounded ($\xi < 10^{-3}$) [133] and ω is a phase. The mixing angle is defined by

$$\tan 2\xi = \frac{2M_{LR}^2}{M_L^2 - M_R^2} = \frac{4g_R g_L v_u v_d}{g_L^2 (v^2 + 2v_L^2) + g_R^2 (v^2 + 2v_R^2)}, \quad (3.33)$$

In the limit $v_L \rightarrow 0$ we get

$$\begin{aligned} M_{W_1}^2 &= \frac{g_L^2}{2} \left[v^2 \cos^2 \xi - 2 \frac{g_R}{g_L} v_u v_d \sin 2\xi + \frac{g_R^2}{g_L^2} (2v_R^2 + v^2) \sin^2 \xi \right], \\ M_{W_2}^2 &= \frac{g_L^2}{2} \left[v^2 \sin^2 \xi + 2 \frac{g_R}{g_L} v_u v_d \sin 2\xi + \frac{g_R^2}{g_L^2} (2v_R^2 + v^2) \cos^2 \xi \right]. \end{aligned} \quad (3.34)$$

Notice that when there is no mixing ($\xi \rightarrow 0$) the mass eigenstates will be exactly $M_{W_1} = M_{W_L}$ and $M_{W_2} = M_{W_R}$.

$$M_{W_L} = v \frac{g_L}{\sqrt{2}}, \quad M_{W_R} = v_R g_R. \quad (3.35)$$

The relation between the masses of W and Z bosons are

$$\frac{M_{W_L}}{M_{Z_L}} = \frac{g_L}{\sqrt{g_L^2 + g_Y^2}} = \cos \theta_W, \quad \frac{M_{W_R}}{M_{Z_R}} = \frac{g_R}{\sqrt{2(g_R^2 + g_{B-L}^2)}} = \frac{\cos \varphi}{\sqrt{2}}. \quad (3.36)$$

The fermion masses are generated through the Yukawa Lagrangian given in eq. (3.16) when the Higgs fields acquire VEVs as in eqs. (3.18) and (3.25). The Dirac fermions receive their masses by coupling to Φ and $\tilde{\Phi}$ bi-doublets which give rise to the following Dirac mass matrices for leptons and quarks

$$\begin{aligned} M_\nu &= y_{ij}^L v_u + \tilde{y}_{ij}^L v_d, & M_e &= y_{ij}^L v_d + \tilde{y}_{ij}^L v_u, \\ M_u &= (y_{ij}^Q v_u + \tilde{y}_{ij}^Q v_d), & M_d &= (y_{ij}^Q v_d + \tilde{y}_{ij}^Q v_u). \end{aligned} \quad (3.37)$$

The left-chiral triplet Δ (the right-chiral triplet Δ^c), on the other hand, only couple to left-handed neutrinos generating light Majorana masses corresponding to the three known neutrino flavors (right-handed neutrinos generating heavy Majorana masses which has yet to be discovered). The mechanism to explain the relative sizes of observed neutrino masses is called the see-saw mechanism and happens through mixing

$$M_\nu \sim \begin{pmatrix} 0 & M_D \\ M_D^\dagger & M_M \end{pmatrix}, \quad (3.38)$$

where M_M is much more higher than M_D . The eigen states are $m_{\nu_1} \sim -M_D^2/M_M$ and $m_{\nu_2} \sim M_M$ [19, 44].

3.2 The Supersymmetric Standard Model

Supersymmetry is a hypothetical symmetry and very different from those we have encountered so far. It is a symmetry that relates bosonic and fermionic degrees of freedoms of particles. Originally, the idea of an existing symmetry between bosons and fermions has been introduced in two-dimensional string theory [134–136]. Afterward, in 1974, a four-dimensional field theory, SUSY, was constructed by Wess and Zumino

[20,21]. What is remarkable about SUSY is that it enlightens the gauge problem of the SM by leading a coupling constant unification. Simple GUT predict that the gauge couplings, when properly normalized, should all be equal at the GUT scale. Since the dependence of the gauge couplings on the energy is very mild logarithmically, the energy scale where the unification occurs is quite high, as can be seen in Figure 5. Unification can be tested via the observed gauge couplings at the Z -boson mass scale. At one loop one has

$$\frac{1}{\alpha_i(Q^2)} = \frac{1}{\alpha_i(M_Z^2)} - 4\pi b_i \ln \frac{Q^2}{M_Z^2}, \quad (3.39)$$

where

$$\begin{pmatrix} b_1 \\ b_2 \\ b_3 \end{pmatrix} = \frac{1}{16\pi^2} \begin{pmatrix} 41/10 \\ -19/6 \\ -7 \end{pmatrix}_{\text{SM}} \quad \text{or} \quad \frac{1}{16\pi^2} \begin{pmatrix} 33/5 \\ 1 \\ -3 \end{pmatrix}_{\text{MSSM}}. \quad (3.40)$$

As can be seen from the Figure 5, the couplings do not unify at a single point when extrapolated assuming SM, but do meet at around 10^{16} GeV when the supersymmetric partners contribution are taken into account.

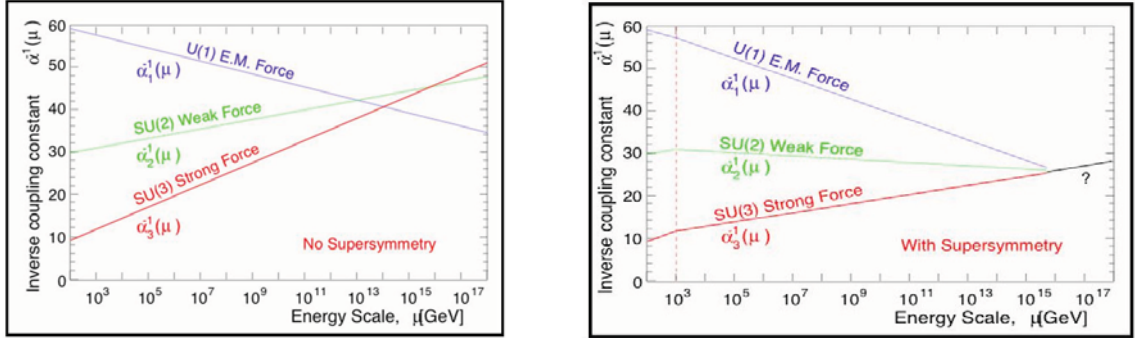


Figure 5: Extrapolation of the gauge couplings in the SM (on the left), in SUSY (on the right).

Another motivation to study SUSY is that it offers a solution to the SM Higgs hierarchy problem in a most ingenious manner. As discussed before the Higgs boson receives a non-vanishing VEV when the Higgs potential term in the SM Lagrangian is minimized. The experimental value for the VEV of Higgs is $v \sim 174$ GeV. Based on the measurements of the properties of the weak interactions, the Higgs mass is expected to be $m_h \sim 100$ GeV. However, it receives quadratically divergent

contributions from the one-loop diagrams shown in Figure 6 left panel. The radiative correction due to top quark will be

$$-i(\Delta m_h^2) = -N_c(-ih_t)^2 \int \frac{d^4k}{(2\pi)^4} \text{Tr} \left(\frac{i}{\not{k} - m_t} \frac{i}{\not{k} - m_t} \right) \sim i \frac{N_c h_t^2}{4\pi^2} \Lambda^2, \quad (3.41)$$

where -1 is because it is a closed fermion loop, $N_c = 3$ counts for the color charge of quarks, $h_t = gm_t/2M_W$ is the vertex factor and Λ is the ultraviolet momentum cut-off used to regulate the loop integral (energy scale at which new physics enters to alter the high-energy behavior of the theory).

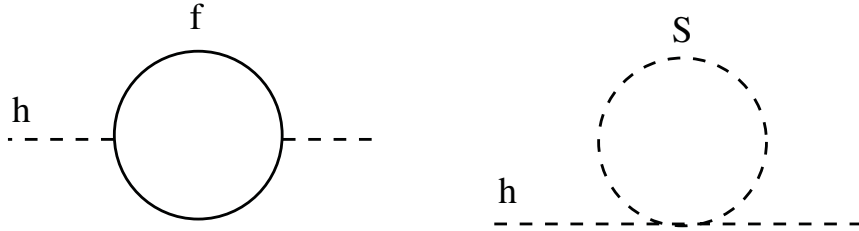


Figure 6: One loop correction to Higgs mass square (m_h^2) due to fermion (f) loop on the left and a scalar (S) on the right.

In SUSY, on the other hand, for every fermionic particle, there is a corresponding bosonic superpartner. Therefore, there will be additional contributions to the Higgs mass coming from superpartners as shown in Figure 6 right panel. It will couple to the Higgs Lagrangian with a term $-\lambda_S H^2 S^2$ which yields a correction

$$-i(\Delta m_h^2) = -2i\lambda_S N_c \int \frac{d^4k}{(2\pi)^4} \frac{i}{k^2 - m_S^2} \sim -i \frac{\lambda_S N_c}{8\pi^2} \Lambda^2, \quad (3.42)$$

If each fermion in the SM is accompanied by two complex scalars with $h_t^2 = \lambda_S$ there is a systematic cancellation between those of the divergences coming from a fermion loop and those of the loop containing its bosonic superpartner, since there is a relative minus sign between them. Unfortunately, the exact cancellation implies that, mass values of superpartners of the each existing particle have to be the same as the corresponding SM particle. Clearly, the SM particles are not degenerate with their superpartners, otherwise they would have been observed by now. Therefore, SUSY cannot be an exact symmetry of nature, and it must be broken. Broken SUSY still provides a solution to the hierarchy problem. Even in the presence of SUSY breaking,

if we consider “soft” SUSY breaking, which is an explicit symmetry breaking, containing only mass terms and coupling parameters with positive mass dimension, the mass splittings between the known SM particles and their superpartners will be determined by the mass scale, and keeping it as small, we will not lose the successful cure for the hierarchy problem. However, general soft breaking terms introduce large number of free parameters. Another motivation for SUSY is, in the case of local supersymmetric gauge invariance of a theory, we must introduce new fields and that will automatically reproduce Einstein’s general relativity, and the resulting theory called supergravity. Moreover, the lightest supersymmetric partner that does not decay and has the right mass and right interactions might also be a dark matter candidate.

3.2.1 Elementary Particles in the Supersymmetric Standard Model

Supersymmetry is elegant in its principles but not economical when it comes to its particle content. It actually requires more than doubling the SM spectrum. In SUSY, each SM particle is assigned a superpartner differing in spin by $1/2$ unit and its Higgs sector is extended. By virtue of the phenomenological reasons, none of the SM bosons or fermions can be partners of each other. The name tagging to differentiate the superparticles from their SM reciprocates is done as follows: The spin-0 superpartners of fermions are prepended with an *s*, (for example the superpartner of electron is named as “*selectron*”), and they are indicated by a tilde on the top of the corresponding fermionic representation. The fermionic (spin $1/2$) superpartner of a bosonic particle, on the other hand, is appended with an *ino* in the end, (for example the superpartner of *W* is named as “*Wino*”) and they are not indicated by tilde on the top of the corresponding bosonic representation, but have different symbols instead. Extensions to supergravity also predict a spin- $3/2$ partner of the graviton(*g*), the gravitino ($g_{3/2}$). In Table 8, the field contents, associated gauge quantum numbers and spin quantum numbers for quarks, leptons and their superpartners are summarized.

Chiral Field	Component Fields	SU(3) _c ⊗ SU(2) _L ⊗ U(1) _Y Quantum Numbers			Spin
Q_1^α	$\begin{pmatrix} u^\alpha \\ d^\alpha \end{pmatrix}$	3	2	$\frac{1}{3}$	1/2
$U_1^{c\alpha}$ $D_1^{c\alpha}$	$u^{c\alpha}$ $d^{c\alpha}$	3* 3*	1 1	$\frac{4}{3}$ $-\frac{2}{3}$	1/2
\tilde{Q}_1^α	$\begin{pmatrix} \tilde{u}^\alpha \\ \tilde{d}^\alpha \end{pmatrix}$	3	2	$\frac{1}{3}$	0
$\tilde{U}_1^{c\alpha}$ $\tilde{D}_1^{c\alpha}$	$\tilde{u}^{c\alpha}$ $\tilde{d}^{c\alpha}$	3* 3*	1 1	$\frac{4}{3}$ $-\frac{2}{3}$	0
L_1	$\begin{pmatrix} \nu_e \\ e \end{pmatrix}$	1	2	-1	1/2
E_1^c	e^c	1	2	-2	1/2
\tilde{L}_1	$\begin{pmatrix} \tilde{\nu}_e \\ \tilde{e} \end{pmatrix}$	1	2	-1	0
\tilde{E}_1^c	\tilde{e}^c	1	1	-2	0

Table 8: First generation of fermions in the SUSY including the corresponding $SU(3)_c \otimes SU(2)_L \otimes U(1)_Y$ gauge and spin quantum numbers together.

Note that the color charge of quarks are indicated by a superscript (α). The sparticles carry the same gauge quantum numbers as their corresponding SM partners. As, supersymmetry must be broken the squarks and sleptons are relatively heavy.

Some properties of gauge bosons and their spin-1/2 gaugino partners are summarized in Table 9 and Table 10 lists the Higgs contents and their superpartners, higgsinos. The higgsinos can mix with winos and bino to produce two mass eigenstate Dirac charginos and four mass eigenstate neutralinos (we will not go into the details of this discussion in this thesis). Also the lightest neutral Higgs boson acts very much like the SM Higgs in the decoupling limit.

Chiral Field	Component Fields	SU(3) _c ⊗ SU(2) _L ⊗ U(1) _{B-L} Quantum Numbers			Spin
B_μ	B_μ	1	1	0	1
$W_{L\mu}$	$W_{L\mu}^+, W_{L\mu}^-, W_{L\mu}^3$	1	3	0	1
G_μ^a	$G_\mu^1, G_\mu^2, \dots, G_\mu^8$	8	1	0	1
$\lambda_{B\mu}$	$\lambda_{B\mu}$	1	1	0	1/2
$\lambda_{L\mu}$	$\lambda_{L\mu}^+, \lambda_{L\mu}^-, \lambda_{L\mu}^3$	1	3	0	1/2
$\lambda_{G\mu}^a$	$\lambda_{G\mu}^1, \lambda_{G\mu}^2, \dots, \lambda_{G\mu}^8$	8	1	0	1/2

Table 9: Gauge Boson content of the SUSY with their corresponding $SU(3)_c \otimes SU(2)_L \otimes U(1)_Y$ gauge and spin quantum numbers.

Chiral Field	Component Fields	SU(3) _c ⊗ SU(2) _L ⊗ U(1) _Y Quantum Numbers			Spin
Φ_d	$\begin{pmatrix} \phi_d^+ \\ \phi_d^0 \end{pmatrix}$	1	2	1	0
Φ_u	$\begin{pmatrix} \phi_u^0 \\ \phi_u^- \end{pmatrix}$	1	2	-1	0
$\tilde{\Phi}_d$	$\begin{pmatrix} \tilde{\phi}_d^+ \\ \tilde{\phi}_d^0 \end{pmatrix}$	1	2	1	1/2
$\tilde{\Phi}_u$	$\begin{pmatrix} \tilde{\phi}_u^0 \\ \tilde{\phi}_u^- \end{pmatrix}$	1	2	-1	1/2

Table 10: Higgs Boson content of the SUSY with their corresponding $SU(3)_c \otimes SU(2)_L \otimes U(1)_Y$ gauge and spin quantum numbers.

In the SM a single Higgs doublet generates masses for both up- and down-type quarks by making use of the conjugate $\tilde{\phi} = i\sigma^2\phi^\dagger$ (this tilde does not represent superpartner). However, SUSY requires more than one Higgs doublet. One reason for this is that if there is only one Higgs doublet, the fermionic superpartner of which will make

nonzero contribution to the traces $\text{Tr}[I_w^3 Y]$ and $\text{Tr}[Y]$, as it carries $Y = \pm 1$ alone, and therefore spoil the anomaly cancellation. This can be avoided if there exist two Higgs doublet with opposite weak hypercharges. Therefore, SUSY does not allow the $\tilde{\phi}$ Yukawa couplings, one needs an extended Higgs sector. In the decoupling limit, the superpartners and the extra Higgs fields are all heavier than the electroweak scale and their contributions to electroweak precision is small, thus giving an excellent agreement with the SM.

3.2.2 The Supersymmetric Lagrangians

In this Subsection we describe the construction of the SUSY Lagrangian by considering a relatively simple supersymmetric model, which embodies a free massless left-chiral Weyl spinor, χ and its superpartner, a free massless complex scalar field, ϕ . A supersymmetry transformation turns a bosonic state into a fermionic one, and vice versa. Let the generator of such transformation be Q , which must be an anticommuting spinor, when applied to fermionic or bosonic states will result in

$$Q|\text{Boson}\rangle = |\text{Fermion}\rangle, \quad Q|\text{Fermion}\rangle = |\text{Boson}\rangle. \quad (3.43)$$

The hermition conjugate of Q is also a symmetry generator. Since they are spinors, they carry spin-1/2 and satisfy the following relations

$$\{Q, Q^\dagger\} = P^\mu, \quad \{Q, Q\} = \{Q^\dagger, Q^\dagger\} = 0, \quad [P^\mu, Q] = [P^\mu, Q^\dagger] = 0, \quad (3.44)$$

where P^μ is the generator of four-momentum translations.

As mentioned before, SUSY requires the number of bosonic and fermionic degrees of freedom to be equal. A Weyl spinor has two complex components, thus, has four degrees of freedom when it is off-shell. On-shell, the equation of motion imposes two constraints, leaving only two degrees of freedom. On the other hand, a complex scalar field has two degrees of freedom. Therefore, on-shell the bosonic and fermionic degrees of freedom are equal, but off-shell they do not match. This makes SUSY algebra closed on-shell but not off-shell. To overcome this problem, we need to add an auxiliary field, F , which is a field with no on-shell degrees of freedom. This could be achieved by setting the equation of motion for this field to be $F = F^\dagger = 0$. The simplest real term we can add in the Lagrangian satisfying this equation of motion is FF^\dagger . So the Lagrangian will be:

$$\mathcal{L}_{\text{free}} = \partial_\mu \phi \partial^\mu \phi^\dagger + \chi^\dagger i \bar{\sigma}^\mu \partial_\mu \chi + FF^\dagger, \quad (3.45)$$

which is invariant up to a total derivative under the following SUSY transformations

$$\begin{aligned}
\delta\phi &= \zeta \cdot \chi, \\
\delta\chi &= -i\sigma^\mu(i\sigma^2\zeta^*)\partial_\mu\phi + F\zeta, \\
\delta F &= -i\zeta^\dagger\bar{\sigma}^\mu\partial_\mu\chi,
\end{aligned}
\tag{3.46}$$

where ζ , being a left-chiral spinor, is the infinitesimal SUSY parameter. It is important to note that we take ζ to be space-time independent; i.e., $\partial_\mu\zeta = 0$. In other words, we are considering global SUSY transformations. The inclusion of the auxiliary field makes the SUSY algebra closed off-shell. One can easily prove that the commutator of two SUSY transformations for all three fields, ϕ , χ , and F will be the same without recourse to any equation of motion such that

$$\delta_\beta\delta_\zeta X - \delta_\zeta\delta_\beta X = -i(\zeta^\dagger\bar{\sigma}^\mu\beta - \beta^\dagger\bar{\sigma}^\mu\zeta)\partial_\mu X,
\tag{3.47}$$

where X stands for any of the three fields ϕ , χ , or F .

Now we include masses and interactions that will preserve SUSY. We must make sure that all the terms added lead to a renormalizable theory, Lorentz invariant, invariant under SUSY transformations given in Eq. (3.46), and finally, satisfy the condition $\mathcal{L}^\dagger = \mathcal{L}$. Call these additional terms as \mathcal{L}_{int}

$$\mathcal{L}_{\text{int}} = \mathcal{G} + W_1 F + W_1^\dagger F^\dagger - \frac{1}{2}W_{11} \chi \cdot \chi - \frac{1}{2}W_{11}^\dagger \bar{\chi} \cdot \bar{\chi},
\tag{3.48}$$

where \mathcal{G} , W_1 , and W_{11} are functions of ϕ and ϕ^\dagger . Applying SUSY transformations given in Eq. (3.46), we get, $\mathcal{G} = 0$, W_1 and W_{11} to be holomorphic in ϕ , and $W_{11} = \frac{\partial W_1}{\partial \phi}$. The most general form for W_1 is therefore,

$$W_1(\phi) = m\phi + \frac{1}{2}y\phi^2 + C,
\tag{3.49}$$

with $[m] = 1$, $[y] = 0$. It is convenient to introduce a superpotential \mathcal{W} such that

$$W_1 = \frac{\partial \mathcal{W}}{\partial \phi},
\tag{3.50}$$

where \mathcal{W} is

$$\mathcal{W} = \frac{1}{2}m\phi^2 + \frac{1}{6}y\phi^3 + C\phi + f(\phi^\dagger).
\tag{3.51}$$

In terms of superpotential, the interaction Lagrangian is given by

$$\mathcal{L}_{\text{int}} = \frac{\partial \mathcal{W}}{\partial \phi} F - \frac{1}{2} \frac{\partial^2 \mathcal{W}}{\partial \phi^2} \chi \cdot \chi + \text{h.c.},
\tag{3.52}$$

The obvious generalization of this Lagrangian to a set of n copies of fields reads

$$\mathcal{L}_{\text{int}} = \frac{\partial \mathcal{W}}{\partial \phi_i} F_i - \frac{1}{2} \frac{\partial^2 \mathcal{W}}{\partial \phi_i \partial \phi_j} \chi_i \cdot \chi_j + \text{h.c.}, \quad (3.53)$$

where there is a sum over i and j . Since we now know that the free Lagrangian given in eq. (3.45) is invariant under supersymmetry transformations, we consider now the change in the interaction Lagrangian. The part involving the for spinors reads,

$$- \frac{1}{2} \frac{\partial \mathcal{W}_{ij}}{\partial \phi_k} (\zeta \cdot \chi_k) (\chi_i \cdot \chi_j) - \frac{1}{2} \frac{\partial \mathcal{W}_{ij}}{\partial \phi_k^\dagger} (\zeta^\dagger \cdot \bar{\chi}_k) (\chi_i \cdot \chi_j) + \text{h.c.} \quad (3.54)$$

Neither of these terms can be canceled by the variation of the any other term. However the first term will vanish assuming

$$\frac{\partial \mathcal{W}_{ij}}{\partial \phi_k} \text{ is symmetric in } i, j, \text{ and } k. \quad (3.55)$$

There is an important identity involving products of three spinors

$$(\zeta \cdot \chi_k) (\chi_i \cdot \chi_j) + (\zeta \cdot \chi_i) (\chi_j \cdot \chi_k) + (\zeta \cdot \chi_j) (\chi_k \cdot \chi_i), \quad (3.56)$$

from which it follows that if the condition in eq. (3.55) is true, then the first term in eq. (3.54) will vanish identically. However, there is no corresponding identity for the second term of eq. (3.54). The only way to get rid of this term is to say W_{ij} cannot depend on ϕ_k^\dagger . This is an additional reason for why SUSY requires more than one Higgs doublet to the one given in Subsection 3.2.1. Bearing in mind the symmetry properties the potential term is

$$\mathcal{W} = \frac{1}{2} m_{ij} \phi_i \phi_j + \frac{1}{6} y_{ijk} \phi_i \phi_j \phi_k + c_i \phi_i, \quad (3.57)$$

and $i, j = 1, \dots, n$. Finally, using the equation of motion for the auxiliary field $F^\dagger = F = 0$, we get

$$F_i^\dagger = -W_i = -\frac{\partial \mathcal{W}}{\partial \phi_i}, \quad (3.58)$$

and

$$F_i = -W_i^\dagger = -\left(\frac{\partial \mathcal{W}}{\partial \phi_i}\right)^\dagger. \quad (3.59)$$

Then the whole Lagrangian becomes

$$\begin{aligned} \mathcal{L} = & \partial_\mu \phi_i^\dagger \partial^\mu \phi_i + \chi_i^\dagger i \bar{\sigma}^\mu \partial_\mu \chi_i - \left| m_{ij} \phi_j + \frac{1}{2} y_{ijk} \phi_j \phi_k + c_i \right|^2 \\ & - \frac{1}{2} (m_{ij} \chi_i \cdot \chi_j + y_{ijk} \phi_k \chi_i \cdot \chi_j + \text{h.c.}), \end{aligned} \quad (3.60)$$

which is called Wess-Zumino Lagrangian [20, 21], with the last two terms called the F terms

$$V_F = \left| m_{ij}\phi_j + \frac{1}{2}y_{ijk}\phi_j\phi_k + c_i \right|^2 - \frac{1}{2}(m_{ij}\chi_i \cdot \chi_j + y_{ijk}\phi_k\chi_i \cdot \chi_j + \text{h.c.}), \quad (3.61)$$

The gauge sector of SUSY Lagrangian contains a massless gauge boson field A_μ^a , its superpartner gaugino λ^a , which is a left chiral Weyl spinor, and an auxiliary scalar field D^a in order to make SUSY algebra closed off-shell.

$$\mathcal{L} = -\frac{1}{4}F_{\mu\nu}^a F^{\mu\nu a} + i\lambda^{a\dagger}\bar{\sigma}^\mu D_\mu\lambda^a + \frac{1}{2}D^a D^a. \quad (3.62)$$

Note that the index $a = 1, \dots, 8$ for $SU(3)_c$, $a = 1, 2, 3$ for $SU(2)_L$, and $a = 1$ for $U(1)_Y$. The SUSY transformations are

$$\begin{aligned} \delta\lambda &= \frac{i}{2}\sigma^\mu\bar{\sigma}^\nu\zeta F_{\mu\nu} + \zeta D, \\ \delta D &= -i\zeta^\dagger\bar{\sigma}^\mu D_\mu\lambda + i(D_\mu\lambda)^\dagger\bar{\sigma}^\mu\zeta, \\ \delta A_\mu &= \zeta^\dagger\bar{\sigma}^\mu\lambda + \lambda^\dagger\bar{\sigma}^\mu\zeta. \end{aligned} \quad (3.63)$$

In the same way as we obtained F terms of the potential, D terms can be obtained as

$$V_D = \frac{g^2}{2}(\phi_i^\dagger T^a \phi_i)(\phi_j^\dagger T^a \phi_j), \quad (3.64)$$

where T_a are the group generators.

A realistic phenomenological model must contain breaking of SUSY. It could be broken spontaneously, or explicitly. However, spontaneous SUSY breaking would force extending the minimal model by adding new particles and interactions at very high scales, and there is no consensus on exactly how this should be done. This is why we consider explicitly breaking SUSY. The SUSY breaking couplings should be soft (of positive mass dimension) to maintain naturally a hierarchy between the EW scale and Plank scale. The possible soft symmetry breaking terms are

$$\begin{aligned} \mathcal{L}'_{\text{soft}} &= -\left(\frac{1}{2}M_a\lambda_a\lambda_a + \frac{1}{6}a_{ijk}\phi_i\phi_j\phi_k + \frac{1}{2}b_{ij}\phi_i\phi_j + t_i\phi_i \right) + \text{h.c.} - m_{ij}^2\phi_i\phi_j^\dagger, \\ \mathcal{L}'_{\text{soft}} &= -\frac{1}{2}c_{ijk}\phi_i^\dagger\phi_j\phi_k + \text{h.c.}, \end{aligned} \quad (3.65)$$

where M_a are gaugino masses for each gauge group, m_{ij} and b_{ij} are scalar squared mass terms, a_{ijk} and c_{ijk} are (scalar)³ couplings, and t_i are tadpole couplings.

Many supersymmetric models introduces a discrete R-parity symmetry [45] which requires that every allowed interaction vertex involves an even number of superpartners. It is given by

$$R = (-1)^{3(B-L)+2S}, \quad (3.66)$$

where S corresponds to the spin quantum number of the particle. The conservation of R-parity ensures that the SUSY partners with $R = -1$ to be produced in pairs and this implies the lightest supersymmetric particle to be absolutely stable, and therefore candidate for dark matter. Neutralinos are the most promising possibility, although scalar neutrinos or the gravitino cannot be excluded.

3.3 The Four-Generation Standard Model

The experimentally observed twelve building blocks of Nature (as summarized in Section 2.1), known as fermions, are successfully described in the SM with three fermion generations. In fact, the first family of fermions is all that is needed to form the ordinary matter that we experience in everyday life. However, it turns out that there are second and third generations of fermions with identical charges as the first generation but larger masses and tendency to decay into particles of lower generations. Presently, the reason for the existence of two other generations is unknown but the presence of minimum three generations of fermions was predicted theoretically by Kobayashi and Maskawa [137] to accommodate the observed CP violation in Weak interactions [138]. The discoveries of the charm [139], bottom [140, 141] and top [119, 120] quarks together with the τ -neutrino in the following years then provided the proof for the existence of three generations. However, there is no definite theoretical reasoning restricting the number of fermion generations to be equal to three as in the SM. Because the existence of the other generations is neither predicted nor disallowed by the SM, we should keep an open mind regarding more generations. The simplest extension will be the Four-Generation Standard Model [28, 29] as it obeys all the symmetries of the SM and does not introduce new ones. In the Introduction, we outlined some of the attractive features of the model. We present here an introduction to the model.

The additional family of fermions will be considered as a heavier replica of the

other three generations existing in the SM. In chiral representation they are given by

$$\begin{aligned} Q_{4,L} &= \begin{pmatrix} t'_L \\ b'_L \end{pmatrix}, & U_{4,R} &= t'_R, & D_{4,R} &= b'_R, \\ L_{4,L} &= \begin{pmatrix} \nu_{\tau'_L} \\ \tau'_L \end{pmatrix}, & E_{4,R} &= \tau'_R, & N_{4,R} &= \nu_{\tau'_R}. \end{aligned} \quad (3.67)$$

Note that we also have a right-chiral four-generation neutrino, as it is required to be heavy.

The inclusion of the fourth generation fermions requires also 4×4 extension of \mathbf{V}_{CKM} quark mixing matrix, given in eq. (2.6), to \mathbf{V}_{CKM4}

$$\mathbf{V}_{\text{CKM4}} = \begin{pmatrix} \tilde{V}_{ud} & \tilde{V}_{us} & \tilde{V}_{ub} & \tilde{V}_{ub'} \\ \tilde{V}_{cd} & \tilde{V}_{cs} & \tilde{V}_{cb} & \tilde{V}_{cb'} \\ \tilde{V}_{td} & \tilde{V}_{ts} & \tilde{V}_{tb} & \tilde{V}_{tb'} \\ \tilde{V}_{t'd} & \tilde{V}_{t's} & \tilde{V}_{t'b} & \tilde{V}_{t'b'} \end{pmatrix}. \quad (3.68)$$

The values of the CKM elements which are obtained from the tree-level weak decays are independent of the number of generations and the current results from the measurements are [114]

$$\begin{aligned} |\tilde{V}_{ud}| &= 0.97418 \pm 0.00027, & |\tilde{V}_{cd}| &= 0.23 \pm 0.011, \\ |\tilde{V}_{us}| &= 0.2255 \pm 0.0019, & |\tilde{V}_{cs}| &= 1.04 \pm 0.06, \\ |\tilde{V}_{ub}| &= (3.93 \pm 0.36) \times 10^{-3}, & |\tilde{V}_{cb}| &= (41.2 \pm 1.1) \times 10^{-3}. \end{aligned} \quad (3.69)$$

Since the V_{td} , V_{ts} elements of the CKM matrix cannot be measured directly (bounds are obtained from decays involving loops) and V_{tb} varies notably with changes on the degree of significance, σ , these three are mainly determined from the unitarity conditions. However, in SM4 the assumption of 3×3 unitarity is invalid, thus giving more space for V_{tq} ($q = d, s, b$) entries. The \mathbf{V}_{CKM4} matrix can also be parametrized as it is done by Wolfenstein for \mathbf{V}_{CKM} , which is given in eq. (2.7), with appropriate choices for the quark phases. The Dighe-Kim parametrization [142, 143] of \mathbf{V}_{CKM4} introduces six real parameters and three phases as follows

$$\mathbf{V}_{\text{CKM4}} = \begin{pmatrix} \# & \lambda & A\lambda^3 C e^{-i\delta_{ub}} & p\lambda^3 e^{-i\delta_{ub'}} \\ \# & \# & A\lambda^2 & q\lambda^2 e^{-i\delta_{cb'}} \\ \# & \# & \# & r\lambda \\ \# & \# & \# & \# \end{pmatrix}, \quad (3.70)$$

where λ is the sine of Cabibbo angle, and the entries denoted by # can be obtained uniquely by the unitarity condition $\mathbf{V}_{\text{CKM4}}^\dagger \mathbf{V}_{\text{CKM4}} = \mathbf{I}$. They have been calculated up to a multiplicative factor of $[1 + \mathcal{O}(\lambda^3)]$ in [144] as

$$\begin{aligned}
\tilde{V}_{ud} &= 1 - \frac{\lambda^2}{2} + \mathcal{O}(\lambda^4), \\
\tilde{V}_{cd} &= -\lambda + \mathcal{O}(\lambda^5), \\
\tilde{V}_{cs} &= 1 - \frac{\lambda^2}{2} + \mathcal{O}(\lambda^4), \\
\tilde{V}_{td} &= A\lambda^3(1 - Ce^{i\delta_{ub}}) + r\lambda^4(qe^{i\delta_{cb'}} - pe^{i\delta_{ub'}}) \\
&\quad + \frac{A}{2}\lambda^5(-r^2 + (C + Cr^2)e^{i\delta_{ub}}) + \mathcal{O}(\lambda^6), \\
\tilde{V}_{ts} &= -A\lambda^2 - qr\lambda^3e^{i\delta_{cb'}} + \frac{A}{2}\lambda^4(1 + r^2 - 2Ce^{i\delta_{ub}}) + \mathcal{O}(\lambda^5), \\
\tilde{V}_{tb} &= 1 - \frac{r^2\lambda^2}{2} + \mathcal{O}(\lambda^4), \\
\tilde{V}_{t'd} &= \lambda^3(qe^{i\delta_{cb'}} - pe^{i\delta_{ub'}}) + Ar\lambda^4(1 + Ce^{i\delta_{ub}}) \\
&\quad + \frac{\lambda^5}{2}(pe^{i\delta_{ub'}} - qr^2e^{i\delta_{cb'}} + pr^2e^{i\delta_{ub'}}) + \mathcal{O}(\lambda^6) \\
\tilde{V}_{t's} &= q\lambda^2e^{i\delta_{cb'}} + Ar\lambda^3 + \lambda^4\left(-pe^{i\delta_{ub'}} + \frac{q}{2}e^{i\delta_{cb'}} + \frac{qr^2}{2}e^{i\delta_{cb'}}\right) + \mathcal{O}(\lambda^5), \\
\tilde{V}_{t'b} &= -r\lambda + \mathcal{O}(\lambda^4), \\
\tilde{V}_{t'b'} &= 1 - \frac{r^2\lambda^2}{2} + \mathcal{O}(\lambda^4). \tag{3.71}
\end{aligned}$$

The presence of additional phases make it possible to explain the deviation of the CP violating measurements in the B-meson system [145–150] from the SM predictions where there is only one single phase. Note that in the limit $p = q = r = 0$ together with the redefinitions $C = \sqrt{\rho^2 + \eta^2}$ and $\delta_{ub} = \tan^{-1}(\eta/\rho)$ the above expansion reduces to the Wolfenstein parametrization given in eq. (2.7) [116].

3.3.1 Experimental Status of the Four-Generation Standard Model

Constraints on the fourth generation fermion masses

The electroweak oblique parameters are a set of three measurable quantities, called S , T , and U which were originally introduced as

$$\begin{aligned}\alpha S &= 4e^2 \frac{d}{dq^2} \left[\Pi_{33}(q^2) - \Pi_{3Q}(q^2) \right] \Big|_{q^2=0}, \\ \alpha T &= 4e^2 \frac{e^2}{x_W \bar{x}_W M_Z^2} \left[\Pi_{11}(0) - \Pi_{33}(0) \right], \\ \alpha U &= 4e^2 \frac{d}{dq^2} \left[\Pi_{11}(q^2) - \Pi_{33}(q^2) \right] \Big|_{q^2=0},\end{aligned}\tag{3.72}$$

where α is the electromagnetic coupling and e is the electron charge. Π_{xy} denotes the virtual self energy contributions to the weak gauge bosons. $x_W = \sin^2 \theta_W$ and $\bar{x}_W = 1 - x_W$ where θ_W is the Weinberg angle. In the presence of the fourth generation, the fermionic contribution to these parameters are calculated by [151] and the measurements of the oblique parameters S and T indicates a correlation between the masses of the fourth generation quarks [152–156]

$$\begin{aligned}m_{t'} &\geq 404 \text{ GeV}, \\ m_{t'} - m_{b'} &\simeq \left[1 + \frac{1}{5} \ln \left(\frac{m_h}{115 \text{ GeV}} \right) \right] \times 50 \text{ GeV},\end{aligned}\tag{3.73}$$

where $m_{t'}$, $m_{b'}$ and m_h are the masses of the fourth generation up-type, down-type quarks and the Higgs boson, respectively. The perturbativity of the Yukawa couplings and unitarity of S-wave scattering amplitudes constraints the masses of the fourth generation to a narrow band. These bounds, however, may be relaxed with the introduction of heavy leptons which have a counter effect on the S and T parameters. Electroweak precision measurements also restrict the mass difference [156, 157] of the fourth generation leptons to be

$$m_{\tau'} - m_{\nu_{\tau'}} \simeq (30 - 60) \text{ GeV},\tag{3.74}$$

where $m_{\tau'}$, $m_{\nu_{\tau'}}$ are the masses of the additional family of lepton and neutrino, respectively. In addition, the invisible width of Z boson gives a mass constraint for the fourth generation neutrino to be heavier than 45 GeV. Even though one would

need a special mechanism for the fourth generation neutrino to be massive while the other three are extremely light, phenomenologically this is allowed.

Recently, there are intensive searches at the LHC aimed at putting exclusion limits on SM4. The direct searches for t' and b' quarks from pp collisions at center-of-mass energy of 7 TeV give lower bounds for their masses. CMS search which is performed with a data sample corresponding to an integrated luminosity of 5.0 fb^{-1} gives $m_{t'} > 557 \text{ GeV}$ at 95% CL with the assumption that it decays 100% in the decay mode $t' \rightarrow bW$, and an integrated luminosity of 4.9 fb^{-1} brings the constraint $m_{b'} > 611 \text{ GeV}$ at 95% CL assuming it decays 100% in the decay channel $b' \rightarrow tW$ [158, 159]. ATLAS detector, on the other hand, with 1.04 fb^{-1} integrated luminosity at 95% CL restricts $m_{b'} > 480 \text{ GeV}$ via the decay channels $b' \rightarrow Wt$ in the lepton + jets channel as $b'b' \rightarrow WtWt \rightarrow l\nu bbqqqqqq$. The $m_{t'} > 450$ limit also comes from ATLAS at 95% CL with 1.04 fb^{-1} integrated luminosity [160, 161].

Constraints on the Fourth-Generation Higgs Mass

Besides direct searches for heavy quarks, Higgs production in gluon-gluon fusion is also an important channel for the SM4 searches [162]. In the SM this channel is basically determined at the Leading Order (LO) by the one-loop diagram of the top quark. Moving from SM to SM4, the LO the production cross-section of a Higgs boson through the gluon-gluon fusion increases about nine times than that of the SM, because in addition to the top quark there are also heavy t' and b' quarks propagating in the loop. The latest results in ATLAS detector exclude the SM4 Higgs mass $m_h > 120 \text{ GeV}$ and $m_h < 600 \text{ GeV}$ with the integrated luminosity of $2 - 2.3 \text{ fb}^{-1}$ for $h \rightarrow ZZ^* \rightarrow l^+l^-l^+l^-$ searches and 1.7 fb^{-1} for $h \rightarrow WW^* \rightarrow l^+\nu l^-\bar{\nu}$ searches at 95% CL [163].

The CMS detector explored the Higgs boson mass in a range $110 - 600 \text{ GeV}$ in five different Higgs boson decay modes: $\gamma\gamma$, bb , $\tau\tau$, WW , and ZZ with an integrated luminosity of $4.6 - 4.8 \text{ fb}^{-1}$ and for an extension of the SM including a fourth generation of fermions and excluded the region $120 < m_h < 600 \text{ GeV}$ at 95% CL [164].

If the bump in the signal announced by LHC is the Higgs boson, this would rule out the SM4 at 95% CL for $m_{h^0} \geq 123 \text{ GeV}$, and at 99.6% if $m_{h^0} = 125 \text{ GeV}$ [165–167]. The limits from the Tevatron [168] also exclude a wide range of Higgs boson masses. So maybe the SM4 is in peril, but not other BSM with four-generations.

3.3.2 Two-Loop Electroweak Corrections to the Higgs Boson Production

Recently, the two-loop electroweak corrections, δ_{EW}^4 , to the Higgs boson production via gluon-gluon fusion have been computed with respect to the LO cross section $\sigma_{\text{SM4}}^{\text{LO}}(gg \rightarrow h)$ in [169–172]

$$\sigma_{\text{SM4}}(gg \rightarrow h_0) = \sigma_{\text{SM4}}^{\text{LO}}(gg \rightarrow h)(1 + \delta_{\text{EW}}^{(4)}). \quad (3.75)$$

The Next-to-Leading Order (NLO) corrections are calculated to be positive for light Higgs boson masses whereas above $m_h > 260$ GeV, become negative as summarized in the following Table 11.

m_h (GeV)	$\delta_{\text{EW}}^{(4)}$ [%]	m_h (GeV)	$\delta_{\text{EW}}^{(4)}$ [%]
100	7.08	180	3.22
110	7.01	190	2.79
120	6.91	200	2.20
130	6.77	210	0.39
140	6.55	220	-1.11
150	6.16	230	-3.84
160	4.87	240	-8.71
170	4.38	250	-17.00

Table 11: Relative NLO electroweak corrections to the $gg \rightarrow h$ cross sections in SM4, for the mass scenario $m_{t'} = 500$ GeV, $m_{b'} = 450$ GeV, $m_{\nu_{t'}} = 375$ GeV, $m_{\tau'} = 450$ GeV. Table is taken courtesy [172].

The decays of $h \rightarrow \gamma\gamma$ in SM4 also receive corrections from t' and b' quarks running in the loops. The amplitude can be written as

$$A = A_{\text{LO}} + X_{\text{W}}A_{\text{NLO}} + X_{\text{W}}^2A_{\text{NNLO}} + \dots, \quad (3.76)$$

with the amplitude square for electroweak NLO corrections

$$|A|^2 \sim |A_{\text{LO}}|^2 + 2X_{\text{W}}\text{Re}[A_{\text{NLO}}A_{\text{LO}}^\dagger] = |A_{\text{LO}}|^2(1 + \delta_{\text{EW}}^{(4)}), \quad (3.77)$$

where $\delta_{\text{EW}}^{(4)} = 2X_{\text{W}}\text{Re}[A_{\text{NLO}}A_{\text{LO}}^\dagger]/|A_{\text{LO}}|^2$. The problem is that in SM4 the cancellation between the fermion and W boson loops is stronger than it is in SM, thus giving a

suppressed LO by two times at the amplitude level. Therefore, one needs to include $X_W^2|A_{\text{NLO}}|^2$ term in the expansion such that

$$|A|^2 \sim |A_{\text{LO}} + X_W A_{\text{NLO}}|^2 = |A_{\text{LO}}|^2(1 + \bar{\delta}_{\text{EW}}^{(4)}), \quad (3.78)$$

where $\bar{\delta}_{\text{EW}}^{(4)} = |A_{\text{LO}} + X_W A_{\text{NLO}}|^2/|A_{\text{LO}}|^2 - 1$. Unfortunately, it turns out that the A_{LO} is small and $X_W A_{\text{NLO}}$ is in the same order as A_{LO} but with opposite sign which make $\bar{\delta}_{\text{EW}}^{(4)}$ large (close to one in absolute value) and non-perturbative. Therefore, it is customary to give the following shifted quantities which include Next-to-Next-to-Leading Order (NNLO) corrections

$$\bar{A}_{\text{LO}} = A_{\text{LO}} + X_W A_{\text{NLO}}, \quad \bar{A}_{\text{NLO}} = A_{\text{NNLO}}, \quad (3.79)$$

yielding the two loop corrected decay width to be

$$\bar{\Gamma}_{\text{LO}} = \Gamma_{\text{LO}}(1 + \bar{\delta}_{\text{EW}}) = \Gamma_{\text{LO}} \frac{|A_{\text{LO}} + X_W A_{\text{NLO}}|^2}{|A_{\text{LO}}|^2}. \quad (3.80)$$

In [172] the \bar{A}_{NLO} is estimated with the assumption $m_{b'} = m_{b''} = m_Q$ and $m_{\tau'} = m_{\nu_{\tau'}} = m_L$ such that the absolute value of the NLO leading coefficient is assigned to the unknown coefficient of NNLO in leading behavior of m_Q^4 and m_L^4 , with no accidental cancellations. Then, the decay rate is corrected by the estimate for the missing higher-order corrections (δ_{THU}) relative to $\bar{\Gamma}_{\text{LO}}$ as

$$\Gamma = \bar{\Gamma}_{\text{LO}}(1 \pm \delta_{\text{THU}}) = \Gamma_{\text{LO}}(1 + \bar{\delta}_{\text{EW}})(1 \pm \delta_{\text{THU}}). \quad (3.81)$$

The numerical values are summarized in the Table 12 below

m_h (GeV)	Γ_{LO}	$\bar{\delta}_{\text{EW}}^{(4)}$ [%]	$\bar{\Gamma}_{\text{LO}}$	δ_{THU} [%]
100	0.602×10^{-6}	-99.4	0.004×10^{-6}	68.3
110	0.938×10^{-6}	-98.2	0.016×10^{-6}	37.1
120	1.466×10^{-6}	-96.3	0.054×10^{-6}	23.8
130	2.322×10^{-6}	-93.4	0.154×10^{-6}	16.4
140	3.802×10^{-6}	-89.2	0.412×10^{-6}	11.6
150	6.714×10^{-6}	-83.1	1.133×10^{-6}	8.3

Table 12: NLO electroweak corrections to the $h \rightarrow \gamma\gamma$ decay width and estimate for the missing higher-order corrections δ_{THU} relative to $\bar{\Delta}_{\text{LO}}$. Table is taken courtesy [172].

3.4 The Warped Extra Dimensions

The SM explains Nature very well up to electroweak scale by providing a unified picture for the electromagnetic, weak and strong forces. The gravitational interaction, on the other hand, is not included in the SM since it is much weaker than the other three forces. However, at the Planck scale the quantum effects of gravity become as strong as the other interactions. One of the main drawbacks of the SM that there is an unnaturally huge discrepancy between the energy scales M_{EW} and M_{Pl} ($M_{\text{Pl}}/M_{\text{EW}} \approx 10^{16}$). Lisa Randall and Raman Sundrum [40, 41] proposed an elegant possibility to explain this significant difference. In their model, two 4D Minkowskian space-time, namely Plank Brane (or UV Brane) and TeV Brane (or IR Brane), are embedded at the boundaries of five-dimensional (5D) anti-de-Sitter (AdS_5) space², and the fifth dimension is compactified on S^1/Z_2 orbifold of size r , labeled by a coordinate ϕ which is invariant under the Z_2 parity transformation $(x^\mu, \phi) \leftrightarrow (x^\mu, -\phi)$, giving $\phi = 0, \pm\pi$. See Fig 7 for S^1/Z_2 orbifold.

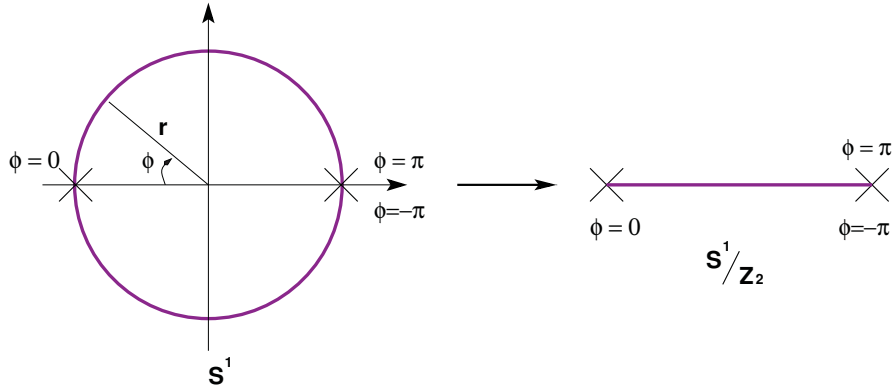


Figure 7: The S^1 and S^1/Z_2 Orbifolds.

In its original form, the metric of the model is given by

$$ds^2 = g_{MN}dx^M dx^N = e^{-2\sigma(\phi)}\eta_{\mu\nu}dx^\mu dx^\nu - r^2d\phi^2, \quad (3.82)$$

²A maximally symmetric space-time with a constant negative scalar curvature.

such that

$$g_{MN} = \begin{pmatrix} e^{-2\sigma(\phi)} & 0 & 0 & 0 & 0 \\ 0 & -e^{-2\sigma(\phi)} & 0 & 0 & 0 \\ 0 & 0 & -e^{-2\sigma(\phi)} & 0 & 0 \\ 0 & 0 & 0 & -e^{-2\sigma(\phi)} & 0 \\ 0 & 0 & 0 & 0 & -r^2 \end{pmatrix}. \quad (3.83)$$

Here x^M ($M = \mu, 5$) are the 5D space-time coordinates, and x^μ ($\mu = 0, \dots, 3$) denote the coordinates in 4D Minkowskian space-time (see Appendix A for the convention of the Minkowski metric). The 4D coordinates are rescaled by an exponential warp factor for every constant value of ϕ . The coefficient, r , independent of ϕ , is the compactification radius of the extra dimensional circle prior to orbifolding. After orbifolding, the size of the extra dimension becomes $L = \pi r$. Planck and TeV branes are placed at the orbifold fixed points $\phi = 0$ and $\phi = \pi$ (or equivalently $\phi = -\pi$), respectively. The region in between the branes is called as the bulk, and it was originally proposed that the only field allowed to propagate in the bulk is gravity, whereas the SM fields are assumed to be confined on the TeV brane. The set-up for the model is shown in Figure 8.

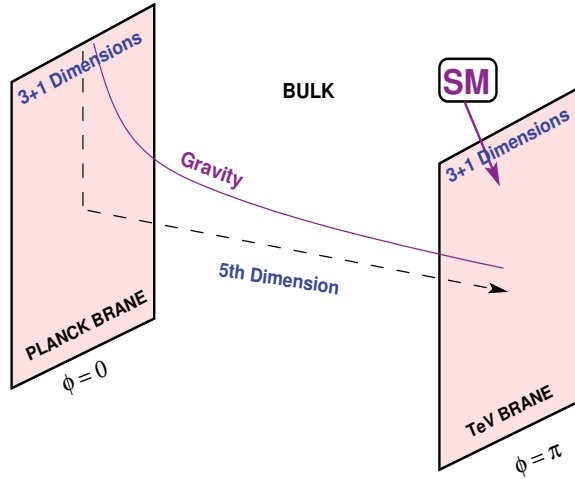


Figure 8: Original setup of Randall-Sundrum model.

The action of the model is given by

$$S = S_{\text{bulk}} + S_{\text{UV}} + S_{\text{IR}}, \quad (3.84)$$

where

$$\begin{aligned}
S_{\text{BULK}} &= \int d^5x \sqrt{g} (-2M^3 R - \Lambda), \\
S_{\text{UV}} &= \int d^4x \sqrt{-g^{\text{UV}}} (\mathcal{L}_{\text{UV}} - V_{\text{UV}}), \\
S_{\text{IR}} &= \int d^4x \sqrt{-g^{\text{IR}}} (\mathcal{L}_{\text{IR}} - V_{\text{IR}}),
\end{aligned} \tag{3.85}$$

where M is the fundamental scale of the theory, Λ is the 5D cosmological constant and R is the Ricci scalar. The Ricci scalar is simply the trace of the Ricci curvature tensor, R_{MN} , which carries information about the curvature of space-time, and constructed out of the Riemann-Christoffel symbols and their derivatives with respect to space-time as

$$R_{MN} = \Gamma_{MN,K}^K - \Gamma_{MK,N}^K - \Gamma_{ML}^K \Gamma_{NK}^L + \Gamma_{MN}^K \Gamma_{KL}^L, \tag{3.86}$$

where

$$\Gamma_{MK,N}^K = \frac{\partial \Gamma_{MK}^K}{\partial x^N}, \tag{3.87}$$

and Christoffel symbols are defined in terms of the space-time metric as

$$\Gamma_{MN}^K = g^{KL} \Gamma_{LMN} = \frac{1}{2} g^{KL} (g_{LM,N} + g_{LN,M} - g_{MN,L}), \tag{3.88}$$

with

$$g_{MN,K} = \frac{\partial g_{MN}}{\partial x^K}. \tag{3.89}$$

As it can be seen from the eqs. (3.86) and (3.88), the Ricci scalar involves two powers of derivative and g_{MN} terms. Since g_{MN} is dimensionless, the mass dimension of R is 2 ($[R] = 2$) which, to keep the action dimensionless, is multiplied by the third power of the fundamental scale of the theory ($[M^3] = 3$) in eq. (3.85). We assume $\mathcal{L}_{\text{IR}} = \mathcal{L}_{\text{SM}}$ since the original scenario assigns the SM fields on the IR brane and $\mathcal{L}_{\text{UV}} = 0$ with the reasoning of no UV localized field. \sqrt{g} in eq. (3.85) corresponds to the square root of the determinant of the 5D metric needed to have an invariant integration measure for the bulk. It can be calculated as

$$\sqrt{g} = \sqrt{\det(g_{MN})} = \sqrt{e^{-8\sigma(\phi)} r^2} = e^{-4\sigma(\phi)} r. \tag{3.90}$$

The branes can support 4D field theories, therefore we need the brane induced metric on them, which are given by

$$\begin{aligned}
g_{\mu\nu}^{\text{UV}}(x^\mu) &\equiv g_{\mu\nu}(x^\mu, \phi = 0), & \sqrt{-g^{\text{UV}}} &= e^{-4\sigma(\phi=0)} \\
g_{\mu\nu}^{\text{IR}}(x^\mu) &\equiv g_{\mu\nu}(x^\mu, \phi = \pi), & \sqrt{-g^{\text{IR}}} &= e^{-4\sigma(\phi=\pi)}.
\end{aligned} \tag{3.91}$$

Note that, the determinant of 4D metric on the branes is negative. Hence, we write them with a negative sign in the square root. Let us write the action in eq. (3.85) in a more compact form

$$S = \int d^5x \sqrt{g} \left(-2M^3 g_{MN} R^{MN} - \Lambda - \frac{1}{\sqrt{-g_{55}}} \sum_i V_i \delta(\phi - \phi_i) \right), \quad (3.92)$$

where i denote the UV and IR branes such that $\phi_i = 0$ on UV brane whereas, $\phi_i = \pi$ for IR brane. Varying it with respect to the special metric given in eq. (3.82) using

$$\delta\sqrt{g} = \frac{1}{2} \delta g_{MN} g^{MN} \sqrt{g}, \quad \delta g^{MN} = -g^{MK} g^{NL} \delta g_{KL}, \quad (3.93)$$

yields

$$\begin{aligned} \delta S &= \int d^5x \delta\sqrt{g} \left[-2M^3 R - \Lambda - \frac{1}{\sqrt{-g_{55}}} \sum_i V_i \delta(\phi - \phi_i) \right] - \sqrt{g} 2M^3 \delta g_{MN} R^{MN} \\ &= \int d^5x \left[2M^3 G^{MN} - \frac{1}{2} \left(\Lambda + \frac{1}{\sqrt{-g_{55}}} \sum_i V_i \delta(\phi - \phi_i) \right) g^{MN} \right] \sqrt{g} \delta g_{MN}, \end{aligned} \quad (3.94)$$

where the term $G_{MN} = R_{MN} - \frac{1}{2} g_{MN} R$ is known as the Einstein tensor and the relation $R_{MN} - \frac{1}{2} g_{MN} R = \kappa^2 T_{MN}$ is the so called Einstein field equation, with T_{MN} the stress-energy tensor and $\kappa^2 = 1/2M^3$. Using $\delta S = 0$ (the action is required to be coordinate invariant), the 5D Einstein equation then becomes

$$\begin{aligned} \sqrt{g} G_{MN} &= \frac{1}{4M^3} \left[\Lambda \sqrt{g} g_{MN} + V_{\text{IR}} \sqrt{-g^{\text{IR}}} g_{\mu\nu}^{\text{IR}} \delta_M^\mu \delta_N^\nu \delta(\phi - \pi) \right. \\ &\quad \left. + V_{\text{UV}} \sqrt{-g^{\text{UV}}} g_{\mu\nu}^{\text{UV}} \delta_M^\mu \delta_N^\nu \delta(\phi) \right]. \end{aligned} \quad (3.95)$$

Before going any further we will pause here to derive a relation between the stress-energy tensor and Ricci curvature tensor which will serve for our purposes later.

$$R_{MN} = \kappa^2 T_{MN} + \frac{1}{2} g_{MN} R. \quad (3.96)$$

Multiplying both hand-sides with g^{MN} and solve for R in 5D

$$R = -\frac{2}{3} \kappa^2 T. \quad (3.97)$$

Substituting into eq. (3.96) one gets

$$R_{MN} = \kappa^2 \left(T_{MN} - \frac{1}{3} g_{MN} T \right). \quad (3.98)$$

3.4.1 Derivation of the Warp Factor

The components of the Ricci Tensor and the Ricci Scalar are calculated explicitly in Appendix C-1 for the metric in eq. (3.82). The $\mu\nu$ -, $\mu 5$ - and 55 -components of the Ricci tensor are obtained as

$$\begin{aligned} R_{\mu\nu} &= \frac{e^{-2\sigma(\phi)}}{r^2} \{4[\sigma'(\phi)]^2 - \sigma''(\phi)\} \eta_{\mu\nu}, \\ R_{55} &= 4\{\sigma''(\phi) - [\sigma'(\phi)]^2\}, \\ R_{\mu 5} &= 0, \end{aligned} \quad (3.99)$$

and the Ricci Scalar is

$$R = \frac{4}{r^2} \{5[\sigma'(\phi)]^2 - 2\sigma''(\phi)\}. \quad (3.100)$$

These yield the components of Einstein Tensor

$$\begin{aligned} G_{\mu\nu} &= R_{\mu\nu} - \frac{1}{2}g_{\mu\nu}R = -\frac{3g_{\mu\nu}}{r^2}(\sigma''(\phi) - 2[\sigma'(\phi)]^2), \\ G_{55} &= R_{55} - \frac{1}{2}g_{55}R = -6[\sigma'(\phi)]^2, \\ G_{\mu 5} &= 0. \end{aligned} \quad (3.101)$$

The explicit form of $\sigma(\phi)$ can be obtained by equating the 55 -component of the Einstein Tensor from eq. (3.95) and (3.101)

$$6[\sigma'(\phi)]^2 = \frac{1}{4M^3}\Lambda(-r^2), \quad (3.102)$$

and solving for $\sigma(\phi)$ by taking into account the orbifold symmetry one gets

$$\sigma(\phi) = \sqrt{\frac{-\Lambda}{24M^3}}r|\phi| = kr|\phi|. \quad (3.103)$$

The integration constant is taken as zero because it is nothing but a rescaling of x^μ , which could be absorbed into the redefinition of the 4D coordinates. Moreover, one can conclude that, the warped geometry is allowed only if there is a negative non-vanishing 5D cosmological constant in the model, resulting an AdS₅ space-time. k is called the RS curvature. Inserting this result in eq. (3.82) the metric becomes

$$ds^2 = g_{MN}dx^M dx^N = e^{-2kr|\phi|}\eta_{\mu\nu}dx^\mu dx^\nu - r^2d\phi^2, \quad (3.104)$$

where the factor $e^{-kr|\phi|}$, named warp factor, describes the change in length scales when moving along the fifth dimension. One can rewrite the metric in a more compact form by a redefinition of the form $y = r|\phi|$ as

$$ds^2 = g_{MN}dx^M dx^N = e^{-2ky}\eta_{\mu\nu}dx^\mu dx^\nu - dy^2, \quad (3.105)$$

Another widely used form of RS background is the conformally flat metric which can be derived as follows

$$ds^2 = g_{MN}dx^M dx^N = e^{-2ky}(\eta_{\mu\nu}dx^\mu dx^\nu - e^{2ky}dy^2). \quad (3.106)$$

After making a change of variables $e^{ky}dy = dz$ and solving for z we have

$$ds^2 = g_{MN}dx^M dx^N = \left(\frac{R}{z}\right)^2 (\eta_{\mu\nu}dx^\mu dx^\nu - dz^2), \quad (3.107)$$

where $1/k = R$, or in matrix form

$$g_{MN} = \left(\frac{R}{z}\right)^2 \begin{pmatrix} 1 & 0 & 0 & 0 & 0 \\ 0 & -1 & 0 & 0 & 0 \\ 0 & 0 & -1 & 0 & 0 \\ 0 & 0 & 0 & -1 & 0 \\ 0 & 0 & 0 & 0 & -1 \end{pmatrix}. \quad (3.108)$$

The orbifold boundaries will also change with the change of variables as $\phi \in [0, \pi] \rightarrow y \in [0, r\pi] \rightarrow z \in [R, R']$ with $R' = \frac{1}{M_{KK}}$ and for the conformally flat metric we can write

$$\sqrt{g} = \left(\frac{R}{z}\right)^5, \quad \sqrt{-g^{\text{UV}}} = 1, \quad \sqrt{-g^{\text{IR}}} = \left(\frac{R}{R'}\right)^4. \quad (3.109)$$

Since we have the explicit form of the warp factor, $\sigma(\phi)$, we can calculate the potentials V_{IR} and V_{UV} on the branes. We substitute the eqs. (3.102) and (3.103) in the $\mu\nu$ -component of the Einstein tensor given in eq. (3.101) and equate this to the corresponding component obtained from eq. (3.95) which yields

$$3\sigma''(\phi)e^{-6kr|\phi|} = \frac{r}{4M^3} \left[V_{\text{IR}}e^{-6kr\pi}\delta(\phi - \pi) + V_{\text{UV}}\delta(\phi) \right]. \quad (3.110)$$

The requirement of the function $\sigma(\phi)$ having delta functions in the second derivatives (see Appendix C-2) can be compensated by the brane vacuum energies such that

$$6kre^{-6kr|\phi|} \left[\delta(\phi) - \delta(\phi - \pi) \right] = \frac{r}{4M^3} \left[V_{\text{IR}}e^{-6kr\pi}\delta(\phi - \pi) + V_{\text{UV}}\delta(\phi) \right], \quad (3.111)$$

thus giving

$$V_{\text{UV}} = -V_{\text{IR}} = 24M^3k. \quad (3.112)$$

At this point the theory possesses three 5D parameters. The fundamental scale M , the RS curvature k and compactification radius r . The parameters of the 4D effective theory, namely the 4D Planck scale, can be derived in terms of these fundamental scales. Note that as for the fifth dimension is not found in present gravity testing experiments the r is required to be small.

The first step is to extend the metric in eq. (3.104) by massless fluctuations around the vacuum solution as

$$ds^2 = e^{-2k\bar{b}(x)|\phi|}[\eta_{\mu\nu} + \bar{h}_{\mu\nu}(x)]dx^\mu dx^\nu - \bar{b}^2 d\phi^2, \quad (3.113)$$

where $\bar{h}_{\mu\nu}$, the deviation from the flat metric, is the physical graviton of the 4D effective theory. $g_{55} = b^2(x)$ is the radion and its zero mode $\bar{b}(x)$ determines the size of the extra dimension, discussed in Subsection 3.4.3. Given that the 4D metric

$$\bar{g}_{\mu\nu} = \eta_{\mu\nu} + \bar{h}_{\mu\nu}(x), \quad (3.114)$$

is smooth, this extended metric can be considered locally the same as the vacuum solution in eq. (3.104) since $\bar{g}_{\mu\nu}$ is locally a 4D Minkowski metric and $b(x)$ is locally constant. Focusing on the curvature term from eq. (3.85) we can write the effective 4D action as

$$S_{\text{eff}} \supset \int d^4x \int_{-\pi}^{\pi} d\phi 2M^3 r e^{-2kr|\phi|} \sqrt{-\bar{g}} \bar{R}, \quad (3.115)$$

where \bar{R} and \bar{g} are the corresponding 4D parameters. Upon performing the ϕ integral explicitly we obtain a purely 4D action which has to be in agreement with the 4D description of gravity given by Einstein-Hilbert action

$$S_{\text{eff}} = \int d^4x 2M_{\text{Pl}}^2 \sqrt{-\bar{g}} \bar{R}. \quad (3.116)$$

Comparing the eqs. (3.115) and (3.116) the reduced 4D Planck scale M_{Pl} emerges from the fundamental scale M

$$M_{\text{Pl}}^2 = \int_{-\pi}^{\pi} d\phi 2M^3 r e^{-2kr|\phi|} = \frac{M^3}{k} [1 - e^{2kr\pi}]. \quad (3.117)$$

For $kr\pi \gg 1$ (necessary for solving the Hierarchy problem), M_{Pl} only depends very weakly on the compactification radius. In order not to produce large hierarchies between the fundamental parameters introduced, we set $k \sim M$ which yields $M \sim M_{\text{Pl}}$.

3.4.2 The Higgs Lagrangian

We will consider the Higgs field as localized on the TeV brane (i.e., $\phi = \pi$)

$$S_{\text{Higgs}} = \int d^4x r \int_{-\pi}^{\pi} d\phi \mathcal{L}_{\text{Higgs}}, \quad (3.118)$$

where in analogy to the Higgs Lagrangian in SM given in eqs. (2.16) and (2.19) we write

$$\mathcal{L}_{\text{Higgs}} = \delta(|\phi| - \pi) \frac{\sqrt{g}}{r^2} \left[g_{\text{IR}}^{\mu\nu} (D_\mu H)^\dagger D_\nu H - V(H) \right], \quad (3.119)$$

and

$$V(H) = -\frac{\mu_5^2}{2} (H^\dagger H) + \frac{\lambda_5}{4} (H^\dagger H)^2. \quad (3.120)$$

Here the form of the Higgs field H is the same as the SM one introduced in eq. (2.28) except the 4D VEV is replaced by v_5 . We rewrite the action with a redefinition $v_5 = \sqrt{-\mu_5^2/\lambda_5}$ as

$$S_{\text{Higgs}} = \int d^4x r \int_{-\pi}^{\pi} d\phi \delta(|\phi| - \pi) \frac{\sqrt{g}}{r^2} \left[g_{\text{IR}}^{\mu\nu} (D_\mu H)^\dagger D_\nu H - \frac{\lambda_5}{4} (H^\dagger H - v_5^2)^2 \right]. \quad (3.121)$$

After taking the integral along the extra dimension, we get the effective 4D action

$$S_{\text{Higgs}} = \int d^4x e^{-4kr\pi} \sqrt{-\tilde{g}} \left[e^{2kr\pi} \tilde{g}_{\text{IR}}^{\mu\nu} (D_\mu H)^\dagger D_\nu H - \frac{\lambda_5}{4} (H^\dagger H - v_5^2)^2 \right], \quad (3.122)$$

where \tilde{g} corresponds to the metric of the effective 4D theory. In order to obtain canonically normalized kinetic terms for the Higgs field, we perform the transformation $H \rightarrow e^{kr\pi} H$.

$$S_{\text{Higgs}} = \int d^4x \sqrt{-\tilde{g}} \left[\tilde{g}_{\text{IR}}^{\mu\nu} (D_\mu H)^\dagger D_\nu H - \frac{\lambda_5}{4} (H^\dagger H - e^{-2kr\pi} v_5^2)^2 \right]. \quad (3.123)$$

One can conclude from the last term in the above equation that, an observer living on the IR brane sees the 5D VEV (v_5) as rescaled by the warp factor, such that the effective VEV (v_4) reads

$$v_4 = e^{-kr\pi} v_5. \quad (3.124)$$

Note that the 5D self interaction constant does not receive any rescaling ($\lambda_5 = \lambda$) whereas μ_5 is rescaled ($\mu = e^{-kr\pi} \mu_5$). Based on eq. (3.124), we observe that any fundamental mass parameter in 5D theory, measured on the IR brane will receive such a rescaling, which in turn explains the gauge hierarchy problem of the SM as follows

$$M_{\text{EW}} \equiv e^{-kr\pi} M_{\text{Pl}} \Rightarrow L = kr\pi \sim 37 \text{ or } kr \sim 12. \quad (3.125)$$

Thus, one can conclude that all the dimensionful parameters of the fundamental theory are almost at the same order, $M \sim M_{\text{Pl}} \sim k \sim 1/r \sim v_5$, and therefore consistent with naturalness arguments.

3.4.3 The Radion Solution

In RS1, it is assumed that the two branes are located at a modest distance apart but this distance is not determined by the dynamics of the model. For this scenario to be relevant, a mechanism for stabilizing the separation of the two branes is necessary. Small shifts in the separation between the two branes will not change the energy. In an effective theory these shifts are described by the fluctuations of a massless particle, the so called radion. However, to be able to recover the ordinary 4D Einstein gravity it must be massive. Goldberger and Wise proposed a way to achieve these requirements by introducing a scalar field (Φ) in the 5D bulk in addition to the graviton [65] with a bulk potential $V(\Phi)$. To stabilize the size of the extra dimension the induced potentials on 4D branes $\lambda_{\text{IR,UV}}(\Phi)$ are also included. The counteraction of the brane and bulk Lagrangians generates a VEV for the radion field that gives rise to a 4D vacuum energy which depends on the size of the extra dimension and is in agreement with the solution of the gauge hierarchy problem without much fine tuning.

The bulk action for this scalar field is

$$S_{\Phi}^{\text{BULK}} = \frac{1}{2} \int d^5x \sqrt{g} \left[g_{MN} \partial^M \Phi \partial^N \Phi - V(\Phi) \right], \quad (3.126)$$

and the induced potential terms on the UV- and IR-branes are

$$\begin{aligned} S_{\Phi}^{\text{UV}} &= - \int d^4x \sqrt{-g^{\text{UV}}} \lambda_{\text{UV}}(\Phi), \\ S_{\Phi}^{\text{IR}} &= - \int d^4x \sqrt{-g^{\text{IR}}} \lambda_{\text{IR}}(\Phi). \end{aligned} \quad (3.127)$$

As we deal with delta functions it is more practical to use the compact form of the metric given in eq. (3.105) with the definition $ky = A(y)$ where the TeV and Plank branes are located at $y = r_0$ and $y = 0$, respectively. To solve the large hierarchy between the Planck and TeV scales, $kr_0 \sim 37$. Let the background VEV for Φ be $\Phi(x, y) = \Phi_0(y)$. The variation of the radion bulk action with respect to the metric yields

$$\delta S_{\Phi}^{\text{BULK}} = \int d^5x \left\{ \frac{1}{2} g^{MN} \left[\frac{1}{2} (\partial\Phi)^2 - V(\Phi) \right] - \frac{1}{2} \partial^M \Phi \partial^N \Phi \right\} \sqrt{g} \delta g_{MN}. \quad (3.128)$$

Including the brane induced potential terms as calculated in eq. (3.94), the stress-energy tensor

$$T_{MN} = \frac{1}{\sqrt{g}} \frac{\delta S}{\delta g^{MN}}, \quad (3.129)$$

reads

$$\begin{aligned} T^{MN} = & \frac{1}{2} g^{MN} \left[\frac{1}{2} (g_{RS} \partial^R \Phi \partial^S \Phi) - V(\Phi) \right] - \frac{1}{2} \partial^M \Phi \partial^N \Phi \\ & - \frac{1}{2\sqrt{-g_{55}}} g_\mu^M g_\nu^N g^{\mu\nu} \sum_i \lambda_i(\phi) \delta(\phi - \phi_i). \end{aligned} \quad (3.130)$$

Using the relation for the stress-energy tensor and Ricci curvature scalar given in eq. (3.98) for $\mu\nu$ -component with the redefined $R_{\mu\nu}$ in terms of $A(y)$ instead of $\sigma(\phi)$ one writes

$$4A'^2 - A'' = -\frac{2\kappa^2}{3} V(\Phi_0) - \frac{\kappa^2}{3} \sum_i \lambda_i(\Phi_0) \delta(y - y_i), \quad (3.131)$$

In addition, the equation of motion for the radion field can be found by using

$$\partial_M \frac{\partial \mathcal{L}}{\partial (\partial_M \Phi)} - \frac{\partial \mathcal{L}}{\partial \Phi} = 0, \quad (3.132)$$

as

$$\Phi_0'' - 4A'\Phi_0' = \frac{\partial V(\Phi_0)}{\partial \Phi} + \sum_i \frac{\partial \lambda_i(\Phi(0))}{\partial \Phi} \delta(y - y_i). \quad (3.133)$$

Here the primes denotes the derivative with respect to the extra dimension (y). The metric itself is supposed to be continuous. However, there is no requirement that the derivative of the metric to be continuous. The jump in the derivative from $A'(0 - \epsilon)$ to $A'(0 + \epsilon)$ can be expressed in the form

$$A'(y=0) \sim [A'(0 + \epsilon) - A'(0 - \epsilon)]U(y), \quad (3.134)$$

where $U(y)$ is the unit step function. The second derivative reads

$$A''(y=0) \sim [A'(0 + \epsilon) - A'(0 - \epsilon)]\delta(y). \quad (3.135)$$

Thus, the delta function is proportional to the jump in the derivative of A' . In the same way, the delta function in the bulk scalar equation of motion will be proportional to the jump in the derivative Φ' . Therefore, the boundary conditions, (or jump equations) are given by

$$[A']|_i = \frac{\kappa^2}{3} \lambda_i(\Phi_0), \quad [\Phi_0']|_i = \frac{\partial \lambda_i(\Phi_0)}{\partial \Phi}. \quad (3.136)$$

These coupled second order differential equations are quite hard to solve. The solution can be simplified only for specific potentials. We are interested in a bulk potential with a cosmological constant term and a mass term which can be chosen as

$$W(\Phi) = \frac{6k}{\kappa^2} - u\Phi^2. \quad (3.137)$$

One can define the potential $W(\Phi)$ such that

$$A' \equiv \frac{\kappa^2}{6}W(\Phi_0), \quad \Phi' \equiv \frac{1}{2} \frac{\partial W}{\partial \Phi_0}, \quad (3.138)$$

and solve for Φ_0 using the boundary condition at $y = 0$, $\Phi_0 = \Phi_P$ which gives

$$\Phi_0(y) = \Phi_P e^{-uy}. \quad (3.139)$$

Then, at the TeV brane (i.e., $y = r_0$) the scalar is determined to be

$$\Phi_T = \Phi_P e^{-ur_0}, \quad (3.140)$$

which means that the the brane separation is no longer arbitrary but given by,

$$r_0 = \frac{1}{u} \ln \frac{\Phi_P}{\Phi_T}. \quad (3.141)$$

This is the so called Golberger Wise mechanism [65]. The background metric will be obtained as

$$A(y) = ky + \frac{\kappa^2 \Phi_P^2}{12} e^{-2uy}, \quad (3.142)$$

where the first term is the usual RS warp factor and the second term is the backreaction of the metric to the non-vanishing scalar field in the bulk. The right hierarchy between M_{Pl} and M_{EW} will be generated ensuring that $kr \sim 30$ as calculated in eq. (3.125). Thus, we get

$$\frac{k}{u} \ln \left(\frac{\Phi_P}{\Phi_T} \right) \sim 37, \quad (3.143)$$

which is the ratio that will set the hierarchy in the RS1 model. Since Φ_P/Φ_T is constant, so u is kept constant.

Once we established the stabilization mechanism of radion, we realize that it is no longer massless. Therefore, one has to extend the AdS metric including the scalar perturbation such that

$$ds^2 = e^{-2(A(y)+F(x,y))} \eta_{\mu\nu} dx^\mu dx^\nu - (1 + 2F(x,y))^2 dy^2, \quad (3.144)$$

where $A(y) = ky$ and $F(x, y)$ is the 5D radion field. In linear order in the fluctuation $F(x, y)$, the metric perturbation reads

$$\delta(ds^2) \approx -2F(x, y) \left(e^{-2A(y)} \eta_{\mu\nu} dx^\mu dx^\nu + 2dy^2 \right). \quad (3.145)$$

The perturbed metric can also be expressed as

$$ds^2 = \left(\frac{R}{z} \right)^2 \left(e^{-2F(x, z)} \eta_{\mu\nu} dx^\mu dx^\nu - (1 + 2F(x, z))^2 dz^2 \right). \quad (3.146)$$

Note that even in z coordinates, the metric is no longer conformally flat. In linear order in $F(x, z)$ we obtain

$$\delta(ds^2) \approx -2F(x, z) \left(\frac{R}{z} \right)^2 (\eta_{\mu\nu} dx^\mu dx^\nu + 2dz^2). \quad (3.147)$$

The radion can be written as $F(x, z) = \phi_0(x)R(z)$ where $\phi_0(x)$ is the 4D radion field. In the limit of small back-reaction, the relation between $\phi_0(x)$ and $F(x, z)$ is

$$F(x, z) = \frac{1}{\sqrt{6}} \frac{R^2}{R'} \left(\frac{z}{R} \right)^2 \phi_0(x) = \frac{\phi_0(x)}{\Lambda_\phi} \left(\frac{z}{R'} \right)^2, \quad (3.148)$$

where $\Lambda_\phi = \sqrt{6}/R'$ is the radion interaction scale. This relation of Λ_ϕ could be slightly modified with the addition of gravity brane kinetic terms, and thus allow some flexibility on the precise definition of Λ_ϕ in terms of the other model parameters.

The mass of the radion depends on the mechanism that stabilizes the size of the extra dimension. In a simple model with a bulk scalar which generates a VEV, the radion field emerges as a pseudo-Goldstone boson associated with breaking of translation symmetry [65].

Generically, the radion may be the lightest new state in a Randall-Sundrum type setup, with a mass typically suppressed with respect to KK fields by a volume factor of ~ 40 [70], which then might put its mass between a few tens to a few hundreds of GeV, with suppressed couplings which allow it to have escaped detection at LEP, and consistent with precision electroweak data.

3.4.4 The SM fields propagating in the bulk

In the original scenario of warped extra dimensions proposed by Randall and Sundrum all the SM fields were localized on the TeV brane and gravity was the only field allowed

to propagate in the bulk. However, this model was suffering from the shortcoming that one can introduce higher dimensional operators of the IR fields which in the 4D effective theory are only suppressed by TeV scales, leading to large flavor violation and rapid proton decay. To address these issues the most popular venue has been to allow the SM fermions and gauge bosons to propagate in the bulk [73–85] which not only reduced the flavor problem, but also provided a compelling theory of flavor, in which hierarchies among the fermion masses arise naturally [86–90].

Bulk Gauge Fields

We assume the gauge symmetry group for the warped extra dimensional scenarios to be the same as the SM one which is given in eq. (2.1). The 4D gauge fields of the SM, on the other hand, have to be extended into the corresponding 5D bulk gauge fields such that $B_\mu \rightarrow B_M$, $W_\mu^i \rightarrow W_M^i$ and $G_\mu^a \rightarrow G_M^a$ which later will be decomposed into the representations of the 4D Lorentz group as the vector B_μ and the scalar B_5 , the vector W_μ^i and the scalar W_5^i , and the vector G_μ^a and the scalar G_5^a . We choose the vector components (to ensure zero modes corresponding to the SM gauge bosons) to be even under the Z_2 orbifold symmetry, while the scalar components are odd. Taking into account the additional dimension in space-time and the non-trivial metric, the action for the gauge fields reads

$$\mathcal{S}_{\text{GB}}^{\text{Kin}} = -\frac{1}{4} \int d^5x \sqrt{g} g^{KM} g^{LN} \left(B_{KL} B_{MN} + \sum_{i=1}^3 W_{KL}^i W_{MN}^i + \sum_{a=1}^8 G_{KL}^a G_{MN}^a \right), \quad (3.149)$$

where the field strength tensors are defined in analogy to the 4D ones as given in eq. (2.13)

$$\begin{aligned} B_{MN} &= \partial_M B_N - \partial_N B_M, \\ W_{MN}^i &= \partial_M W_N^i - \partial_N W_M^i + g \epsilon^{ijk} W_M^j W_N^k, \quad i, j, k = 1, \dots, 3, \\ G_{MN}^a &= \partial_M G_N^a - \partial_N G_M^a - g_s f^{abc} G_M^b G_N^c, \quad a, b, c = 1, \dots, 8. \end{aligned} \quad (3.150)$$

After EWSB, to diagonalize the gauge boson mass terms we use the redefinitions

$$W_M^\pm = \frac{1}{\sqrt{2}} (W_M^1 \mp i W_M^2), \quad (3.151)$$

and

$$\begin{pmatrix} Z_M \\ A_M \end{pmatrix} = \begin{pmatrix} \cos \theta_w & -\sin \theta_w \\ \sin \theta_w & \cos \theta_w \end{pmatrix} \begin{pmatrix} W_M^3 \\ B_M \end{pmatrix}, \quad (3.152)$$

where θ_w is the 5D Weinberg angle defined as

$$\sin \theta_w = \frac{g'_5}{\sqrt{g_5^2 + g_5'^2}} = \frac{g'}{\sqrt{g^2 + g'^2}}, \quad \cos \theta_w = \frac{g_5}{\sqrt{g_5^2 + g_5'^2}} = \frac{g}{\sqrt{g^2 + g'^2}}, \quad (3.153)$$

with the 4D gauge coupling introduced as

$$g = \frac{g_5}{\sqrt{2\pi r}} = \frac{g_5}{\sqrt{2R \ln(z/R)}}, \quad (3.154)$$

and similar for the other gauge couplings. Here, g_5 and g'_5 are the 5D gauge couplings of the groups $SU(2)_L$ and $U(1)_Y$, respectively. Evaluating the four-vector part of the Higgs kinetic Lagrangian one can see that the bulk gauge fields get masses

$$M_W = \frac{g_5 v}{\sqrt{2}}, \quad M_Z = \sqrt{\frac{g_5^2 + g_5'^2}{2}} v, \quad (3.155)$$

while the photon remains massless $M_A = 0$. The actions for the radion couplings to the gauge bosons are

$$S_W = \int d^5x \sqrt{g} \left(-\frac{1}{2} g^{MN} g^{KL} W_{MK}^\dagger W_{NL} + g^{\mu\nu} \frac{\delta(z-R')}{\sqrt{-g_{55}}} (g_5 v)^2 W_\mu^\dagger W_\nu \right), \quad (3.156)$$

and

$$S_Z = \int d^5x \sqrt{g} \left(-\frac{1}{4} g^{MN} g^{KL} Z_{MK}^\dagger Z_{NL} + \frac{1}{2} g^{\mu\nu} \frac{\delta(z-R')}{\sqrt{-g_{55}}} \times (\sqrt{g_5^2 + g_5'^2} v)^2 Z_\mu^\dagger Z_\nu \right). \quad (3.157)$$

For the massless gauge bosons we have

$$S_{\text{massless}} = -\frac{1}{4g_5^2} \int d^5x \sqrt{g} F_{MN} F^{MN} - \frac{1}{4} \int d^5x \sqrt{-g_{\text{IR}}} \tau_{\text{IR}} F_{\mu\nu} F^{\mu\nu} - \frac{1}{4} \int d^5x \sqrt{-g_{\text{UV}}} \tau_{\text{UV}} F_{\mu\nu} F^{\mu\nu}, \quad (3.158)$$

where $\tau_{\text{IR,UV}}$ parametrize the kinetic terms induced on Plank and TeV branes. The Feynman rules are summarized in Appendix E-2.

Bulk Fermions

By allowing the SM fermions to propagate in the bulk of the extra dimension one can suppress the contributions from higher dimensional operators leading to rapid proton decay, and also explain the fermion mass hierarchy by fermion localization in the

extra dimension [86–90]. The drawback is that, in the minimal models, excitations of the bulk fields are subjected to tight bounds from precision electroweak tests and flavor physics [93,94,173], and constrained to be heavier than a few TeV, which makes it very hard to produce and observe heavy resonances of these masses at the LHC.

We will focus on 5D fermions of the down quark sector which are in Weyl notation given by

$$Q_i = \begin{pmatrix} \mathcal{Q}_L^i \\ \bar{\mathcal{Q}}_R^i \end{pmatrix}, \quad D_i = \begin{pmatrix} \mathcal{D}_L^i \\ \bar{\mathcal{D}}_R^i \end{pmatrix}. \quad (3.159)$$

One can perform a “mixed” KK decomposition as

$$\begin{aligned} \mathcal{Q}_L^i(x, z) &= \sum_j Q_L^{ij}(z) q_L^j(x), & \bar{\mathcal{Q}}_R^i(x, z) &= \sum_j Q_R^{ij}(z) \bar{d}_R^j(x), \\ \mathcal{D}_L^i(x, z) &= \sum_j D_L^{ij}(z) q_L^j(x), & \bar{\mathcal{D}}_R^i(x, z) &= \sum_j D_R^{ij}(z) \bar{d}_R^j(x). \end{aligned} \quad (3.160)$$

Here $q_L^j(x)$ and $\bar{d}_R^j(x)$ are the 4D fermions and $Q_{L,R}^{ij}(z)$ and $D_{L,R}^{ij}(z)$ are the corresponding profiles along the extra dimension. The action for the bulk fermions in 5D is

$$S_{\text{fermion}} = \int d^5x \sqrt{g} \left[\frac{i}{2} (\bar{Q} \Gamma^M D_M Q - D_M \bar{Q} \Gamma^M Q) + \frac{c_q}{R} \bar{Q} Q + (Q \rightarrow D) \right], \quad (3.161)$$

where c_q and c_d (c_d comes with a minus sign) are the 5D fermion mass coefficients. $\Gamma^M = \gamma^a e_a^M$ are the 5D gamma matrices with $\gamma^a = (\gamma^\mu, i\gamma^5)$ providing an appropriate 4D representation of Dirac matrices in 5D, and e_a^M are 5D vielbeins defined by $e_a^M e_b^N \eta^{ab} = g^{MN}$. To linear order in F they are given by

$$e_M^a = \text{diag} \frac{z}{R} (1 + F, 1 + F, 1 + F, 1 + F, 1 - 2F). \quad (3.162)$$

The covariant derivative is $D_M = \partial_M + \omega_M$ and $\omega_M = \frac{1}{2} \omega_{bcM} \sigma^{bc}$ where ω 's are the spin connections and $\sigma^{bc} = \frac{i}{2} [\gamma^b, \gamma^c]$. Substituting the explicit form of vielbeins, 5D gamma matrices, 5D spinors in Weyl notation (see Appendix A), and the covariant derivative we obtain the action as

$$\begin{aligned} S_{\text{fermion}} = & \frac{\phi_0}{\sqrt{6}} \frac{R^2}{R^2} \int d^5x \left(\frac{R}{z} \right)^2 \left[-i (\mathcal{Q}_L \sigma^\mu \partial_\mu \bar{\mathcal{Q}}_R + \bar{\mathcal{Q}}_L \bar{\sigma}^\mu \partial_\mu \mathcal{Q}_R) \right. \\ & \left. + 2 (\mathcal{Q}_L \overleftrightarrow{\partial}_5 \mathcal{Q}_R) - \bar{\mathcal{Q}}_L \overleftrightarrow{\partial}_5 \bar{\mathcal{Q}}_R + \frac{2c}{z} (\mathcal{Q}_L \mathcal{Q}_R + \bar{\mathcal{Q}}_L \bar{\mathcal{Q}}_R) \right]. \end{aligned} \quad (3.163)$$

To obtain a chiral spectrum choose boundary conditions as

$$Q_L(++), \quad Q_R(--), \quad D_L(--), \quad D_R(++). \quad (3.164)$$

where $+$ ($-$) and $-$ signs on the left(right) are the boundary condition for the vector components (scalar component) and $+$ ($-$) sign indicates that the components are even(odd) under the Z_2 orbifold symmetry. Then only Q_L and D_L have zero modes with the wave functions

$$Q_L^0(z) = f(c_q) \frac{R'^{-1/2+c_q}}{R^2} z^{2-c_q}, \quad (3.165)$$

$$D_L^0(z) = f(c_d) \frac{R'^{-1/2+c_d}}{R^2} z^{2-c_d}, \quad (3.166)$$

$$(3.167)$$

where

$$f(c) \equiv \sqrt{\frac{1-2c}{1-\frac{R}{R'}^{1-2c}}}. \quad (3.168)$$

Note that for $c_q > 1/2$ ($c_q < 1/2$) the zero modes are localized towards UV-brane (IR-brane). The KK modes are all localized at IR-brane. The wave functions of KK modes of Q_L and D_R are all localized on the IR-brane, whereas the ones for Q_R and D_L vanish due to their boundary conditions. The 4D SM fermions satisfies the Dirac equation

$$-i\bar{\sigma}^\mu \partial_\mu q_L^i + m_{ij}^d \bar{d}_R^j = 0, \quad (3.169)$$

$$-i\sigma^\mu \partial_\mu \bar{d}_R^i + m_{ij}^d q_L^j = 0. \quad (3.170)$$

The 4D SM fermion mass matrix m_{ij} is the eigenvalue which emerges from the solution of the coupled bulk equations of motion, and is not necessarily diagonal in flavor space. The couplings between the radion and SM fermions can be obtained by inserting the perturbed metric of eq. (3.146) and the 5D fermion KK decompositions of eq. (3.160) into the action of eq. (3.163). We proceed by using a perturbative approach in treating the 4D fermion masses m_{ij} as small expansion parameters and keeping only first order terms. A 5D bulk Higgs field perturbation contains itself some radion degree of freedom. Including all the contributions, the radion coupling to fermions can be expressed finally as

$$\mathcal{L}_{\text{FV}}(\phi_0) = -\frac{\phi_0(x)}{\Lambda_\phi} (q_L^i d_R^j + \bar{q}_L^i \bar{d}_R^j) m_{ij}^d [\mathcal{I}(c_{q_i}) + \mathcal{I}(c_{d_j})] + (d \rightarrow u), \quad (3.171)$$

with the definition

$$\mathcal{I}(c) = \left[\frac{(\frac{1}{2} - c)}{1 - (R/R')^{1-2c}} + c \right] \approx \begin{cases} c & (c > 1/2) \\ \frac{1}{2} & (c < 1/2) \end{cases}. \quad (3.172)$$

This result from [174] is consistent with the original calculation obtained for the case of a brane Higgs and a single family of fermions in [70].

The terms of the Higgs field interacting with fermions are included in the Yukawa Lagrangian. As mentioned before delocalized fermions provide a natural explanation of the flavor structure of the SM. Starting from anarchic 5D Yukawa couplings (i.e., they are all $\mathcal{O}(1)$), large hierarchies can be generated by localizing fermions at different points in the fifth dimension. For the brane localized Higgs scenario we have

$$S_{\text{brane}} = \int d^4x dz \delta(z - R') \left(\frac{R}{z} \right)^4 H (Y_1^{5D} R \bar{Q}_L \mathcal{D}_R + Y_2^{5D} R \bar{Q}_R \mathcal{D}_L + \text{h.c.}). \quad (3.173)$$

Here the Yukawa couplings $[Y_1^{5D}]$ and $[Y_2^{5D}]$ are independent and $\dim[Y_{1,2}^{5D}] = 0$. The equations of motions are obtained as follows

$$\begin{aligned} -m_d Q_L - \partial_z Q_R + \frac{c_q + 2}{z} Q_R + v_4 \delta(z - R') Y_1^{5D} R' D_R &= 0, \\ -m_d^* Q_R - \partial_z Q_L + \frac{c_q - 2}{z} Q_L + v_4 \delta(z - R') Y_2^{5D} R' D_L &= 0, \\ -m_d D_L - \partial_z D_R + \frac{c_d + 2}{z} D_R + v_4 \delta(z - R') Y_2^{5D} R' Q_R &= 0, \\ -m_d^* D_R - \partial_z D_L + \frac{c_d - 2}{z} D_L + v_4 \delta(z - R') Y_1^{5D} R' D_L &= 0. \end{aligned} \quad (3.174)$$

The odd wave functions Q_R and D_L vanish at the TeV brane due to their boundary conditions. However, in the above equations the delta functions give a jump at the TeV brane creating an ambiguity. To remove this ambiguity the following regularization can be imposed on the delta function

$$\delta(z - R') = \lim_{\epsilon \rightarrow 0} \begin{cases} \frac{1}{\epsilon}, & \text{if } R' - \epsilon < z < R' \\ 0, & \text{if } z < R' - \epsilon. \end{cases} \quad (3.175)$$

We use the Dirichlet boundary conditions

$$Q_R(R') = D_L(R') = 0, \quad (3.176)$$

and integrate the equations of motion to obtain the profiles near the IR brane as

$$\begin{aligned} Q_R(z) &= v_4 Y_1^{5D} R' D_R(R') \left(\frac{z - R'}{\epsilon} \right), \quad \text{for } R' - \epsilon < z < R', \\ D_L(z) &= -v_4 Y_1^{5D*} R' Q_L(R') \left(\frac{z - R'}{\epsilon} \right), \quad \text{for } R' - \epsilon < z < R', \end{aligned} \quad (3.177)$$

3.4.5 Flavor Misalignment

As mentioned in the beginning of the Subsection 2.4, in an effective field theory, it is possible to have terms with mass dimension $D > 4$ as long as the inverse power of the scale of new physics appears. Below we write the the lowest order operators which generate misalignment in flavor space between the Higgs Yukawa couplings and the SM fermion masses. For simplicity, we concentrate on the down-quark sector and write the dimension six operators of the 4D effective Lagrangian [175–179]

$$\lambda_{ij} \frac{H^2}{\Lambda^2} H \bar{\mathcal{Q}}_{L_i} \mathcal{D}_{R_j}, \quad k_{ij}^{\mathcal{D}} \frac{H^2}{\Lambda^2} \bar{\mathcal{D}}_{R_i} \not{\partial} \mathcal{D}_{R_j}, \quad k_{ij}^{\mathcal{Q}} \frac{H^2}{\Lambda^2} \bar{\mathcal{Q}}_{L_i} \not{\partial} \mathcal{Q}_{L_j}, \quad (3.178)$$

where λ_{ij} , $k_{ij}^{\mathcal{D}}$, and $k_{ij}^{\mathcal{Q}}$ are complex couplings with i, j being the flavor indices and \mathcal{Q}_{L_i} , \mathcal{D}_{R_j} are the fermionic gauge eigen states. Upon EWSB the Higgs field will receive a VEV such that $H = \frac{h}{\sqrt{2}} + v_4$, where h is the physical Higgs field and $v_4 = 174$ GeV. The original Yukawa (y_{ij}^d are the original Yukawa couplings) and kinetic terms are modified as follows

$$\begin{aligned} & y_{ij}^d \left(\frac{h}{\sqrt{2}} + v_4 \right) \bar{\mathcal{Q}}_{L_i} \mathcal{D}_{R_j} + \frac{\lambda_{ij}}{\Lambda^2} \left(\frac{h^3}{2\sqrt{2}} + \frac{3h^2}{\sqrt{2}} v_4 + \frac{3h}{\sqrt{2}} v_4^2 + v_4^3 \right) \bar{\mathcal{Q}}_{L_i} \mathcal{D}_{R_j}, \\ & \frac{\delta_{ij}}{2} \bar{\mathcal{D}}_{R_i} \not{\partial} \mathcal{D}_{R_j} + \frac{k_{ij}^{\mathcal{D}}}{\Lambda^2} \left(\frac{h^2}{2} + \frac{2h}{\sqrt{2}} v_4 + v_4^2 \right) \bar{\mathcal{D}}_{R_i} \not{\partial} \mathcal{D}_{R_j}, \\ & \frac{\delta_{ij}}{2} \bar{\mathcal{Q}}_{L_i} \not{\partial} \mathcal{Q}_{L_j} + \frac{k_{ij}^{\mathcal{Q}}}{\Lambda^2} \left(\frac{h^2}{2} + \frac{2h}{\sqrt{2}} v_4 + v_4^2 \right) \bar{\mathcal{Q}}_{L_i} \not{\partial} \mathcal{Q}_{L_j}. \end{aligned} \quad (3.179)$$

The addition of dimension six operators give rise to corrections to the fermion mass and kinetic terms in the following way

$$v_4 \left(y_{ij}^d + \lambda_{ij} \frac{v_4^2}{\Lambda^2} \right) \bar{\mathcal{Q}}_{L_i} \mathcal{D}_{R_j}, \quad \left(\frac{\delta_{ij}}{2} + k_{ij}^{\mathcal{D}} \frac{v_4^2}{\Lambda^2} \right) \bar{\mathcal{D}}_{R_i} \not{\partial} \mathcal{D}_{R_j}, \quad \left(\frac{\delta_{ij}}{2} + k_{ij}^{\mathcal{Q}} \frac{v_4^2}{\Lambda^2} \right) \bar{\mathcal{Q}}_{L_i} \not{\partial} \mathcal{Q}_{L_j}. \quad (3.180)$$

As a result of these alterations, the mass and kinetic terms of the fermions are not diagonal anymore. Therefore, one has to redefine the fermion fields to canonically normalize the new kinetic energy terms and one more transformation will be needed to diagonalize the resulting mass matrix. In addition, there will be corrections to Higgs-fermion-fermion couplings given by

$$\left(y_{ij}^d + 3\lambda_{ij} \frac{v_4^2}{\Lambda^2} \right) \frac{h}{\sqrt{2}} \bar{\mathcal{Q}}_{L_i} \mathcal{D}_{R_j}, \quad \left(2k_{ij}^{\mathcal{D}} \frac{v_4}{\Lambda^2} \right) \frac{h}{\sqrt{2}} \bar{\mathcal{D}}_{R_i} \not{\partial} \mathcal{D}_{R_j}, \quad \left(2k_{ij}^{\mathcal{Q}} \frac{v_4}{\Lambda^2} \right) \frac{h}{\sqrt{2}} \bar{\mathcal{Q}}_{L_i} \not{\partial} \mathcal{Q}_{L_j}. \quad (3.181)$$

These cannot be diagonalized with the fermion redefinitions and rotations obtained from eq. (3.180), and thus generate tree-level flavor changing Higgs couplings, with a generic size v_4^2/Λ^2 .

In warped extra dimensional scenarios we can easily estimate the size of a misalignment of this kind by using mass insertion approximation. For a bulk Higgs localized near the IR brane, the zero-zero-Higgs, zero-KK-Higgs, KK-KK-Higgs Yukawa couplings are given approximately by

$$Y_{d,00} \sim Y_* f(c_q) f(c_d), \quad (3.182)$$

$$Y_{d,0n} \sim Y_* f(c_q) \text{ or } Y_* f(c_d), \quad (3.183)$$

$$Y_{d,nm} \sim Y_*, \quad (3.184)$$

where $Y_* = Y_d/\sqrt{R}$ is the $\mathcal{O}(1)$ dimensionless 5D Yukawa coupling, (typically not larger than a value of 3 due to perturbativity constraints). Terms with $\mathcal{O}(1)$ factors other than 5D Yukawa couplings are omitted in the previous equations. The SM fermions are mostly zero mode fermions with some small amount of mixing with KK mode fermions. Therefore, we can use the mass insertion approximation to calculate the corrections to the masses and Yukawa couplings of SM fermions.

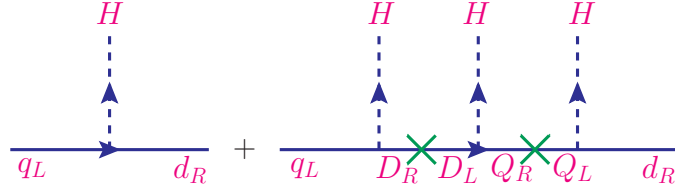


Figure 9: Correction to fermion masses and to physical Yukawa couplings (right diagram) of SM fermions using the mass insertion approximation.

This is shown in Fig. 9. From the Feynman diagrams given in this Figure the SM fermion mass can be written by

$$\begin{aligned} m_{SM}^d &\approx Y_{d,00} v_4 - Y_{d,0n} Y_{d,nm} Y_{d,m0} v_4 \frac{v_4^2}{M_{KK}^2} f(c_d) Y_* v_4 \\ &\approx f(c_q) Y_* f(c_d) v_4 - f(c_q) \frac{Y_*^2 v_4^2}{M_{KK}^2} f(c_d) Y_* v_4, \end{aligned} \quad (3.185)$$

where we assume that all KK fermion masses are of the same order (M_{KK}). The 4D effective Yukawa couplings of SM fermions can be calculated using the same diagram, but the correction will be different. This is because in the second diagram of Figure 9, we have to set two external Higgs bosons H to their VEV v_4 while the other one

becomes the physical Higgs h , and there are three different ways to do this. Thus, we obtain the 4D Yukawa couplings

$$y_{SM}^d \approx f(c_q)Y_*f(c_d) - 3f(c_q)\frac{Y_*^2v_4^2}{M_{KK}^2}f(c_d)Y_*. \quad (3.186)$$

We see that the SM fermion masses and the 4D Yukawa couplings are not universally proportional but there is a shift with respect to the SM prediction of $m_{SM}^d = y_{SM}^d v_4$. This shift, or misalignment, is defined as $\Delta^d = m_{SM}^d - y_{SM}^d v_4$ and equal to

$$\Delta_1^d \approx 2f(c_q)\frac{Y_*^2v_4^2}{M_{KK}^2}f(c_d)v_4Y_*. \quad (3.187)$$

We call this as the first misalignment and indicate it by a subscript 1. The second source of the shift comes from the corrections to the kinetic terms as shown in Figure 10.

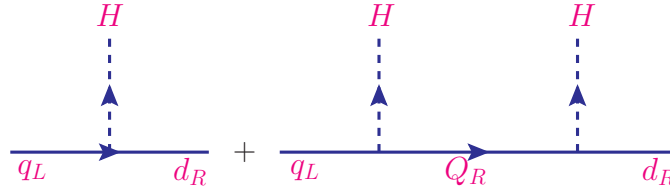


Figure 10: Correction to kinetic terms using the insertion approximation.

The kinetic term also receives a correction induced by the mixing of SM fermions with KK modes as

$$\left(1 + Y_{d,0n}Y_{d,n0}\frac{H^2}{M_{KK}^2}\right)\bar{q}_L^{\text{SM}}i\not{\partial}q_L^{\text{SM}} \approx \left(1 + f(c_q)^2Y_*^2\frac{H^2}{M_{KK}^2}\right)\bar{q}_L^{\text{SM}}i\not{\partial}q_L^{\text{SM}}. \quad (3.188)$$

To get the canonically normalized kinetic terms we redefine the fields which leading a new shift between the masses and the Yukawa couplings of the SM fields given by

$$\Delta_2^d \approx f(c_q)^3Y_*^2\frac{v_4^2}{M_{KK}^2}f(c_d)v_4Y_*. \quad (3.189)$$

Similarly for the down sector we have

$$\Delta_2^{d'} \approx f(c_q)Y_*^2\frac{v_4^2}{M_{KK}^2}f(c_d)^3v_4Y_*. \quad (3.190)$$

The total shift will be

$$\Delta^d = \Delta_1^{d'} + \Delta_2^d + \Delta_2^{d'} \approx f(c_q)Y_*^2\frac{v_4^2}{M_{KK}^2}[2 + f(c_q)^2 + f(c_d)^2]. \quad (3.191)$$

For the first two generations $f(c_{q,d}) \ll 1$. Therefore, the main misalignment comes from the first shift.

In the case of an exactly brane localized Higgs there is a subtlety. Since the wave functions of q_R^{KK} and d_L^{KK} vanish at the TeV brane, their couplings to brane localized Higgs should also vanish. However, upon EWSB the wave functions of the q_R^{KK} and d_L^{KK} fields become discontinuous at the brane location [180] and the jump is proportional to v_4 . The discontinuity requires a regularization which results in infinitesimally small couplings with Higgs. But as we sum over an infinite tower of fermion KK modes, this may yield a finite non-zero result in the end. The shift in the masses and Yukawa couplings in the case of brane Higgs is shown in Figure 11

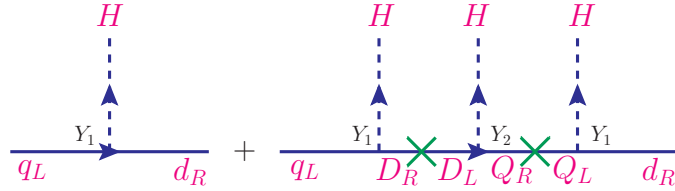


Figure 11: Correction to fermion masses and to physical Yukawa couplings (right diagram) of SM fermions using the mass insertion approximation for brane Higgs scenario.

is

$$\begin{aligned} \Delta_1^d &= 2(Y_2^{5D})^*(Y_1^{5D})^2 R'^3 v_4^3 d_R(R') q_L^*(R') \left(\frac{R}{R'}\right)^4 \int_{R'-\epsilon}^{R'} dz \frac{1}{\epsilon} \left(\frac{z-R'}{\epsilon}\right)^2 \\ &= \frac{2}{3} m_d (Y_2^{5D})^* Y_1^{5D} R'^3 v_4^3 d_R(R') q_L^*(R') \left(\frac{R}{R'}\right)^4 \end{aligned} \quad (3.192)$$

and the SM fermion mass is given by

$$m_d \approx \left(\frac{R}{R'}\right)^4 v_4 Y_1^{5D} R' q_L^*(R') d_R(R'). \quad (3.193)$$

The misalignment including $\mathcal{O}(1)$ terms only becomes [181]

$$\Delta_1^d = \frac{2}{3} m_d Y_1^{5D} (Y_2^{5D})^* v_4^2 R'^2 = \frac{2}{3} |m_d|^2 m_d R'^2 \left(\frac{Y_2^{5D}}{Y_1^{5D}}\right)^* \frac{1}{f(c_q)^2 f(-c_d)^2}. \quad (3.194)$$

Note the presence of the independent couplings Y_2^{5D} which are not necessary for generating fermion masses. It is technically possible to set their values as small as

necessary and suppress the misalignment. Nevertheless this seems to go against the main philosophy of our approach which assumes that the value of all dimensionless 5D parameters is of order one. Moreover in the case where the Higgs is a bulk scalar field we have $Y_1 = Y_2$, which is the simplifying assumption we make for our numerical computations.

There is another contribution to the misalignment can be also calculated and is given by [181]

$$\Delta_2^d = m_d |m_d|^2 R'^2 [K(c_q) + K(-c_d)], \quad (3.195)$$

with

$$K(c) \equiv \frac{1}{1-2c} \left[-\frac{1}{\epsilon^{2c-1}-1} + \frac{\epsilon^{2c-1}-\epsilon^2}{(\epsilon^{2c-1}-1)(3-2c)} + \frac{\epsilon^{1-2c}-\epsilon^2}{(1+2c)(\epsilon^{2c-1}-1)} \right]. \quad (3.196)$$

The two contributions to the misalignment, Δ_1^d and Δ_2^d , can be of the same parametric order only for IR localized fermions (heavy quarks). In the case of light fermions, the Δ_2^d contribution will be highly suppressed, effectively leaving only the contribution from the Δ_1^d term.

3.4.6 Radion-Higgs Mixing

Since the radion and the Higgs bosons have the same quantum numbers, it is possible for them to mix via kinetic factors:³

$$S_\xi = \xi \int d^4x \sqrt{-g_{\text{IR}}} R(g^{\text{IR}}) \hat{H}^\dagger \hat{H}, \quad (3.197)$$

The effective 4D Lagrangian up to quadratic order is

$$\mathcal{L} = -\frac{1}{2}(1+6\gamma^2\xi)\phi_0\Box\phi_0 - \frac{1}{2}h_0\Box h_0 - 6\gamma\xi\phi_0\Box h_0 - \frac{1}{2}\phi_0 m_{\phi_0}^2 \phi_0 - \frac{1}{2}h_0 m_{h_0}^2 h_0, \quad (3.198)$$

where the first three are kinetic energy terms and the rest are mass terms with m_{h_0} and m_{ϕ_0} are being the Higgs and radion masses before mixing, respectively. Let the states diagonalizing the kinetic terms be h' and ϕ' . They can be introduced as

$$\begin{pmatrix} h_0 \\ \phi_0 \end{pmatrix} = \begin{pmatrix} d' & c' \\ b' & a' \end{pmatrix} \begin{pmatrix} h' \\ \phi' \end{pmatrix}. \quad (3.199)$$

³We note that in the case of a bulk Higgs, there will be Higgs-radion mixing at the level of the bulk scalar potential, without the need to introduce kinetic mixing. For simplicity, we will assume that the Higgs is highly localized on the brane and consider only brane kinetic mixing.

Substituting the redefinitions from eq. (3.199) we obtain the kinetic terms as

$$\begin{aligned}\mathcal{L}^{Kin} &= -\frac{1}{2}\left(c'^2 + (1 + 6\gamma^2\xi)a'^2 + 12\gamma\xi a'c'\right)\phi'\square\phi' \\ &\quad -\frac{1}{2}\left(d'^2 + (1 + 6\gamma^2\xi)b'^2 + 12\gamma\xi b'd'\right)h'\square h' \\ &\quad -\left(c'd' + (1 + 6\gamma^2\xi)a'b' + 6\gamma\xi(a'd' + b'c')\right)h'\square\phi'.\end{aligned}\quad (3.200)$$

Assuming ϕ' and h' to be the physical fields, the coefficients of $\phi'\square\phi'$ and $h'\square h'$ terms are equal to $(-1/2)$. Hence we have

$$c'^2 + (1 + 6\gamma^2\xi)a'^2 + 12\gamma\xi a'c' - 1 = 0, \quad (3.201)$$

$$d'^2 + (1 + 6\gamma^2\xi)b'^2 + 12\gamma\xi b'd' - 1 = 0, \quad (3.202)$$

and the coefficient of $h'\square\phi'$ is required to be zero which yields

$$\left(c'd' + (1 + 6\gamma^2\xi)a'b' + 6\gamma\xi(a'd' + b'c')\right)h'\square\phi' = 0. \quad (3.203)$$

We have three equations and four unknowns. Solving for a' , c' and d' in terms of b'

$$d' = -6\gamma\xi b' \pm \sqrt{1 - b'^2 Z^2}, \quad a' = \pm \frac{\sqrt{1 - b'^2 Z^2}}{|Z|}, \quad c' = \mp \frac{6\gamma\xi \sqrt{1 - b'^2 Z^2}}{|Z|} + |b'Z| \quad (3.204)$$

where $Z^2 = 1 + 6\gamma^2\xi(1 - 6\xi) = \beta - 36\xi^2\gamma^2$. After undoing the kinetic mixing Z becomes the coefficient of the radion kinetic term, and is therefore required to be positive definite bringing theoretical limits on the ξ parameter

$$\frac{1}{12}\left(1 - \sqrt{1 + \frac{4}{\gamma^2}}\right) \leq \xi \leq \frac{1}{12}\left(1 + \sqrt{1 + \frac{4}{\gamma^2}}\right). \quad (3.205)$$

The parameter ξ is also subject to strong restrictions coming from precision electroweak constraints (on S and T parameters), LEP/LEP2 data, and Tevatron bounds [70, 72]. Assuming $b' = 0$ the kinetic terms are diagonalized by the shift

$$\begin{pmatrix} h_0 \\ \phi_0 \end{pmatrix} = \begin{pmatrix} 1 & \frac{6\gamma\xi}{Z} \\ 0 & -\frac{1}{Z} \end{pmatrix} \begin{pmatrix} h' \\ \phi' \end{pmatrix}. \quad (3.206)$$

We check whether or not this redefinition diagonalizes the mass terms as well. Substituting the redefinitions from eq. (3.199) we obtain the mass terms

$$\begin{aligned}\mathcal{L}^{Mass} &= -\frac{1}{2}(a'^2 m_{\phi_0}^2 + c'^2 m_{h_0}^2)\phi'^2 - \frac{1}{2}(b'^2 m_{\phi_0}^2 + d'^2 m_{h_0}^2)h'^2 \\ &\quad - (a'b' m_{\phi_0}^2 + c'd' m_{h_0}^2)h'\phi'.\end{aligned}\quad (3.207)$$

The coefficients of ϕ'^2 and h'^2 are required to be equal to $(-1/2)m_{\phi'}^2$ and $(-1/2)m_{h'}^2$, respectively where $m_{h'}$ and $m_{\phi'}$ are assumed to be the corresponding masses after mixing and the coefficient of the mass mixing term in eq. (3.207) has to be zero. By focusing on the last term one can easily realize that

$$a' b' m_{\phi_0}^2 + c' d' m_{h_0}^2 = \frac{6\gamma\xi}{Z} m_{h_0}^2 \neq 0. \quad (3.208)$$

Therefore, we need one more transformation. Let

$$\begin{pmatrix} h' \\ \phi' \end{pmatrix} = \begin{pmatrix} \cos\theta & \sin\theta \\ -\sin\theta & \cos\theta \end{pmatrix} \begin{pmatrix} h \\ \phi \end{pmatrix}. \quad (3.209)$$

or equivalently

$$\begin{pmatrix} h_0 \\ \phi_0 \end{pmatrix} = \begin{pmatrix} d & c \\ b & a \end{pmatrix} \begin{pmatrix} h \\ \phi \end{pmatrix} = \begin{pmatrix} \cos\theta - \frac{6\gamma\xi}{Z} \sin\theta & \sin\theta + \frac{6\gamma\xi}{Z} \cos\theta \\ \frac{\sin\theta}{Z} & -\frac{\cos\theta}{Z} \end{pmatrix} \begin{pmatrix} h \\ \phi \end{pmatrix} \quad (3.210)$$

It is important to remark that this transformation is not orthogonal. It is a combination of an non-orthogonal transformation which diagonalizes the the kinetic terms and an orthogonal transformation which diagonalizes the mass terms in the 4D effective Lagrangian. The Lagrangian including the mass terms then becomes

$$\begin{aligned} \mathcal{L}^{Mass} &= -\frac{1}{2} \left[\frac{\cos^2\theta}{Z^2} m_{\phi_0}^2 + \left(\sin^2\theta + \frac{6\gamma\xi \sin 2\theta}{Z} + \frac{36\gamma^2\xi^2 \cos^2\theta}{Z^2} \right) m_{h_0}^2 \right] \phi^2 \\ &\quad -\frac{1}{2} \left[\frac{\sin^2\theta}{Z^2} m_{\phi_0}^2 + \left(\cos^2\theta - \frac{6\gamma\xi \sin 2\theta}{Z} + \frac{36\gamma^2\xi^2 \sin^2\theta}{Z^2} \right) m_{h_0}^2 \right] h^2 \\ &\quad + \left[\left\{ \frac{m_{\phi_0}^2 - (Z^2 - 36\gamma^2\xi^2) m_{h_0}^2}{2Z^2} \right\} \sin 2\theta - \frac{6\gamma\xi m_{h_0}^2}{Z} \cos 2\theta \right] h\phi. \quad (3.211) \end{aligned}$$

The coefficients of ϕ^2 and h^2 are supposed to be equal to $-m_{\phi}^2/2$ and $-m_h^2/2$, respectively, yielding

$$\begin{aligned} m_{\phi}^2 &= \frac{\cos^2\theta}{Z^2} m_{\phi_0}^2 + \left(\sin^2\theta + \frac{6\gamma\xi \sin 2\theta}{Z} + \frac{36\gamma^2\xi^2 \cos^2\theta}{Z^2} \right) m_{h_0}^2, \\ m_h^2 &= \frac{\sin^2\theta}{Z^2} m_{\phi_0}^2 + \left(\cos^2\theta - \frac{6\gamma\xi \sin 2\theta}{Z} + \frac{36\gamma^2\xi^2 \sin^2\theta}{Z^2} \right) m_{h_0}^2. \quad (3.212) \end{aligned}$$

Requiring the coefficient of the last term in eq. (3.211), which is the mixing between the h and ϕ , to be zero we get the mixing angle θ of the orthogonal transformation as

$$\tan 2\theta = 12\gamma\xi Z \frac{m_{h_0}^2}{m_{\phi_0}^2 - m_{h_0}^2 (Z^2 - 36\gamma^2\xi^2)}. \quad (3.213)$$

The difference between the h and ϕ masses gives

$$m_h^2 - m_\phi^2 = \frac{m_{\phi_0}^2 - m_{h_0}^2 (Z^2 - 36\gamma^2\xi^2)}{Z^2} \cos 2\theta + \frac{12\gamma\xi}{Z} m_{h_0}^2 \sin 2\theta \quad (3.214)$$

which yields using eq. (3.213) gives

$$\sin 2\theta = \frac{12\gamma\xi m_{h_0}^2}{Z(m_\phi^2 - m_h^2)}. \quad (3.215)$$

In addition, there are theoretically excluded parameter regions which do not satisfy requirements of $m_h - m_\phi$ degeneracy. The mass squared values for the physical states are obtained as

$$m_\pm^2 = \frac{1}{2Z^2} \left(m_{\phi_0}^2 + \beta m_{h_0}^2 \pm \sqrt{(m_{\phi_0}^2 + \beta m_{h_0}^2)^2 - 4Z^2 m_{\phi_0}^2 m_{h_0}^2} \right), \quad (3.216)$$

where the larger(smaller) of m_h and m_ϕ will be identified as m_+ (m_-) leading

$$m_+^2 + m_-^2 = \frac{1}{Z^2} (m_{\phi_0}^2 + \beta m_{h_0}^2), \quad m_{\phi_0}^2 m_{h_0}^2 = Z^2 m_+^2 m_-^2. \quad (3.217)$$

We solve for the bare masses in terms of the physical ones. Substituting the equation for $m_+^2 + m_-^2$ given above into m_\pm^2 we get

$$m_\pm^2 = \frac{1}{2Z^2} \left[(m_+^2 + m_-^2) Z^2 \pm \sqrt{(m_+^2 + m_-^2)^2 Z^4 - 4Z^2 m_{\phi_0}^2 m_{h_0}^2} \right]. \quad (3.218)$$

Using eqs. (3.217) and (3.218) we solve for $m_{h_0}^2$ and $m_{\phi_0}^2$ as follows

$$[\beta m_{h_0}^2, m_{\phi_0}^2] = \frac{Z^2}{2} \left[m_+^2 + m_-^2 \pm \sqrt{(m_+^2 + m_-^2)^2 - \frac{4\beta m_+^2 m_-^2}{Z^2}} \right]. \quad (3.219)$$

To keep the masses real, the term inside the square root has to be positive

$$(m_+^2 + m_-^2)^2 - \frac{4\beta m_+^2 m_-^2}{Z^2} > 0. \quad (3.220)$$

Expanding and taking into the parenthesis of m_-^4

$$m_-^4 \left[\frac{m_+^4}{m_-^4} + \left(2 - \frac{4\beta}{Z^2} \right) \frac{m_+^2}{m_-^2} + 1 \right] > 0. \quad (3.221)$$

Since $m_-^4 > 0$, the remaining term in the parenthesis is required to be greater than zero leaving the inequality

$$\frac{m_+^2}{m_-^2} > 1 + \frac{2\beta}{Z^2} \left(1 - \frac{Z^2}{\beta} \right) + \frac{2\beta}{Z^2} \left(1 - \frac{Z^2}{\beta} \right)^{1/2}. \quad (3.222)$$

to keep the bare masses real.

There is an ambiguity regarding the bare masses about which one to take as larger. We resolve this by assuming $m_{h_0}^2 \rightarrow m_h^2$ in the limit $\xi \rightarrow 0$. In this limit $Z \rightarrow 1$ and $\beta \rightarrow 1$ it yields

$$[m_{h_0}^2, m_{\phi_0}^2] = \frac{1}{2} \left[m_+^2 + m_-^2 \pm \sqrt{(m_+^2 + m_-^2)^2 - 4m_+^2 m_-^2} \right]. \quad (3.223)$$

When $m_{h_0}^2 > m_{\phi_0}^2$ we take the plus sign and $m_{h_0}^2 \rightarrow m_+^2$, and for $m_{h_0}^2 < m_{\phi_0}^2$ we get $m_{h_0}^2 \rightarrow m_-^2$. The presence of mixing will modify the couplings to fermions, gluons, photons, W 's and Z 's of both the radion and the Higgs boson and thus change the corresponding decay branching ratios as well as the production rates.

Chapter 4

HIGGS BOSONS in a MINIMAL *R*-PARITY CONSERVING LEFT-RIGHT SUPERSYMMETRIC MODEL

The LRSM, introduced in Section 3.1, has a hierarchy problem similar to the one in the SM, where the masses of the fundamental Higgs scalars diverge quadratically. To cancel these divergences, parameters of the theory have to be fine tuned. Including SUSY can cure this problem with the cancellation of quadratic divergences by the contributions from the corresponding superpartners.

There are also other arguments in favor of a left-right symmetric extension of SUSY, as it resolves several problems of the popular MSSM. The most important one is that the *R*-parity is an exact symmetry of the model, hence, preventing the rapid proton decay [46–48]¹. In addition, it offers a solution to the strong CP problem. Originally, the term

$$\mathcal{L}_{\theta_{\text{QCD}}} = \theta_{\text{QCD}} \frac{g_s^2}{64\pi^2} \epsilon^{\mu\nu\rho\sigma} G_{\mu\nu}^a G_{\rho\sigma}^a, \quad (4.1)$$

was absent in the SM. It is induced, however, due to fermion field redefinitions while diagonalizing the mass terms for quarks and leptons and violates the combined CP invariance in the sector of strong interactions. As this term can contribute to the neutron electric dipole moment, the current experimental limit for the parameter

¹Note that *R* can be broken spontaneously, through $\langle \tilde{\nu}_R \rangle \neq 0$, but *B* is still conserved.

θ_{QCD} is $\theta_{\text{QCD}} \leq 10^{-9}$. Its being unnaturally small is called the strong CP problem. In LRSUSY, since the Yukawa couplings are Hermitian the determinant of the quark mass matrices are ensured to be real, thus proving a solution to the strong CP problem [49, 50].

However, the model in its minimal form seems to suffer from a serious shortcoming. In the global minimum of the theory R -parity is conserved while parity is violated, which breaks electric charge and is therefore unacceptable. Accordingly, the minimization of the Higgs potential requires either spontaneous R -parity breaking by the VEV of the right-chiral scalar neutrino [182] which consecutively results the SUSY dark matter candidate to be lost; or introduction of higher scale non-renormalizable operators [183, 184] which make θ_{QCD} large. A new version of the theory is suggested by Babu and Mohapatra [185], which allows for both R -parity conservation and the absence of higher-dimensional operators by inclusion of the Yukawa coupling of the heavy Majorana neutrino in the effective Lagrangian. The gauge group of the model is the same as LRSM given in eq. (3.1).

4.1 The Particle Content of the Left-Right Supersymmetric Model

In this Subsection we introduce the field content of the LRSUSY. In Table 13 we give the first family of fermions and their bosonic partners, which differ in spin by $1/2$, with the corresponding left-right symmetric assignments under the gauge group G_{LRSM} . Employing left-right symmetry requires the right-chiral fields to be doublets under $SU(2)_R$ as their left-chiral counterparts are under $SU(2)_L$ (see Appendix A for the representations of the fields). We use a superscript (c) for the right-chiral conjugates of left-chiral fields and the supersymmetric partners are denoted by tilde on the top of the fermionic partner. Note that the color charge of quarks are indicated by a superscript (α).

Chiral Field	Component Fields	$SU(3)_c \otimes SU(2)_L \otimes SU(2)_R \otimes U(1)_{B-L}$ Quantum Numbers				Spin
Q_1^α	$\begin{pmatrix} u^\alpha \\ d^\alpha \end{pmatrix}$	3	2	1	$\frac{1}{3}$	1/2
$Q_1^{c\alpha}$	$\begin{pmatrix} d^{c\alpha} \\ -u^{c\alpha} \end{pmatrix}$	3*	1	2	$-\frac{1}{3}$	1/2
\tilde{Q}_1^α	$\begin{pmatrix} \tilde{u}^\alpha \\ \tilde{d}^\alpha \end{pmatrix}$	3	2	1	$\frac{1}{3}$	0
$\tilde{Q}_1^{c\alpha}$	$\begin{pmatrix} \tilde{d}^{c\alpha} \\ -\tilde{u}^{c\alpha} \end{pmatrix}$	3*	1	2	$-\frac{1}{3}$	0
L_1	$\begin{pmatrix} \nu_e \\ e \end{pmatrix}$	1	2	1	-1	1/2
L_1^c	$\begin{pmatrix} e^c \\ -\nu_e^c \end{pmatrix}$	1	1	2	1	1/2
\tilde{L}_1	$\begin{pmatrix} \tilde{\nu}_e \\ \tilde{e} \end{pmatrix}$	1	2	1	-1	0
\tilde{L}_1^c	$\begin{pmatrix} \tilde{e}^c \\ -\tilde{\nu}_e^c \end{pmatrix}$	1	1	2	1	0

Table 13: First generation of fermions and their bosonic superpartners in the LRSUSY including the corresponding $SU(3)_c \otimes SU(2)_L \otimes SU(2)_R \otimes U(1)_{B-L}$ gauge and spin quantum numbers.

In Table 14, we give the field contents, associated gauge quantum numbers and spin quantum numbers for the bosons and their fermionic superpartners in LRSUSY.

Chiral Field	Component Fields	SU(3) _c ⊗ SU(2) _L ⊗ SU(2) _R ⊗ U(1) _{B-L}				Spin
		Quantum Numbers				
V_μ	V_μ	1	1	1	0	1
$W_{L\mu}$	$W_{L\mu}^+, W_{L\mu}^-, W_{L\mu}^3$	1	3	1	0	1
$W_{R\mu}$	$W_{R\mu}^+, W_{R\mu}^-, W_{R\mu}^3$	1	1	3	0	1
G_μ^a	$G_\mu^1, G_\mu^2, \dots, G_\mu^8$	8	1	1	0	1
$\lambda_{V\mu}$	$\lambda_{V\mu}$	1	1	1	0	$\frac{1}{2}$
$\lambda_{L\mu}$	$\lambda_{L\mu}^+, \lambda_{L\mu}^-, \lambda_{L\mu}^3$	1	3	1	0	$\frac{1}{2}$
$\lambda_{R\mu}$	$\lambda_{R\mu}^+, \lambda_{R\mu}^-, \lambda_{R\mu}^3$	1	1	3	0	$\frac{1}{2}$
\tilde{G}_μ^a	$\tilde{G}_\mu^1, \tilde{G}_\mu^2, \dots, \tilde{G}_\mu^8$	8	1	1	0	$\frac{1}{2}$

Table 14: Gauge Bosons and their fermionic partners in the LRSUSY.

A significant difference between the SUSY and LRSUSY concerns the Higgs sector. In the supersymmetrization of the theory, the number of bi-doublets is doubled in order to generate charged leptons and quark masses, and achieve a non-vanishing CKM quark mixing matrix. The number of triplets is doubled for the sake of anomaly cancellations. The right-chiral ($\Delta^c + \bar{\Delta}^c$) fields are needed for $SU(2)_R \otimes U(1)_{B-L}$ symmetry breaking without R -parity violating couplings, and $(\Delta + \bar{\Delta})$ fields are their left-chiral partners, needed for parity invariance. A parity-odd singlet is appended to the theory so that R -parity breaking occurs in the supersymmetric limit.

Higgs Field	Matrix Representation	Vacuum Expectation Values
$\Delta(1, 3, 1, 2)$	$\begin{pmatrix} \frac{\delta^+}{\sqrt{2}} & \delta^{++} \\ \delta^0 & -\frac{\delta^+}{\sqrt{2}} \end{pmatrix}$	$\begin{pmatrix} 0 & 0 \\ v_L & 0 \end{pmatrix}$
$\bar{\Delta}(1, 3, 1, -2)$	$\begin{pmatrix} \frac{\bar{\delta}^-}{\sqrt{2}} & \bar{\delta}^0 \\ \bar{\delta}^{--} & -\frac{\bar{\delta}^-}{\sqrt{2}} \end{pmatrix}$	$\begin{pmatrix} 0 & \bar{v}_L \\ 0 & 0 \end{pmatrix}$
$\Delta^c(1, 1, 3, -2)$	$\begin{pmatrix} \frac{\delta^{c-}}{\sqrt{2}} & \delta^{c0} \\ \delta^{c--} & -\frac{\delta^{c-}}{\sqrt{2}} \end{pmatrix}$	$\begin{pmatrix} 0 & v_R \\ 0 & 0 \end{pmatrix}$
$\bar{\Delta}^c(1, 1, 3, 2)$	$\begin{pmatrix} \frac{\bar{\delta}^{c+}}{\sqrt{2}} & \bar{\delta}^{c++} \\ \bar{\delta}^{c0} & -\frac{\bar{\delta}^{c+}}{\sqrt{2}} \end{pmatrix}$	$\begin{pmatrix} 0 & 0 \\ \bar{v}_R & 0 \end{pmatrix}$
$\Phi_1(1, 2, 2, 0)$	$\begin{pmatrix} \phi_1^+ & \phi_2^0 \\ \phi_1^0 & \phi_2^- \end{pmatrix}$	$\begin{pmatrix} 0 & \kappa'_1 \\ \kappa_1 & 0 \end{pmatrix}$
$\Phi_2(1, 2, 2, 0)$	$\begin{pmatrix} \chi_1^+ & \chi_2^0 \\ \chi_1^0 & \chi_2^- \end{pmatrix}$	$\begin{pmatrix} 0 & \kappa_2 \\ \kappa'_2 & 0 \end{pmatrix}$
S	-	S

Table 15: Minimal Higgs sector in the Supersymmetric Left-Right Model

Here the VEVs of the bi-doublets $\kappa_{1,2}$ are of the order of electroweak scale. The VEV of the right-chiral triplets v_R and \bar{v}_R , on the other hand, has to be much more larger in order the right-chiral gauge bosons to be sufficiently heavy. The VEVs of the left-chiral triplet fields $\Delta, \bar{\Delta}$, which determine the tree-level left-chiral neutrino masses, must be extremely small and are assumed to be zero. In this case, the left-chiral triplet fields decouple and thus their addition amounts only to the proliferation of Higgs masses and representations in this model.

Phenomenological aspects of LRSUSY has been studied previously in [22–26]. In our work [27], we revisit the Higgs sector of minimal R -parity conserving LRSUSY by constructing the mass matrices for the doubly-charged, singly charged and neutral bosons (both scalar and pseudoscalar sectors). Although the model depends on many parameters, we show that the masses are sensitive to only a few, and thus the model is predictive. Light doubly-charged Higgs bosons emerge naturally. The LRSUSY model predicts neutral scalar and pseudoscalar Higgs bosons that violate flavor at tree level. We impose conditions coming from phenomenology: $K^0 - \bar{K}^0$, $D^0 - \bar{D}^0$ and $B_{d,s}^0 - \bar{B}_{d,s}^0$ mixing. We show that one can have light neutral and charged Higgs bosons that conserve flavor, while the flavor violating bosons are in the 600 GeV- 100 TeV scale, as required by meson mixing constraints. We pinpoint the parameters that the masses are most sensitive to, and show that they satisfy the constraints in a limited range of these parameters. We set up the structure of the Higgs potential, masses and mixing, including the constraints, while leaving the study of the characteristic signals at the LHC for a future study.

4.2 R -parity Conserving the Left-Right Supersymmetric Model

As mentioned before, R -parity, given in eq. (3.66), is imposed in the MSSM to avoid dangerous baryon and lepton number violating operators. Otherwise explicit Yukawa terms that violate R -parity can exist in the Lagrangian. This explicit R -parity breaking is forbidden in LRSUSY models by the symmetries of the model. In early LRSUSY models $SU(2)_R$ doublets were used to break the gauge symmetry. Later $SU(2)_{L,R}$ triplets were introduced to provide the see-saw mechanism for neutrino masses [19], and both left- and right-chiral triplet Higgs bosons are required by parity conservation. The model was described extensively in several previous works [24]. However R -parity may not be conserved in this setup. The reason is that the minimum of the potential prefers a solution in which the right-chiral scalar neutrino gets a VEV, thus breaking R -parity spontaneously. Two scenarios have been proposed which remedy this situation. One is the model of Babu and Mohapatra [185] where an extra singlet Higgs boson is added to the model and one-loop corrections to the potential show that an R -parity conserving minimum can be found. The second model is that

of Aulakh *et. al.* [186], where the addition of two more triplets, $\Omega(1, 3, 1, 0)$ and $\Omega_c(1, 1, 3, 0)$, with zero lepton number, achieves left-right symmetry breaking with conserved R -parity at tree-level. In our work, we adopt the former, as it is a minimal model.

The superpotential of this model is given by

$$\begin{aligned}
W &= Y_u Q^T \tau_2 \Phi_1 \tau_2 Q^c + Y_d Q^T \tau_2 \Phi_2 \tau_2 Q^c + Y_\nu L^T \tau_2 \Phi_1 \tau_2 L^c + Y_\ell L^T \tau_2 \Phi_2 \tau_2 L^c + \text{h.c.} \\
&+ i f L^{cT} \tau_2 \Delta^c L^c \\
&+ S [\lambda \text{Tr}(\Delta^c \bar{\Delta}^c) + \lambda_{ij} \text{Tr}(\Phi_i^T \tau_2 \Phi_j \tau_2) - \mathcal{M}_R^2] + W',
\end{aligned} \tag{4.2}$$

where

$$W' = [M_\Delta \text{Tr}(\Delta^c \bar{\Delta}^c)] + \mu_{ij} \text{Tr}(\Phi_i^T \tau_2 \Phi_j \tau_2) + \mathcal{M}_S S^2 + \lambda_S S^3. \tag{4.3}$$

Here $Y_{u,d}$ and $Y_{\nu,\ell}$ in eq. (4.2) are quark and lepton Yukawa coupling matrices, while f is the Majorana neutrino Yukawa coupling. We choose to work with $W' = 0$, which leads to an enhanced R -symmetry and a natural interpretation of the supersymmetric μ term, as explained below.

The VEVs of the Higgs fields in this model needed to break the symmetries as described above. If we assume that the VEVs of the bi-doublet Higgs are real, the fermion mass matrices become Hermitian. In the supersymmetric limit, the VEV of the singlet S Higgs boson is zero, but after SUSY breaking, $\langle S \rangle \sim m_{\text{SUSY}}$. Thus the μ term for the bidoublet Φ will arise from the coupling λ_{ij} , with a magnitude of order m_{SUSY} [185]. In the SUSY limit,

$$|v_R| = |\bar{v}_R|, \quad \lambda v_R \bar{v}_R = \mathcal{M}_R^2, \quad \langle S \rangle = 0. \tag{4.4}$$

The VEV of S field, generated after SUSY breaking, arises from linear terms in SUSY breaking

$$V_{\text{soft}} = A_\lambda \lambda S \text{Tr}(\Delta^c \bar{\Delta}^c) - C_\lambda \mathcal{M}_R^2 S + \text{h.c.} \tag{4.5}$$

Minimization of the resulting potential yields $\langle S^* \rangle = \frac{1}{2\lambda}(C_\lambda - A_\lambda)$, which is of order m_{SUSY} . If the coupling λ is small, then $\langle S \rangle$ can be above the SUSY breaking scale. This feature can be used to make one pair of Higgs doublet superfields heavier than the SUSY breaking scale. However, the masses of doubly charged fermionic fields, which are equal to $\lambda \langle S \rangle$ must remain below a TeV. Consistency of the model (non-vanishing CKM mixing angle) requires the asymmetry $\mu_{12} = \mu_{21} + \epsilon$.

The full potential of the model relevant for symmetry breaking includes the F term, the D term and soft SUSY-breaking contributions as explained in Subsection 3.2.2. They are given by

$$\begin{aligned}
V_F &= |\lambda \text{Tr}(\Delta^c \bar{\Delta}^c) + \lambda_{ij} \text{Tr}(\Phi_i^T \tau_2 \Phi_j \tau_2) - \mathcal{M}_R^2|^2 + \lambda^2 |S|^2 |\text{Tr}(\Delta^c \Delta^{c\dagger}) + \text{Tr}(\bar{\Delta}^c \bar{\Delta}^{c\dagger})|, \\
V_{\text{soft}} &= M_1^2 \text{Tr}(\Delta^{c\dagger} \Delta^c) + M_2^2 \text{Tr}(\bar{\Delta}^{c\dagger} \bar{\Delta}^c) + M_3^2 \Phi_1^\dagger \Phi_1 + M_4^2 \Phi_2^\dagger \Phi_2 + M_S^2 |S|^2 \\
&\quad + \{A_\lambda \lambda S \text{Tr}(\Delta^c \bar{\Delta}^c) - C_\lambda \mathcal{M}_R^2 S + \text{h.c.}\}, \\
V_D &= \frac{g_L^2}{8} \sum_i \left| \text{Tr}(\Phi_a \tau_i^T \Phi_b^\dagger) \right|^2 + \frac{g_R^2}{8} \sum_i \left| \text{Tr}(2\Delta^{c\dagger} \tau_i \Delta^c + 2\bar{\Delta}^{c\dagger} \tau_i \bar{\Delta}^c + \Phi_a \tau_i^T \Phi_b^\dagger) \right|^2 \\
&\quad + \frac{g'^2}{2} \left| \text{Tr}(-\Delta^{c\dagger} \Delta^c + \bar{\Delta}^{c\dagger} \bar{\Delta}^c) \right|^2. \tag{4.6}
\end{aligned}$$

We use this potential and proceed the usual way to find the masses and mixing matrices for the Higgs bosons in this model.

4.3 Higgs Boson Composition and Masses

The Higgs boson spectrum was previously analyzed in a variant of the model [187] with R -parity violation. The new features of the present analysis are 1) we employ a version of the model that uses the right-chiral neutrino couplings to the triplet Higgs bosons to eliminate the need for L -number violation; and 2) we include constraints from FCNC processes to predict the range of Higgs masses and parameters in LRSUSY. Effectively, we are looking at a very different model and Higgs sector than in [187].

We minimize the full potential of the model given in eq. (4.6) which is relevant for symmetry breaking by using

$$\frac{\partial V}{\partial \kappa_1} = \frac{\partial V}{\partial \kappa_2} = \frac{\partial V}{\partial v_R} = \frac{\partial V}{\partial \bar{v}_R} = \frac{\partial V}{\partial \langle S \rangle} = 0, \tag{4.7}$$

to obtain masses and compositions of the Higgs bosons. However, this procedure does not lead to the correct potential minimum. The reason is that all the terms in the scalar potential are identical for the configurations in which VEVs are given to the neutral right-chiral triplet Higgs, except for the D -term, which is lower for the charge breaking configuration:

$$\langle \Delta^c \rangle = \frac{1}{\sqrt{2}} \begin{pmatrix} 0 & v_R \\ v_R & 0 \end{pmatrix}, \quad \langle \bar{\Delta}^c \rangle = \frac{1}{\sqrt{2}} \begin{pmatrix} 0 & \bar{v}_R \\ \bar{v}_R & 0 \end{pmatrix}. \tag{4.8}$$

Previous solutions suggested are breaking R -parity, which would have the attractive feature that $v_R \sim 1$ TeV, but which abandons the LSP as the candidate for dark matter [182]; or introducing higher dimensional operators to lower the charge conserving vacuum, with $v_R \sim 10^{11}$ GeV, but losing the solution to strong and weak CP violation [186]. More recently, a new version of the model [185] examined the effects of introducing one loop Coleman-Weinberg effective potential generated by one family right-chiral neutrino to the Δ^c field:

$$V_{\text{eff}}^{1\text{-loop}} = \frac{1}{16\pi^2} \sum_i (-1)^{2s} (2s+1) M_i^4 \left[\ln \left(\frac{M_i^2}{\mu^2} \right) - \frac{3}{2} \right]. \quad (4.9)$$

Expanding this potential in the limit in which the SUSY breaking parameters are small with respect to the triplet VEVs (v_R, \bar{v}_R) , one obtains an effective form in terms of the small parameter

$$x = \frac{\text{Tr}(\Delta^c \Delta^c) \text{Tr}((\Delta^{c\dagger} \Delta^{c\dagger}))}{[\text{Tr}((\Delta^{c\dagger} \Delta^c)^2)],}$$

the 1-loop potential becomes:

$$\begin{aligned} V_{\text{eff}}^{1\text{-loop}} \simeq & - \frac{|f|^2 m_{L^c}^2 \text{Tr}(\Delta^c \Delta^c) \text{Tr}(\Delta^{c\dagger} \Delta^{c\dagger})}{128\pi^2 |v_R|^2} \\ & \times \left\{ (a_1 - a_2) g_R^2 \left(2 \ln \frac{|f v_R|^2}{\mu^2} + \ln x - 2 \ln 2 - 2 \right) \right. \\ & \left. - [2 + (a_1 + a_2) g_{B-L}^2] (\ln x - 2 \ln 2) \right\}. \quad (4.10) \end{aligned}$$

Here a_1 and a_2 vanish in the SUSY limit (when D-terms vanish) and $m_{L^c}^2$ are soft right-chiral scalar lepton masses. The effect of this potential is to mimic the effects of the higher dimensional operators in previous versions, without the need to introduce them explicitly, thus solving the problem of the global minimum. Whereas before the global minimum contained at least one doubly-charged Higgs boson with zero mass, after 1-loop corrections all the masses are positive. The advantage of such a formalism is that the masses are very predictive, as they do not depend on coefficients of ad-hoc higher order terms, or sneutrino VEVs. In the next section, we study explicitly the implications for the Higgs masses in this model. Before, we wish to point out that, should the model have included left-chiral triplet Higgs bosons, their mass would remain negative and cannot be fixed by the first order loop corrections. A left-chiral counterpart of the one loop correction would not work, as the VEV of this field v_L

is zero, or very small. Thus, one would have to consider higher order corrections or additional Higgs representations.

In the explicit expressions of the bare and the physical Higgs boson mass terms, we use the following abbreviations

$$\begin{aligned}
\kappa_{dif}^2 &= \kappa_1^2 - \kappa_2^2, \\
\rho_{dif}^2 &= v_R^2 - \bar{v}_R^2 + \frac{1}{2}(\kappa_1^2 - \kappa_2^2), \\
Y &= A_\lambda \lambda S + \lambda(-M_R^2 - 2\lambda_{21}\kappa_1\kappa_2 + \lambda v_R \bar{v}_R), \\
M &= 2\lambda_{21}(-M_R^2 - 2\lambda_{21}\kappa_1\kappa_2 + \lambda v_R \bar{v}_R), \\
f(\epsilon) &= \epsilon \left(\frac{M}{2\lambda_{21}} - 2\lambda_{21}\kappa_1\kappa_2 - \epsilon\kappa_1\kappa_2 \right), \\
g(\epsilon) &= \epsilon\lambda\kappa_1\kappa_2, \\
h(\epsilon) &= \epsilon\kappa_1\kappa_2(4\lambda_{21} + \epsilon),
\end{aligned} \tag{4.11}$$

with $\epsilon = \mu_{21} - \mu_{12}$, small but non-zero after symmetry breaking.

4.3.1 Doubly Charged Higgs Boson Masses

Mass matrices for the doubly charged Higgs fields are of block diagonal form of one two by two matrix for $(\delta^{c^{--*}}, \bar{\delta}^{c^{++}})$ fields

$$M_{\delta^{c^{--*}} \bar{\delta}^{c^{++}}}^2 = \begin{pmatrix} -2g_R^2 \rho_{dif}^2 - \frac{\bar{v}_R}{v_R} Y' & Y' \\ Y' & 2g_R^2 \rho_{dif}^2 - \frac{v_R}{\bar{v}_R} Y' \end{pmatrix}, \tag{4.12}$$

where $Y' = Y - g(\epsilon)$. From these expressions we can find the exact analytic forms for the doubly charged Higgs masses. Setting $\tan \delta = \frac{\bar{v}_R}{v_R}$, these are:

$$M_{H_{1,2}^{++}}^2 = -\frac{Y'}{\sin 2\delta} \pm \sqrt{4g_R^4 \rho_{dif}^4 + \frac{Y'^2}{\sin^2 2\delta} - 4Y'g_R^2 \rho_{dif}^2 \cot 2\delta}. \tag{4.13}$$

It is clear that one must require $Y' < 0$, but even so, one of the mass eigenvalues will be negative. It is thus essential that we include the first order correction to the doubly charged Higgs masses, which arises from derivatives of the quartic potential (4.10) with respect to the doubly charged Higgs boson fields. The corrected (Mass²)

matrix elements are

$$\begin{aligned}
M_{\delta^{c--*} \delta^{c--}}^2 &= -\frac{f^2 m_{L^c}^2}{16\pi^2} \left[a_1 g_R^2 \left(2 \ln \left(\frac{|f v_R|}{\mu} \right) - 1 \right) + \ln 2 \left(2 - a_1 (g_R^2 - g_{B-L}^2) \right) \right] \\
&\quad - 2g_R^2 \rho_{dif}^2 - \frac{\bar{v}_R}{v_R} Y', \\
M_{\delta^{c++} \delta^{c--}}^2 &= Y', \\
M_{\delta^{c--*} \delta^{c++*}}^2 &= Y', \\
M_{\bar{\delta}^{c++} \bar{\delta}^{c++*}}^2 &= 2g_R^2 \rho_{dif}^2 - \frac{\bar{v}_R}{v_R} Y',
\end{aligned} \tag{4.14}$$

yielding a positive correction to the masses, for $m_{L^c}^2 < 0$. The first order correction is not finite at $x = 0$, however, the divergence is very mild (logarithmic) and higher order effects cure it without altering the masses significantly.

4.3.2 Singly Charged Higgs Boson Masses

Mass matrices for the singly charged Higgs fields are of block diagonal form of one two by two matrix for (ϕ_1^+, χ_2^{-*}) fields and one four by four matrix for $(\delta^{c+}, \bar{\delta}^{c-*}, \phi_2^{-*}, \chi_1^+)$ fields respectively,

$$M_{\phi_1^+, \chi_2^{-*}}^2 = \begin{pmatrix} \frac{\kappa_2}{\kappa_1} M'' & M' \\ M' & \frac{\kappa_1}{\kappa_2} M' \end{pmatrix}, \tag{4.15}$$

where $M' = M + f(\epsilon)$. The elements of the four by four matrix are

$$\begin{aligned}
M_{\delta^{c-*} \delta^{c-}}^2 &= g_R^2 v_R^2 - g_R^2 \rho_{dif}^2 - \frac{\bar{v}_R}{v_R} Y', \\
M_{\delta^{c-*} \bar{\delta}^{c+*}}^2 &= -g_R^2 v_R \bar{v}_R + Y', \\
M_{\delta^{c-*} \phi_2^-}^2 &= -\frac{1}{\sqrt{2}} g_R^2 \kappa_1 v_R, \\
M_{\delta^{c-*} \chi_1^{+*}}^2 &= -\frac{1}{\sqrt{2}} g_R^2 \kappa_2 v_R, \\
M_{\delta^{c+} \bar{\delta}^{c+*}}^2 &= g_R^2 \bar{v}_R^2 + g_R^2 \rho_{dif}^2 - \frac{v_R}{\bar{v}_R} Y', \\
M_{\delta^{c+} \phi_2^-}^2 &= \frac{1}{\sqrt{2}} g_R^2 \kappa_1 \bar{v}_R, \\
M_{\delta^{c+} \chi_1^{+*}}^2 &= \frac{1}{\sqrt{2}} g_R^2 \kappa_2 \bar{v}_R,
\end{aligned}$$

$$\begin{aligned}
M_{\phi_2^* \phi_2^-}^2 &= \frac{1}{2} \kappa_1^2 (g_L^2 + g_R^2) - \frac{1}{2} g_L^2 \kappa_{dif}^2 - g_R^2 \rho_{dif}^2 + \frac{\kappa_2}{\kappa_1} M', \\
M_{\phi_2^* \chi_1^{+*}}^2 &= \frac{1}{2} \kappa_1 \kappa_2 (g_L^2 + g_R^2) + M', \\
M_{\chi_1^+ \chi_1^-}^2 &= \frac{1}{2} \kappa_2^2 (g_L^2 + g_R^2) + \frac{1}{2} g_L^2 \kappa_{dif}^2 + g_R^2 \rho_{dif}^2 + \frac{\kappa_1}{\kappa_2} M'.
\end{aligned} \tag{4.16}$$

4.3.3 Neutral Higgs Boson Masses

Mass matrices for the neutral scalar Higgs fields are of block diagonal form of one two by two matrix for $(\phi_2^{0r}, \chi_1^{0r})$ fields and one five by five matrix for $(\delta^{c0r}, \bar{\delta}^{c0r}, \phi_1^{0r}, \chi_2^{0r}, S^{0r})$ fields respectively,

$$M_{\phi_2^{0r}, \chi_1^{0r}}^2 = \begin{pmatrix} -\frac{1}{2} g_L^2 \kappa_{dif}^2 - g_R^2 \rho_{dif}^2 + \frac{\kappa_2}{\kappa_1} M' & -M' \\ -M' & \frac{1}{2} g_L^2 \kappa_{dif}^2 + g_R^2 \rho_{dif}^2 + \frac{\kappa_1}{\kappa_2} M' \end{pmatrix}. \tag{4.17}$$

The elements of the five by five matrix are

$$\begin{aligned}
M_{\delta^{c0r} \delta^{c0r}}^2 &= 2v_R^2 (g_{B-L}^2 + g_R^2) + \lambda^2 \bar{v}_R^2 - \frac{\bar{v}_R}{v_R} Y', \\
M_{\delta^{c0r} \bar{\delta}^{c0r}}^2 &= -2v_R \bar{v}_R (g_{B-L}^2 + g_R^2) + \lambda^2 v_R \bar{v}_R + Y', \\
M_{\delta^{c0r} \phi_1^{0r}}^2 &= g_R^2 \kappa_1 v_R - 2\lambda \lambda_{21} \kappa_2 \bar{v}_R - 2 \frac{\bar{v}_R}{\kappa_1} g(\epsilon), \\
M_{\delta^{c0r} \chi_2^{0r}}^2 &= -g_R^2 \kappa_2 v_R - 2\lambda \lambda_{21} \kappa_1 \bar{v}_R - \frac{\bar{v}_R}{\kappa_2} g(\epsilon), \\
M_{\delta^{c0r} S^{0r}}^2 &= 2\lambda^2 S v_R + A_\lambda \lambda \bar{v}_R, \\
M_{\bar{\delta}^{c0r} \bar{\delta}^{c0r}}^2 &= 2(g_{B-L}^2 + g_R^2) \bar{v}_R^2 + \lambda^2 v_R^2 - \frac{v_R}{\bar{v}_R} Y', \\
M_{\bar{\delta}^{c0r} \phi_1^{0r}}^2 &= -g_R^2 \kappa_1 \bar{v}_R - 2\lambda \lambda_{21} \kappa_2 v_R - \frac{v_R}{\kappa_1} g(\epsilon), \\
M_{\bar{\delta}^{c0r} \chi_2^{0r}}^2 &= g_R^2 \kappa_2 \bar{v}_R - 2\lambda \lambda_{21} \kappa_1 v_R - \frac{v_R}{\kappa_2} g(\epsilon), \\
M_{\bar{\delta}^{c0r} S^{0r}}^2 &= 2\lambda^2 S \bar{v}_R + A_\lambda \lambda v_R, \\
M_{\phi_1^{0r} \phi_1^{0r}}^2 &= \frac{1}{2} \kappa_1^2 (g_L^2 + g_R^2) + 4\lambda_{21}^2 \kappa_2^2 + \frac{\kappa_2}{\kappa_1} [M' + h(\epsilon)], \\
M_{\phi_1^{0r} \chi_2^{0r}}^2 &= -\frac{1}{2} \kappa_1 \kappa_2 (g_L^2 + g_R^2) + 4\lambda_{21}^2 \kappa_1 \kappa_2 - [M' - h(\epsilon)], \\
M_{\phi_1^{0r} S^{0r}}^2 &= 0, \\
M_{\chi_2^{0r} \chi_2^{0r}}^2 &= \frac{1}{2} \kappa_2^2 (g_L^2 + g_R^2) + 4\lambda_{21}^2 \kappa_1^2 + \frac{\kappa_1}{\kappa_2} [M' + h(\epsilon)], \\
M_{\chi_2^{0r} S^{0r}}^2 &= 0, \\
M_{S^{0r} S^{0r}}^2 &= M_S^2 + \lambda^2 (v_R^2 + \bar{v}_R^2).
\end{aligned} \tag{4.18}$$

Mass matrices for the neutral pseudoscalar Higgs fields are similarly of block diagonal form of one two by two matrix for $(\phi_2^{0i}, \chi_1^{0i})$ fields and one five by five matrix for $(\delta^{c0i}, \bar{\delta}^{c0i}, \phi_1^{0i}, \chi_2^{0i}, S^{0i})$ fields respectively,

$$M_{\phi_2^{0i}, \chi_1^{0i}}^2 = \begin{pmatrix} -\frac{1}{2}g_L^2\kappa_{dif}^2 - g_R^2\rho_{dif}^2 + \frac{\kappa_2}{\kappa_1}M' & M' \\ M' & \frac{1}{2}g_L^2\kappa_{dif}^2 + g_R^2\rho_{dif}^2 + \frac{\kappa_1}{\kappa_2}M' \end{pmatrix}. \quad (4.19)$$

The elements of the five by five matrix are

$$\begin{aligned} M_{\delta^{c0i} \delta^{c0i}}^2 &= \lambda^2 \bar{v}_R^2 - \frac{\bar{v}_R}{v_R} Y', \\ M_{\delta^{c0i} \bar{\delta}^{c0i}}^2 &= \lambda^2 v_R \bar{v}_R - Y', \\ M_{\delta^{c0i} \phi_1^{0i}}^2 &= -2\lambda\lambda_{21}\kappa_2 \bar{v}_R - \frac{\bar{v}_R}{\kappa_1} g(\epsilon), \\ M_{\delta^{c0i} \chi_2^{0i}}^2 &= -2\lambda\lambda_{21}\kappa_1 \bar{v}_R - \frac{\bar{v}_R}{\kappa_2} g(\epsilon), \\ M_{\delta^{c0i} S^{0i}}^2 &= -A_\lambda \lambda \bar{v}_R, \\ M_{\bar{\delta}^{c0i} \bar{\delta}^{c0i}}^2 &= \lambda^2 v_R^2 - \frac{v_R}{\bar{v}_R} Y', \\ M_{\bar{\delta}^{c0i} \phi_1^{0i}}^2 &= -2\lambda\lambda_{21}\kappa_2 v_R - \frac{v_R}{\kappa_1} g(\epsilon), \\ M_{\bar{\delta}^{c0i} \chi_2^{0i}}^2 &= -2\lambda\lambda_{21}\kappa_1 v_R - \frac{v_R}{\kappa_2} g(\epsilon), \\ M_{\bar{\delta}^{c0i} S^{0i}}^2 &= -A_\lambda \lambda v_R, \\ M_{\phi_1^{0i} \phi_1^{0i}}^2 &= 4\lambda_{21}^2 \kappa_2^2 + \frac{\kappa_2}{\kappa_1} [M' + h(\epsilon)], \\ M_{\phi_1^{0i} \chi_2^{0i}}^2 &= 4\lambda_{21}^2 \kappa_2 \kappa_1 + [M' + h(\epsilon)], \\ M_{\phi_1^{0i} S^{0i}}^2 &= 0, \\ M_{\chi_2^{0i} \chi_2^{0i}}^2 &= 4\lambda_{21}^2 \kappa_1^2 + \frac{\kappa_1}{\kappa_2} [M' + h(\epsilon)], \\ M_{\chi_2^{0i} S^{0i}}^2 &= 0, \\ M_{S^{0i} S^{0i}}^2 &= M_S^2 + \lambda^2 (v_R^2 + \bar{v}_R^2). \end{aligned} \quad (4.20)$$

4.4 Constraints on the Higgs sector

4.4.1 Flavor Changing Neutral Higgs Bosons

As any model with more than one Higgs doublet, the LRSUSY is plagued by tree-level FCNC-inducing Higgs bosons [188]. We proceed first by isolating the flavor-violating and flavor-conserving field combinations, then subject them to constraints coming

from mixings in the kaon, B and D neutral meson states. We show explicitly the expressions for the down-quark sector; the up-quark sector can be obtained simply by the same method. The Yukawa Lagrangian in the quark sector is given by

$$\mathcal{L}_Y = \bar{\mathbf{d}}_{\mathbf{L}} \mathbf{Y}_{\mathbf{u}} \phi_2^0 \mathbf{d}_{\mathbf{R}} + \bar{\mathbf{d}}_{\mathbf{L}} \mathbf{Y}_{\mathbf{d}} \chi_2^0 \mathbf{d}_{\mathbf{R}} + \bar{\mathbf{u}}_{\mathbf{L}} \mathbf{Y}_{\mathbf{u}} \phi_1^0 \mathbf{u}_{\mathbf{R}} + \bar{\mathbf{u}}_{\mathbf{L}} \mathbf{Y}_{\mathbf{d}} \chi_1^0 \mathbf{u}_{\mathbf{R}} + \text{h.c.}, \quad (4.21)$$

where $\mathbf{Y}_{\mathbf{u}}$ and $\mathbf{Y}_{\mathbf{d}}$ are 3×3 Hermitian matrices in flavor space. When the bi-doublets acquire VEVs as in Table 15, with κ_1 , κ_2 , κ'_1 and κ'_2 real, the up and the down type quark mass matrices are given by:

$$\mathbf{M}_{\mathbf{u}} = \mathbf{Y}_{\mathbf{u}} \kappa_1 + \mathbf{Y}_{\mathbf{d}} \kappa'_2 \quad \mathbf{M}_{\mathbf{d}} = \mathbf{Y}_{\mathbf{u}} \kappa'_1 + \mathbf{Y}_{\mathbf{d}} \kappa_2. \quad (4.22)$$

Inserting the expressions obtained for Y_u and Y_d in terms of masses, the Yukawa Lagrangian in the down type quark sector reads

$$\begin{aligned} \mathcal{L}_Y^N(d) = & \frac{[d_L^{i*} M_u^{ij} d_R^j (\kappa_2 \phi_2^0 - \kappa'_2 \chi_2^0) + d_L^{i*} M_d^{ij} d_R^j (\kappa_1 \chi_2^0 - \kappa'_1 \phi_2^0)]}{\kappa_1 \kappa_2 - \kappa'_1 \kappa'_2} \\ & + \frac{[d_R^{j*} M_u^{ij*} d_L^i (\kappa_2 \phi_2^{0*} - \kappa'_2 \chi_2^{0*}) + d_R^{j*} M_d^{ij*} d_L^i (\kappa_1 \chi_2^{0*} - \kappa'_1 \phi_2^{0*})]}{\kappa_1 \kappa_2 - \kappa'_1 \kappa'_2}. \end{aligned} \quad (4.23)$$

To obtain the physical states we diagonalize the mass matrices by the unitary transformations

$$M_u^{ij} = U_u^{ik} \hat{M}_u^{km} W_u^{jm*} \delta^{km}, \quad M_d^{ij} = U_d^{ik} \hat{M}_d^{km} W_d^{jm*} \delta^{km}, \quad (4.24)$$

where $\hat{\mathbf{M}}_{\mathbf{u}}$ and $\hat{\mathbf{M}}_{\mathbf{d}}$ are diagonal up and down type quark mass matrices. Since $\mathbf{d}_{\mathbf{L}}$ and $\mathbf{d}_{\mathbf{R}}$ are weak eigenstates, unitary transformations convert them into mass eigenstates

$$d_L^i \rightarrow U_d^{ij} d_L^j, \quad d_R^i \rightarrow W_d^{ij} d_R^j. \quad (4.25)$$

We define $U_d^{ji*} U_u^{ik} = V_L^{jk}$ and $W_u^{lj*} W_d^{jm} = V_R^{lm}$ where $\mathbf{V}_{\mathbf{L}}$ and $\mathbf{V}_{\mathbf{R}}$ are the components of the left-chiral and right-chiral CKM matrices. Then the Yukawa Lagrangian for down type quark fields is given by

$$\begin{aligned} \mathcal{L}_Y^N(d) = & \frac{d_L^{n*} V_L^{kn*} \hat{M}_u^{km} V_R^{ml} d_R^l \delta^{km} (\kappa_2 \phi_2^0 - \kappa'_2 \chi_2^0)}{\kappa_1 \kappa_2 - \kappa'_1 \kappa'_2} \\ & + \frac{d_L^{n*} \delta^{nk} \hat{M}_d^{km} \delta^{ml} d_R^l \delta^{km} (\kappa_1 \chi_2^0 - \kappa'_1 \phi_2^0)}{\kappa_1 \kappa_2 - \kappa'_1 \kappa'_2} \\ & + \frac{d_R^{m*} V_R^{mn*} \hat{M}_u^{km*} V_L^{kl} d_L^l \delta^{km} (\kappa_2 \phi_2^{0*} - \kappa'_2 \chi_2^{0*})}{\kappa_1 \kappa_2 - \kappa'_1 \kappa'_2} \\ & + \frac{d_R^{m*} \delta^{nm} \hat{M}_d^{km*} \delta^{kl} d_L^l \delta^{km} (\kappa_1 \chi_2^{0*} - \kappa'_1 \phi_2^{0*})}{\kappa_1 \kappa_2 - \kappa'_1 \kappa'_2}, \end{aligned} \quad (4.26)$$

where the up and down mass matrices are Hermitian since the VEVs of bi-doublets are taken to be real. For simplicity, we assume $\mathbf{V}_L = \mathbf{V}_R = \mathbf{V}$. The fields ϕ_2^0 and χ_2^0 are complex. Thus we can isolate two terms in the Lagrangian, one flavor violating, and one FCNC-conserving. Writing the neutral and imaginary parts separately, the FCNC Lagrangian reads

$$\begin{aligned}
\mathcal{L}_{FCNC}(d) &= \frac{d_L^{n*} V^{kn*} \hat{M}_u^{kk} V^{kl} d_R^l (\kappa_2 \phi_2^{0r} - \kappa_2' \chi_2^{0r})}{\kappa_1 \kappa_2 - \kappa_1' \kappa_2'} \\
&+ \frac{id_L^{n*} V^{kn*} \hat{M}_u^{kk} V^{kl} d_R^l (\kappa_2 \phi_2^{0i} - \kappa_2' \chi_2^{0i})}{\kappa_1 \kappa_2 - \kappa_1' \kappa_2'} \\
&+ \frac{d_R^{n*} V^{kn*} \hat{M}_u^{kk*} V^{kl} d_R^l (\kappa_2 \phi_2^{0r} - \kappa_2' \chi_2^{0r})}{\kappa_1 \kappa_2 - \kappa_1' \kappa_2'} \\
&- \frac{id_R^{n*} V^{kn*} \hat{M}_u^{kk*} V^{kl} d_R^l (\kappa_2 \phi_2^{0i} - \kappa_2' \chi_2^{0i})}{\kappa_1 \kappa_2 - \kappa_1' \kappa_2'}, \tag{4.27}
\end{aligned}$$

where ϕ_2^{0r} and χ_2^{0r} are the two of the nine bare scalar fields and ϕ_2^{0i} and χ_2^{0i} are the two of the nine bare pseudo-scalar fields appearing in LRSUSY Lagrangian. The $d-s$ coupling in Eq. (4.27) allows a $\Delta S = 2$ transition at tree level. To evaluate explicitly, we use the Wolfenstein parametrization [116] of the CKM matrix given in eq. (2.7)

$$V^{kd*} \hat{M}_u^{kk} V^{ks} = (m_u - m_c) \left(\lambda - \frac{\lambda^3}{2} \right) - m_t A^2 \lambda^5 (1 - \rho + i\eta). \tag{4.28}$$

We express the bare scalar and pseudoscalar neutral Higgs fields as

$$\begin{aligned}
\psi^{0rT} &= (\delta^{c0r} \bar{\delta}^{c0r} \phi_1^{0r} \phi_2^{0r} \chi_1^{0r} \chi_2^{0r} S^{0r}), \\
\psi^{0iT} &= (\delta^{c0i} \bar{\delta}^{c0i} \phi_1^{0i} \phi_2^{0i} \chi_1^{0i} \chi_2^{0i} S^{0i}), \tag{4.29}
\end{aligned}$$

for the CP even Higgs fields and the physical ones as

$$\begin{aligned}
H^{0rT} &= (H_1^{0r} H_2^{0r} H_3^{0r} H_4^{0r} H_5^{0r} H_6^{0r} H_7^{0r}), \\
H^{0iT} &= (H_1^{0i} H_2^{0i} H_3^{0i} H_4^{0i} H_5^{0i} H_6^{0i} H_7^{0i}), \tag{4.30}
\end{aligned}$$

for the CP odd Higgs fields. Call A_{ij} the transformation matrix which transforms the bare scalar fields into the physical CP even ones, and B_{ij} matrix which transforms the bare pseudo-scalar fields into the physical CP odd ones: $H_i^{0r} = A_{ij} \psi_j^{0r}$, $H_i^{0i} = B_{ij} \psi_j^{0i}$. Substituting these into the Eq. (4.27), we obtain the explicit Lagrangian responsible

for FCNC in the down-sector

$$\begin{aligned}
\mathcal{L}_{FCNC}^{\Delta S=2}(d) &= \frac{m_t \lambda}{\kappa_1 \kappa_2 - \kappa'_1 \kappa'_2} \left(\left[\left(\frac{m_u}{m_t} - \frac{m_c}{m_t} \right) \left(1 - \frac{\lambda^2}{2} \right) - A^2 \lambda^4 (1 - \rho) \right] (\kappa_2 A_{i4}^* - \kappa'_2 A_{i6}^*) H_i^{0r} \right. \\
&\times \left. (\bar{d} P_{RS} + \bar{d} P_{LS}) + A^2 \lambda^4 \eta (\kappa_2 B_{i4}^* - \kappa'_2 B_{i6}^*) H_i^{0i} (\bar{d} P_{RS} - \bar{d} P_{LS}) \right) \\
&+ \frac{i m_t \lambda}{\kappa_1 \kappa_2 - \kappa'_1 \kappa'_2} \left(\left[\frac{m_u}{m_t} - \frac{m_c}{m_t} \right] \left(1 - \frac{\lambda^2}{2} \right) - A^2 \lambda^4 (1 - \rho) \right] (\kappa_2 B_{i4}^* - \kappa'_2 B_{i6}^*) H_i^{0i} \\
&\times \left. (\bar{d} P_{RS} - \bar{d} P_{LS}) - A^2 \lambda^4 \eta (\kappa_2 A_{i4}^* - \kappa'_2 A_{i6}^*) H_i^{0r} (\bar{d} P_{RS} + \bar{d} P_{LS}) \right). \quad (4.31)
\end{aligned}$$

We proceed in similar fashion to evaluate the flavor-conserving and flavor-violating Higgs contributions to the up sector. The Yukawa Lagrangian for the up quark sector is

$$\mathcal{L}_Y^N(u) = u_L^{i*} Y_u^{ij} \phi_1^0 u_R^j + u_L^{i*} Y_d^{ij} \chi_1^0 u_R^j + u_R^{j*} \phi_1^{0*} Y_u^{ji*} u_L^i + u_R^{j*} \chi_1^{0*} Y_d^{ji*} u_L^i. \quad (4.32)$$

We use the same substitutions as before and express the Lagrangian in terms of the complex fields ϕ_2^0 and χ_2^0 . The first and third terms in the Lagrangian above are flavor-conserving. Writing the neutral and imaginary parts separately, the FCNC Lagrangian reads

$$\begin{aligned}
\mathcal{L}_{FCNC}(u) &= \frac{u_L^{n*} V^{nk} \hat{M}_d^{kk} V^{lk*} u_R^l (\kappa_2 \phi_1^{0r} - \kappa'_2 \chi_1^{0r})}{\kappa_1 \kappa_2 - \kappa'_1 \kappa'_2} \\
&+ \frac{i u_L^{n*} V^{nk} \hat{M}_d^{kk} V^{lk*} u_R^l (\kappa_2 \phi_1^{0i} - \kappa'_2 \chi_1^{0i})}{\kappa_1 \kappa_2 - \kappa'_1 \kappa'_2} \\
&+ \frac{u_R^{n*} V^{nk} \hat{M}_d^{kk*} V^{lk*} u_L^l (\kappa_2 \phi_1^{0r} - \kappa'_2 \chi_1^{0r})}{\kappa_1 \kappa_2 - \kappa'_1 \kappa'_2} \\
&- \frac{i u_R^{n*} V^{nk} \hat{M}_d^{kk*} V^{lk*} u_L^l (\kappa_2 \phi_1^{0i} - \kappa'_2 \chi_1^{0i})}{\kappa_1 \kappa_2 - \kappa'_1 \kappa'_2}, \quad (4.33)
\end{aligned}$$

where ϕ_1^{0r} and χ_1^{0r} are the two of the nine bare scalar fields and ϕ_1^{0i} and χ_1^{0i} are the two of the nine bare pseudo-scalar fields appearing in LRSUSY Lagrangian. The $u-c$ coupling in eq. (4.33) allows a $\Delta C = 2$ transition at tree level. Inserting $V^{uk} \hat{M}_u^{kk} V^{ck*}$ in terms of Wolfenstein parameters,

$$V^{uk} \hat{M}_u^{kk} V^{ck*} = (m_s - m_c) \left(\lambda - \frac{\lambda^3}{2} \right) - m_b A^2 \lambda^5 (-\rho + i\eta), \quad (4.34)$$

and using physical states instead of ϕ_1^{0r} and χ_1^{0r} we obtain the explicit form of the Lagrangian responsible for FCNC in the up-sector

$$\begin{aligned}
\mathcal{L}_{FCNC}^{\Delta C=2}(u) &= \frac{m_b \lambda}{\kappa_1 \kappa_2 - \kappa'_1 \kappa'_2} \left(\left[\left(\frac{m_s}{m_b} - \frac{m_d}{m_b} \right) \left(1 - \frac{\lambda^2}{2} \right) + A^2 \lambda^4 \rho \right] (\kappa_2 A_{i3}^* - \kappa'_2 A_{i5}^*) H_i^{0r} \right. \\
&\times (\bar{u} P_{RC} + \bar{u} P_{LC}) + A^2 \lambda^4 \eta (\kappa_2 B_{i3}^* - \kappa'_2 B_{i5}^*) H_i^{0i} (\bar{u} P_{RC} - \bar{u} P_{LC}) \left. \right) \\
&+ \frac{i m_b \lambda}{\kappa_1 \kappa_2 - \kappa'_1 \kappa'_2} \left(\left[\left(\frac{m_s}{m_b} - \frac{m_d}{m_b} \right) \left(1 - \frac{\lambda^2}{2} \right) + A^2 \lambda^4 \rho \right] (\kappa_2 B_{i3}^* - \kappa'_2 B_{i5}^*) H_i^{0i} \right. \\
&\times (\bar{u} P_{RC} - \bar{u} P_{LC}) - A^2 \lambda^4 \eta (\kappa_2 A_{i3}^* - \kappa'_2 A_{i5}^*) H_i^{0r} (\bar{u} P_{RC} + \bar{u} P_{LC}) \left. \right). \quad (4.35)
\end{aligned}$$

These expressions will be used to calculate the real and imaginary parts of the $K^0 - \bar{K}^0$, $D^0 - \bar{D}^0$ and $B^0 - \bar{B}^0$ mixing.

ϵ_K and $K^0 - \bar{K}^0$ Mixing

We evaluate the real and imaginary parts of the $K^0 - \bar{K}^0$ transition. We assume a common mass for scalar and pseudoscalar Higgs fields. In the following calculations we will use the compact forms $\langle \tilde{Q}_1(\mu) \rangle + \langle Q_1(\mu) \rangle = \langle Q_1^{\text{tot}} \rangle$ and $\langle \tilde{Q}_2(\mu) \rangle + \langle Q_2(\mu) \rangle = \langle Q_2^{\text{tot}} \rangle$.

$$\begin{aligned}
\text{Re} \langle \bar{K}^0 | H_{eff} | K^0 \rangle &= \frac{m_t^2 \lambda^2}{4M_i^2 (\kappa_1 \kappa_2 - \kappa'_1 \kappa'_2)^2} \left\{ \left[\left(\frac{m_u}{m_t} - \frac{m_c}{m_t} \right) (2 - \lambda^2) - 2A^2 \lambda^4 (1 - \rho) \right] \right. \\
&\times \left([(\kappa_2 A_{i4}^* - \kappa'_2 A_{i6}^*)^2 - (\kappa_2 B_{i4}^* - \kappa'_2 B_{i6}^*)^2] \langle Q_1^{\text{tot}} \rangle \right. \\
&+ [(\kappa_2 A_{i4}^* - \kappa'_2 A_{i6}^*)^2 + (\kappa_2 B_{i4}^* - \kappa'_2 B_{i6}^*)^2] \langle Q_2^{\text{tot}} \rangle \left. \right) \\
&+ 4A^4 \lambda^8 \eta^2 \left([(\kappa_2 A_{i4}^* - \kappa'_2 A_{i6}^*)^2 + (\kappa_2 B_{i4}^* - \kappa'_2 B_{i6}^*)^2] \langle Q_1^{\text{tot}} \rangle \right. \\
&\left. \left. + [(\kappa_2 A_{i4}^* - \kappa'_2 A_{i6}^*)^2 - (\kappa_2 B_{i4}^* - \kappa'_2 B_{i6}^*)^2] \langle Q_2^{\text{tot}} \rangle \right) \right\}, \quad (4.36)
\end{aligned}$$

and

$$\begin{aligned}
\text{Im} \langle K^0 | H_{eff} | \bar{K}^0 \rangle &= \frac{i m_t^2 \lambda^2}{4M_i^2 (\kappa_1 \kappa_2 - \kappa'_1 \kappa'_2)^2} \left[\left(\frac{m_u}{m_t} - \frac{m_c}{m_t} \right) (2 - \lambda^2) A^2 \lambda^4 \eta - 2A^4 \lambda^8 (1 - \rho) \eta \right] \\
&\times \left([(\kappa_2 B_{i4}^* - \kappa'_2 B_{i6}^*)^2 - (\kappa_2 A_{i4}^* - \kappa'_2 A_{i6}^*)^2] \langle Q_1^{\text{tot}} \rangle \right. \\
&\left. - [(\kappa_2 B_{i4}^* - \kappa'_2 B_{i6}^*)^2 + (\kappa_2 A_{i4}^* - \kappa'_2 A_{i6}^*)^2] \langle Q_2^{\text{tot}} \rangle \right), \quad (4.37)
\end{aligned}$$

The $\Delta F = 2$ process are described by the Hamiltonian [189, 190]

$$\mathcal{H}_{eff}^{\Delta F=2} = \sum_{a=1}^5 C_a Q_a^{q_i q_j} + \sum_{a=1}^3 \tilde{C}_a \tilde{Q}_a^{q_i q_j}, \quad (4.38)$$

with

$$\begin{aligned} Q_1^{q_i q_j} &= \bar{q}_{jL}^\alpha \gamma_\mu q_{iL}^\alpha \bar{q}_{jL}^\beta \gamma^\mu q_{iL}^\beta, & Q_2^{q_i q_j} &= \bar{q}_{jR}^\alpha q_{iL}^\alpha \bar{q}_{jR}^\beta q_{iL}^\beta, & Q_3^{q_i q_j} &= \bar{q}_{jR}^\alpha q_{iL}^\beta \bar{q}_{jR}^\beta q_{iL}^\alpha, \\ Q_4^{q_i q_j} &= \bar{q}_{jR}^\alpha q_{iL}^\alpha \bar{q}_{jL}^\beta q_{iR}^\beta, & Q_5^{q_i q_j} &= \bar{q}_{jR}^\alpha q_{iL}^\beta \bar{q}_{jL}^\beta q_{iR}^\alpha, \end{aligned} \quad (4.39)$$

where α, β are color indices. The operators \tilde{Q}_a are obtained from Q_a by exchange $L \leftrightarrow R$. Here, we only use $Q_1, Q_2, \tilde{Q}_1,$ and \tilde{Q}_2 . The other quark operators will be useful in the following chapters. The matrix elements are, [191]

$$\begin{aligned} \langle Q_1(\mu) \rangle &= -\frac{5}{24} \left(\frac{m_a}{m_{q_1}(\mu) + m_{q_2}(\mu)} \right)^2 m_a F_a^2 B_1(\mu), \\ \langle Q_2(\mu) \rangle &= \frac{1}{4} \left(\frac{m_a}{m_{q_1}(\mu) + m_{q_2}(\mu)} \right)^2 m_a F_a^2 B_2(\mu), \end{aligned} \quad (4.40)$$

where $a = K, B_d, B_s, D$ mesons, and no summation is assumed. F_a is the decay constant of the corresponding meson and $B_1(\mu)$ and $B_2(\mu)$ are the bag parameters calculated in NDR scheme for an energy scale μ . The numerical values for all the parameters involved in the calculation of $K^0 - \bar{K}^0, D^0 - \bar{D}^0$ and $B_{d,s}^0 - \bar{B}_{d,s}^0$ mixings are summarized in Table 16. Same expressions for the operators Q_1 and Q_2 are valid for the operators \tilde{Q}_1 and \tilde{Q}_2 .

	$\mathbf{K}^0 - \bar{\mathbf{K}}^0$	$\mathbf{B}_d^0 - \bar{\mathbf{B}}_d^0$	$\mathbf{B}_s^0 - \bar{\mathbf{B}}_s^0$	$\mathbf{D}^0 - \bar{\mathbf{D}}^0$
μ	2 GeV	m_b	m_b	2 GeV
\mathbf{q}_1	s	b	b	u
\mathbf{q}_2	d	d	s	c
\mathbf{m}_a	498 MeV	5.28 GeV	5.37 GeV	1.86 GeV
\mathbf{F}_a	160 MeV	0.21 GeV	0.25 GeV	232 MeV
$\mathbf{B}_1(\mu)$	0.76	0.82	0.83	1
$\mathbf{B}_2(\mu)$	1.30	1.16	1.17	1
ΔM_a (GeV)	3.483×10^{-15}	3.337×10^{-13}	117×10^{-13}	1.57313×10^{-20}
ϵ_a	2.228×10^{-3}	-	-	-

Table 16: QCD parameters used for meson mixings.

In the table above, ΔM_a values are taken from PDG [114] and indirect CP violation in $K \rightarrow \pi\pi$ [138] and in $K \rightarrow \pi l\nu$ decays is given by [114]. Substituting $\mu = 2$ GeV in the expressions for ΔM_K and CP violating parameter ϵ_K given below

$$\Delta M_K = 2\text{Re}\langle\bar{K}^0|H_{eff}|K^0\rangle, \quad \Delta\epsilon_K = \frac{1}{\sqrt{2}\Delta M_K}\text{Im}\langle\bar{K}^0|H_{eff}|K^0\rangle, \quad (4.41)$$

we get

$$\Delta M_K = \frac{6.9269 \times 10^{-7} A_{i4}^{2*} + 2.0088 \times 10^{-7} B_{i4}^{2*}}{M_i^2} \sec \beta^2, \quad (4.42)$$

and

$$\epsilon_K = \frac{9.9975 \times 10^6 A_{i4}^{2*} - 9.8616 \times 10^{-9} A_{i4}^* B_{i4}^* + 2.8993 \times 10^7 B_{i4}^{2*}}{M_i^2} \sec \beta^2. \quad (4.43)$$

By comparing the calculated expressions with their experimental values given in Table 16, we obtain on the sources of flavor and CP violation in the LRSUSY. We give below the analytical expressions for the constraints on the parameters in the neutral scalar and pseudoscalar mixing from K meson mixing. Taking the lightest neutral Higgs mass to be $M_{H_i^0r} = M_{H_i^0i} = M_i$, ΔM_K yields the constraint

$$M_i^2 \geq (1.9888 \times 10^8 A_{i4}^{2*} + 5.7675 \times 10^8 B_{i4}^{2*}) \sec \beta^2 \text{ GeV}^2, \quad (4.44)$$

while the value of ϵ_K yields the constraint

$$M_i^2 \geq (4.4872 \times 10^9 A_{i4}^{2*} - 4.4262 \times 10^{-6} A_{i4}^* B_{i4}^* + 1.3013 \times 10^{10} B_{i4}^{2*}) \sec \beta^2 \text{ GeV}^2. \quad (4.45)$$

In the above expressions we assumed that the lightest Higgs mass provides the dominant contribution, and neglected the rest, while in our numerical evaluations we have summed over all mass contributions, as in (4.20) and (4.21). These become, for example, when $\tan \beta = 10$, for ΔM_K

$$M_i^2 \geq (2.0087 \times 10^{10} A_{i4}^{2*} + 5.8251 \times 10^{10} B_{i4}^{2*}) \text{ GeV}^2, \quad (4.46)$$

and for ϵ_K

$$M_i^2 \geq (4.5320 \times 10^{11} A_{i4}^{2*} - 4.4704 \times 10^{-4} A_{i4}^* B_{i4}^* + 1.3143 \times 10^{12} B_{i4}^{2*}) \text{ GeV}^2. \quad (4.47)$$

We tried varying the lightest relative masses in the scalar and pseudoscalar sector and found that the results do not change.

$B_d^0 - \bar{B}_d^0$ Mixing

We proceed the same way as for $K^0 - \bar{K}^0$ mixing to evaluate the constraints from the B_d^0 , B_s^0 meson mixing. We use again four quark operators Q_1 , Q_2 , \tilde{Q}_1 , and \tilde{Q}_2 defined previously. Setting as before the Higgs mass to be equal to the lightest scalar mass $M_{H_i^{0r}} = M_{H_i^{0i}} = M_i$ the expression for ΔM_{B_d} becomes

$$\Delta M_{B_d} = \frac{(9.4139 \times 10^{-6} A_{i4}^{2*} + 3.6405 \times 10^{-5} B_{i4}^{2*}) \sec \beta^2}{M_i^2} \text{ GeV}^3. \quad (4.48)$$

Using the experimental of ΔM_{B_d} from Table 16, we obtain, assuming as before dominance by the lightest mass

$$M_i^2 \geq (2.8211 \times 10^7 A_{i4}^{2*} + 1.6909 \times 10^8 B_{i4}^{2*}) \sec \beta^2 \text{ GeV}^2, \quad (4.49)$$

which becomes, for $\tan \beta = 10$

$$M_i^2 \geq (2.8493 \times 10^9 A_{i4}^{2*} + 1.1019 \times 10^{10} B_{i4}^{2*}) \text{ GeV}^2. \quad (4.50)$$

$B_s^0 - \bar{B}_s^0$ Mixing

We proceed exactly as in the previous subsection, substituting s instead of d quark. The parameters for $B_s^0 - \bar{B}_s^0$ mixing are given in Table 16.

$$\Delta M_{B_s} = \frac{(4.2314 \times 10^{-4} A_{i4}^{*2} + 1.6469 \times 10^{-3} B_{i4}^{*2}) \sec \beta^2}{M_i^2} \text{ GeV}^3. \quad (4.51)$$

Using the experimental value of ΔM_{B_s} from Table 16,

$$M_i^2 \geq (3.6166 \times 10^7 A_{i4}^{2*} + 1.4076 \times 10^8 B_{i4}^{2*}) \sec \beta^2 \text{ GeV}^2, \quad (4.52)$$

or, for $\tan \beta = 10$

$$M_i^2 \geq (3.6528 \times 10^9 A_{i4}^{2*} + 1.4217 \times 10^{10} B_{i4}^{2*}) \text{ GeV}^2. \quad (4.53)$$

$D^0 - \bar{D}^0$ Mixing

We have already evaluated the real and imaginary parts of the $D^0 - \bar{D}^0$ transition Subsection 4.4.1. We assume as before a common mass for scalar and pseudo-scalar

Higgs fields.

$$\begin{aligned}
\text{Re}\langle\bar{D}^0|H_{eff}|D^0\rangle &= \frac{m_b^2\lambda^2}{4M_i^2(\kappa_1\kappa_2 - \kappa'_1\kappa'_2)^2} \left\{ \left[\left(\frac{m_s}{m_b} - \frac{m_d}{m_b} \right) (2 - \lambda^2) + 2A^2\lambda^4\rho \right]^2 \right. \\
&\times \left([(\kappa_2 A_{i3}^* - \kappa'_2 A_{i5}^*)^2 - (\kappa_2 B_{i3}^* - \kappa'_2 B_{i5}^*)^2] \langle Q_1^{\text{tot}} \rangle \right. \\
&+ [(\kappa_2 A_{i3}^* - \kappa'_2 A_{i5}^*)^2 + (\kappa_2 B_{i3}^* - \kappa'_2 B_{i5}^*)^2] \langle Q_2^{\text{tot}} \rangle \left. \right) \\
&+ 4A^4\lambda^8\eta^2 \left([(\kappa_2 A_{i3}^* - \kappa'_2 A_{i5}^*)^2 + (\kappa_2 B_{i3}^* - \kappa'_2 B_{i5}^*)^2] \langle Q_1^{\text{tot}} \rangle \right. \\
&\left. \left. + [(\kappa_2 A_{i3}^* - \kappa'_2 A_{i5}^*)^2 - (\kappa_2 B_{i3}^* - \kappa'_2 B_{i5}^*)^2] \langle Q_2^{\text{tot}} \rangle \right) \right\}, \quad (4.54)
\end{aligned}$$

where Q_1 , Q_2 , \tilde{Q}_1 , and \tilde{Q}_2 are the four quark operators defined as before, the mass difference $\Delta M_D = 2\text{Re}\langle\bar{D}^0|H_{eff}|D^0\rangle$ is obtained as

$$\Delta M_D = \frac{5.2816 \times 10^{-10} A_{i5}^{2*} + 5.8097 \times 10^{-9} B_{i5}^{2*}}{M_i^2} \text{csc } \beta^2 \text{ GeV}^3. \quad (4.55)$$

Comparing the calculated expression with the experimental value from Table 16 we obtain

$$M_i^2 \geq (3.3574 \times 10^{10} A_{i5}^{2*} + 3.6931 \times 10^{11} B_{i5}^{2*}) \text{csc } \beta^2 \text{ GeV}^2, \quad (4.56)$$

which becomes for $\tan \beta = 10$,

$$M_i^2 \geq (3.3909 \times 10^{10} A_{i5}^{2*} + 3.7300 \times 10^{11} B_{i5}^{2*}) \text{ GeV}^2. \quad (4.57)$$

4.5 Numerical Results and Discussion

The FCNCs tree-level diagrams are mediated by the physical scalar fields H_2^0 and H_6^0 , and the pseudoscalars A_1^0 and A_4^0 . These fields are linear superpositions of the χ_1^{0r} or ϕ_2^{0r} (χ_1^{0i} or ϕ_2^{0i} , respectively, for the pseudoscalars) components from the bidoublet Higgs.

As the fields H_2^0 and H_6^0 must be heavy, the light neutral scalars would likely be linear combinations of the complimentary χ_2^{0r} or ϕ_1^{0r} components from the bidoublets, or δ^{0r} , $\bar{\delta}^{0r}$, δ^{c0r} , and $\bar{\delta}^{c0r}$ from the triplet Higgs. We set v_R in the interval obtained from the requirement that the doubly charged Higgs are light (3 – 10 TeV). Varying v_R

outside this range adversely affects the masses of the lightest doubly charged Higgs, and some of the light neutral and singly charged scalars.

The mass of the lightest scalar field H_1^0 (the SM-like) changes at most a few GeV, if we vary any of the parameters, whereas the second lightest scalar field H_2^0 is highly dependent on the changes in the parameter v_R . Similarly, the lightest pseudoscalar field A_1^0 behaves like the second lightest neutral scalar field and is also affected by the changes in v_R . H_1^0 is SM-like, and the parameter that seems to affect H_1^0 mass the most is the λ_{21} coupling. (This parameter is the coupling that generates the $\mu_{21} = \lambda_{21}\langle S \rangle$ Higgsino coupling). The dependence is not smooth, but varying $|\lambda_{21}|$ in the interval $0.01 - 1$ produces a 30% change in $M_{H_1^0}$.

The tree-level flavor-changing neutral currents in the down-quark sector are governed by H_6^0 and A_4^0 . The mass values of the fields H_6^0 and A_4^0 are the same, and they are dependent on the parameters λ_{21} , v_R , λ , $\tan\beta$ and M_R . Numerical investigation reveals that only $\tan\beta$ and M_R can affect the H_6^0 and A_4^0 masses significantly, while there is practically no variation on the mass with v_R . These masses are dependent on the parameters M_R and $\tan\beta$ such that when they increase, mass values of these physical fields also increase. The dependence of the H_6^0 mass on the parameter M_R is more dominant than on $\tan\beta$. Requiring $M_R \sim 100$ TeV insures that Higgs-mediated FCNCs in K and B neutral mesons are suppressed to levels consistent with experimental data. The variations of H_6^0 mass with these parameters are shown in Fig. 4.5.

The fields H_2^0 and A_1^0 are responsible for flavor-changing neutral currents in the up-quark sector. Their masses are the same (as one can infer from the mass matrices in Section 4.3), and although they depend in principle on v_R , $\tan\beta$ and λ_{21} , the only significant dependence is on v_R , such that if v_R increases from 3 to 10 TeV, their mass values increase approximately 3 – 12 times. The mass also varies with the ratio $\tan\delta = \bar{v}_R/v_R$, while almost independent of the changes in the other parameters. The parameter dependence is shown in Fig. 13, where we plot the explicit v_R dependence for three values of $\tan\delta$, as well as a more extensive illustration of the $v_R - \bar{v}_R$ dependence in a contour plot. $D^0 - \bar{D}^0$ mixing constraints require $v_R \geq 3$ TeV. While the dependence on both $\tan\beta$ and λ_{21} is very weak, the dependence on v_R is almost linear.

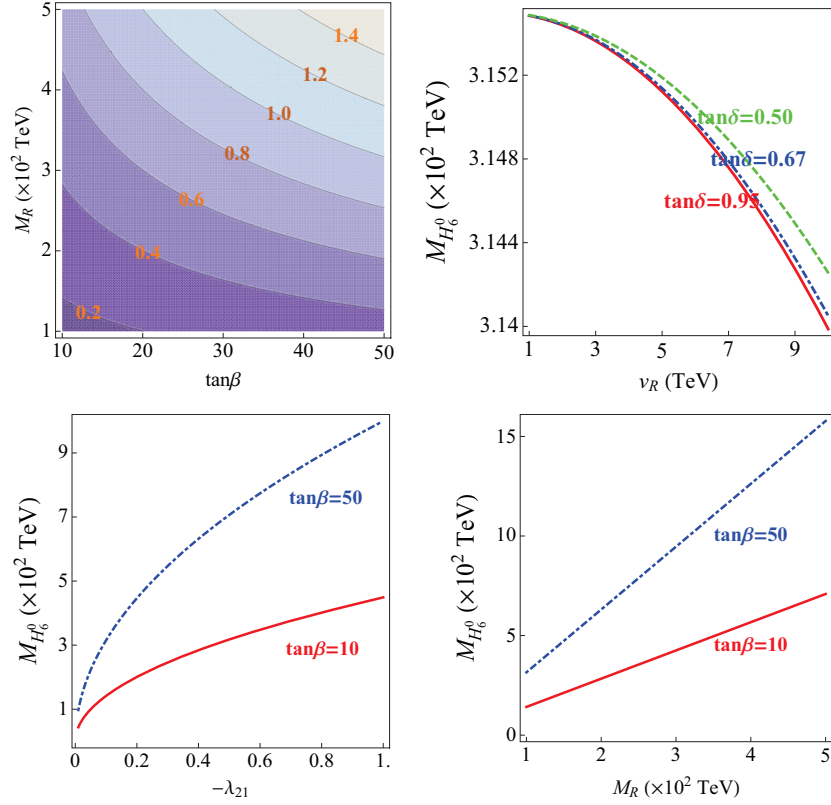


Figure 12: The variation of the FCNC neutral Higgs H_6^0 mass with the parameters of the LRSUSY model. H_6^0 induces tree-level FCNC in the down-quark sector. Shown are: contour plots in the $M_R - \tan \beta$ plane (the contour values are given in TeV when multiplied by 10^3), the variation of $M_{H_6^0}$ with M_R , and with v_R , for three values of $\tan \delta = \bar{v}_R/v_R$.

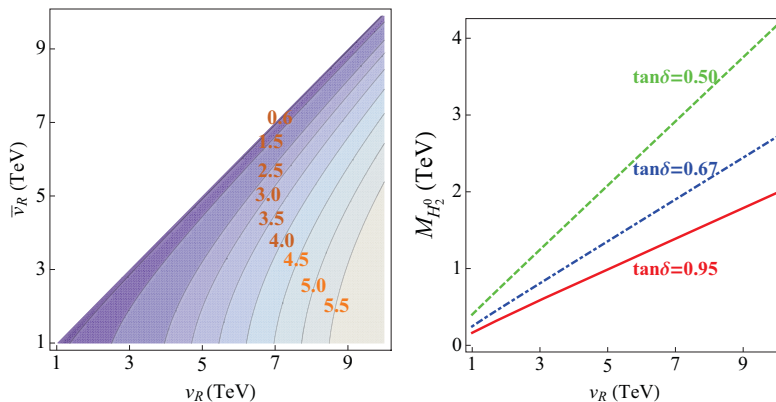


Figure 13: The variation of the FCNC neutral Higgs H_2^0 mass with the parameters of the LRSUSY model. H_2^0 induces tree-level FCNC in the up-quark sector. To the left, a contour plot in the $v_R - \bar{v}_R$ plane (the contour values are given in TeV) and, at the right, as a function of v_R for three values of $\tan \delta = \bar{v}_R/v_R$.

From the approximate analytical expressions in Section 4.3, the mass of the lightest doubly charged physical field $H_1^{\pm\pm}$ depends on v_R , λ , M_R as well as on the soft slepton masses $m_{L^c}^2$. Analysis shows that only the dependence on v_R and $m_{L^c}^2$ is significant. However, the exact mass also depends on \bar{v}_R through the ratio $\tan \delta = \bar{v}_R/v_R$.

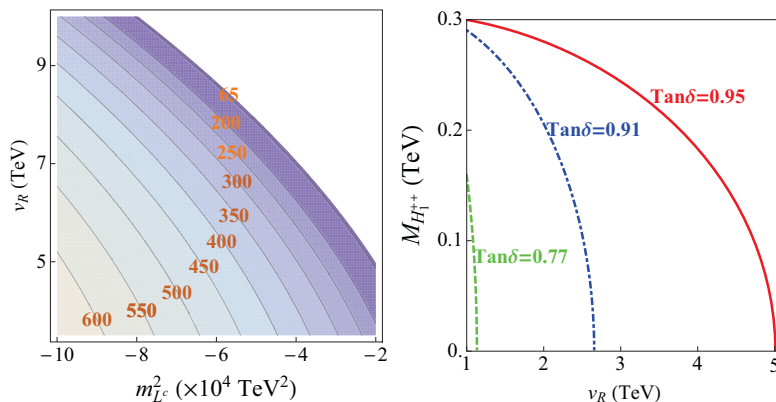


Figure 14: The masses of the lightest doubly-charged Higgs boson as a contour plot (the contours values are given in GeV) in the $v_R - m_{L^c}^2$ plane (left) and as a function of v_R plane for three values of $\tan \delta = \bar{v}_R/v_R$ (right).

As before we show, in Fig. 14, the dependence of these parameters as a function of v_R for different values of $\tan \delta$, as well as a contour plot in the $v_R - m_{L^c}^2$ plane. The

mass of $H_1^{\pm\pm}$ increases with the increasing values of v_R , as shown on the right hand side of Fig. 14, for three values of $\tan\delta$, while it is basically independent on M_R . One can see that the mass is highly dependent on \bar{v}_R/v_R .

For example, when we change v_R from 3 to 10 TeV, the $H_1^{\pm\pm}$ mass values increase approximately 4 times. Of course, in all cases, different $m_{L^c}^2 < 0$ are needed to keep the masses positive. Within the parameter space considered, $m_{L^c} \in (4.5i - 10i)$ TeV. The effect of varying the other parameters is negligible for the lightest doubly charged Higgs, whereas the mass of the heavier doubly charged Higgs $H_2^{\pm\pm}$ depends almost exclusively on M_R .

The lightest singly charged physical field H_1^\pm mass corresponds to the MSSM-like charged Higgs boson. The singly charged state that is triplet-like is H_2^\pm and is heavy. The other triplet-like charged Higgs boson is the Goldstone boson G_2^\pm responsible for giving mass to W_R^\pm bosons. The other charged Higgs which come from bidoublet components are heavy, a consequence of requiring the mass parameters to satisfy FCNC bounds.

Finally, we present in Tables 17 and 18 two explicit numerical scenarios for the Higgs masses, which obey the constraints from meson mixings: one for $v_R = 3.5$ TeV and $\tan\beta = 10$, the other for $v_R = 5$ TeV and $\tan\beta = 50$. The other parameters in both scenarios are taken to be $\tan\delta \equiv \bar{v}_R/v_R = 1/1.05$, $M_R = 100$ TeV, $\lambda = 1$, $\lambda_{21} = -0.1$, $C_\lambda = 2.5$ TeV, $\langle S \rangle = 1$ TeV, $M_S = 1$ TeV. We give masses and compositions in terms of the bare states. One can see that, except for raising the lightest neutral Higgs mass, increasing $\tan\beta$ has little effect on the spectrum. However raising v_R increases the mass of the lighter non-SM-like Higgs bosons in the neutral scalar and pseudoscalar sector, as well as in the singly and doubly charged Higgs sectors. While we did not prove in general that the model conserves R -parity, the numerical results obtained from minimizing the masses confirm the results of [185]. Both of these scenarios allow for a flavor-conserving neutral scalar Higgs boson; one light doubly charged Higgs boson, and only two other Higgs bosons with masses below 1TeV, one neutral and one singly-charged. The FCNC Higgs responsible for mixing in the up ($D^0 - \bar{D}^0$) or down ($K^0 - \bar{K}^0$ and $B_{d,s}^0 - \bar{B}_{d,s}^0$) quark sectors are heavy and satisfy the experimental constraints in each sector. This scenario is completely consistent with the Tevatron [192] and LHC data [193] on Higgs boson searches.

Particle	Mass (GeV)	Composition
H_1^0	111.6	$0.100\phi_1^{0r} + 0.995\chi_2^{0r}$
H_2^0	680.9	$-0.100\phi_2^{0r} - 1.000\chi_1^{0r}$
H_3^0	4557.4	$0.720\delta^{c^{0r}} + 0.685\bar{\delta}^{c^{0r}} + 0.001\chi_2^{0r} - 0.129S^{0r}$
H_4^0	11140.6	$0.045\delta^{c^{0r}} + 0.043\bar{\delta}^{c^{0r}} + 0.998S^{0r}$
H_5^0	141537.9	$0.690\delta^{c^{0r}} - 0.724\bar{\delta}^{c^{0r}}$
H_6^0	141686.6	$-1.000\phi_2^{0r} + 0.100\chi_1^{0r}$
H_7^0	141688.2	$0.001\delta^{c^{0r}} - 0.001\bar{\delta}^{c^{0r}} + 1.000\phi_1^{0r} - 0.100\chi_2^{0r}$
A_1^0	680.9	$0.100\phi_2^{0i} - 1.000\chi_1^{0i}$
A_2^0	11106.8	$1.000S^{0i}$
A_3^0	141502.0	$0.690\delta^{c^{0i}} + 0.724\bar{\delta}^{c^{0i}} - 0.003\phi_2^{0i}$
A_4^0	141686.6	$-1.000\phi_2^{0i} - 0.100\chi_1^{0i}$
A_5^0	141688.2	$-0.002\delta^{c^{0i}} - 0.002\bar{\delta}^{c^{0i}} - 1.000\phi_1^{0i} - 0.100\chi_2^{0i}$
H_1^+	690.2	$-0.018\delta^{c^{-*}} - 0.018\bar{\delta}^{c^+} - 0.099\phi_2^{-*} + 0.995\chi_1^+$
H_2^+	141454.6	$0.690\delta^{c^{-*}} - 0.724\bar{\delta}^{c^+}$
H_3^+	141686.6	$-0.995\phi_1^+ - 0.100\chi_2^{-*}$
H_4^+	449688.2	$-0.995\phi_2^{-*} - 0.100\chi_1^+$
H_1^{++}	217.9	$-0.724\delta^{c^{--*}} - 0.690\bar{\delta}^{c^{++}}$
H_2^{++}	141419.9	$-0.690\delta^{c^{--*}} + 0.724\bar{\delta}^{c^{++}}$
G_1^0	0	$0.568\delta^{c^{0i}} + -0.540\bar{\delta}^{c^{0i}} + 0.062\phi_1^{0i} - 0.617\chi_2^{0i}$
G_2^0	0	$-0.449\delta^{c^{0i}} + 0.428\bar{\delta}^{c^{0i}} + 0.078\phi_1^{0i} - 0.780\chi_2^{0i}$
G_1^+	0	$0.100\phi_1^+ - 0.995\chi_2^{-*}$
G_2^+	0	$-0.724\delta^{c^{-*}} - 0.690\bar{\delta}^{c^+} + 0.003\phi_2^{-*} - 0.025\chi_1^+$

Table 17: Masses and compositions of physical Higgs fields and unphysical Goldstone bosons. Parameters are chosen as follows: $\tan \beta = 10$, $\tan \delta = 1/1.05$, $v_R = 3.5$ TeV, $M_R = 100$ TeV, $\lambda = 1$, $\lambda_{21} = -0.1$, $C_\lambda = 2.5$ TeV, $\langle S \rangle = 1$ TeV, $M_S = 1$ TeV, $m_{L^c}^2 = -20$ TeV², $f = 1$.

Particle	Mass (GeV)	Composition
H_1^0	113.6	$0.020\phi_1^{0r} + 1.000\chi_2^{0r}$
H_2^0	998.6	$-0.020\phi_2^{0r} - 1.000\chi_1^{0r}$
H_3^0	6797.1	$0.714\delta^{c^{0r}} + 0.680\bar{\delta}^{c^{0r}} - 0.168S^{0r}$
H_4^0	12214.8	$0.068\delta^{c^{0r}} + 0.061\bar{\delta}^{c^{0r}} + 0.996S^{0r}$
H_5^0	141575.2	$-0.690\delta^{c^{0r}} + 0.724\bar{\delta}^{c^{0r}}$
H_6^0	315121.9	$-1.000\phi_2^{0r} + 0.020\chi_1^{0r}$
H_7^0	315123.5	$-1.000\phi_1^{0r} + 0.020\chi_2^{0r}$
A_1^0	998.6	$0.020\phi_2^{0i} - 1.000\chi_1^{0i}$
A_2^0	12152.2	$1.000S^{0i}$
A_3^0	141502.0	$0.690\delta^{c^{0i}} + 0.724\bar{\delta}^{c^{0i}}$
A_4^0	315121.9	$-1.000\phi_2^{0i} - 0.020\chi_1^{0i}$
A_5^0	315123.5	$-1.000\phi_1^{0i} - 0.020\chi_2^{0i}$
H_1^+	995.3	$-0.013\delta^{c^{-*}} - 0.012\bar{\delta}^{c^+} - 0.020\phi_2^{-*} + 1.000\chi_1^+$
H_2^+	141405.3	$0.690\delta^{c^{-*}} - 0.724\bar{\delta}^{c^+}$
H_3^+	315121.9	$-1.000\phi_1^+ - 0.020\chi_2^{-*}$
H_4^+	315123.5	$-1.000\phi_2^{-*} - 0.020\chi_1^+$
H_1^{++}	215.3	$-0.724\delta^{c^{-**}} - 0.690\bar{\delta}^{c^{++}}$
H_2^{++}	141334.2	$-0.690\delta^{c^{-**}} + 0.724\bar{\delta}^{c^{++}}$
G_1^0	0	$-0.138\delta^{c^{0i}} + 0.131\bar{\delta}^{c^{0i}} + 0.019\phi_1^{0i} - 0.961\chi_2^{0i}$
G_2^0	0	$0.710\delta^{c^{0i}} - 0.677\bar{\delta}^{c^{0i}} + 0.004\phi_1^{0i} - 0.981\chi_2^{0i}$
G_1^+	0	$0.020\phi_1^+ - 1.000\chi_2^{-*}$
G_2^+	0	$0.724\delta^{c^{-*}} + 0.690\bar{\delta}^{c^+} + 0.018\chi_1^+$

Table 18: Masses and compositions of physical Higgs fields and unphysical Goldstone bosons. Parameters are chosen as follows: $\tan\beta = 50$, $\tan\delta = 1/1.05$, $v_R = 5$ TeV, $M_R = 100$ TeV, $\lambda = 1$, $\lambda_{21} = -0.1$, $C_\lambda = 2.5$ TeV, $\langle S \rangle = 1$ TeV, $M_S = 1$ TeV, $m_{Lc}^2 = -30$ TeV², $f = 1$.

Finally we comment on the scalar leptons and gaugino masses. In [185], the authors attempt a complete model building, incorporating general (approximate) constraints on doubly charged Higgs boson fields and scalar lepton masses, as functions of gaugino masses. Using two-loop MSSM renormalization group equations

[194], the relations between these parameters are

$$\begin{aligned}
M_{++}^2(m_Z) &< \frac{24}{5b_1} M_{\bar{1}}^2(m_Z) \left[\frac{\alpha_{B-L}^2(v_R)}{\alpha_{B-L}^2(m_Z)} - 1 \right] \\
M_{\bar{\tau}_R}^2(m_Z) &< \frac{5}{6b_1} M_{\bar{1}}^2(m_Z) \left[\frac{\alpha_{B-L}^2(v_R)}{\alpha_{B-L}^2(m_Z)} - 1 \right] \\
M_{\bar{\tau}_L}^2(m_Z) &< \frac{3}{10b_1} M_{\bar{1}}^2(m_Z) \left[\frac{\alpha_{B-L}^2(v_R)}{\alpha_{B-L}^2(m_Z)} - 1 \right] + \frac{3}{2b_2} M_{\bar{L}}^2(m_Z) \left[\frac{\alpha_L^2(v_R)}{\alpha_L^2(m_Z)} - 1 \right]
\end{aligned} \tag{4.58}$$

where $M_{\bar{1}}, M_{\bar{L}}$ are gaugino masses, b_1, b_2 are RGE coefficients, M_{++} is the soft doubly charged Higgs mass, and the last two equations give bounds on the the right and left tau slepton masses. We use the renormalization group equations for the LRSUSY model with triplets and an arbitrary number of singlets [195] to evaluate the mass bounds². In our case, taking v_R in the 3.5 – 10 TeV region, the limits become:

$$\begin{aligned}
M_{++}^2(m_Z) &< \frac{1}{8} M_{\bar{1}}^2(m_Z) \left[\frac{\alpha_{B-L}^2(v_R)}{\alpha_{B-L}^2(m_Z)} - 1 \right] + M_{\bar{R}}^2(m_Z) \left[\frac{\alpha_{\bar{R}}^2(v_R)}{\alpha_{\bar{R}}^2(m_Z)} - 1 \right] \\
M_{\bar{\tau}_R}^2(m_Z) &< \frac{1}{32} M_{\bar{1}}^2(m_Z) \left[\frac{\alpha_{B-L}^2(v_R)}{\alpha_{B-L}^2(m_Z)} - 1 \right] + \frac{3}{16} M_{\bar{R}}^2(m_Z) \left[\frac{\alpha_{\bar{R}}^2(v_R)}{\alpha_{\bar{R}}^2(m_Z)} - 1 \right] \\
M_{\bar{\tau}_L}^2(m_Z) &< \frac{1}{32} M_{\bar{1}}^2(m_Z) \left[\frac{\alpha_{B-L}^2(v_R)}{\alpha_{B-L}^2(m_Z)} - 1 \right] + \frac{3}{16} M_{\bar{L}}^2(m_Z) \left[\frac{\alpha_L^2(v_R)}{\alpha_L^2(m_Z)} - 1 \right]
\end{aligned} \tag{4.59}$$

The approximate bounds on the soft masses depend critically on the relationship between the $U(1)_{B-L}, SU(2)_L$ and $SU(2)_R$ gaugino masses. For instance, for $M_{\bar{L}} = M_{\bar{R}} = M_{\bar{1}} : M_{++}(m_Z) < 0.24 M_{\bar{1}}(m_Z), M_{\bar{\tau}_R}(m_Z) < 0.11 M_{\bar{1}}(m_Z)$ and $M_{\bar{\tau}_L}(m_Z) < 0.11 M_{\bar{1}}(m_Z)$; for $M_{\bar{L}} = M_{\bar{R}} = 2M_{\bar{1}}$ the bounds become $M_{++}(m_Z) < 0.4 M_{\bar{1}}(m_Z), M_{\bar{\tau}_R}(m_Z) < 0.2 M_{\bar{1}}(m_Z)$ and $M_{\bar{\tau}_L}(m_Z) < 0.2 M_{\bar{1}}(m_Z)$; while for $2M_{\bar{L}} = M_{\bar{R}} = 4M_{\bar{1}}$, the limits are $M_{++}(m_Z) < 0.7 M_{\bar{1}}(m_Z), M_{\bar{\tau}_R}(m_Z) < 0.32 M_{\bar{1}}(m_Z)$ and $M_{\bar{\tau}_L}(m_Z) < 0.2 M_{\bar{1}}(m_Z)$. While no precise conclusions can be reached, the bounds push the gaugino mass parameter $M_{\bar{1}}$ to be very large, which is not inconsistent with soft slepton masses in the TeV range. Note that these mass bounds are only a rough estimate, as we include gaugino masses but neglect other terms. The purpose of our calculations was to show that a self-consistent Higgs sector can be obtained within the framework of the minimal model, leaving the door open for a more thorough exploration of the model.

²These bounds are completely consistent with what we obtain using relations given in [185] for $M_{\bar{1}} = M_{\bar{L}} = M_{\bar{R}}$.

4.6 Summary and Conclusion

In this Chapter we analyzed the Higgs sector of a minimal LRSUSY model with automatic R -parity violation. Symmetries of the model forbid explicit R -parity violation. Inclusion of the effects of the Yukawa coupling of the heavy Majorana neutrino insures a global minimum which is charge conserving, thus avoiding spontaneous R -parity breaking or the need to introduce higher dimensional terms.

The Higgs sector contains four doubly charged, six singly charged Higgs fields, nine neutral scalar fields, and seven pseudoscalar fields (in addition to two neutral Goldstone bosons, and two charged ones). One would expect that, with so many free parameters in the Lagrangian, and so many free masses, almost any scenario is possible for the Higgs masses in this model. We show that the requirement that 1) there is a light neutral scalar Higgs boson, flavor conserving, which is the counterpart to the SM Higgs boson; 2) there exists at least one light doubly charged Higgs boson (as it is interesting for phenomenology); and 3) the flavor-violating neutral Higgs bosons satisfy the constraints imposed by the experimental data from $K^0 - \bar{K}^0$, $D^0 - \bar{D}^0$, and $B_{d,s}^0 - \bar{B}_{d,s}^0$ mixings, makes the Higgs sector fairly predictive and fixes some of the parameters in a narrow range. The masses of the light neutral and doubly charged Higgs bosons depend on very few parameters. For instance, we find that requirement 1) and 2) are related, and satisfied by $v_R \in (3, 10)$ TeV range. Assuming $v_R \sim \bar{v}_R$ and $g_L = g_R$, this predicts masses for the W_R around 4 – 13 TeV (assuming negligible mixing with W_L), and for Z_R bosons in the 3 – 10 TeV range. Thus, while the model can allow for light neutral, singly and doubly charged Higgs bosons, it predicts new gauge bosons just outside the range $M_{W_R} < 2(4)$ TeV which can be observed at the LHC with a luminosity of 1(30) fb^{-1} [196].

The parameter M_R , associated with the singlet Higgs field in the superpotential, must be of $\mathcal{O}(100)$ TeV, which insures high masses for the FCNC Higgs. And our rough estimates show that requiring some of the Higgs bosons to be light likely push the scale of supersymmetry above 1 TeV.

Our analysis is important for two reasons: first, we have shown that a reasonable Higgs mass spectrum is possible in LRSUSY. This analysis shows that, except for these three bosons, the rest are heavy (with only three, one neutral scalar, one pseudoscalar and one singly charged) just below the TeV scale. Second, as most Higgs masses are sensitive to few parameters, the model is very predictive and free

of additional parameters, such as the sneutrino VEVs or extra higher-dimensional terms. The best signal for this model from the Higgs sector remains the observation of a doubly charged Higgs boson, decaying copiously to charged leptons. Observation of a light non-MSM like Higgs (neutral or singly charged) will invalidate the model, at least within the present minimal prescription for the Higgs sector. This analysis can now form the basis of a consistent phenomenological study of signals from such a Higgs sector, including production and decay rates, and has implications for the masses of the additional gauge bosons, of the right-chiral neutrinos, as well as for the supersymmetric partners.

Chapter 5

HIGGS PHENOMENOLOGY in WARPED EXTRA DIMENSIONS with a 4th GENERATION

Previously, in Section 3.3 Four-Generation Standard Model and in Section 3.4 Warped Extra Dimensions has been introduced. There have been many extensive studies of the SM4. However, there are few analyzes of BSM scenarios with four generations (see however [99]). The reason is that the fourth generation typically imposes severe restrictions on the models. We have mentioned before the advantages of introducing a fourth generation into models with warped extra dimensions.

As mentioned earlier, KK particles could be just barely beyond the reach of the LHC. Nevertheless there are implications of the warped scenarios that could leave an imprint on lower energy physics. For instance, recently it was pointed out that warped extra-dimensional models introduce new flavor-violating operators in the Higgs sector. In a composite Higgs sector with strong dynamics, flavor changing neutral currents (FCNC) can arise at tree level, generated by a misalignment between the Higgs Yukawa matrices and the fermion mass matrices [175,176,181]. The full set of operators responsible for the misalignment has been thoroughly analyzed, showing that the effect is generically large and phenomenologically important [181] and even could alter considerably the couplings of Higgs to gluons [197,198], thus affecting the main production mechanism of the Higgs at hadron colliders.

These flavor violating effects will be even more pronounced if the matter sector is

extended by extra fermionic generations. And for the Higgs bosons, it is well known that the effects of a fourth generation are quite spectacular in modifying the Higgs boson cross-section at hadron colliders, which can be tested easily with Tevatron and early LHC data within this or the next year. The Tevatron has published limits on the Higgs boson cross-section in the fourth generation model, excluding a wide range of Higgs boson masses [168], and recently the CMS collaboration carried out a similar study [193].

As Higgs production can be modified within warped scenarios due to flavor violating effects in the Higgs sector [198], it may be possible to distinguish signals coming from SM4 from those coming from a fourth generation model associated with a warped extra-dimension (or a composite scenario), given the searches for the Higgs boson underway at the LHC. The inclusion of the fourth generation will also affect low-energy precision observables, as well as limits on rare decays. In the lines of [181], we explore here the effect of FCNC Higgs couplings with a fourth generation in a warped extra dimensional model with fermions in the bulk.

5.1 Flavor Structure with four families

The model is introduced in detail in Section 3.4. We now proceed to add to the scenario the remaining families of quarks and leptons, including a new fourth generation. This will of course create a richer structure of flavor, not only in the Higgs sector, but in the electroweak sector, where the flavor changing charged current mediated by W bosons now contains new contributions with the addition of t' and b' .

The fermion zero-mode wavefunctions evaluated at the TeV brane, $f(c)$, are now diagonal matrices as follows

$$\begin{aligned}
 \mathbf{F}_{\mathbf{Q}} &= \begin{pmatrix} f_{Q_1} & 0 & 0 & 0 \\ 0 & f_{Q_2} & 0 & 0 \\ 0 & 0 & f_{Q_3} & 0 \\ 0 & 0 & 0 & f_{Q_4} \end{pmatrix}, & \mathbf{F}_{\mathbf{u}} &= \begin{pmatrix} f_{u_1} & 0 & 0 & 0 \\ 0 & f_{u_2} & 0 & 0 \\ 0 & 0 & f_{u_3} & 0 \\ 0 & 0 & 0 & f_{u_4} \end{pmatrix}, \\
 \mathbf{F}_{\mathbf{d}} &= \begin{pmatrix} f_{d_1} & 0 & 0 & 0 \\ 0 & f_{d_2} & 0 & 0 \\ 0 & 0 & f_{d_3} & 0 \\ 0 & 0 & 0 & f_{d_4} \end{pmatrix}. & & (5.1)
 \end{aligned}$$

Here small differences in the c 's will produce large hierarchies in the values of $f(c)$ (i.e. geographical fermion localization in the extra dimension) giving rise to a highly hierarchical structure in \mathbf{F}_i where $i = Q, u, d$. This is shown in Figure 15.

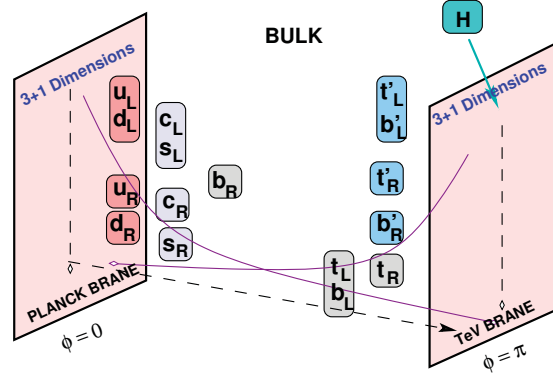


Figure 15: Typical geographic location of quarks in RS-4GEN (RS with a fourth family) such that large quark mass hierarchies and small mixing angles are generic. The Higgs boson and the heavier fermions (top and fourth generation quarks and charged leptons) are localized near the TeV brane, whereas light fermions are localized towards the Planck brane.

5.1.1 The quark mixing matrix V_{CKM4}

The mass matrices are given by

$$\begin{aligned} \mathbf{M}_u &= v_4 \mathbf{F}_Q \mathbf{Y}_u \mathbf{F}_u, \\ \mathbf{M}_d &= v_4 \mathbf{F}_Q \mathbf{Y}_d \mathbf{F}_d. \end{aligned} \quad (5.2)$$

Here, the matrices \mathbf{Y}_u and \mathbf{Y}_d are composed of 5D Yukawa couplings and are 4×4 with complex entries. Because most of the elements in the diagonal matrices \mathbf{F}_i are naturally hierarchical (for UV-localized fermions), the physical fermion mass matrices \mathbf{M}_u and \mathbf{M}_d will inherit their hierarchical structure independently of the nature of the true 5D Yukawa couplings, the latter of which can therefore contain all of their entries with similar size of $\mathcal{O}(1)$, and have no definite flavor structure. This is the main idea behind scenarios of so-called flavor anarchy, which we consider here, applied to a four-family scenario. The introduction of the fourth family is simply realized by assuming that the new fermions are localized near the TeV brane, like the top quark, and therefore will be naturally heavy. Mixing angles should typically be small except

among the heavy fermions where large mixings could be possible. To diagonalize the mass matrices we use

$$\mathbf{U}_{\mathbf{Q}_u} \mathbf{M}_u \mathbf{W}_u^\dagger = \mathbf{M}_u^{\text{diag}}, \quad (5.3)$$

$$\mathbf{U}_{\mathbf{Q}_d} \mathbf{M}_d \mathbf{W}_d^\dagger = \mathbf{M}_d^{\text{diag}}. \quad (5.4)$$

One can in fact obtain a relatively simple formulation of the rotation matrices $\mathbf{U}_{\mathbf{Q}_u}$, $\mathbf{U}_{\mathbf{Q}_d}$, \mathbf{W}_u and \mathbf{W}_d by expanding their entries in powers of ratios f_i/f_j , where $i < j$ and with $i = 1, 2$ and $j = 1, 2, 3, 4$. In Appendix D-1 we have calculated the unitary transformation matrices $\mathbf{U}_{\mathbf{Q}_u}$ and $\mathbf{U}_{\mathbf{Q}_d}$ for four generations of fermions by keeping only the leading terms. Here we will only give the final results of our calculation. For the three family case see [199].

$$\mathbf{U}_{\mathbf{Q}_u} = \begin{pmatrix} 1 & \frac{[\mathbf{Y}_u]_{21}}{[\mathbf{Y}_u]_{11}} \frac{f_{Q_1}}{f_{Q_2}} & \mathcal{U}_{13}^{Q_u} & \mathcal{U}_{14}^{Q_u} \\ -\frac{[\mathbf{Y}_u]_{21}^*}{[\mathbf{Y}_u]_{11}^*} \frac{f_{Q_1}}{f_{Q_2}} & 1 & \mathcal{U}_{23}^{Q_u} & \mathcal{U}_{24}^{Q_u} \\ \frac{[\mathbf{Y}_u]_{31}}{[\mathbf{Y}_u]_{11}} \frac{f_{Q_1}}{f_{Q_3}} & -\frac{[\mathbf{Y}_u]_{11,32}^*}{[\mathbf{Y}_u]_{11,22}^*} \frac{f_{Q_2}}{f_{Q_3}} & c_{Q_u} & s_{Q_u} \\ -\frac{[\mathbf{Y}_u]_{41}}{[\mathbf{Y}_u]_{11}} \frac{f_{Q_1}}{f_{Q_4}} & \frac{[\mathbf{Y}_u]_{11,42}^*}{[\mathbf{Y}_u]_{11,22}^*} \frac{f_{Q_2}}{f_{Q_4}} & -s_{Q_u}^* & c_{Q_u}^* \end{pmatrix}, \quad (5.5)$$

$$\mathbf{U}_{\mathbf{Q}_d} = \begin{pmatrix} 1 & \frac{[\mathbf{Y}_d]_{21}}{[\mathbf{Y}_d]_{11}} \frac{f_{Q_1}}{f_{Q_2}} & \mathcal{U}_{13}^{Q_d} & \mathcal{U}_{14}^{Q_d} \\ -\frac{[\mathbf{Y}_d]_{21}^*}{[\mathbf{Y}_d]_{11}^*} \frac{f_{Q_1}}{f_{Q_2}} & 1 & \mathcal{U}_{23}^{Q_d} & \mathcal{U}_{24}^{Q_d} \\ \frac{[\mathbf{Y}_d]_{31}}{[\mathbf{Y}_d]_{11}} \frac{f_{Q_1}}{f_{Q_3}} & -\frac{[\mathbf{Y}_d]_{11,32}^*}{[\mathbf{Y}_d]_{11,22}^*} \frac{f_{Q_2}}{f_{Q_3}} & c_{Q_d} & s_{Q_d} \\ -\frac{[\mathbf{Y}_d]_{41}}{[\mathbf{Y}_d]_{11}} \frac{f_{Q_1}}{f_{Q_4}} & \frac{[\mathbf{Y}_d]_{11,42}^*}{[\mathbf{Y}_d]_{11,22}^*} \frac{f_{Q_2}}{f_{Q_4}} & -s_{Q_d}^* & c_{Q_d}^* \end{pmatrix}, \quad (5.6)$$

where, in particular we have

$$\mathcal{U}_{23}^{Q_d} = c_{Q_d} \frac{f_{Q_2}}{f_{Q_3}} \frac{[\mathbf{Y}_d]_{11,32}}{[\mathbf{Y}_d]_{11,22}} + s_{Q_d}^* \frac{f_{Q_2}}{f_{Q_4}} \frac{[\mathbf{Y}_d]_{11,42}}{[\mathbf{Y}_d]_{11,22}}, \quad (5.7)$$

$$\mathcal{U}_{13}^{Q_d} = c_{Q_d} \frac{f_{Q_1}}{f_{Q_3}} \frac{[\mathbf{Y}_d]_{21,32}}{[\mathbf{Y}_d]_{11,22}} + s_{Q_d}^* \frac{f_{Q_1}}{f_{Q_4}} \frac{[\mathbf{Y}_d]_{21,42}}{[\mathbf{Y}_d]_{11,22}}. \quad (5.8)$$

The $\mathcal{U}_{13}^{Q_u}$ and $\mathcal{U}_{23}^{Q_u}$ entries cannot be simplified as in the down sector since m_t is heavy. However, we do not need them to calculate the CKM entries. The 4D CKM matrix for the left handed quarks are

$$\mathbf{V}_{\text{CKM}} = \mathbf{U}_{\mathbf{Q}_u}^\dagger \mathbf{U}_{\mathbf{Q}_d}, \quad (5.9)$$

The $\mathcal{U}_{13}^{Q_d}$ and $\mathcal{U}_{23}^{Q_d}$ are needed for calculating the elements V_{cb} and V_{ub} . Using the mass hierarchy $m_b \ll m_{b'}$, we can also write the simple expansions for c_{Q_d} and $s_{Q_d}^*$ as

$$c_{Q_d} = v_4 f_{Q_4} f_{d_4} |Y_{44}^d| / m_{b'}, \quad s_{Q_d}^* = v_4 f_{Q_3} f_{d_4} Y_{34}^{d*} / m_{b'} e^{i \arg(Y_{44}^d)}. \quad (5.10)$$

Now, we give the analytical expressions for some of the CKM entries. The details of the calculations are given in Appendix D-1. It is important to note that even though the 5D Yukawa matrices are all $\mathcal{O}(1)$, we can still have the observed hierarchy structure in CKM matrix by virtue of the f_i parameters.

$$V_{us} = \frac{f_{Q_1}}{f_{Q_2}} \left(\frac{[\mathbf{Y}_d]_{21}}{[\mathbf{Y}_d]_{11}} - \frac{[\mathbf{Y}_u]_{21}}{[\mathbf{Y}_u]_{11}} \right), \quad (5.11)$$

$$, \quad (5.12)$$

and

$$\begin{aligned} V_{ub} &= c_{Q_d} \frac{f_{Q_1}}{f_{Q_3}} \left(\frac{[\mathbf{Y}_u]_{31}}{[\mathbf{Y}_u]_{11}} + \frac{[\mathbf{Y}_d]_{21,32}}{[\mathbf{Y}_d]_{11,22}} - \frac{[\mathbf{Y}_u]_{21}}{[\mathbf{Y}_u]_{11}} \frac{[\mathbf{Y}_d]_{11,32}}{[\mathbf{Y}_d]_{11,22}} \right) \\ &+ s_{Q_d}^* \frac{f_{Q_1}}{f_{Q_4}} \left(\frac{[\mathbf{Y}_u]_{41}}{[\mathbf{Y}_u]_{11}} + \frac{[\mathbf{Y}_d]_{21,42}}{[\mathbf{Y}_d]_{11,22}} - \frac{[\mathbf{Y}_u]_{21}}{[\mathbf{Y}_u]_{11}} \frac{[\mathbf{Y}_d]_{11,42}}{[\mathbf{Y}_d]_{11,22}} \right). \end{aligned} \quad (5.13)$$

If the 5D Yukawa matrix elements are all of order 1, then the observed hierarchies among the CKM elements can still be explained by hierarchies among the f_i parameters. The explicit dependence on the 5D Yukawa couplings gives a more precise prediction for the mixing angles, which is quite useful when looking for phenomenologically viable points in parameter space. The results of such a scan are presented in the next subsection. The $\mathbf{W}_{\mathbf{u},\mathbf{d}}$ matrices are obtained in the same

way as $\mathbf{U}_{\mathbf{Q}_{u,d}}$ and are given by (see Appendix D-1)

$$\mathbf{W}_{\mathbf{u}} = \begin{pmatrix} 1 & \frac{[\mathbf{Y}_{\mathbf{u}}]_{12}^* f_{u_1}}{[\mathbf{Y}_{\mathbf{u}}]_{11}^* f_{u_2}} & \mathcal{W}_{13}^u & \mathcal{W}_{14}^u \\ -\frac{[\mathbf{Y}_{\mathbf{u}}]_{12} f_{u_1}}{[\mathbf{Y}_{\mathbf{u}}]_{11} f_{u_2}} & 1 & \mathcal{W}_{23}^u & \mathcal{W}_{24}^u \\ \frac{[\mathbf{Y}_{\mathbf{u}}]_{13} f_{u_1}}{[\mathbf{Y}_{\mathbf{u}}]_{11} f_{u_3}} & -\frac{[\mathbf{Y}_{\mathbf{u}}]_{11,23} f_{u_2}}{[\mathbf{Y}_{\mathbf{u}}]_{11,22} f_{u_3}} & c_u^* & s_u^* \\ -\frac{[\mathbf{Y}_{\mathbf{u}}]_{14} f_{u_1}}{[\mathbf{Y}_{\mathbf{u}}]_{11} f_{u_4}} & \frac{[\mathbf{Y}_{\mathbf{u}}]_{11,24} f_{u_2}}{[\mathbf{Y}_{\mathbf{u}}]_{11,22} f_{u_4}} & -s_u & c_u \end{pmatrix}, \quad (5.14)$$

and

$$\mathbf{W}_{\mathbf{d}} = \begin{pmatrix} 1 & \frac{[\mathbf{Y}_{\mathbf{d}}]_{12}^* f_{d_1}}{[\mathbf{Y}_{\mathbf{d}}]_{11}^* f_{d_2}} & \mathcal{W}_{13}^d & \mathcal{W}_{14}^d \\ -\frac{[\mathbf{Y}_{\mathbf{d}}]_{12} f_{d_1}}{[\mathbf{Y}_{\mathbf{d}}]_{11} f_{d_2}} & 1 & \mathcal{W}_{23}^d & \mathcal{W}_{24}^d \\ \frac{[\mathbf{Y}_{\mathbf{d}}]_{13} f_{d_1}}{[\mathbf{Y}_{\mathbf{d}}]_{11} f_{d_3}} & -\frac{[\mathbf{Y}_{\mathbf{d}}]_{11,23} f_{d_2}}{[\mathbf{Y}_{\mathbf{d}}]_{11,22} f_{d_3}} & c_d^* & s_d^* \\ -\frac{[\mathbf{Y}_{\mathbf{d}}]_{14} f_{d_1}}{[\mathbf{Y}_{\mathbf{d}}]_{11} f_{d_4}} & \frac{[\mathbf{Y}_{\mathbf{d}}]_{11,24} f_{d_2}}{[\mathbf{Y}_{\mathbf{d}}]_{11,22} f_{d_4}} & -s_d & c_d \end{pmatrix}. \quad (5.15)$$

5.1.2 Tree level Higgs FCNC couplings

We now extend the one-family results presented in Subsection 3.4.5 to the case of four generations. To leading order in Yukawa couplings, the SM fermion mass matrix is

$$\hat{\mathbf{m}}^{\mathbf{d}} = \hat{\mathbf{F}}_{\mathbf{Q}} \hat{\mathbf{Y}}_1^{5\text{D}} \hat{\mathbf{F}}_{\mathbf{d}} v_4, \quad (5.16)$$

where $\hat{\cdot}$ indicates a 4×4 matrix in flavor space. The misalignment in flavor space between the fermion mass matrix and the Yukawa coupling matrix is defined as

$$\hat{\Delta}^{\mathbf{d}} = \hat{\mathbf{m}}^{\mathbf{d}} - v_4 \hat{\mathbf{y}}_4^{\mathbf{d}}, \quad (5.17)$$

where $\hat{\mathbf{y}}_4^{\mathbf{d}}$ is the 4D effective coupling matrix between the physical scalar Higgs and the quarks.

Similarly to the one family case, the misalignment can be separated into two components, $\hat{\Delta}_1^{\mathbf{d}} + \hat{\Delta}_2^{\mathbf{d}}$, with

$$\hat{\Delta}_1^{\mathbf{d}} = \frac{2}{3} \hat{\mathbf{m}}^{\mathbf{d}} \frac{1}{\hat{\mathbf{F}}_{\mathbf{d}}} (\hat{\mathbf{Y}}_2^{5\text{D}})^\dagger \frac{1}{\hat{\mathbf{F}}_{\mathbf{Q}}} \hat{\mathbf{m}}^{\mathbf{d}} (v_4 R'^2), \quad (5.18)$$

and

$$\hat{\Delta}_2^d = \hat{\mathbf{m}}^d \left(\hat{\mathbf{m}}^{d\dagger} \hat{\mathbf{K}}(\mathbf{c}_q) + \hat{\mathbf{K}}(-\mathbf{c}_d) \hat{\mathbf{m}}^{d\dagger} \right) \hat{\mathbf{m}}^d R'^2 \quad (5.19)$$

The crucial observation is that $\hat{\mathbf{m}}^d$ and $\hat{\Delta}^d$ are generally not aligned in flavor space. Thus when we diagonalize the quark mass matrix with a bi-unitary transformation $\hat{\mathbf{m}}^d \rightarrow \mathbf{U}_{\mathbf{Q}_L}^\dagger \hat{\mathbf{m}}^d \mathbf{W}_d$, the Yukawa couplings will not be diagonal. To be more specific, in models of flavor anarchy, we have

$$(U_{Q_d}, W_d)_{i,j} \sim \frac{f_{Q_i, d_i}}{f_{Q_j, d_j}} \quad \text{for } i < j. \quad (5.20)$$

Then the off-diagonal Yukawa coupling will be dominated by

$$\hat{\mathbf{Y}}_{ij}^{\text{off}} = -(\mathbf{U}_{\mathbf{d}_L}^\dagger \hat{\Delta}^d \mathbf{W}_{\mathbf{d}_R})_{ij} \frac{1}{v_4} \sim \frac{2}{3} f_{Q_i} \bar{Y}^3 f_{d_j} v_4^2 R'^2, \quad (5.21)$$

where \bar{Y} is the typical value of the dimensionless 5D Yukawa coupling.

Since the Higgs couplings now contain off-diagonal entries, we must choose a convenient parametrization for them. A common choice is to normalize the couplings with the fermion masses and write the Higgs Yukawa couplings as¹

$$\mathcal{L}_{HFV} = a_{ij}^d \sqrt{\frac{m_i^d m_j^d}{v_4^2}} H \bar{d}_L^i d_R^j + \text{h.c.} + (d \leftrightarrow u). \quad (5.22)$$

5.1.3 Analytical Estimates of Higgs FCNC Couplings in Flavor Anarchy

In Section 3.4 the tree level Higgs FCNCs are presented. In this subsection we will estimate analytically flavor changing couplings of Higgs to fermions with 4 generation in warped extra dimensional model. We follow the same procedure as in [181] where there are three families only. We then compare these analytical results to our numerical scan.

We use eqs. (5.20) and (5.21) to estimate the sizes of $a_{ij}^{u,d}$. For example, we have

$$a_{12}^d \sim \frac{2}{3} f_{Q_1} \bar{Y}^3 f_{d_2} v_4^2 R'^2 \sqrt{\frac{v_4^2}{m_s m_d}} \sim \frac{2}{3} \lambda \bar{Y}^2 v_4^2 R'^2 \sqrt{\frac{m_s}{m_d}}, \quad (5.23)$$

¹This is a particular realization of the Cheng-Sher *Ansatz* [200].

where λ is the Wolfenstein parameter (see Section 2.3), and we used $f_{q_1}/f_{q_2} \sim (U_{dL})_{12} \sim (V_{CKM})_{12} \sim \lambda$. We can find the other $a_{ij}^{u,d}$ in similar fashion. We obtain:

$$a_{ij}^d \sim \delta_{ij} - \frac{2}{3} \bar{Y}^2 v_4^2 R'^2 \begin{pmatrix} 1 & \lambda \sqrt{\frac{m_s}{m_d}} & \lambda^3 \sqrt{\frac{m_b}{m_d}} & \lambda^3 \sqrt{\frac{m_{b'}}{m_d}} \\ \frac{1}{\lambda} \sqrt{\frac{m_d}{m_s}} & 4 & \lambda^2 \sqrt{\frac{m_b}{m_s}} & \lambda^2 \sqrt{\frac{m_{b'}}{m_s}} \\ \frac{1}{\lambda^3} \sqrt{\frac{m_d}{m_b}} & \frac{1}{\lambda^2} \sqrt{\frac{m_s}{m_b}} & 12 & \sqrt{\frac{m_{b'}}{m_b}} \\ \frac{1}{\lambda^3} \sqrt{\frac{m_d}{m_{b'}}} & \frac{1}{\lambda^2} \sqrt{\frac{m_s}{m_{b'}}} & \sqrt{\frac{m_b}{m_{b'}}} & 12 \end{pmatrix}, \quad (5.24)$$

$$a_{ij}^u \sim \delta_{ij} - \frac{2}{3} \bar{Y}^2 v_4^2 R'^2 \begin{pmatrix} 1 & \lambda \sqrt{\frac{m_c}{m_u}} & \lambda^3 \sqrt{\frac{v_4^2}{m_t m_u}} & \lambda^3 \sqrt{\frac{v_4^2}{m_{t'} m_u}} \\ \frac{1}{\lambda} \sqrt{\frac{m_u}{m_c}} & 4 & \lambda^2 \sqrt{\frac{v_4^2}{m_t m_c}} & \lambda^2 \sqrt{\frac{v_4^2}{m_{t'} m_c}} \\ \frac{1}{\lambda^3} \sqrt{\frac{m_u}{m_t}} & \frac{1}{\lambda^2} \sqrt{\frac{m_c}{m_t}} & 16 & \sqrt{\frac{m_{t'} m_t}{v_4^2}} \\ \frac{1}{\lambda^3} \sqrt{\frac{m_u}{m_{t'}}} & \frac{1}{\lambda^2} \sqrt{\frac{m_c}{m_{t'}}} & \sqrt{\frac{v_4^2}{m_{t'} m_t}} & 16 \end{pmatrix}. \quad (5.25)$$

The effect clearly decouples since it depends on $R'^2 \sim \frac{1}{M_{KK}^2}$. Taking the typical Yukawa size $\bar{Y} = 2$ and $1/R' = 1500$ GeV, and using the known SM masses evaluated at the KK scale, along with $m_{t'} = 400$ GeV and $m_{b'} = 350$ GeV, one can obtain the typical values of these couplings:

$$a_{ij}^d \sim \begin{pmatrix} 0.96 & 0.03 & 0.01 & 0.14 \\ 0.04 & 0.86 & 0.01 & 0.15 \\ 0.13 & 0.19 & 0.57 & 0.45 \\ 0.01 & 0.007 & 0.003 & 0.57 \end{pmatrix}, \quad (5.26)$$

$$a_{ij}^u \sim \begin{pmatrix} 0.96 & 0.16 & 0.15 & 0.09 \\ 0.008 & 0.86 & 0.04 & 0.02 \\ 0.01 & 0.04 & 0.42 & 0.05 \\ 0.007 & 0.03 & 0.003 & 0.42 \end{pmatrix}. \quad (5.27)$$

Note that the results presented here are just estimates for the size of $a_{ij}^{u,d}$, which enter without sign or phases. However, we observe that for the third and fourth generation quarks, the corrections to the diagonal Yukawa couplings are always negative (suppressions) if $Y_1 = Y_2$ and are larger than the previous estimates. This point was argued in [181] and we address it again the next subsection for completeness.

An interesting feature of these matrices is the asymmetry of a_{ij}^d in the $b_L b'_R$ and $b'_L b_R$ entries, asymmetry not shared by the up-quark matrix a_{ij}^u . This asymmetry in the couplings produces an asymmetry in the decays, as well as in the shift in the vertex functions g_L^b, g_R^b for $Z \rightarrow b\bar{b}$. This asymmetry will be typical for the (34 – 43) entries and thus non-universal. We expect the same feature in the charged lepton mass matrix.

5.1.4 Numerical Results for Higgs FCNC Couplings

In order to obtain a better prediction of the typical size of the off-diagonal Yukawa couplings, and to compare with the previous estimates we perform a scan in parameter space. The results should be in general consistent with the rough estimates of Eqs. (5.26) and (5.27). Some differences observed can nevertheless be explained, (see also [181]) so that one can still be confident of the generic size of the flavor violating couplings predicted in the flavor anarchy paradigm in RS type scenarios with four generations.

We proceed as follows:

- We fix $m_{t'} = 400$ GeV and $m_{b'} = 350$ GeV as well as SM quark masses at the KK scale, taken to be $m_t = 140$ GeV, $m_b = 2.2$ GeV, $m_c = 0.55$ GeV, $m_s = 5 \times 10^{-2}$ GeV, $m_u = 1.5 \times 10^{-3}$ GeV, $m_d = 3.0 \times 10^{-3}$ GeV. We take the KK scale as $R'^{-1} = 1500$ GeV.
- Then we generate random complex entries for Y_u and Y_d , such that $|Y_i| \in [0.3, 3.5]$. We also generate random f_{Q_4} such that $f_{Q_4} \sim \mathcal{O}(1)$.
- We then obtain f_{Q_3} from $|V_{ub}|/|V_{us}|/|V_{cb}|$, f_{Q_2} from $|V_{ub}|/|V_{us}|$ and f_{Q_1} from $|V_{us}|$ (see Eqs. (5.11), (5.12) and (5.13)).
- We then obtain the right-handed down quark entries f_{d_4} from $m_{b'}$.
- Similarly for the up right-handed matrix entries, we obtain $f_{u_1}, f_{u_2}, f_{d_1}, f_{d_2}$ and f_{d_3} from m_u, m_c, m_d, m_s and m_b . We also obtain f_{u_3} and f_{u_4} from m_t and $m_{t'}$.
- Finally we check that the generated Y_u and Y_d along with the obtained \hat{F}_q, \hat{F}_u and \hat{F}_d do indeed produce the observed masses and mixings of the SM. If so

we keep the point in parameter space and continue until we obtain 1000 points which satisfy all constraints.

- For each acceptable point, we use Eqs. (5.18) and (5.19) to compute the flavor violating Higgs Yukawa couplings, parametrized by the a_{ij} 's as defined in Eq. (5.22).

We present the results of the scan as follows: we give the 25% quantile and the 75% quantile of the obtained couplings. This means that 50% of our acceptable points contain a coupling in between the quoted values. Also it means that 25% of the generated points predict higher values than the range quoted, while 25% of the points predict lower values than the range quoted.

We find the following ranges for a_{ij}^d , a_{ij}^u matrix couplings²

$$a_{ij}^d \sim \begin{pmatrix} 0.919 - 0.987 & 0.025 - 0.081 & 0.011 - 0.044 & 0.130 - 0.532 \\ 0.049 - 0.148 & 0.827 - 0.934 & 0.0017 - 0.059 & 0.249 - 0.934 \\ 0.140 - 0.470 & 0.142 - 0.446 & 0.620 - 0.819 & 0.873 - 2.508 \\ 0.018 - 0.061 & 0.017 - 0.058 & 0.008 - 0.120 & 0.375 - 0.643 \end{pmatrix}, \quad (5.28)$$

$$a_{ij}^u \sim \begin{pmatrix} 0.927 - 1.000 & 0.089 - 0.364 & 0.091 - 0.410 & 0.139 - 0.612 \\ 0.015 - 0.052 & 0.816 - 0.949 & 0.065 - 0.197 & 0.092 - 0.300 \\ 0.019 - 0.068 & 0.071 - 0.236 & 0.545 - 0.772 & 0.127 - 0.343 \\ 0.0167 - 0.062 & 0.060 - 0.191 & 0.064 - 0.168 & 0.403 - 0.651 \end{pmatrix}, \quad (5.29)$$

to be compared with the rough estimates Eqs. (5.26) and (5.27).

5.1.5 Cumulative Effect on Diagonal Yukawa Couplings when $Y_1 = Y_2$

We observe that the rough estimates are slightly smaller than the results of the scan, specially for the third and fourth generation couplings. This was already pointed out in [181] for the three generation case. The argument given is that due to the presence of a fourth generation some of the coefficients will be different and typically the cumulative effect will be larger.

²This scans were produced by Dr. Manuel Toharia.

We assume that $Y_1 = Y_2$. This is an important choice, and without it no extra enhancements would appear. Nevertheless this choice is natural if the Higgs boson is to be considered as a highly localized 5D scalar field, and then 5D Lorentz invariance imposes $Y_1 = Y_2$. Let us consider the element (33) of the Yukawa coupling in the up quark sector as an example

$$\begin{aligned}
a_{tt} - 1 &= -\frac{2R'^2}{3m_t} \left[\mathbf{U}_{\mathbf{Q}_u}^\dagger \mathbf{M}_u \frac{1}{\hat{F}_u^2} \mathbf{M}^{u\dagger} \frac{1}{\hat{F}_Q^2} \mathbf{M}_u \mathbf{W}_u \right]_{33} \\
&= -\frac{2R'^2}{3m_t} \left(\mathbf{M}_u^{\text{diag}} \right)_{33} \left(\mathbf{W}_u^\dagger \frac{1}{\hat{F}_u^2} \mathbf{W}_u \right)_{3j} \left(\mathbf{M}_u^{\text{diag}} \right)_{jj} \\
&\quad \times \left(\mathbf{U}_{\mathbf{Q}_u}^\dagger \frac{1}{\hat{F}_Q^2} \mathbf{U}_{\mathbf{Q}_u} \right)_{j3} \left(\mathbf{M}_u^{\text{diag}} \right)_{33}. \tag{5.30}
\end{aligned}$$

First let's look at the contribution to a_{tt} when the j index is equal to 3 (i.e. for mass matrix $(\mathbf{M}_u^{\text{diag}})_{33} = m_t$). In this case, there will be 16 terms in phase, each proportional to $-\frac{2R'^2\bar{Y}^2v_4^2}{3}$, and it is important to realize that every one of them will be real and negative, because $(\mathbf{W}_u^\dagger \frac{1}{\hat{F}_u^2} \mathbf{W}_u)_{33} \geq 0$. When $j = 2$ ($(\mathbf{M}_u^{\text{diag}})_{22} = m_c$) there will be 2 terms $\sim \frac{2R'^2\bar{Y}^2v_4^2}{3}$ but every one of them will have generically a random complex phase (the 14 remaining terms are much smaller). For $j = 1$ ($(\mathbf{M}_u^{\text{diag}})_{11} = m_u$) there is only one term $\sim \frac{2R'^2\bar{Y}^2v_4^2}{3}$ contributing, with the rest 15 terms being again suppressed. So, summing over all terms, the dominant contribution to a_{tt} will consist of 19 terms, 16 of which are negative and the rest 3 have random complex phases. Generically each of these terms are of the same size $\sim \frac{2R'^2\bar{Y}^2v^2}{3}$ so from a statistical argument, $a_{tt} - 1$ should receive a negative contribution $\sim -16 \left(\frac{2R'^2\bar{Y}^2v^2}{3} \right)$. This cumulative effect is confirmed by the numerical scan.

One can perform the same analysis for the rest of elements of the Yukawa matrix, including the off diagonal ones, and realize that typically there are a number of aligned terms in each case which enhance the naive estimate by an $\mathcal{O}(1)$ factor (and which also can be estimated). This fact gives us confidence that both our scan and our estimates are consistent and that our numerical results predict correctly in this scenario the generic size of the flavor violating couplings in the Higgs sector.

5.1.6 Higgs FCNC Couplings in the Lepton Sector

We proceed in a similar fashion to evaluate Higgs flavor violation in the lepton sector. The difficulty with the lepton sector is that mixing matrices are not well-established here. The neutrinos can be either Dirac or Majorana, the charged lepton mixing matrix (PMNS) is not as well established as the CKM matrix, and there are several mechanisms to explain the large mixing angles and light masses for the neutrinos (see for example [201, 202]). For all cases, the Lagrangian can then be parametrized as:

$$\mathcal{L}_{HFV} = a_{ij}^l \sqrt{\frac{m_i^l m_j^l}{v_4^2}} H \bar{L}^i e^j + h.c. \quad (5.31)$$

Following [181, 202], we analyze two types of scenarios. Depending on the neutrino model, the left-handed charged lepton profiles can be either hierarchical and UV localized, or similar and UV localized. The profiles of the right-handed charged leptons are always hierarchical and localized near the UV brane. We outline both cases below.

- (A) In the case where the left-handed and right-handed profiles are hierarchical, they satisfy the following relations:

$$f_L^i f_e^i \sim \frac{m_i^l}{\bar{Y} v_4}, \quad (O_{L,e})^{i,j} \sim \frac{f_{L,e}^i}{f_{L,e}^j}, \quad i < j. \quad (5.32)$$

where $f_{L,e}$ are profiles of the left-handed and right-handed fields and $(O_{L,e})^{i,j}$ is the intergenerational mixing. Then the a_{ij}^l become:

$$a_{ij}^l \sim \frac{2}{3} \bar{Y}^2 (v_4^2 R'^2) \sqrt{\frac{f_L^i f_e^j}{f_L^j f_e^i}}. \quad (5.33)$$

This a_{ij}^l are maximal when $\frac{f_L^i}{f_L^j} \sim \frac{f_e^i}{f_e^j} \sim \sqrt{\frac{m_i^l}{m_j^l}}$, i.e., when the hierarchy of charged lepton masses acquires equal contributions from the left-handed and right-handed fields.

- (B) If right-handed profiles are hierarchical and left-handed profiles are similar, $f_L^1 \sim f_L^2 \sim f_L^3$, the profiles satisfy the following relations:

$$f_L^i f_e^i \sim \frac{m_i^l}{\bar{Y} v_4}, \quad \frac{f_L^i}{f_L^j} \sim O(1), \quad \frac{f_e^i}{f_e^j} \sim \frac{m_i^l}{m_j^l}, \quad i < j, \quad (5.34)$$

and the the parameter a_{ij}^l becomes:

$$a_{ij}^l \sim \frac{2}{3} \bar{Y}^2 (v_4^2 R'^2) \sqrt{\frac{f_e^j}{f_e^i}}. \quad (5.35)$$

These flavor violating Higgs Yukawa couplings to leptons can also lead to interesting collider signals for the decays of the fourth generation leptons, as discussed in the next section.

5.1.7 Tree Level Z^0 Flavor Violating Couplings

FCNC couplings of the Z^0 boson have been studied before in the context of warped scenarios with 3 generations [199]. These couplings arise basically from two sources. First, the bulk profiles of the lowest-lying massive gauge bosons (the SM Z^0 and W^0) are not flat, yielding non-trivial and non-universal overlap integrals with the fermion profiles. Second, even if the Z^0 and W^0 profiles were flat, there would still be a non-universal correction to these couplings due to misalignments in the fermion kinetic terms. In fact the correction has the exact same origin as the misalignment $\hat{\Delta}_2^d$ in the Higgs sector shown in Eq. (5.19).

For light quarks, the first source of misalignment dominates due to Yukawa suppression of the fermion kinetic term misalignments. But for heavier quarks, and specially fourth generation quarks, this last source of flavor should dominate and this is the one we consider in the following.

We can write the couplings of fermions with Z^0 as:

$$\mathcal{L}_Z = \left[g_L \delta_{ij} + \left(\hat{\delta}_{g_L} \right)_{ij} \right] \bar{d}_L^i \not{Z} d_L^j + \left[g_R \delta_{ij} + \left(\hat{\delta}_{g_R} \right)_{ij} \right] \bar{d}_R^i \not{Z} d_R^j + (d \leftrightarrow u), \quad (5.36)$$

where $g_L = \frac{g}{\cos \theta_W} (T_3 - Q \sin^2 \theta_W)$ and $g_R = \frac{g}{\cos \theta_W} Q \sin^2 \theta_W$ are the usual diagonal SM couplings with g the $SU(2)_L$ coupling constant, and Q and T_3 the charge and the isospin of the quark in question. The corrections coming from the kinetic term misalignment are, for the down quarks,

$$\hat{\delta}_{g_L}^{kin} = -\frac{g T_3^d}{\cos \theta_W} \mathbf{M}_d^\dagger \hat{\mathbf{K}}_{c_d} \mathbf{M}_d R'^2, \quad (5.37)$$

$$\hat{\delta}_{g_R}^{kin} = \frac{g T_3^d}{\cos \theta_W} \mathbf{M}_d \hat{\mathbf{K}}_{c_d} \mathbf{M}_d^\dagger R'^2. \quad (5.38)$$

where \mathbf{M}^d is the fermion mass matrix before diagonalization, R'^{-1} is the KK scale and $\hat{\mathbf{K}}$ is a diagonal matrix whose entries $K(c)$ were defined in Eq. (3.196). Upon diagonalization of the fermion mass matrix in order to go to the physical basis, these corrections will not be diagonal and will produce flavor violating coupling for the Z^0 boson. The same mechanism applies in the up-sector.

Once in the physical basis, we can parametrize the off-diagonal quark couplings in the Lagrangian by $(a_L^{u,d})_{ij}$ and $(a_R^{u,d})_{ij}$, with

$$\mathcal{L}_{Z^0} = -\frac{gT_3^d}{\cos\theta_W} \left[(a_L^d)_{ij} \bar{d}_L^i \not{Z} d_L^j - (a_R^d)_{ij} \bar{d}_R^i \not{Z} d_R^j \right] + (d \leftrightarrow u). \quad (5.39)$$

The Z^0 FCNC couplings $(a_L^{u,d})_{ij}$, $(a_R^{u,d})_{ij}$ can then be obtained from the same scan used to obtain numerical values for the Higgs FCNC couplings. For example, for the (43) entries in the up and down sector, we find typical ranges

$$(a_L^u)_{43} = 0.00350 - 0.0176, \quad (a_R^u)_{43} = 0.0274 - 0.0952, \quad (5.40)$$

$$(a_L^d)_{43} = 0.00356 - 0.0161, \quad (a_R^d)_{43} = 0.0209 - 0.0830. \quad (5.41)$$

To obtain these values we followed the same procedure explained previously in the subsection “*Numerical results for Higgs FCNC couplings*”.

5.2 Phenomenology

5.2.1 Bounds on Higgs-mediated FCNC Couplings

The off-diagonal Higgs Yukawa couplings induce FCNC, which affect many low energy observables and also give possible signatures at colliders. In this section, we discuss first bounds on Higgs flavor violation coming from tree-level processes $\Delta F = 2$, such as $K - \bar{K}$, $B - \bar{B}$, $D - \bar{D}$ mixing. We then study the effects on loop processes, such as b and t flavor-changing decays, as well as on $Z \rightarrow b\bar{b}$, $\tau^+\tau^-$. The radiative processes are enhanced due to heavy quarks in the loop, and strong off-diagonal Yukawa couplings.

Tree-level Processes

The $\Delta F = 2$ processes are introduced in Subsection 4.4.1. For $K - \bar{K}$, $B_d - \bar{B}_d$, $B_s - \bar{B}_s$, $D - \bar{D}$ mixing, $q_i q_j$ in eq. (4.39) are replaced by sd , bd , bs and uc , respectively.

The exchange of the flavor-violating Higgs bosons gives rise to new contribution to C_2 , \tilde{C}_2 and C_4 operators [94]. These contributions have been analyzed in the context of SM4 [203]. The 3-generation constraints have been included in [181], and the basic bounds on the coefficients are not altered. We present them here, for completeness, in a more general fashion, with no relation to the possible numerical values of the entries in the Higgs Yukawa mass matrix. We use the model-independent bounds on BSM contributions as in [189], and present coupled constraints on the Higgs flavor violating Yukawa couplings parametrized by the a_{ij} couplings and the Higgs mass m_h .

- **$\mathbf{K}^0 - \bar{\mathbf{K}}^0$ mixing:** the coefficients C_2 , \tilde{C}_2 and C_4 will set limits on the real and imaginary of the Yukawa couplings a_{12}^d , a_{21}^d , and their product. Specifically, for the values of parameters used in the previous sections, we obtain, from ΔM_K , respectively:

$$\begin{aligned} |(a_{12}^d)| \left(\frac{500 \text{ GeV}}{m_h} \right) &\leq 0.78, & |(a_{21}^d)| \left(\frac{500 \text{ GeV}}{m_h} \right) &\leq 0.78, & (5.42) \\ |(a_{12}^d a_{21}^{d*})| \left(\frac{500 \text{ GeV}}{m_h} \right)^2 &\leq (0.44)^2. \end{aligned}$$

The bounds obtained from ϵ_K are very stringent, and restrict the phases of the off-diagonal Higgs Yukawa couplings:

$$\begin{aligned} \text{Im}(a_{12}^d)^2 \left(\frac{500 \text{ GeV}}{m_h} \right)^2 &\leq (5.75 \times 10^{-2})^2, \\ \text{Im}(a_{21}^d)^2 \left(\frac{500 \text{ GeV}}{m_h} \right)^2 &\leq (5.75 \times 10^{-2})^2, \\ \text{Im}(a_{12}^d a_{21}^{d*}) \left(\frac{500 \text{ GeV}}{m_h} \right)^2 &\leq (2.75 \times 10^{-2})^2. & (5.43) \end{aligned}$$

- **$\mathbf{D}^0 - \bar{\mathbf{D}}^0$ mixing:** the mixing constrains the (12, 21) off-diagonal entries in the up-quark flavor changing mixings.

$$\begin{aligned} |(a_{12}^u)| \left(\frac{500 \text{ GeV}}{m_h} \right) &\leq 0.89, & |(a_{21}^u)| \left(\frac{500 \text{ GeV}}{m_h} \right) &\leq 0.89, \\ |(a_{12}^u a_{21}^{u*})| \left(\frac{500 \text{ GeV}}{m_h} \right)^2 &\leq (0.59)^2. & (5.44) \end{aligned}$$

- **$\mathbf{B}_d^0 - \bar{\mathbf{B}}_d^0$ mixing:** the mixing is fairly constrained, resulting in bounds on the (13, 31) entries in the down-quark flavor changing mixings.

$$\begin{aligned}
|(a_{13}^d)| \left(\frac{500 \text{ GeV}}{m_h} \right) &\leq 0.675, & |(a_{31}^d)| \left(\frac{500 \text{ GeV}}{m_h} \right) &\leq 0.675, \\
|(a_{13}^d a_{31}^{d*})| \left(\frac{500 \text{ GeV}}{m_h} \right)^2 &\leq (0.44)^2.
\end{aligned} \tag{5.45}$$

- **$\mathbf{B}_s^0 - \bar{\mathbf{B}}_s^0$ mixing:** The mass mixing in the $B_s^0 - \bar{B}_s^0$ is less restricted than in the B_d^0 sector, resulting in bounds on the (23, 32) entries in the down-quark flavor changing mixings. At first, these bounds may not appear useful; however, one must note that the matrix entries a_{ij} are not otherwise constrained (*e.g.*, by unitarity).

$$\begin{aligned}
|(a_{23}^d)| \left(\frac{500 \text{ GeV}}{m_h} \right) &\leq 1.38, & |(a_{32}^d)| \left(\frac{500 \text{ GeV}}{m_h} \right) &\leq 1.38, \\
|(a_{23}^d a_{32}^{d*})| \left(\frac{500 \text{ GeV}}{m_h} \right)^2 &\leq (0.8)^2.
\end{aligned} \tag{5.46}$$

With the exception of ϵ_K , these bounds are not too restrictive over the estimated size of the flavor violating couplings of the Higgs as our numerical evaluation show, except perhaps for very light $m_h \simeq 120$ GeV. In what follows, we compare the tree-level bounds with precision bounds coming from loop-generated processes including a heavy fermion in the loop.

One-loop processes

We evaluate flavor-violating radiative type processes of the form $q_i \rightarrow q_j \gamma$, and $l_i \rightarrow l_j \gamma$ as well as $Z \rightarrow b\bar{b}$ and $Z \rightarrow \tau^+ \tau^-$. Though occurring at one-loop level, these processes are tightly constrained experimentally. For a recent calculation of these warped penguin diagrams due to radiative exchanges of heavy KK states see [204]. In our scenario each process receives additional non-universal contributions from the fourth generation quarks or leptons and Higgs bosons running in the loop.

The contribution is enhanced for couplings with the third generation, as the FCNC couplings are larger. The basic process is illustrated in Fig. 3, where F represent fourth generation quarks or leptons, f_i, f_j , second or third generation quarks or leptons, and h is the Higgs boson. For instance, for $b \rightarrow s \gamma$, $F = b'$, $f_i = b$ and

$f_j = s$ quarks, while for $Z \rightarrow \tau^+\tau^-$, $F = \tau'$, and $f_i = \tau^+$, $f_j = \tau^-$. We analyze each process in detail.

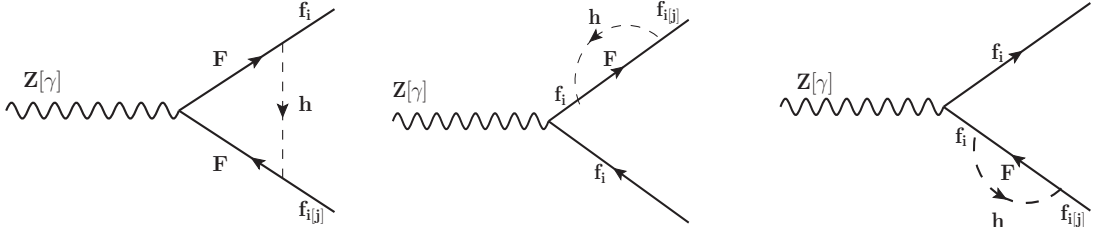


Figure 16: Generic loop diagrams enhanced by FCNC couplings between Higgs boson and 4th generation fermions. Here F stand for a 4th generation quark (or lepton), while f_i, f_j are 2nd or 3rd generation quarks (or leptons). The left-hand side graph is the vertex diagram, while the other two are self-energy diagrams.

- $b \rightarrow s\gamma$ induced by Higgs FCNC couplings

The decay rate of $b \rightarrow s\gamma$ is

$$\Gamma(b \rightarrow s\gamma) = \frac{\langle \mathcal{M}^2 \rangle}{16\pi m_b^3} \sqrt{m_b^4 + m_s^4 - 2m_b^2 m_s^2}. \quad (5.47)$$

where the most dominant term in the matrix element \mathcal{M}^2 is

$$\begin{aligned} \langle \mathcal{M}^2 \rangle &= \frac{em_b^4 m_b m_s}{(24\pi^2 v_4^2)^2} |a_{42}^d a_{34}^d|^2 (m_b^4 + m_s^4 - 2m_b^2 m_s^2) \\ &\quad \times C_0^2 \left(P_1^2, P_2^2, (P_1 + P_2)^2, m_{b'}^2, m_h^2, m_{b'}^2 \right), \end{aligned} \quad (5.48)$$

and where C_0 is a three point integral as defined in Looptools [205] Using the experimental value of the branching ratio of $\bar{B} \rightarrow X_s \gamma$

$$Br(\bar{B} \rightarrow X_s \gamma) = (3.55 \pm 0.24 \pm 0.09) \times 10^{-4}, \quad (5.49)$$

we can put a bound on a_{ij}^d 's such that $|a_{42}^d a_{34}^d| \leq 1.3$. This is a very conservative bound. If we require the branching ratio to be the sum of the SM and the new physics contribution, and use the NLO result $Br(\bar{B} \rightarrow X_s \gamma)_{E_\gamma > 1.6 \text{ GeV}} = (3.60 \pm 0.30) \times 10^{-4}$ [206], we obtain $|a_{42}^d a_{34}^d| \leq 0.45$. These values start to be quite restrictive, as compared to the expected size predicted by our scenario $|a_{42}^d a_{34}^d| \simeq 0.85$ (obtained from our numerical scan).

- $\tau \rightarrow \mu\gamma$, $\tau \rightarrow e\gamma$, $\mu \rightarrow e\gamma$ induced by Higgs FCNC couplings

The same operators will contribute to lepton FCNC decays. The experimental limits on these processes are [114]

$$\begin{aligned} Br(\tau \rightarrow \mu\gamma) &\leq 4.4 \times 10^{-8}, \\ Br(\tau \rightarrow e\gamma) &\leq 3.3 \times 10^{-8}, \\ Br(\mu \rightarrow e\gamma) &\leq 1.2 \times 10^{-11}. \end{aligned} \quad (5.50)$$

The Higgs mediated diagrams with a heavy τ' in the loop yield limits on the a_{ij}^l parameters. Specifically, we get

$$|a_{34}^l a_{42}^l| \leq 0.11, \quad |a_{34}^l a_{41}^l| \leq 1.45, \quad |a_{24}^l a_{41}^l| \leq 0.002. \quad (5.51)$$

We also calculated the a_{ij}^l values by using the two different scenarios. In scenario (A) where both the left-handed and right-handed profiles are hierarchical, we have

$$|a_{34}^l a_{42}^l| = |a_{34}^l a_{41}^l| = |a_{24}^l a_{41}^l| \simeq 0.0065. \quad (5.52)$$

However, in scenario (B) where right-handed profiles are hierarchical and left-handed profiles are not, we get

$$|a_{34}^l a_{42}^l| \simeq 0.0016, \quad |a_{34}^l a_{41}^l| \simeq 0.00011, \quad |a_{24}^l a_{41}^l| \simeq 0.00045. \quad (5.53)$$

Using the a_{ij}^l values in scenario (A) and $\bar{Y} = 3$ we calculated the branching ratios as $Br(\tau \rightarrow \mu\gamma) = 1.4 \times 10^{-10}$, $Br(\tau \rightarrow e\gamma) = 6.7 \times 10^{-13}$ and $Br(\mu \rightarrow e\gamma) = 6.2 \times 10^{-11}$.

For scenario (B) (keeping $\bar{Y} = 3$) we have $Br(\tau \rightarrow \mu\gamma) = 7.8 \times 10^{-12}$, $Br(\tau \rightarrow e\gamma) = 1.9 \times 10^{-16}$ and $Br(\mu \rightarrow e\gamma) = 2.9 \times 10^{-13}$. The predicted size of flavor violating τ decays lies just below experimental bounds, but the branching ratio for $\mu \rightarrow e\gamma$ is above the experimental bounds in scenario (A), and therefore sets some bounds on our scenario. More stringent limits can be set when (expected) new experimental results become available.

- $t \rightarrow c\gamma$ induced by Higgs FCNC couplings Using the formalism from $b \rightarrow s\gamma$ we can estimate the branching ratio for $t \rightarrow c\gamma$. We obtain

$$Br(t \rightarrow c\gamma) = 1.55 \times 10^{-9} \left[|a_{42}^u a_{34}^u|^2 + |a_{43}^u a_{24}^u|^2 + 0.25 \Re(a_{24}^u a_{43}^u a_{42}^u a_{34}^u) \right]. \quad (5.54)$$

which for the values of the scanned Higgs couplings becomes $\text{Br}(t \rightarrow c\gamma) = 1.33 \times 10^{-12}$, too small to be detected anytime soon, and comparable to the SM estimate $\text{Br}(t \rightarrow c\gamma) = 4.5 \times 10^{-13}$ [207].

- $Z \rightarrow b\bar{b}$ decay and $Z \rightarrow \tau^+\tau^-$ For completeness we also computed the loop corrections to $Z \rightarrow b\bar{b}$ decay and $Z \rightarrow \tau^+\tau^-$. The b' and τ' running in these loops make these diagrams larger than the corresponding case with three generations but are still too small to place any useful bound on the Higgs FCNC couplings.

Higgs Production and Decay

The Higgs in RS with 4 generations is in fact quite similar to the SM4. The tree level couplings are still proportional to the masses of the particles it couples to. One of the main differences between four generations and three generations, from the Higgs perspective, are the new radiative contributions to the coupling of Higgs to photons and gluons. This last coupling is typically enhanced by a factor of $\sim \mathcal{O}(3)$ (due to three heavy quarks running in the loops instead of only the top quark), and since the Higgs is mainly produced through gluon fusion at LHC, one expects roughly an enhancement in production cross section of $\sim \mathcal{O}(9)$. Of course this enhancement must be carefully calculated as it is still sensitive to the relative mass between the Higgs and the heavy quarks. In any case the production cross section for this Higgs allows the appearance of many more Higgs bosons than predicted by the minimal SM. Therefore the SM Higgs bounds from Tevatron now become quite stringent, and even early LHC data allows exclusions of regions in the parameter space [163, 164, 208, 209]. In particular a Higgs mass in the 120 – 600 GeV is already excluded by hadron collider bounds (assuming that no new decay channels exist for the Higgs) [163, 164]. We take 100 GeV as a lower bound for the Higgs scalar and study the possible decay channels that such a Higgs could have. The grey shaded regions represent regions of the parameter space excluded by LHC for the SM4 scenario. The dark-grey regions represent higher-confidence parameter regions, while the light-grey regions lower likelihood exclusion regions. As shown in [198] the production and decays of Higgs in RS can alter the values of mass parameters with respect to the SM. The branching ratio bands represent 50% likelihood for the branching ratio, as given in our numerical scan. (That is, 25% of all the parameter points from the numerical scan lie below and 25% lie above the shown interval.) The results are shown in Figure

17, where the branching fraction for each channel is presented. Not surprisingly the dominant decay modes for heavy Higgs ($m_h > 200$ GeV) are $h \rightarrow W^\pm W^\mp$ and $h \rightarrow Z^0 Z^0$ where both W pairs and Z^0 pairs are on-shell. These are the same dominant channels as in the SM; of course once above threshold the Higgs should also decay into pairs of heavy fermions. The typical expectation for models with four generations is that Higgs decays into $t\bar{t}$, $t'\bar{t}'$, $b'\bar{b}'$, $\tau'^+\tau'^-$ (fourth generation charged lepton pair) or $\nu'_\tau\nu'_\tau$ (fourth generation neutrino pair) all have branchings similar to the branching of $h \rightarrow t\bar{t}$, given that the masses of these fermions should typically be in the hundreds of GeV (except maybe the ν'_τ). That yields branching fractions at the 10% level, and this is confirmed in Figure 17.

The new and very interesting result is the prediction of sizable branching fractions for exotic decays of the Higgs into fermion pairs of different flavor. In particular we observe that $h \rightarrow \tau\tau'$, $h \rightarrow bb'$ and $h \rightarrow tt'$ are among the most important new flavor violating channels, a fact not surprising since for heavier fermions one expects larger couplings to the Higgs. An interesting remark for these new channels is that the threshold mass at which they become kinematically allowed is basically set by the mass of the heaviest fermion. This means that while some or most of the flavor diagonal decays into fermions might be closed, there are good chances of an open channel such as $h \rightarrow \tau\tau'$ or $h \rightarrow bb'$. For the chosen parameters (KK scale of $1/R' = 1500$ GeV and typical 5D Yukawa couplings of $\mathcal{O}(2)$) we obtain generic flavor violating Higgs couplings which place the branching ratios of these exotic decay modes on the order of 10^{-2} . Note that since the flavor violating couplings scale as $(\bar{Y}R')^2$, the branching ratios should in turn scale as $(\bar{Y}R')^4$, showing great sensitivity to both the 5D Yukawa couplings and the KK scale.

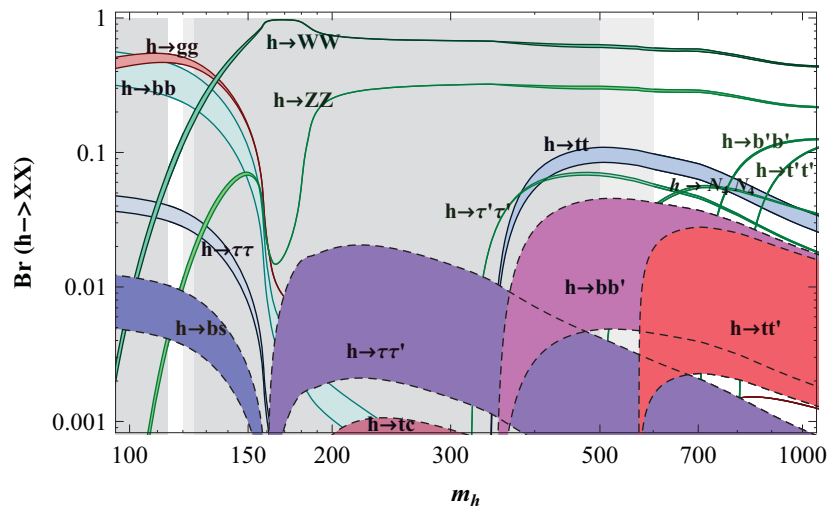


Figure 17: Decay branching fractions of the Higgs scalar in a warped scenario with four generations of fermions. The bands represent 50% likelihood for the branching ratio, according to our numerical scan, as explained in the text. The light and dark gray regions vertical regions are excluded by both Tevatron and LHC (with varying degree of confidence, see discussion in the text). The flavor anarchy setup (masses and mixings explained through fermion localization, with random 5D Yukawa couplings) predicts generic FV couplings of the Higgs, leading to a few new interesting decay channels such as $h \rightarrow bb'$ and $h \rightarrow \tau\tau'$. The masses chosen for this plot are $m_{b'} = 350$ GeV, $m_{t'} = 400$ GeV, $m_{\tau'} = 160$ GeV and $m_{\nu_{\tau'}} = 250$ GeV ($N_4 \equiv \nu_{\tau'}$), and the KK scale is $(R')^{-1} = 1500$ GeV. (Figure on the curtesy of Dr. Manuel Toharia).

The production cross section at the LHC of a heavy Higgs of 400 GeV³, in a scenario with fourth generation quarks is expected to be about $50 - 70$ pb [114]. Since the new exotic decays have branching ratios at the percent level, one expects the cross section of these modes to be somewhere near 500 fb. This means that with 1 or 2 fb⁻¹ of integrated luminosity at the LHC (early stages) one could have at least a few hundred of these events. Of course given the large production cross section, there would be no problem in quickly discovering the Higgs via the four lepton mode ($h \rightarrow Z^0 Z^0 \rightarrow 4l$) or maybe through ($h \rightarrow W^\pm W^\mp$). With the Higgs mass properly set, a complementary search for some of the new exotic channels should be much easier.

³We assume that our branching ratios modify predictions for the m_h from the colliders, thus allowing lighter m_h for RS with four generations.

Of particular interest is the mode $h \rightarrow \tau\tau'$ since it may actually compete as the main production mechanism for the fourth generation charged lepton. If $m_h < 2m_{\tau'}$, the decay into pairs of τ' is forbidden and so the other possible production for heavy leptons is through s -channel processes involving electroweak bosons [210] and their KK partners [105]. The typical cross section for $\tau' - \nu'_\tau$ production via s -channel W is $10 - 100$ fb [210], which means that the flavor violating production through s -channel on-shell Higgs of $\tau^\pm\tau'^\mp$ can be a few times larger than this. The subsequent decay of the $\tau'^\mp \rightarrow \nu'_\tau W^\mp$, and then of $\nu'_\tau \rightarrow Wl$ should give a signal of $pp \rightarrow h \rightarrow \tau^\pm\tau'^\mp \rightarrow \tau^\pm W^\mp Wl$, where all particles are produced and decayed on-shell. The signs of the second W and the charged lepton l are not fixed and depend on the nature of ν'_τ . One would look for same sign dilepton events coming from leptonic decays of the first W along with the last lepton of the chain. This type of signature is quite clean thanks to the minimal background and would in principle allow for easy confirmation of the signal, which could become the discovery signal for the τ' along with the confirmation of Higgs flavor violating couplings.

Another interesting decay mode, if kinematically allowed, is $h \rightarrow bb'$, where the b' would subsequently decay as $b' \rightarrow qW$ or $b' \rightarrow bZ^0$. In the first possibility, q stands for t if kinematically allowed, and for c or u . The partial width of these channels depend on the size of the CKM4 angles $V_{tb'}$, $V_{cb'}$ and $V_{ub'}$ which are typically constrained to be small [144]. A channel which could compete is $b' \rightarrow bZ^0$, since in the RS scenario under study these flavor violating couplings appear at tree-level, in a similar fashion to the Higgs sector [199,211]. Thus depending on the decay branching ratios of the b' heavy quark (see next section) the events could be $pp \rightarrow h \rightarrow bb' \rightarrow bW^-t \rightarrow bbW^\pm W^\mp$ or $pp \rightarrow h \rightarrow bb' \rightarrow bW^-j$ or $pp \rightarrow h \rightarrow bb' \rightarrow bbZ^0$. A careful study of these signals and their background is beyond the scope of this work, but we should mention that a clear prediction of our scenario is that the $h - b - b'$ coupling is highly asymmetric (see Eq. (5.24)) with a definite preference for $h \rightarrow b'_R b_L$ decay over the $h \rightarrow b'_L b_R$. Thus one should also look for the angular correlations in the signals in order to search for this asymmetric property of the couplings (see refs. [212] for studies along these lines).

Heavy Fermion Decays

- Heavy quark decays

If the Higgs masses are lighter than the masses of the fourth generation fermions, channels in which the heavy fermions decay to the Higgs boson and a fermion from one of the lighter families are open. Pair production of heavy quark flavors is expected to have a cross section of $\sim 4 - 4.5$ pb for a mass of 500 GeV⁴ at the LHC with $\sqrt{s} = 14$ TeV [213], thus should be within reach, and the properties of the fourth generation fermions would then become apparent. As the FCNC couplings of the Higgs to the fermions are proportional to fermion masses, the dominant decays would be to the third generation fermions. The flavor violating couplings of Higgs will lead to tree-level decays $t' \rightarrow th$ and $b' \rightarrow bh$ in the kinematically allowed regions $m_{t'} > m_h + m_t$ and $m_{b'} > m_h + m_b$. The decay rates for these processes are calculated as

$$\begin{aligned} \Gamma(Q_j \rightarrow q_i h) &= \frac{m_i m_j}{16\pi m_j^3 v_4^2} \sqrt{m_i^4 + m_j^4 + m_h^4 - 2m_i^2 m_j^2 - 2m_i^2 m_h^2 - 2m_j^2 m_h^2} \\ &\times \left[(|a_{ij}^{u(d)}|^2 + |a_{ji}^{u(d)}|^2)(m_j^2 + m_i^2 - m_h^2) \right. \\ &\left. + 4\Re(a_{ij}^{u(d)} a_{ji}^{u(d)}) m_i m_j \right]. \end{aligned} \quad (5.55)$$

These decays can have significant decay width, and branching ratios. By comparison, the other dominant two body decay modes are $t' \rightarrow bW$ and $b' \rightarrow tW$, given by [214]

$$\begin{aligned} \Gamma(Q_j \rightarrow q_i W) &= \frac{\alpha |V_{ji}|^2}{16M_W^2 m_j^3} \sqrt{m_i^4 + m_j^4 + M_W^4 - 2m_i^2 m_j^2 - 2m_i^2 M_W^2 - 2m_j^2 M_W^2} \\ &\times \left(m_i^4 + m_j^4 - 2M_W^4 - 2m_i^2 m_j^2 + m_j^2 M_W^2 \right), \end{aligned} \quad (5.56)$$

by substituting the corresponding quarks in the two body decays. The flavor-changing couplings of quarks to the Z^0 boson allow FCNC quark decays via the process $Q \rightarrow qZ^0$. The branching ratio is [199]

$$\begin{aligned} \Gamma(Q_j \rightarrow q_i Z^0) &= \frac{\alpha T_3^2}{8M_Z^2 \cos^2 \theta_W m_j^3} \sqrt{m_i^4 + m_j^4 + M_Z^4 - 2m_i^2 m_j^2 - 2m_i^2 M_Z^2 - 2m_j^2 M_Z^2} \\ &\times \left\{ (m_j^2 - m_i^2)^2 + M_Z^2 (m_j^2 - 2M_Z^2) \left[\left| (a_L^{u,d})_{34} \right|^2 + \left| (a_R^{u,d})_{34} \right|^2 \right] \right. \\ &\left. + 12 m_i m_j^3 \Re \left[(a_L^{u,d})_{34}^* (a_R^{u,d})_{34} \right] \right\}, \end{aligned} \quad (5.57)$$

with T_3 the third quark isospin component and with the flavor-changing couplings $a_L^{u,d}$ and $a_R^{u,d}$ as defined in given as in Eq. (5.39). We define the total width to be the

⁴ The cross sections are estimated based on QCD effects only, and are based on approximate knowledge of PDF, thus should be only seen as indicative.

sum of the dominant two body-decays

$$\Gamma(Q_j \rightarrow 2X) = \Gamma(Q_j \rightarrow q_i W) + \Gamma(Q_j \rightarrow q_i h) + \Gamma(Q_j \rightarrow q_i Z^0). \quad (5.58)$$

Although the decays $Q_j \rightarrow q'_i W$, $Q_j \rightarrow q_i Z$ and $Q_j \rightarrow q_i h$, $i = 1, 2$ should be subdominant due to CKM and Yukawa suppression, for completeness we include them in our numerical calculations and plots.

Although the Higgs bosons with masses from 120 to 600 GeV appear to be excluded by the LHC [163, 164], we allow for possible suppression in production in RS with four generations versus SM4 scenarios [198], we plot the branching ratios of the heavy quarks for $m_h = 500$ GeV. Should the Higgs mass be larger, the graphs would shift to the right, but the same features hold.

In Figure 18 we illustrate the branching ratios for the t' quark for two choices of KK mass scales, $R'^{-1} = 1.5$ TeV and $R'^{-1} = 3$ TeV, and for two choices of the CKM4 mixing involved, i.e $V_{t'b} = 0.1$ and $V_{t'b} = 0.3$. The latter will affect the tree-level decay $t' \rightarrow b W$, typically assumed to be the dominant decay for the usual choice $m_{t'} - m_{b'} \sim 50$ GeV. The characteristic bands appearing in these figures are due to the fact that the flavor violating couplings for both Higgs and Z^0 are obtained from numerical scans, performed for different values of the heavy quark masses. To visualize the generic region in parameter space that the branchings should cover, we show the interval of couplings inside which 30% of all the generated points lie, such that 35% lie below that interval and 35% lie above. This procedure will define “bands” in the figures which should be understood as the generic region predicted by flavor anarchy.

We compare the dominant branching ratios for tree level decays: $t' \rightarrow b W$, $t' \rightarrow t h$ and $t' \rightarrow t Z^0$, and also the subdominant decays $t' \rightarrow q' W$, $t' \rightarrow q Z$ and $t' \rightarrow q h$ with $q' = d, s$ and $q = c, u$. Compared to these tree-level decays, the branching ratios of loop-induced processes such as $\text{Br}(t' \rightarrow t \gamma) \simeq \mathcal{O}(10^{-7})$ are much smaller. In all three plots we observe the importance of the decay rate $t' \rightarrow t h$, which will generically dominate for a KK scale of 1.5 TeV and a moderate CKM4 entry $V_{t'b} = 0.1$, when kinematically allowed. By increasing the KK scale or $V_{t'b}$, the branching ratio of $t' \rightarrow b W$ is enhanced, but we observe that the decay into Higgs and *bottom* remains well above 20% in the worst case considered.

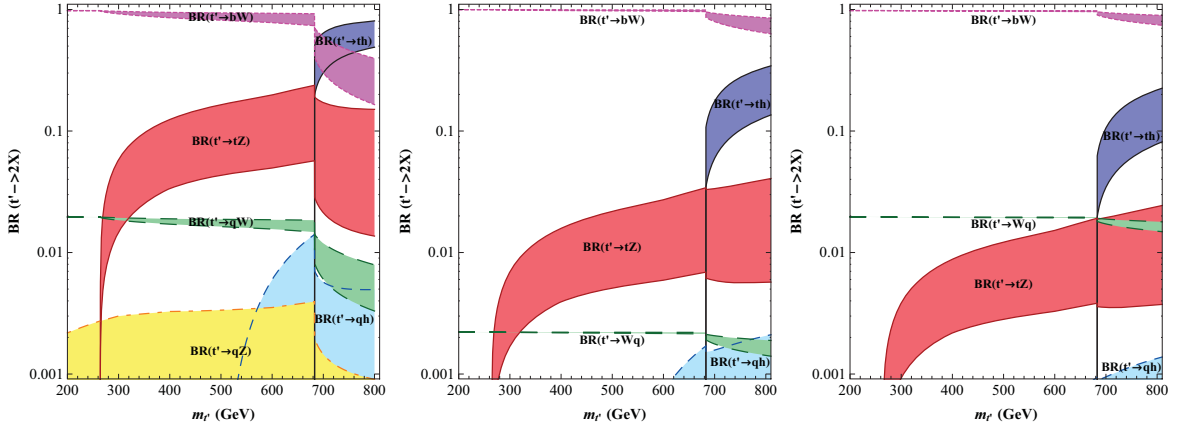


Figure 18: Branching ratios for 2-body t' decays with CKM4 mixing angle $V_{t'b} = 0.1$ and KK scale $R'^{-1} (\equiv M_{KK}) = 1.5$ TeV (left panel), $V_{t'b} = 0.3$, $R'^{-1} = 1.5$ TeV (middle panel) and $V_{t'b} = 0.1$, $R'^{-1} = 3$ TeV (right panel). We take $V_{t's} = V_{t'd} = 0.01$ and $m_h = 500$ GeV throughout. The bands represent 30% likelihood for the branching ratio, according to our numerical scan, as explained in the text.

In general one can see that the flavor violating decays of the t' are significant for all parameter values chosen, and, as long as they are kinematically allowed, they clearly dominate over the intuitive channel $t' \rightarrow bW$. Of course, the effect depends on $(R'^2 \bar{Y}^2)^2$ and will decouple for a large enough increase of the KK scale R'^{-1} . Therefore, which decay is dominant depends sensitively on the KK scale R'^{-1} and also on the CKM mixing $V_{t'b}$. In particular, for $R'^{-1} = 1.5$ TeV and $V_{t'b} = 0.1$ (a value favored in the fits of [144]), the branching ratio for $t' \rightarrow th$ seems to be predicted to be dominant and about twice as large as the one for $t' \rightarrow bW$ over the allowed parameter space. While for $R'^{-1} = 3$ TeV and $V_{t'b} = 0.1$, the branching ratio for $t' \rightarrow th$ is predicted to be about two to three times smaller than that of $t' \rightarrow bW$. For the intermediate choice, $R'^{-1} = 1.5$ TeV and $V_{t'b} = 0.3$ the branching ratio for $t' \rightarrow bW$ overlaps with that for $t' \rightarrow th$ over a significant range of parameter space.

In all three plots, the flavor violating decay $t' \rightarrow tZ^0$ is subdominant above the th threshold, but significant over a large region of parameter space, with possible branchings ranging from about 1% to 10%. This channel becomes specially interesting when the decay into Higgs is kinematically forbidden, namely for t' masses below the threshold $m_t + m_h \simeq 670$ GeV, but the decay into top and Z is open.

We also include the suppressed decays $t' \rightarrow q_i h$, $t' \rightarrow q_i Z^0$ and $t' \rightarrow q_j W$, $i, j = 1, 2$. The Z^0 decay width is sometimes too small and the corresponding branching

ratio falls below 10^{-3} , which is why it does not appear in the plot. We take a generic value for $V_{t'q_j} = 0.01$ and include FCNC coefficients $a_{4i(i4)}^u, (a_L^u)_{4i(i4)}$ from our scan.

Thus the decay $t' \rightarrow th$, if kinematically allowed, is a promising channel for observing t' pair production as well as a novel Higgs pair production channel, in the subsequent decays of the heavy quarks.

It may even be possible to see simultaneously the two dominant decays⁵ if the branching ratios happen to be of similar size, giving rise to interesting pair production processes and decays:

- $pp \rightarrow t't' \rightarrow tthh,$
- $pp \rightarrow t't' \rightarrow tbhW,$
- $pp \rightarrow t't' \rightarrow bbWW,$

all potentially accessible and thus providing an indirect confirmation (or at least a consistency check) of the warped extra dimensional model and its parameter space. In particular, the relative importance of these signals would provide valuable hints on the size of the KK scale as well as of the CKM4 angle $V_{t'b}$. Note also that if the KK scale is such that $R'^{-1} = 1.5$ TeV, the lightest KK particle in the minimal scenario would have a mass of $\mathcal{O}(3$ TeV) and may escape detection at the LHC, while the exotic flavor violating decays (caused by the presence of KK particles) of the fourth generation quarks would still be observable.

We perform the same analysis for the decays of the b' quark as shown in Fig. 19. As before, we choose three parameter combinations for the KK scale and for the main CKM4 mixing angle involved in these decays, i.e $R'^{-1} = 1.5$ TeV and $V_{tb'} = 0.1$, then $R'^{-1} = 1.5$ TeV and $V_{tb'} = 0.3$, and finally $R'^{-1} = 3$ TeV and $V_{tb'} = 0.1$. The dependence of the branching ratios of FCNC decays of the b' quark is more or less similar to the corresponding ones for the t' quark, with the decay $b' \rightarrow bh$ dominating over all others for $R'^{-1} = 1.5$ TeV and $V_{tb'} = 0.1$ (and where kinematically allowed), while for the two other parameter choices the decay $b' \rightarrow tW$ has the largest width for $m_{b'} \geq 250$ GeV.

The flavor violating decay $b' \rightarrow bZ^0$ has a lower kinematic threshold than $b' \rightarrow bh$ and therefore can occur for b' masses just above the Z^0 mass. But the W-mediated

⁵ One might also be able to observe the decays $t' \rightarrow tZ^0$ even if subdominant over the parameter space.

decays of the b' start at a larger mass threshold than in the previous CKM decays of the t' , since charged current decays of b' will involve a *top* quark and a W , both heavy. This means that in the low b' mass region, the Z^0 FCNC decay dominates. Of course as the mixing angle $V_{tb'}$ is increased, the relative importance of the charged current decay grows as expected. As before, we include the CKM4 and a_{ij}^d , $(a_L^d)_{ij}$ suppressed decays $b' \rightarrow q_i h$, $b' \rightarrow q_i Z^0$ and $b' \rightarrow q_j W$, $i, j = 1, 2$, with a generic value for $V_{b'q_j} = 0.01$ and including the FCNC couplings $a_{4i(i4)}^d$, $(a_L^d)_{4i(i4)}$ from our scan.

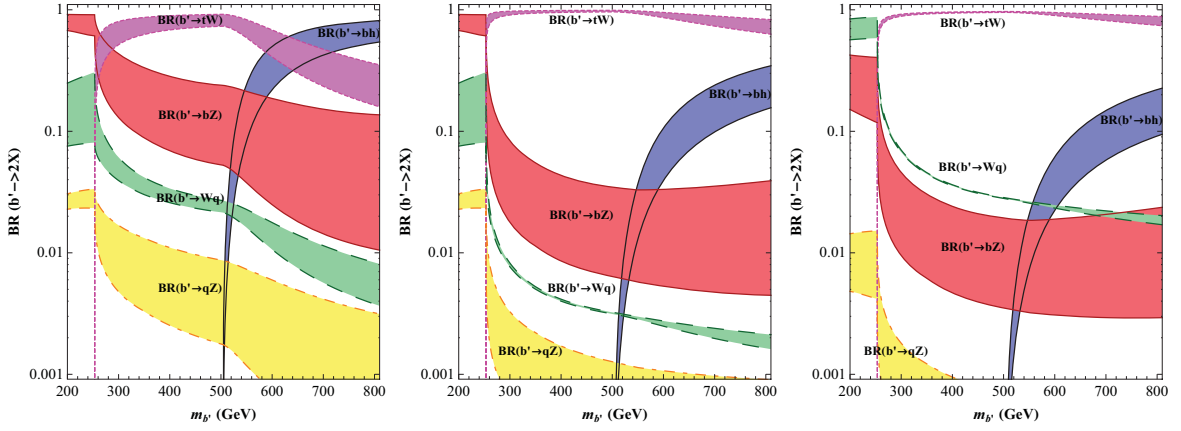


Figure 19: Branching ratios for 2-body b' decays with CKM4 mixing angle $V_{tb'} = 0.1$ and KK scale $R'^{-1}(\equiv M_{KK}) = 1.5$ TeV (left panel), $V_{tb'} = 0.3$, $R'^{-1} = 1.5$ TeV (middle panel) and $V_{tb'} = 0.1$, $R'^{-1} = 3$ TeV (right panel). We take $V_{cb'} = V_{ub'} = 0.01$ throughout as well as $m_h = 500$ GeV. The bands represent 30% likelihood for the branching ratio, according to our numerical scan, as explained in the text.

Again, the $b' \rightarrow h b$ decay is important above h threshold for all the parameter points considered, being dominant for low KK scale and small CKM4 mixing angles, and then competing with the decay $b' \rightarrow t W$ when KK scale or $V_{tb'}$ are increased. In this region the decay $b' \rightarrow b Z^0$ is suppressed relative to the other two, but still important, with branching ratios reaching 1% -6%.

As before, we include the CKM and Yukawa suppressed decays $b' \rightarrow q' W$, $b' \rightarrow q h$ and $b' \rightarrow q Z$, with $q' = u, d$ and $q = s, d$.

Again, FCNC decays of b' through Higgs or Z^0 bosons would provide an indirect indication of the warped space scenario, even for large KK scales such as $R'^{-1} = 3$ TeV. From the plots one see that it may again be possible to observe at the same

time the dominant decay modes of the b' quark (since these are produced in pairs).

For completeness, we include two plots for t' and b' decays for a light Higgs, roughly in the Higgs window still open. We take $m_h = 120$ GeV, and show, in the plots below the branching ratios for $t' \rightarrow th$ for $V_{t'b} = 0.1$ and KK scale $R'^{-1}(\equiv M_{KK}) = 1.5$ TeV (left panel) and for $b' \rightarrow bh$ for $V_{tb'} = 0.1$ and KK scale $R'^{-1}(\equiv M_{KK}) = 1.5$ TeV (right panel). The branching ratios are shown in Fig. 20. For such a light Higgs boson, the FCNC branching ratios $t' \rightarrow th$ and $b' \rightarrow bh$ are of $\mathcal{O}(1)$ and dominate over the other 2-body branching ratios when kinematically accessible: over the whole parameter space for b' decays, and for $m_{t'} \leq 300$ GeV for t' decays.

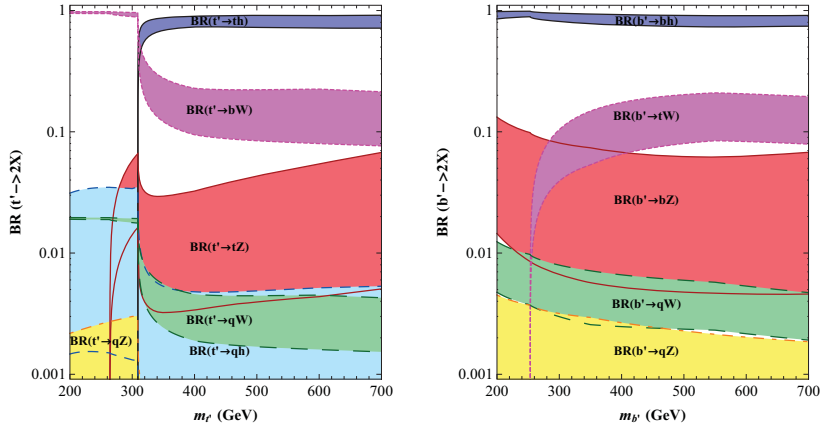


Figure 20: Branching ratios for 2-body t' decays with CKM4 mixing angle $V_{t'b} = 0.1$ and KK scale $R'^{-1}(\equiv M_{KK}) = 1.5$ TeV (left panel) and b' decays with CKM4 mixing angle $V_{tb'} = 0.1$ and KK scale $R'^{-1}(\equiv M_{KK}) = 1.5$ TeV (right panel), for $m_h = 120$ GeV. The bands represent 30% likelihood for the branching ratio, according to our numerical scan, as explained in the text.

For a lighter b' , below the threshold for $b' \rightarrow tW$, i.e. $m_{b'} < 250$ GeV the FCNC decays into Higgs and into Z^0 might dominate over decays into W and light quarks (and hence might substantially alter the current experimental bounds on the b' mass where CKM decays are assumed). In that situation it may be possible to observe a mixture of events:

- $pp \rightarrow b'b' \rightarrow bbhh,$
- $pp \rightarrow b'b' \rightarrow bbZZ,$
- $pp \rightarrow b'b' \rightarrow qWqW,$
- $pp \rightarrow b'b' \rightarrow qWbh,$
- $pp \rightarrow b'b' \rightarrow bZbh,$
- $pp \rightarrow b'b' \rightarrow bZqW.$

For a heavier b' , it appears that two modes should dominate, namely the FCNC decays onto Higgs and the decays into a W and a top quark (due to our assumption of $V_{tb'}$ being the largest of the CKM4 mixing angles involved). The possible mixed events could now be

- $pp \rightarrow b'b' \rightarrow bbhh,$
- $pp \rightarrow b'b' \rightarrow tWbh.$
- $pp \rightarrow b'b' \rightarrow tWtW,$

All events would be easy to identify at the LHC and their relative importance would provide again valuable information on the model parameters of this scenario.

- Heavy lepton decays

Once the τ' lepton is produced at a collider, its FCNC decay will proceed in the same manner as that of the b' quark. As the mass bounds on new τ' leptons and ν'_τ neutrinos are close, it may be that the decay $\tau' \rightarrow W\nu'_\tau$ is kinematically forbidden, and the decay of τ' to lighter neutrinos ($\tau' \rightarrow W\nu_i, i = 1, 2, 3$) depends on the specific model of neutrino masses and mixing and may be suppressed. Thus the FCNC decays $\tau' \rightarrow h\tau$ (for the light Higgs boson scenario), and $\tau' \rightarrow \tau Z^0$ could be the dominant decays. Since we are assuming that $m_h + m_\tau < m_{\tau'}$, the production of τ' should happen via s -channel W bosons and KK partners, and therefore would typically come with associated production of ν'_τ (if the mixing to lighter neutrinos is smaller).

The subsequent FCNC decays of τ' should be easily disentangled at the LHC as they involve several possible processes with many leptons, such as $pp \rightarrow \tau'\nu_\tau \rightarrow \tau h W l$ for the case of $\tau' \rightarrow \tau h$ decays. The Higgs, being heavier than 200 GeV, should mainly decay into pairs of gauge bosons giving rise to final states of $WWWl\tau$ or $ZZWl\tau$, i.e. three gauge bosons, one light lepton and a τ , a clean enough signal at hadron

machine. These might give rise to same-sign dilepton events, trilepton events, and pushing it, to 6 leptons plus τ events, when every boson decays leptonically.

In the case of $\tau' \rightarrow \tau Z^0$ decays, one would similarly obtain processes like $pp \rightarrow \tau' \nu_\tau \rightarrow \tau Z W l$. Again one might observe same-sign dilepton events, trilepton events and when the all bosons decay leptonically one could obtain events with four leptons and a τ .

As in the previous section, a realistic analysis of these signals is beyond the scope of this work, however, it seems clear that it would not be hard to disentangle them, as the branching ratios are subdominant to $\tau' \rightarrow h\tau$, but nonetheless significant.

5.3 Conclusions and Outlook

In this Chapter we analyzed the effects of Higgs flavor-violating couplings in the framework of warped extra dimensions on a fourth generation of quarks and leptons. The Higgs Yukawa couplings are misaligned with the fermion mass matrices, and this effects is even more pronounced in a model with a sequential fourth fermion family, due to cumulative effects in flavor space.

We presented both an analytical evaluation and a numerical estimate of the size of the Higgs FCNC couplings in models with flavor anarchy. The only requirement is that the three-generations quark masses and mixing angles should be reproduced in the present scheme, while the fourth generations masses and mixings are allowed to be free, limited only by V_{CKM4} unitarity. We briefly discussed the possibilities for the lepton sector, which is unfortunately complicated by the lack of a well-defined model of neutrino masses and mixings; as well as revisited the FCNC couplings of the Z^0 boson with a fourth generation.

After setting up the model and evaluating the Yukawa couplings, we analyzed the new effects on low energy FCNC observables. At tree level, the new off-diagonal couplings affect the $K^0 - \bar{K}^0$, $D^0 - \bar{D}^0$ and $B_{d,s}^0 - \bar{B}_{d,s}^0$ mixings. We use the data to set constraints on the a_{ij} , the most stringent bound coming from ϵ_K constraining the phases of the FCNC Yukawa couplings. The constraints are similar to those obtained in the three-generations scenario [181] and the bounds imposed are not stringent, even if we expect the 3×3 Yukawa couplings to be reduced in the four-generation model. The Yukawa FCNC couplings contribute to loop-level processes

such as $b \rightarrow s\gamma$, $t \rightarrow c\gamma$, $\tau \rightarrow e, (\mu)\gamma$ and $\mu \rightarrow e\gamma$. For the quark radiative decays, the effect is negligible compared to SM values and Wq diagrams. For leptons, depending on the size of the FCNC Higgs Yukawa couplings, the radiative decays might become more important and restrict the a_{ij}^l beyond the expectation from the numerical scan, especially from the $\mu \rightarrow e\gamma$ decays, and even more as the bounds on lepton-flavor violation are expected to improve in the near future.

As the present limits on the Higgs masses are pushed higher, especially for the case of four generations, the Higgs boson decay patterns can be substantially modified from the SM and even SM4 expectations. FCNC decay channels such as $\tau\tau'$, bb' and even tt' open for $m_h \sim 600$ GeV, for present bounds on four-generation masses. Both $h \rightarrow \tau\tau'$ could prove to be fertile grounds for discovery of the fourth generation leptons, if the decay $h \rightarrow \tau'\tau'$ is kinematically forbidden. Similarly, the decay $h \rightarrow bb'$ could be an important channel for b' discovery if off-diagonal fourth generation mixing angles $V_{ub'}$, $V_{cb'}$ and $V_{tb'}$ are small. The decays are important for the whole parameter space $m_{t'} \geq 400$ GeV, $m_{b'} \geq 200$ GeV and would provide a clear indication of the model.

If the fourth generation quarks and leptons are heavier than the Higgs boson, their decay into lighter quarks and Higgs bosons would be a promising channel for their discovery and identification. In particular, the branching ratios for $t' \rightarrow th$ and $b' \rightarrow bh$ compete with $t' \rightarrow tZ^0$ and $b' \rightarrow bZ^0$ whenever kinematically accessible, and approach 1 for a significant range of $V_{t'b}$, $V_{tb'}$ and $m_{t'}$, $m_{b'}$ parameter space for $m_h \simeq 120$ GeV. And the fourth generation lepton which can only decay through electroweak processes, may not be able to decay into $W\nu'_\tau$ or $W\nu_\tau$ (depending on mass and mixing constraints in the leptonic sector), making $\tau' \rightarrow \tau h$ a dominant decay mode, and competing with $\tau' \rightarrow \tau Z^0$.

Thus, even if the KK scale is heavy, and KK particles cannot be seen at the LHC, residual effects due to Higgs FCNC could provide the most promising indirect signals for the warped space scenario. Our analysis shows that in a four-generation model, which is natural in this scenario, the results could be enhanced over the model with three generations and yield measurable signals at the LHC.

Chapter 6

RADION PHENOMENOLOGY with 3 and 4 GENERATIONS

Allowing SM fermions and gauge fields to propagate in the bulk effectively solves the large flavor violation and rapid proton decay problems of the original RS scenario and can also be used to explain the fermion mass hierarchy by fermion localization [86–90]. However, tight bounds from precision electroweak tests and from flavor physics [93, 94, 173], constraint the excitations of the bulk fields to be heavier than a few TeV, making it very hard to produce and observe heavy resonances of these masses at the LHC. The scalar field radion associated with the fluctuations in the size of the extra dimension and its associated phenomenology might be promising for observing new states from these scenarios. Generically, the radion may be the lightest new state in an RS-type setup, with its mass suppressed with respect to KK fields by a volume factor of ~ 40 , at least in the small backreaction limit [70]. This might put its mass between a few tens to hundreds of GeV, with couplings allowing it to have escaped detection at LEP, and consistent with precision EW data [215] (see Subsection 3.4.3 for more information about radion). Radion phenomenology has been discussed in several papers [71, 215–218]. More recently it has been shown that a tree-level misalignment between the flavor structure of the Yukawa couplings of the radion and the fermion mass matrix will appear when the fermion bulk parameters are not all degenerate [174]. The mechanism responsible for these FCNC's is different than the one producing Higgs mediated FCNC's in these same models [175, 181].

In the previous chapter we have shown that, if the fourth generation is

incorporated into warped space models, the flavor-changing couplings of the Higgs boson can be enhanced, and both the production and decays of the Higgs bosons and the decay pattern of the heavy quarks and leptons is altered significantly with respect to the patterns expected in SM4, thus giving rise to distinguishing signals at the colliders [107]. It is thus expected that in a warped scenario with extra generations (seen as a natural extension of the warped space model), the flavor-changing couplings of the radion will also yield characteristic signals at colliders.

Also, contrary to the Higgs case in these models [107], exotic flavor violating decays of heavy quarks into radions $Q \rightarrow \phi q$ should be highly suppressed with the new flavor violating couplings of the radion. These will become important in radion decays into quarks $\phi \rightarrow qq, qq'$ as well as into leptons $\phi \rightarrow \tau'\tau$ and $\phi \rightarrow \nu_{\tau'}\nu_{\tau}$. Data from ATLAS [163] and CMS [164] experiments at the LHC indicating that a four generations Higgs boson must be very heavy, does not affect the radion mass directly, but sets limits on the combined radion mass interaction scale parameter space. While we stated that the phenomenology with three and four generations is quite similar for the radion, there are (new) FCNC effects of fourth generation quarks and leptons interacting with the radion. The radion model is described in Subsection 3.4.3 and flavor structure with four families presented in the previous chapter.

6.1 Flavor-Changing Neutral Couplings of the Radion

The couplings between bulk SM fermions and the radion were calculated in [70] for the case of one generation. Including the flavor structure and the possibility of a bulk Higgs, these couplings are the same for four generations as in the three-generation case, presented in [174] and take the form of Eq. (3.171). After diagonalization of the fermion mass matrix, flavor violating couplings will be generated. One can see this explicitly by performing the bi-unitary rotation leading to the fermion mass basis, and writing the radion couplings to fermions in that basis (in matrix form):

$$-\frac{\phi(x)}{\Lambda_{\phi}} \bar{\mathbf{d}}_L^{\text{phys}} \left[\mathbf{U}_{\mathbf{Q}_d}^{\dagger} \hat{\mathcal{I}}(\mathbf{c}_{\mathbf{q}_i}) \mathbf{U}_{\mathbf{Q}_d} \hat{\mathbf{m}}_d^{\text{diag}} + \hat{\mathbf{m}}_d^{\text{diag}} \mathbf{W}_d^{\dagger} \hat{\mathcal{I}}(\mathbf{c}_{\mathbf{d}_i}) \mathbf{W}_d \right] \mathbf{d}_R^{\text{phys}}. \quad (6.1)$$

Here, \mathbf{d}^{phys} is the physical state and is now a 4-vector in flavor space, given that we have introduced an extra (fourth) generation. Also we have defined $\hat{\mathcal{I}}(\mathbf{c}_{\mathbf{q}_i}) =$

$\text{diag}[\mathcal{I}(\mathbf{c}_{q_i})]$ and $\hat{\mathcal{I}}(\mathbf{c}_{d_i}) = \text{diag}[\mathcal{I}(\mathbf{c}_{d_i})]$. One observes that unless the diagonal matrices $\hat{\mathcal{I}}(\mathbf{c}_{q_i})$ and $\hat{\mathcal{I}}(\mathbf{c}_{d_i})$ are both proportional to the unit matrix,¹ there must be some degree of flavor misalignment in the radion couplings. The extension to the up quark sector and charged leptons is immediate.

6.1.1 Radion FCNC's in Flavor Anarchy—Analytical Results

We explicitly parametrize the radion couplings with fermions by highlighting the mass dependence as

$$\mathcal{L}_{q,FV} = -\frac{\tilde{a}_{ij}^d}{\Lambda_\phi} \sqrt{m_{d_i} m_{d_j}} \phi \bar{d}_L^i d_R^j - \frac{\tilde{a}_{ij}^u}{\Lambda_\phi} \sqrt{m_{u_i} m_{u_j}} \phi \bar{u}_L^i u_R^j + \text{h.c.}, \quad (6.2)$$

where d^i, u^i are the quark mass eigenstates with masses m_{d_i}, m_{u_i} . Due to the simplicity of the flavor structure in the radion couplings, it is now possible to give analytical expressions for these couplings, to leading order in ratios of f_i/f_j . The general expressions are, for $i < j$:

$$\begin{aligned} \tilde{a}_{ij}^d &= \sqrt{\frac{m_{d_j}}{m_{d_i}}} \sum_{k=1}^3 \left[(\mathcal{I}(c_{q_k}) - \mathcal{I}(c_{q_4})) U_{ki}^{Q_d} U_{kj}^{Q_d} \right] + \mathcal{O}\left(\frac{m_{d_i}}{m_{d_j}}\right), \\ \tilde{a}_{ij}^u &= \sqrt{\frac{m_{u_j}}{m_{u_i}}} \sum_{k=1}^3 \left[(\mathcal{I}(c_{q_k}) - \mathcal{I}(c_{q_4})) U_{ki}^{Q_u} U_{kj}^{Q_u} \right] + \mathcal{O}\left(\frac{m_{u_i}}{m_{u_j}}\right), \end{aligned} \quad (6.3)$$

and for $i > j$:

$$\begin{aligned} \tilde{a}_{ij}^d &= \sqrt{\frac{m_{d_i}}{m_{d_j}}} \sum_{k=1}^3 \left[(\mathcal{I}(c_{d_k}) - \mathcal{I}(c_{d_4})) W_{ki}^d W_{kj}^{d*} \right] + \mathcal{O}\left(\frac{m_{d_j}}{m_{d_i}}\right), \\ \tilde{a}_{ij}^u &= \sqrt{\frac{m_{u_i}}{m_{u_j}}} \sum_{k=1}^3 \left[(\mathcal{I}(c_{u_k}) - \mathcal{I}(c_{u_4})) W_{ki}^u W_{kj}^{u*} \right] + \mathcal{O}\left(\frac{m_{u_j}}{m_{u_i}}\right). \end{aligned} \quad (6.4)$$

Note that when $i < j$ the couplings are controlled by “left-handed” bulk masses (c_q) and mixings (\mathbf{U}_Q), and when $i > j$, the couplings are controlled by “right-handed” bulk masses ($c_{u,d}$) and mixings ($\mathbf{W}_{u,d}$). The resulting 3×3 substructure of these couplings, i.e. without the fourth generation, matches the results presented in [174]. The expansion of the mixing angles in terms of ratios of f 's gives $U_{ij}^{Q(d,u)} \sim$

¹Note that this can be achieved if the bulk mass parameters, the c_i 's, are all degenerate, but then the scenario cannot be used to produce/explain fermion hierarchies.

f_{Q_i}/f_{Q_j} , $W_{ij}^d \sim f_{d_i}/f_{d_j}$, and $W_{ij}^u \sim f_{u_i}/f_{u_j}$. With these, we can obtain the parametric dependence of the radion couplings up to corrections of order one.²

The diagonal terms are simply

$$\tilde{a}_{ii}^d \approx \mathcal{I}(c_{q_i}) + \mathcal{I}(c_{d_i}), \quad \tilde{a}_{ii}^u \approx \mathcal{I}(c_{q_i}) + \mathcal{I}(c_{u_i}). \quad (6.5)$$

As the function $\mathcal{I}(c)$, defined in Eq. (3.172), tends to c for $c > 1/2$, and approaches quickly the value $1/2$ for $c < 1/2$, the diagonal terms in the down sector can be written as

$$\tilde{a}_{11}^d \approx (c_{q_1} + c_{d_1}), \quad \tilde{a}_{22}^d \approx (c_{q_2} + c_{d_2}), \quad \tilde{a}_{33}^d \approx \left(\frac{1}{2} + c_{d_3}\right), \quad \tilde{a}_{44}^d \approx 1,$$

while the off-diagonal terms also get very simple expressions

$$\begin{aligned} \tilde{a}_{12}^d &\approx \sqrt{\frac{m_s}{m_d}} (c_{q_1} - c_{q_2}) \frac{f_{Q_1}}{f_{Q_2}}, & \tilde{a}_{21}^d &\approx \sqrt{\frac{m_s}{m_d}} (c_{d_1} - c_{d_2}) \frac{f_{d_1}}{f_{d_2}}, \\ \tilde{a}_{13}^d &\approx \sqrt{\frac{m_b}{m_d}} \left(c_{q_1} - \frac{1}{2}\right) \frac{f_{Q_1}}{f_{Q_3}}, & \tilde{a}_{31}^d &\approx \sqrt{\frac{m_b}{m_d}} (c_{d_1} - c_{d_3}) \frac{f_{d_1}}{f_{d_3}}, \\ \tilde{a}_{23}^d &\approx \sqrt{\frac{m_b}{m_s}} \left(c_{q_2} - \frac{1}{2}\right) \frac{f_{Q_2}}{f_{Q_3}}, & \tilde{a}_{32}^d &\approx \sqrt{\frac{m_b}{m_s}} (c_{d_2} - c_{d_3}) \frac{f_{d_2}}{f_{d_3}}, \\ \tilde{a}_{14}^d &\approx \sqrt{\frac{m_{b'}}{m_d}} \left(c_{q_1} - \frac{1}{2}\right) \frac{f_{Q_1}}{f_{Q_4}}, & \tilde{a}_{41}^d &\approx \sqrt{\frac{m_{b'}}{m_d}} \left(c_{d_1} - \frac{1}{2}\right) \frac{f_{d_1}}{f_{d_4}}, \\ \tilde{a}_{24}^d &\approx \sqrt{\frac{m_{b'}}{m_s}} \left(c_{q_2} - \frac{1}{2}\right) \frac{f_{Q_2}}{f_{Q_4}}, & \tilde{a}_{42}^d &\approx \sqrt{\frac{m_{b'}}{m_s}} \left(c_{d_2} - \frac{1}{2}\right) \frac{f_{d_2}}{f_{d_4}}, \\ \tilde{a}_{34}^d &\approx \sqrt{\frac{m_{b'}}{m_b}} [\mathcal{I}(c_{q_3}) - \mathcal{I}(c_{q_4})] \frac{f_{Q_3}}{f_{Q_4}}, & \tilde{a}_{43}^d &\approx \sqrt{\frac{m_{b'}}{m_s}} \left(c_{d_3} - \frac{1}{2}\right) \frac{f_{d_3}}{f_{d_4}}. \end{aligned} \quad (6.6)$$

Note that in the above we took $c_{q_3} \approx c_{q_4} \approx c_{d_4} = 1/2$ except in \tilde{a}_{34}^d where the dominant term comes from the (expected small) difference between c_{q_4} and c_{q_3} .

²See Appendix for details.

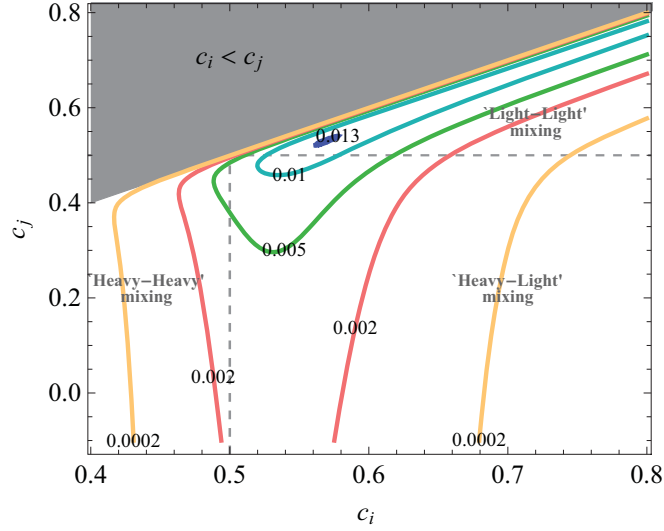


Figure 21: Contours in the plane (c_i, c_j) of the function $\hat{a}_{ij} = [\mathcal{I}(c_i) - \mathcal{I}(c_j)] \frac{f(c_i)}{f(c_j)}$, which sets the size of radion FCNC couplings with fermions. These are estimated to be $\tilde{a}_{ij} \simeq \sqrt{\frac{m_i}{m_j}} \hat{a}_{ij}$ and so from these contours one can quickly estimate the size of these couplings by knowing the values of the bulk mass parameter c_i of each fermion. (Figure on the courtesy of Dr. Manuel Toharia).

Similarly, in the up sector, we obtain

$$\tilde{a}_{11}^u \approx (c_{q_1} + c_{u_1}), \quad \tilde{a}_{22}^u \approx (c_{q_2} + c_{u_2}), \quad \tilde{a}_{33}^u \approx 1, \quad \tilde{a}_{44}^u \approx 1,$$

and for the off-diagonal terms:

$$\begin{aligned} \tilde{a}_{12}^u &\approx \sqrt{\frac{m_c}{m_u}} (c_{q_1} - c_{q_2}) \frac{f_{Q_1}}{f_{Q_2}}, & \tilde{a}_{21}^u &\approx \sqrt{\frac{m_c}{m_u}} (c_{u_1} - c_{u_2}) \frac{f_{u_1}}{f_{u_2}}, \\ \tilde{a}_{13}^u &\approx \sqrt{\frac{m_t}{m_u}} \left(c_{q_1} - \frac{1}{2}\right) \frac{f_{Q_1}}{f_{Q_3}}, & \tilde{a}_{31}^u &\approx \sqrt{\frac{m_t}{m_u}} \left(c_{u_1} - \frac{1}{2}\right) \frac{f_{d_1}}{f_{d_3}}, \\ \tilde{a}_{23}^u &\approx \sqrt{\frac{m_t}{m_c}} \left(c_{q_2} - \frac{1}{2}\right) \frac{f_{Q_2}}{f_{Q_3}}, & \tilde{a}_{32}^u &\approx \sqrt{\frac{m_t}{m_c}} \left(c_{u_2} - \frac{1}{2}\right) \frac{f_{u_2}}{f_{u_3}}, \\ \tilde{a}_{14}^u &\approx \sqrt{\frac{m_{t'}}{m_u}} \left(c_{q_1} - \frac{1}{2}\right) \frac{f_{Q_1}}{f_{Q_4}}, & \tilde{a}_{41}^u &\approx \sqrt{\frac{m_{t'}}{m_u}} \left(c_{u_1} - \frac{1}{2}\right) \frac{f_{u_1}}{f_{u_4}}, \\ \tilde{a}_{24}^u &\approx \sqrt{\frac{m_{t'}}{m_c}} \left(c_{q_2} - \frac{1}{2}\right) \frac{f_{Q_2}}{f_{Q_4}}, & \tilde{a}_{42}^u &\approx \sqrt{\frac{m_{t'}}{m_c}} \left(c_{u_2} - \frac{1}{2}\right) \frac{f_{u_2}}{f_{u_4}}, \\ \tilde{a}_{34}^u &\approx \sqrt{\frac{m_{t'}}{m_t}} [\mathcal{I}(c_{q_3}) - \mathcal{I}(c_{q_4})] \frac{f_{Q_3}}{f_{Q_4}}, & \tilde{a}_{43}^u &\approx \sqrt{\frac{m_{t'}}{m_t}} (\mathcal{I}(c_{u_3}) - \mathcal{I}(c_{u_4})) \frac{f_{u_3}}{f_{u_4}}. \end{aligned} \quad (6.7)$$

Here we assumed $c_{q_3} \approx c_{q_4} \approx c_{u_3} \approx c_{u_4} = 1/2$ except in $\tilde{a}_{34}^u, \tilde{a}_{43}^u$, for the same reasons given for the down sector. This situation is very different from the case

of FCNC couplings of the Higgs boson [107] where the couplings a_{34} , a_{43} are large due to significant misalignment in the 3-4 family. It is clear from the expressions for \tilde{a}_{ij}^d , \tilde{a}_{ij}^u that the flavor changing couplings of the radion are of the simple form $\sqrt{\frac{m_j}{m_i}} [\mathcal{I}(c_i) - \mathcal{I}(c_j)] \frac{f_i}{f_j}$. We explore typical values of this function as contours in a c_i, c_j plane, and determine the localization coefficients for which this function is maximal. In Fig. 21, we show contours of the in the plane of the \tilde{a}_{ij} as a function of two bulk mass parameters, (c_i, c_j) for $c_i < c_j$. The light-light regions correspond to mixing among the first two families, and b_R . Corresponding to the localization of light quarks, these are maximal and the FCNC couplings of the radion \tilde{a}_{ij} can reach a maximum of 0.013. The heavy-light mixing correspond to fourth family mixing, or third family doublet, or t_R mixing, with the two light two families and b_R . These mixings can reach 0.01, although they are more likely to be in the $(0.002 - 0.005)$ region. Finally the heavy-heavy mixing (among fourth families, $(t b)_L$ and u_R) can reach 0.02 as c_{q3}, c_{u3} deviate from $1/2$. The results of the analytic calculations agree with our numerical scan presented in the next subsection.

6.1.2 Radion FCNC's in Flavor Anarchy—Numerical Results

We complement our analytical consideration by performing a numerical scan over the parameter space. We proceed as follows. We generate random complex entries for $\mathbf{Y}_{\mathbf{u}}$ and $\mathbf{Y}_{\mathbf{d}}$, then obtain values for f_{u_i}, f_{d_i} and f_{Q_i} in the same way as for the Higgs FCNC couplings [107], in matrix form. Using $f(c)$ from Eq. (3.168), we solve for the coefficients c_i . We then use the expression for $\mathcal{I}(c_i)$ to calculate mass matrices $\hat{\mathbf{m}}_{\mathbf{u}}, \hat{\mathbf{m}}_{\mathbf{d}}$, then obtain the eigenvalues, and the matrices $\mathbf{W}_{\mathbf{u},\mathbf{d}}$ and $\mathbf{U}_{\mathbf{Q},\mathbf{d}}$. We then have all the ingredients to calculate the fermion-radion couplings. From the scan in parameter space, we find the $\tilde{a}_{ij}^d, \tilde{a}_{ij}^u$ as follows

$$\tilde{a}_{ij}^d \sim \begin{pmatrix} 1.295 - 1.315 & 0.017 - 0.039 & 0.010 - 0.025 & 0.089 - 0.290 \\ 0.013 - 0.034 & 1.215 - 1.231 & 0.006 - 0.016 & 0.065 - 0.179 \\ 0.080 - 0.201 & 0.016 - 0.050 & 1.129 - 1.151 & 0.0002 - 0.001 \\ 0.024 - 0.076 & 0.018 - 0.049 & 0.004 - 0.012 & 1.000 - 1.001 \end{pmatrix}, \quad (6.8)$$

$$\tilde{a}_{ij}^u \sim \begin{pmatrix} 1.294 - 1.320 & 0.065 - 0.164 & 0.081 - 0.212 & 0.094 - 0.268 \\ 0.022 - 0.055 & 1.135 - 1.158 & 0.019 - 0.047 & 0.019 - 0.053 \\ 0.030 - 0.098 & 0.042 - 0.103 & 1.002 - 1.016 & 0.0003 - 0.002 \\ 0.023 - 0.078 & 0.030 - 0.075 & 0.001 - 0.005 & 1.000 - 1.002 \end{pmatrix}. \quad (6.9)$$

The above ranges show the 50% quantile of acceptable points, which means that 25% of points found predict lower $\tilde{a}_{ij}^u, \tilde{a}_{ij}^d$ values and 25% of points predict higher values than those shown in the matrices. The results of the scan are consistent with the values obtained through analytical considerations and from the values estimated using Fig. 21, once typical sizes of the bulk masses are associated to the appropriate fermions.

6.1.3 Radion FCNC's in Flavor Anarchy–Leptons

We proceed in a similar fashion to calculate the FCNC couplings of the radion with the leptons. Assuming the neutrinos to be Dirac-type, we parametrize the couplings as

$$\mathcal{L}_{l,FV} = -\frac{\tilde{a}_{ij}^l}{\Lambda_\phi} \sqrt{m_{l_i} m_{l_j}} \phi \bar{l}_L^i l_R^j - \frac{\tilde{a}_{ij}^\nu}{\Lambda_\phi} \sqrt{m_{\nu_i} m_{\nu_j}} \phi \bar{\nu}_L^i \nu_R^j + \text{h.c.} \quad (6.10)$$

The couplings of the charged leptons resemble those of the down-type quarks, the only difference being that $c_{L_3} \neq \frac{1}{2}$. The coefficients c_{L_i} , $i = 1, 2, 3$ are very close to each other and can be large, while $c_{L_4} = \frac{1}{2}$. The matrix $\hat{\mathcal{I}}(\mathbf{c}_{L_j}) = \text{diag}[\mathcal{I}(c_{L_j})]$, $j = 1, 2, 3, 4$ in Eq. 3.171 can be written as a diagonal matrix plus a non-diagonal one, with entries $\text{diag}(0, 0, 0, \Delta c)$, where $\Delta c = c_{L_4} - c_{L_i}$ can be large.

As the neutrinos are massless, the only FCNC non-zero couplings involve the fourth family, that is $\tilde{a}_{ij}^\nu \neq 0$ only if either $i = 4$ and/or $j = 4$. While couplings with quark are restricted by the CKM matrix (the 3×3 substructure of CKM4), the lepton mixing matrix \mathbf{U}^{PMNS} is not as well known, and thus restrictions on the $U_{i4}^{\text{PMNS}}, U_{4j}^{\text{PMNS}}$ are even less established. We assume that the left-handed matrix \mathbf{U}_L is hierarchical, thus almost diagonal and \mathbf{U}_ν non-hierarchical, and almost the same as \mathbf{U}^{PMNS} .

This would imply the same type of parametric dependence as in the quark sector:

$$\begin{aligned}
\tilde{a}_{14}^\nu &= \sqrt{\frac{m_{\nu_4}}{m_{\nu_1}}} [c_{L_1} - \mathcal{I}(c_{L_4})] \frac{f_{L_1}}{f_{L_4}} \mathcal{O}(1), \\
\tilde{a}_{24}^\nu &= \sqrt{\frac{m_{\nu_4}}{m_{\nu_2}}} [c_{L_2} - \mathcal{I}(c_{L_4})] \frac{f_{L_2}}{f_{L_4}} \mathcal{O}(1), \\
\tilde{a}_{34}^\nu &= \sqrt{\frac{m_{\nu_4}}{m_{\nu_3}}} [c_{L_3} - \mathcal{I}(c_{L_4})] \frac{f_{L_3}}{f_{L_4}} \mathcal{O}(1),
\end{aligned} \tag{6.11}$$

where the coefficients c_{L_i} describe the localization of the lepton doublets and can be large, and f_{L_i} are the values of the zero-mode wavefunctions for the doublet lepton i at the IR brane. For the right-handed neutrinos, W^ν is almost diagonal to insure small neutrino masses. Thus \tilde{a}_{4j} , $j \neq 4$ are small and can be neglected. Here the dominant term could be \tilde{a}_{34}^ν . For $c_{L_i}, c_{\nu_i} > 1/2$, the zero modes wavefunctions are localized towards the UV brane; if $c_{L_i}, c_{\nu_i} < 1/2$, they are localized towards the IR brane. However the size of \tilde{a}_{34}^ν is also determined by the mixing terms $U_{33}^L U_{34}^{L*}$, as given in Eq. (6.3). Thus the mixing will be proportional to $f(c)$. By choosing a value for c_{L_3} which maximizes the expression $\tilde{a}_{34}^\nu \approx [\mathcal{I}(c_{L_3}) - \mathcal{I}(c_{L_4})] f(c_{L_3})$, these values correspond to the region of Fig. 21 for the light-heavy region.

6.2 Phenomenology

6.2.1 Bounds on Radion Mediated FCNC couplings

The off-diagonal Yukawa couplings induce FCNC in both quark and lepton interactions, which affect low energy observables and also give possible signatures at colliders. In this section, we discuss restrictions on radion flavor violation coming from tree-level processes $\Delta F = 2$, such as $K - \bar{K}$, $B - \bar{B}$, $D - \bar{D}$ mixing. We use an effective Lagrangian approach, introduced in Subsection 4.4.1, to isolate the contributions. For $K - \bar{K}$, $B_d - \bar{B}_d$, $B_s - \bar{B}_s$, $D - \bar{D}$ mixings $q_i q_j$ in eq. (4.39) are replaced by sd , bd , bs and uc , respectively.

Exchange of the flavor-violating radions gives rise to additional contributions to C_2 , \tilde{C}_2 and C_4 operators. These are given below, using the model-independent bounds on BSM contributions as in [189] to present coupled constraints on \tilde{a}_{ij} couplings and the radion mass m_ϕ .

At the scale $m_\phi = 60$ GeV, the limits on the C_2 , \tilde{C}_2 and C_4 operators are:

$$\begin{aligned}
\text{Re}C_K^2 &\leq \left(\frac{1}{5.3 \times 10^6 \text{ GeV}}\right)^2, & \text{Re}C_K^4 &\leq \left(\frac{1}{9.1 \times 10^6 \text{ GeV}}\right)^2, \\
\text{Im}C_K^2 &\leq \left(\frac{1}{9.5 \times 10^7 \text{ GeV}}\right)^2, & \text{Im}C_K^4 &\leq \left(\frac{1}{1.2 \times 10^8 \text{ GeV}}\right)^2, \\
|C_D^2| &\leq \left(\frac{1}{1.8 \times 10^6 \text{ GeV}}\right)^2, & |C_D^4| &\leq \left(\frac{1}{2.6 \times 10^6 \text{ GeV}}\right)^2, \\
|C_{B_d}^2| &\leq \left(\frac{1}{8.7 \times 10^5 \text{ GeV}}\right)^2, & |C_{B_d}^4| &\leq \left(\frac{1}{1.3 \times 10^6 \text{ GeV}}\right)^2, \\
|C_{B_s}^2| &\leq \left(\frac{1}{1.0 \times 10^5 \text{ GeV}}\right)^2, & |C_{B_s}^4| &\leq \left(\frac{1}{1.6 \times 10^5 \text{ GeV}}\right)^2.
\end{aligned} \tag{6.12}$$

Using these bounds we obtain the constraints on radion flavor violating Yukawa couplings (to be compared to the \tilde{a}_{ij} in the scan)

$$\begin{aligned}
\Omega^2 \text{Re}(\tilde{a}_{12}^{d*})^2 &\leq 2.6, & \Omega^2 \text{Re}(\tilde{a}_{21}^d)^2 &\leq 2.6, & \Omega^2 \text{Re}(\tilde{a}_{12}^{d*} \tilde{a}_{21}^d) &\leq 0.90, \\
\Omega^2 \text{Im}(\tilde{a}_{12}^{d*})^2 &\leq 0.0082, & \Omega^2 \text{Im}(\tilde{a}_{21}^d)^2 &\leq 0.0082, & \Omega^2 \text{Im}(\tilde{a}_{12}^{d*} \tilde{a}_{21}^d) &\leq 0.0050, \\
\Omega^2 |\tilde{a}_{13}^{u*}|^2 &\leq 3.2, & \Omega^2 |\tilde{a}_{31}^u|^2 &\leq 3.2, & \Omega^2 |\tilde{a}_{31}^{u*} \tilde{a}_{13}^u| &\leq 1.4, \\
\Omega^2 |\tilde{a}_{13}^{d*}|^2 &\leq 1.9, & \Omega^2 |\tilde{a}_{31}^d|^2 &\leq 1.9, & \Omega^2 |\tilde{a}_{13}^{d*} \tilde{a}_{31}^d| &\leq 0.87, \\
\Omega^2 |\tilde{a}_{32}^{d*}|^2 &\leq 6.5, & \Omega^2 |\tilde{a}_{23}^d|^2 &\leq 6.5, & \Omega^2 |\tilde{a}_{32}^{d*} \tilde{a}_{23}^d| &\leq 2.8,
\end{aligned} \tag{6.13}$$

where $\Omega = \left(\frac{60 \text{ GeV}}{m_\phi}\right) \left(\frac{2 \text{ TeV}}{\Lambda_\phi}\right)$. Using our analytic results, the bounds translate parametrically on restrictions on the bulk mass parameters of the appropriate fermions. From the ϵ_K bounds

$$\begin{aligned}
\text{Im}(\tilde{a}_{12}^{d*} \tilde{a}_{21}^d) &= -\frac{m_s}{m_d} (c_{q_1} - c_{q_2})(c_{d_1} - c_{d_2}) \frac{f_{Q_1} f_{d_1}}{f_{Q_2} f_{d_2}} \text{Im} \left(\frac{[Y_d]_{21}^* [Y_d]_{12}^*}{([Y_d]_{11}^*)^2} \right) \\
&= \mathcal{O}(1)(c_{q_1} - c_{q_2})(c_{d_1} - c_{d_2}),
\end{aligned} \tag{6.14}$$

where in the last expression we used the hierarchic nature of the Yukawa couplings. This is a remarkable result, as it relates the magnitude of ϵ_K directly to the bulk mass parameters (or the localization coefficients) of the d , s quarks in the $U(1)_R$ singlet and $SU(2)_L$ doublet representations. Similarly we can obtain appropriate expressions for restrictions on the bulk mass parameters coming from $B^0 - \bar{B}^0$ and $D^0 - \bar{D}^0$ mixing:

$$\begin{aligned}
|\tilde{a}_{13}^{d*} \tilde{a}_{31}^d| &= \mathcal{O}(1)(c_{q_1} - \frac{1}{2})(c_{d_1} - c_{d_3}), \\
|\tilde{a}_{32}^{d*} \tilde{a}_{23}^d| &= \mathcal{O}(1)(c_{q_2} - \frac{1}{2})(c_{d_2} - c_{d_3}), \\
|\tilde{a}_{13}^{u*} \tilde{a}_{31}^u| &= \mathcal{O}(1)(c_{q_1} - \frac{1}{2})(c_{d_1} - \frac{1}{2}).
\end{aligned} \tag{6.15}$$

One can see from the bounds, that unless the radion is very light ($m_\phi \sim 10$ GeV), the most significant constraints come from the ϵ_K bounds, especially those on the coefficient C_4 . We use these bounds as the main flavor constraints on our model, and present the restrictions in Fig. 22 in the $m_\phi - \Lambda_\phi$ plane (for the typical value of $\tilde{a}_{12}^d \sim \tilde{a}_{21}^d \sim 0.05$). The region below the $a_{ds} = 0.05$ curve is named “flavor disfavored”, since typical flavor anarchy parameter points would produce too large contributions to ϵ_K in that region. Note that we considered the scenarios with both 3 and 4 generations of fermions, and the bounds are basically the same. The small difference is due to the renormalization group running of operators, which is slightly altered by the presence of extra fermion families.

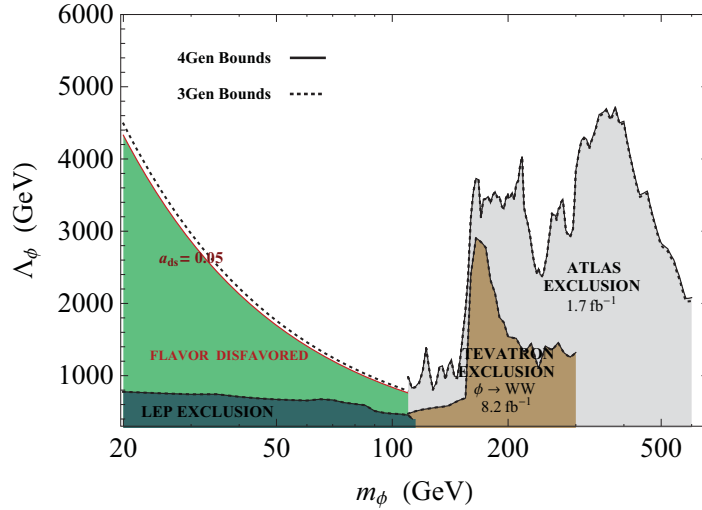


Figure 22: Restrictions in the $m_\phi - \Lambda_\phi$ plane from collider exclusion limits and flavor constraints for ϵ_K (we have defined $a_{ds} = \sqrt{\text{Im}(\tilde{a}_{12}^{d*} \tilde{a}_{21}^d)}$). One sees that for lighter radion ($m_\phi < 160$ GeV) direct bounds are quite weak and flavor physics provide stronger constraints (although less robust). Heavier radions are mostly constrained by the “golden mode” $pp \rightarrow \phi \rightarrow ZZ$ and also $pp \rightarrow \phi \rightarrow WW$ at the LHC, while $p\bar{p} \rightarrow \phi \rightarrow WW$ is used at Tevatron. (Figure on the curtesy of Dr. Manuel Toharia).

In the same figure we present the most recent direct bounds on radion phenomenology coming from collider data. Indeed one can easily use the existing Higgs bounds to restrict regions in the $m_\phi - \Lambda_\phi$ plane, since the search strategy for both the Higgs and the radion are identical. This is due to the fact that the couplings of the radion with particles are proportional to the mass of the particles (just like the couplings

of the Higgs). The main difference is that the Higgs couplings are controlled by the electroweak scale v , whereas the radion couplings are controlled (suppressed) by the much heavier scale Λ_ϕ .

LEP bounds [126] do apply for very light radion, although the restrictions on Λ_ϕ are not too strong, and one sees that in that region the generic flavor bounds are much stronger (although less robust).

For heavier radion, the Tevatron and the LHC have put strong bounds on the allowed parameter region of our scenario. In both experiments, the main production mechanism for the radion is via gluon fusion but, unlike the Higgs, the other possible production mechanisms such as vector boson fusion or associated W and Z production are extremely suppressed. This is due to the enhancement of the coupling of radion to gluons through the trace anomaly. The consequence of this fact is that Higgs searches must be appropriately translated into radion bounds by subtracting events coming from scalars produced via vector boson fusion. One can do this roughly by adjusting the production cross section of the Higgs in order to only obtain the gluon fusion cross section. A better way of translating Higgs searches into radion is to use fourth generation Higgs searches. This is because a Higgs with 4 generations will mainly be produced in gluon fusion (with almost no other production channel) and so there will be no need of subtracting events coming from other production mechanisms.

Another important issue when translating Higgs bounds into the radion bounds is that the width of a heavier Higgs ($m_h > 200$ GeV) starts to be relevant (i.e. becomes larger than the experimental resolution). This means that more background events must be integrated in order to optimize signal events. But the radion width is always going to remain much smaller than experimental resolution due to its couplings being suppressed by Λ_ϕ (and not v as in the Higgs case). We must therefore adjust again the Higgs limits in order to take this fact into account, since much less background events should be kept in a pure radion search [68].

With all this in mind, we translate Tevatron and LHC bounds from Higgs searches and show the excluded regions in Figure 22. From the Tevatron collider, we use the CDF and D0 combined search for a fourth generation Higgs, which allows interesting bounds up to masses of $m_\phi = 300$ GeV [209]. This search focuses on the Higgs decay into pairs of W bosons and for an integrated luminosity of 8.2 fb^{-1} . As for the LHC, we use the recent results from the ATLAS experiment [163], in which they perform

a combination of different channels, with integrated luminosities up to 1.7 fb^{-1} . As one can see, LHC data from a single experiment outperforms the Tevatron and quite interesting bounds can be set up to a mass of $m_\phi = 600 \text{ GeV}$. We note that because the relative importance of different channels is not exactly the same for Higgs and radion (specially the branching of the $\phi \rightarrow \gamma\gamma$ channel differs from $h \rightarrow \gamma\gamma$), in the lower mass region $m_h < 160 \text{ GeV}$ we avoid the combination and use exclusively the ATLAS limits from $h \rightarrow \gamma\gamma$ search. Above that point the branchings of Higgs and radion into heavy vector bosons are essentially the same, specially if we assume for the plot that the fourth generation of fermions (if it exists) is heavy enough, with masses greater than 300 GeV .

Finally we note from this figure that radion phenomenology does not really change due to the addition of a fourth family³. This might seem surprising because the Higgs phenomenology is greatly affected by the presence of a fourth family of fermions (specially fourth family quarks) due to an important enhancement in the Higgs production cross section. This does not happen in the case of the radion, because its couplings with massless gauge bosons are quite indifferent to the addition of new heavy degrees of freedom. Even though the new added fields will produce new loop contributions to $\phi \rightarrow gg$ or to $h \rightarrow \gamma\gamma$, their presence will also alter the β functions of the appropriate gauge groups, which will affect the couplings of the radion to massless bosons through the trace anomaly. The new trace anomaly effects coming from a fourth family will in fact cancel the previous loop contributions in the limit of very heavy new states [70], and so basically the radion couplings to photons and gluons remains the same, controlled only by the light degrees of freedom of the theory [219].

6.3 Flavor Changing Radion Decays in the 4 Generation Model

Radion couplings to fermions, massive and massless gauge bosons have all been analyzed before [70, 174]. Here we investigate the changes in branching ratios due to the effect of a fourth generation, and of flavor-changing interactions. We assume no Higgs-radion mixing. We present our results in Fig. 23. Note that we keep the

³We assume here that the radion decays to fourth generation fermions (especially leptons and neutrinos) is negligible. For an alternative scenario, see next section.

radion mass to be above $\sim 5 - 10$ GeV to avoid constraints from B-meson decays and astrophysical data [220].

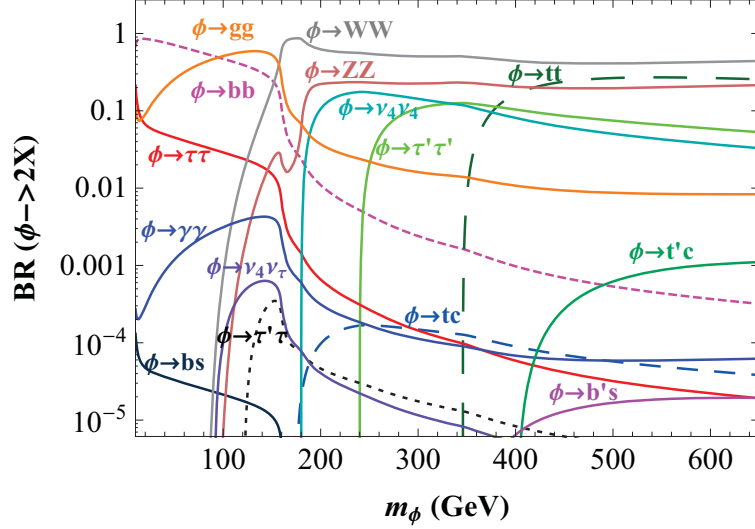


Figure 23: Decay branching fractions of the radion in a warped scenario with four generations of fermions. The flavor anarchy setup (masses and mixings explained through fermion localization, with random 5D Yukawa couplings) predicts generic FV couplings of the radion, leading to a few new interesting decay channels such as $\phi \rightarrow bb'$ and $\phi \rightarrow \tau\tau'$. The masses chosen for this plot are $m_{b'}$ = 350 GeV, $m_{\tau'}$ = 400 GeV, $m_{\tau'}$ = 120 GeV and m_{ν_4} = 90 GeV, and the KK scale is $(R')^{-1} = (\sqrt{6})1500$ GeV (~ 3675 GeV).

Depending on the masses of the fourth generation leptons and neutrinos, FCNC decay channels ($\phi \rightarrow \tau\tau'$, $\nu_\tau\nu_4$) could open for $m_\phi \geq 100$ GeV. At higher radion masses, the WW , ZZ and $t\bar{t}$ dominate. In this region, the radion could be observed through the semi-leptonic channel $\phi \rightarrow W_{lep}W_{had}$, and similarly $\phi \rightarrow t\bar{t} \rightarrow b\bar{b}W_{had}W_{lep}$ (avoiding the fully hadronic channel which suffers from large QCD dijet background), but the decays rate would be comparable to that of a direct Higgs boson production.

Finally, for light (Dirac) fourth-generation neutrinos or leptons, near the present bounds, radion branching ratios to $\nu_4\nu_4$ and $\tau'\tau'$ can be significant and compete with ZZ and WW decays, and thus significantly alter radion decay patterns for $m_\phi > 200$ GeV.

6.4 Conclusions and Outlook

In this Chapter, we have investigated the phenomenology of the couplings, especially the flavor-violating ones, of the radion to fermions in a warped model with three and four generations where the fermions are allowed to propagate in the bulk. We have shown how to obtain these couplings analytically, and presented leading order expressions for them in a compact form. Although the radion FCNC couplings have been analyzed before, some of the analytic expressions presented here are new. We also explored the regions in which the couplings lie, and maximal values for these, as contour plots in a plane defined by coefficients describing quark localization with respect to the TeV brane. We are able to predict typical (and maximal) values for the radion coupling to heavy-heavy, light-light, and heavy-light quarks, and these results are confirmed by an extensive numerical scan.

Applying these to phenomenology of the radion, we calculated the tree-level FCNC contributions to $K^0 - \bar{K}^0$, ϵ_K , $D^0 - \bar{D}^0$ and $B^0 - \bar{B}^0$ mixing, and the restrictions imposed on the couplings. We obtain simple expressions relating quark localization to these experimental values. The most stringent constraints are from ϵ_K , yielding a region of space in $m_\phi - \Lambda_\phi$ parameter space disfavored by flavor violation consideration. We add to these the most recent constraints on Higgs masses, from ATLAS and CMS, translating them into combined radion mass-scale limits. Our analysis shows that a large range around a light radion mass-low scale ($\Lambda_\phi \sim 2$ TeV, $m_\phi \sim 60$ GeV) survives. We also show that, unlike the case of the Higgs boson, there are minute differences between radion mass-scale limits in 3 and 4 generations, and thus these limits are quite independent of the number of generations. This conclusion stands in the case where the radion decays are not significantly influenced by decays into fourth generation fermions (in particular to fourth generation neutrinos or leptons, which have the lowest mass bounds). In a complete analysis, we include all branching ratios of the radion. Expected to be light, the radion decays primarily to gg and $b\bar{b}$ at low masses ($m_\phi \leq 100$ GeV), while for heavier radions ($m_\phi \approx 100$ GeV), FCNC decay channel such as $\nu_4\nu_\tau$ (assuming Dirac neutrinos) and $\tau'\tau$ open, with branching ratios of 10^{-3} . These are the most promising FCNC decays of the radion, barring the unlikely appearance of $\phi \rightarrow t'c$ at the high $m_{t'} = 400$ GeV threshold. However, flavor-conserving radion decays into fourth generation leptons and neutrinos can be large (for $m_{\nu_4}, m_{\tau'} \simeq 100$ GeV) and alter the dominant decay

modes for a heavier radion $r \rightarrow ZZ, WW$. These are typical decay for a radion in a model with four generations and would provide a distinguishing signal for the model. If a heavy Higgs-like state is discovered at the LHC with the usual “golden mode”, $pp \rightarrow h \rightarrow ZZ$, a width measurement could rule out a conventional Higgs boson. A careful study for different and/or exotic decay channels of that resonance might be the key to discover both a fourth generation of fermions and a warped extra dimension.

Chapter 7

SAVING the FOURTH GENERATION HIGGS with RADION MIXING

The Higgs and radion fields carry the same quantum numbers. Therefore, there is the possibility of having physical fields as the mixed states of radion and Higgs fields (see Section 3.4.6 for the details). The mixing of the two fields is introduced with an additional parameter (ξ), which is the coefficient of the curvature-scalar term [68]. Previously in Section 2.6, we have mentioned the ATLAS and CMS announcements of the discovery of a spin-zero particle at a resonance 125 – 126 GeV consistent with a Higgs boson. We presented the exclusion regions at 95% CL for a SM Higgs boson reported by ATLAS and CMS experiments as well. However, we need a thorough analysis of more accumulated data to settle the issue of whether or not the observed particle is a SM Higgs boson. Since the window for new physics is still open, one can naturally ask if the new state is a Higgs, a radion, or a Higgs-radion mixed state. This possibility could have even more dramatic consequences for the scenario with an additional generation of fermions (see Section 3.3), which is a natural extension of the warped space model as in [104, 105]. The exclusion limits for SM4 Higgs boson are introduced in Section 3.3. It appears that if the bump in the signal at the LHC is the Higgs boson, this would rule out the SM4 at 95% CL for $m_{h_0} \geq 123$ GeV, and at 99.6% if $m_{h_0} = 125$ GeV [165–167]. The limits from the Tevatron [168] also exclude a wide range of Higgs boson masses.

In Chapter 5 we have shown that if the fourth generation is incorporated into the framework of warped space models, both the production and decay patterns of the Higgs bosons can be altered significantly with respect to the patterns expected in the standard model with four generations, thus giving rise to distinguishing signals at the colliders [107]. In the next Chapter, radion phenomenology was discussed and it was pointed out that the radion is less sensitive to the presence of an extra generation than the Higgs boson [108].

As the mechanism responsible for the radion FCNCs is different from the one for the Higgs in these same models [175, 181], and the branching ratios for decays into gluons and photons for three and four generations also differs, we can expect the phenomenology of the Higgs-radion mixed state to present an interesting interplay of the two mechanisms responsible, and to yield different effects. In particular, this mixing may help evade the apparent constraints on low Higgs masses in the four generation scenario. Motivated by these expectations, we study the phenomenology of the Higgs-radion mixed state, paying particular attention to the signals for $gg \rightarrow \phi \rightarrow \gamma\gamma$, $gg \rightarrow \phi \rightarrow ZZ^*$ as well as $gg \rightarrow h \rightarrow \gamma\gamma$, $gg \rightarrow h \rightarrow ZZ^*$, where ϕ and h stand for the mixed Higgs-radion states. We use the ATLAS [221] and CMS data [222] available as of 2011 for scalar searches, which are summarized in Section 2.6, to identify regions in the parameter space where the data is compatible with one or the other of these states. The model is introduced in Chapter 3.4 and the radion couplings are given in Appendix E-2.

7.1 Production and Decays of a Mixed Higgs-Radion State with Four Generations

The main production mechanism of the Higgs particles at the hadron colliders is through the gluon-gluon fusion channel, $\sigma(gg \rightarrow h_{SM})$, via triangular loops of heavy quarks. However, for heavier Higgs bosons, the weak vector boson fusion channel, $\sigma(qq \rightarrow qqh_{SM})$, becomes competitive with the gluon-gluon fusion mode. Therefore, as a good approximation one can write the ratio of the production cross section of the h physical mode to the production cross section of SM Higgs as

$$\frac{\sigma(gg \rightarrow h) + \sigma(qq \rightarrow qqh)}{\sigma(gg \rightarrow h_{SM}) + \sigma(qq \rightarrow qqh_{SM})}, \quad (7.1)$$

and this becomes

$$\left(\frac{\sigma(gg \rightarrow h)}{\sigma(gg \rightarrow h_{SM})} + \frac{\sigma(qq \rightarrow qqh)}{\sigma(gg \rightarrow h_{SM})} \right) \left(\frac{1}{1 + \frac{\sigma(qq \rightarrow qqh_{SM})}{\sigma(gg \rightarrow h_{SM})}} \right). \quad (7.2)$$

The ratio of the Higgs production cross section via the weak vector boson fusion channel to the production cross section of the SM Higgs is closely correlated with the partial widths such that

$$\frac{\sigma(qq \rightarrow qqh)}{\sigma(qq \rightarrow qqh_{SM})} = \frac{\Gamma(h \rightarrow WW)}{\Gamma(h_{SM} \rightarrow WW)}, \quad (7.3)$$

which in warped extra dimensional scenarios with Higgs-radion mixing and fields in the bulk simply becomes

$$\frac{\Gamma(h \rightarrow WW)}{\Gamma(h_{SM} \rightarrow WW)} = \left\{ d + b\gamma \left[1 - 3 \ln \left(\frac{\sqrt{6}M_{Pl}}{\Lambda_\phi} \right) \frac{M_W^2}{\Lambda_\phi^2} \right] \right\}^2. \quad (7.4)$$

Substituting this result in Eq. 7.2 we obtain

$$\left[\frac{\sigma(gg \rightarrow h)}{\sigma(gg \rightarrow h_{SM})} + \left\{ d + b\gamma \left[1 - 3 \ln \left(\frac{\sqrt{6}M_{Pl}}{\Lambda_\phi} \right) \frac{M_W^2}{\Lambda_\phi^2} \right] \right\}^2 \frac{\sigma(qq \rightarrow qqh_{SM})}{\sigma(gg \rightarrow h_{SM})} \right] \times \left(\frac{1}{1 + \frac{\sigma(qq \rightarrow qqh_{SM})}{\sigma(gg \rightarrow h_{SM})}} \right), \quad (7.5)$$

where the first term in the brackets is simply the ratio of couplings to gluons $c_g^2/c_{g_{SM}}^2$. Similarly we can calculate the same ratio for the field ϕ ,

$$\left[\frac{\sigma(gg \rightarrow \phi)}{\sigma(gg \rightarrow h_{SM})} + \left\{ c + a\gamma \left[1 - 3 \ln \left(\frac{\sqrt{6}M_{Pl}}{\Lambda_\phi} \right) \frac{M_W^2}{\Lambda_\phi^2} \right] \right\}^2 \frac{\sigma(qq \rightarrow qqh_{SM})}{\sigma(gg \rightarrow h_{SM})} \right] \times \left(\frac{1}{1 + \frac{\sigma(qq \rightarrow qqh_{SM})}{\sigma(gg \rightarrow h_{SM})}} \right). \quad (7.6)$$

The production mechanism of an unmixed Higgs boson through the gluon-gluon fusion channel increases about nine times with an additional fourth family of fermions, because in addition to the top quark there are also heavy t' and b' quarks propagating in the loop. Recently, the two-loop EW corrections, δ_{EW}^4 , to the Higgs boson production via gluon-gluon fusion has been computed with respect to the leading order cross section in [169–172] which are summarized in Section 3.3. This enters as a correction to the Higgs field prior to mixing. For δ_{EW}^4 we have taken the (Higgs-mass dependent) values from Table 11.

Also, in order to take into account the effects of KK fields in the loop, we assume an additional correction to the h_0 couplings squared to massless gauge bosons of $\pm 20\%$ for gluons and $\pm 10\%$ for photons. The estimated values of the corrections are based on the results presented in [198], where it was shown that either enhancements or suppressions in the rates are possible, depending on the phases present at the level of the 5D Yukawa couplings. In the figures, the effect will be illustrated with bands in parameter space representing this “theoretical uncertainty”.

With these considerations the couplings of the physical Higgs and radion fields are calculated and are given in Appendix E. Note that while the bare Higgs (h_0) couplings are corrected by $(1 + \delta_{EW}^4)$, there is no such correction for the bare radion (ϕ_0) couplings. The reason is that the latter are dominated by the trace anomaly, and so higher order loop effects are much smaller. We have also included the corrections to the $h_0 \rightarrow \gamma\gamma$ coupling due to loop effects, as given in Table 12. A note of caution is warranted with these corrections. The authors show that the NLO EW corrections are of the same order as the LO estimate, and negative, due to the strong cancellation between the W and fermion loops with four generations. This might be indicative of a non-perturbative regime, and the authors rely on an estimation of the higher-order corrections, without any certainty that the perturbation series converges. Moreover, in our scenario, heavy Kaluza-Klein fermions are known to affect $h_0 \rightarrow \gamma\gamma$ at lowest order [197,198], and therefore any higher order correction should also include the effect of heavy fermions, not present in SM4. Given these uncertainties, we will present the figures for both LO and EW-corrected branching ratios to $\gamma\gamma$, expressed as in [172], and comment on the differences. We mostly focus on the decays of Higgs-radion mixed states to $\gamma\gamma$ and ZZ^* for the low mass region, and to ZZ channel for larger masses. The ratio of discovery significances for both the h and the ϕ with respect to the SM Higgs can be defined as

$$R_h(XX) = \left[\frac{\sigma(gg \rightarrow h) + \sigma(qq \rightarrow qqh)}{\sigma(gg \rightarrow h_{SM}) + \sigma(qq \rightarrow qqh_{SM})} \right] \frac{BR(h \rightarrow XX)}{BR(h_{SM} \rightarrow XX)} w_{corr}(h), \quad (7.7)$$

and

$$R_\phi(XX) = \left[\frac{\sigma(gg \rightarrow \phi) + \sigma(qq \rightarrow qq\phi)}{\sigma(gg \rightarrow h_{SM}) + \sigma(qq \rightarrow qqh_{SM})} \right] \frac{BR(\phi \rightarrow XX)}{BR(h_{SM} \rightarrow XX)} w_{corr}(\phi), \quad (7.8)$$

where the terms in square brackets are defined in Eqs. (7.5) and (7.6) and where

$$w_{corr}(s) = \begin{cases} \sqrt{\frac{\max(\Gamma_{tot}(h_{SM}), \Delta M_{4l})}{\max(\Gamma_{tot}(s), \Delta M_{4l})}} & \text{for } \Gamma_{tot}(s) > \Gamma_{tot}(h_{SM}), \\ 1 & \text{for } \Gamma_{tot}(s) < \Gamma_{tot}(h_{SM}). \end{cases} \quad (7.9)$$

The term w_{corr} represents a crude and fast approximation of the effects of a large width of either $s = h$ or $s = \phi$. Indeed if the physical state h (or ϕ) has a much larger width than the SM Higgs, and if this width is larger than the experimental resolution of the detector, then an LHC search looking for the SM Higgs would somewhat underestimate the integrated signal as this one would be distributed in a much wider resonance. We have checked numerically using a Breit-Wigner distribution shape that the correction induced indeed scales roughly as in w_{corr} , which was originally introduced as a width-effect correction for the radion in [68].

Finally, the experimental resolution in the 4-lepton channel is estimated to be [68]

$$\frac{\Delta M_{4l}}{M_{4l}} = \frac{0.1}{\sqrt{M_{4l}(\text{GeV})}} + 0.005, \quad (7.10)$$

We use all this information to explore the parameter space for m_ϕ and m_h consistent with the LHC data, which indicates an excess in the mass region 120 – 128 GeV. Let us review the data collected by 2011.

- ATLAS data indicates an enhanced signal in $\gamma\gamma$ and $ZZ^* \rightarrow 4\ell$ near 125 GeV [221] with observed excesses: $R(\gamma\gamma) = 2_{-0.8}^{+0.8}$, $R(4\ell) = 0.5_{-0.5}^{+1.5}$.
- CMS data [222] indicates an excess
 - At 124 GeV: $R(\gamma\gamma) = 1.7_{-0.7}^{+0.8}$, $R(4\ell) = 0.5_{-0.5}^{+1.1}$, $R(b\bar{b}) = 1.2_{-1.2}^{+2.0}$.
 - At 120 GeV in ZZ^* only: $R(4\ell) = 2_{-1}^{+1.5}$, $R(b\bar{b}) = 0.2_{-0.2}^{+1.9}$, while $R(\gamma\gamma) < 0.5$.
 - At 137 GeV in $\gamma\gamma$, $R(\gamma\gamma) = 1.5_{-0.8}^{+0.8}$ but not in ZZ^* , $R(4\ell) < 0.2$.
- Additionally, from the plots we inferred the additional constraints for heavier Higgs bosons, which we used in generating our graphs: for $m_h = 320$ GeV, $R(ZZ) < 0.5$; for $m_h = 400$ GeV, $R(ZZ) < 0.2$; for $m_h = 500$ GeV, $R(ZZ) < 0.5$; and for $m_h = 600$ GeV, $R(ZZ) < 0.95$.

The error bars on the data are still large, but they can be used to restrict the parameter for the four generation Higgs-radion mixed states. In order for these states to fit the data, we should either have one of the states at 124 – 126 GeV, and another one hidden (*i.e.* below the LHC signal), or one state at 124 GeV and the other either at 120 or 137 GeV, both which should respect the CMS signal characteristics.

Based on the experimental constraints, we investigate the production and decay of the two scalar particles in our scenario, m_ϕ and m_h , and divide the parameter space as follows. In the first scenario, we attempt to fit h as the scalar particle observed at LHC at an invariant mass of ~ 125 GeV, while requiring ϕ to be consistent with constraints of the rest of the spectrum from LEP, Tevatron and/or LHC; while in the second scenario, we attempt the same thing for ϕ , while h must be consistent with the previous collider data.

- Scenario 1a: $m_h = 124$ GeV, m_ϕ light (< 300 GeV); in particular, paying specific attention to $m_\phi = 120$ GeV, $m_\phi = 137$ GeV, as these seem possible parameter space points for the CMS data.
- Scenario 1b: $m_h = 125$ GeV, m_ϕ heavy (> 300 GeV).
- Scenario 2a: $m_\phi = 125$ GeV, m_h light (< 300 GeV); in particular, paying specific attention to the point $m_h = 120$ GeV.
- Scenario 2b: $m_\phi = 125$ GeV, m_h heavy (> 300 GeV).

We illustrate some regions of parameter space with different masses of h and ϕ in the following figures. The results will depend on the mass of the fourth family charged lepton (τ') and so we divide our considerations into two parts. We first assume that $m_{\tau'} \geq 150$ GeV, thus preventing flavor-changing decays into $\tau'\tau$, which are potentially large in this model [107, 108]. However, if the τ' is light, this might modify substantially the branching ratios, potentially yielding significantly different signals. We comment on this case in this section, and investigate it in more detail in the next section.

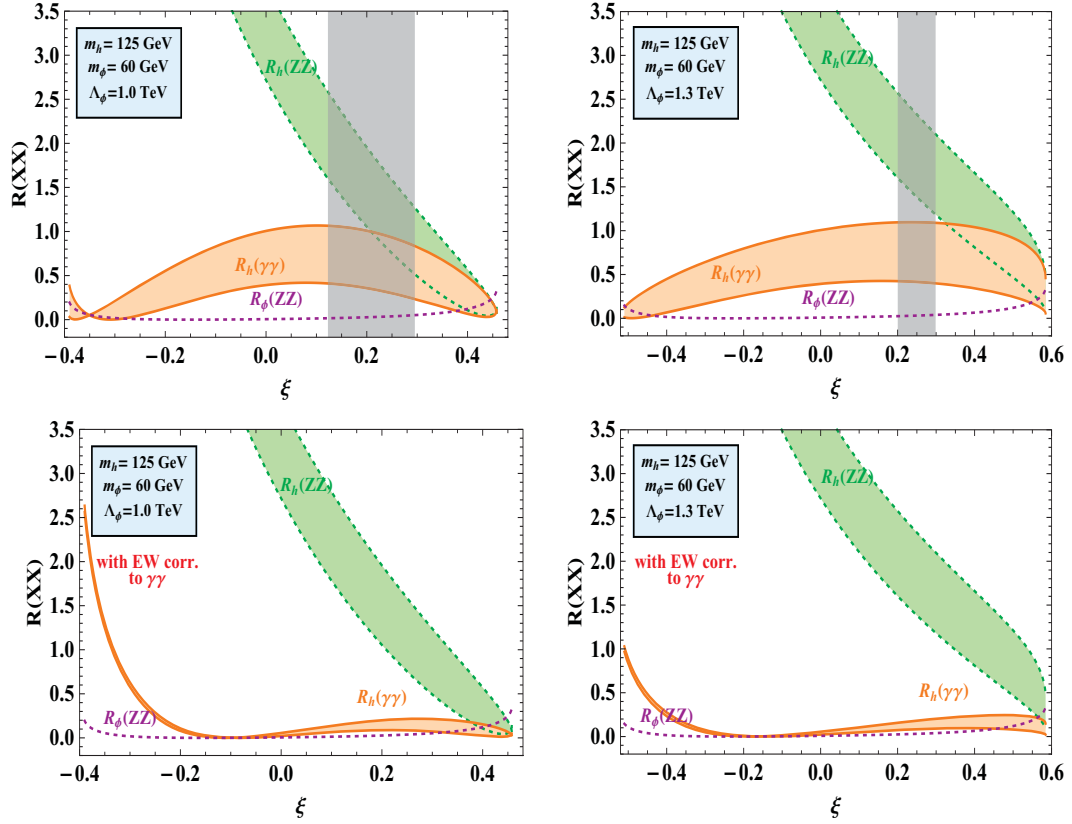


Figure 24: Ratio of discovery significances $R(XX) \sim \sigma/\sigma_{SM}$, defined in the text, for $m_h = 125$ GeV, $m_\phi = 60$ GeV and for different values of Λ_ϕ and $m_{\tau'}$, for $m_{\tau'} = 100$ GeV. In the upper panels we show the LO, and in the lower panels the EW corrected branching ratio to $\gamma\gamma$. The light green bands indicate the theoretical uncertainties in the $gg \rightarrow h \rightarrow ZZ^*$ rate, while those for $\gamma\gamma$ are depicted in orange. The dashed purple lines marked by $R_\phi(ZZ)$ indicate the ratio of $\phi Z^* Z^*$ couplings with respect to the $h_{SM} Z^* Z^*$ one. The vertical gray bands indicate the allowed parameter space for ξ .

- For Scenario 1a, if $m_\phi \leq 100$ GeV, the LEP and Tevatron constraints apply. We find that, constraining $R_\phi(Z^* Z^*)$ to be in the required range (< 0.5) forces $\xi < 0.3$ and $R_h(ZZ^*) < 1.6$. If we do not take into account the higher order EW corrections to the $h\gamma\gamma$ coupling, we find that for $m_\phi = 60$ GeV the experimental constraints (including LEP) are satisfied for $\Lambda_\phi = 1.0$ TeV if $m_{\tau'} = 150$ GeV, and for $\Lambda_\phi = 1.0, 1.3$ TeV if $m_{\tau'} = 100$ GeV, as shown in the upper panel of Fig. 24. The tight LEP constraints on the $\Lambda_\phi - \xi$ parameter space disallows greater values of Λ_ϕ in the very light m_ϕ parameter region. However, when the large EW

corrections to the $\gamma\gamma$ channel are included, we find no regions allowed anymore in this scenario (lower panel of Fig. 24). However, if $m_\phi = 120$ GeV, there exist points in the parameter space still consistent with all the experimental data for light τ' leptons. As both of the h and ϕ states are light, we graph the decays to $\gamma\gamma$, $b\bar{b}$ and ZZ^* . The $m = 120$ GeV is a point in the CMS data, and may or may not survive the latest round of data analysis. As both Higgs-radion mixed states are light, their branching ratios will depend on the τ' mass. If $m_{\tau'} = 100$ GeV, ϕ can decay into $\tau'\tau$, and the branching ratios to $b\bar{b}$, ZZ^* and $\gamma\gamma$ are modified. We present these in Fig. 25 for $\Lambda_\phi = 1.5$ and 2 TeV. From the figure (upper panels) one can note that, not including higher order EW corrections to $\gamma\gamma$, there exist allowed regions of the parameter space. Again in this Scenario, if we include EW corrections to $\gamma\gamma$ (lower panels) all allowed region disappears due to the reduced branching into $\gamma\gamma$.

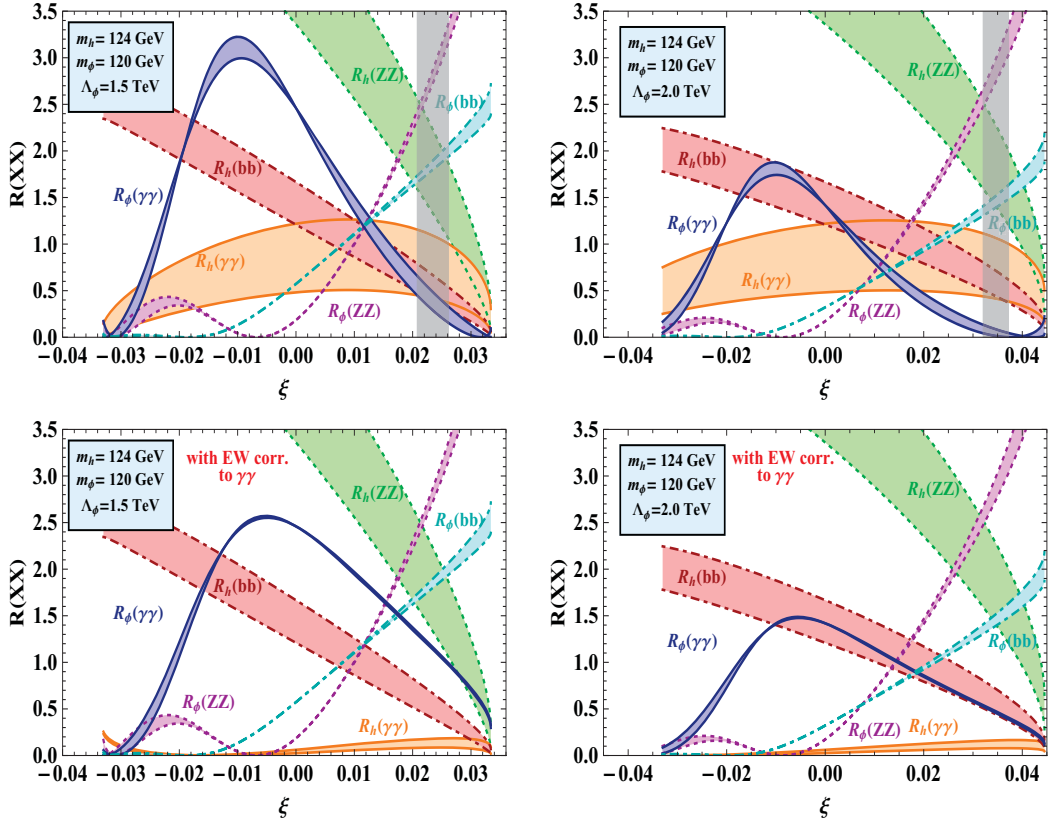


Figure 25: Ratio of discovery significances $R(XX) \sim \sigma/\sigma_{SM}$, defined in the text, for $m_h = 124$ GeV, $m_\phi = 120$, $m_{\tau'}$ = 100 GeV and for different values of Λ_ϕ . In the upper panels we show the LO, and in the lower panel the EW corrected branching ratio to $\gamma\gamma$. The light green bands indicate the theoretical uncertainties in the ZZ^* signal, red for $b\bar{b}$ and orange for $\gamma\gamma$. For ϕ the uncertainties are depicted in pink for ZZ^* , light blue for $b\bar{b}$ and purple for $\gamma\gamma$. The vertical gray bands indicate the allowed parameter space for ξ .

If $m_h = 124$ GeV, $m_\phi = 137$ GeV, we are unable to find points in the parameter space which satisfy the experimental constraints, with or without higher order EW corrections to $\gamma\gamma$. If $R_\phi(ZZ^*) < 0.2$ as required, $R_\phi(\gamma\gamma) > 2.3$, and $R_h(ZZ^*) < 1.6$ for $\Lambda_\phi = 1, 1.3, 1.5$ TeV, and the branching ratios worsen for higher Λ_ϕ .

- For Scenario 1b, increasing m_ϕ only makes the situation worse and we do not find any region of parameters in which an h state at 125 GeV and a heavy ϕ are allowed by the branching ratio constraints, and we thus choose not to show

any figure for this case.

We have so far found that only scenario 1a, allows some regions of parameter space, but with a very restrictive Λ_ϕ , and only if we do not consider the large suppressions in the $\gamma\gamma$ channel due to higher order EW corrections.

- In Scenario 2a, where $m_\phi = 124$ GeV and h is light, and for $m_{\tau'} = 150$ GeV, we do not find any allowed region in which all bounds and observed signals are respected. For regions where $R_h(\gamma\gamma) < 0.5$, $R_\phi(ZZ^*) < 1.6$. However, if the fourth generation charged lepton τ' is light enough for the Higgs-radion mixed state(s) to decay into it (through flavor-violating decays $\tau\tau'$), the branching ratios are modified and the parameter space can shift. We show this in Fig. 26, for $m_h = 120$ GeV, $m_\phi = 124$ GeV and $\Lambda_\phi = 1.3$ TeV and $\Lambda_\phi = 1.5$ TeV. For $m_{\tau'} = 100$ GeV, the possibility of decays into $\tau\tau'$ reduces the branching ratios to the other channels, thus widening the allowed ξ parameter range and of Λ_ϕ for the Higgs-radion states. On the upper panels we do not include higher order corrections to $\gamma\gamma$ while these are taken into account in the lower panels. One can see that the reduction in $h \rightarrow \gamma\gamma$ due to these corrections enhances somewhat the allowed region since a the reduction in $\gamma\gamma$ happens mostly for the h scalar, and this is preferred for $m_h = 120$ GeV.

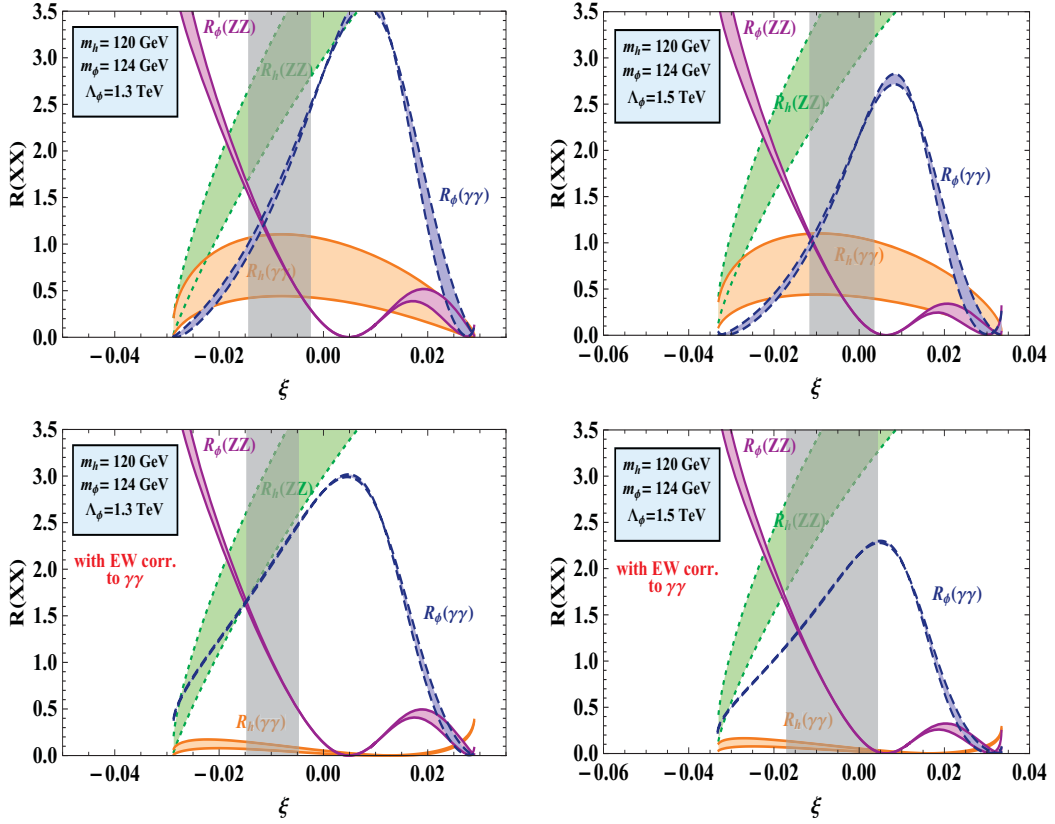


Figure 26: Ratio of discovery significances $R(XX) \sim \sigma/\sigma_{SM}$, defined in the text, for $m_h = 120$ GeV, $m_\phi = 125$ GeV and for different values of Λ_ϕ , for $m_{\tau'} = 100$ GeV. In the upper panels we show the LO, and in the lower panel the EW corrected branching ratio to $\gamma\gamma$. The light green bands indicate the theoretical uncertainties in the ZZ^* signal and the orange the ones are for $\gamma\gamma$. For the ϕ the theoretical uncertainties in ZZ^* are given by pink bands and the ones for $\gamma\gamma$ are in purple. The vertical gray bands indicate the allowed parameter space for ξ .

- In Scenario 2b, we find that as long as h is heavy enough, there are regions of parameter space where all experimental constraints are satisfied. This is true independent of whether $m_{\tau'} = 100$ or 150 GeV, and also of whether one includes the higher order EW corrections to $\gamma\gamma$. However, the results are quite sensitive to the value of Λ_ϕ and to the large experimental and theoretical uncertainties in the rates. We illustrate the situation for two values of Λ_ϕ , i.e $\Lambda_\phi = 1$ TeV in Fig. 27 and for $\Lambda_\phi = 1.3$ TeV in Fig. 28, for different h masses $m_h = 320, 400, 500$ and 600 GeV. These figures are not affected by higher order EW corrections to

$\gamma\gamma$, as these mostly change the couplings of the heavy h field, whose couplings to $\gamma\gamma$ are irrelevant. Note that while for $\Lambda_\phi = 1$ TeV there are allowed bands for 600, 500 and 320 GeV, the parameter space for $\Lambda_\phi = 1.3$ TeV is much more restrictive and we can only fit the data for $m_h = 600$ GeV.

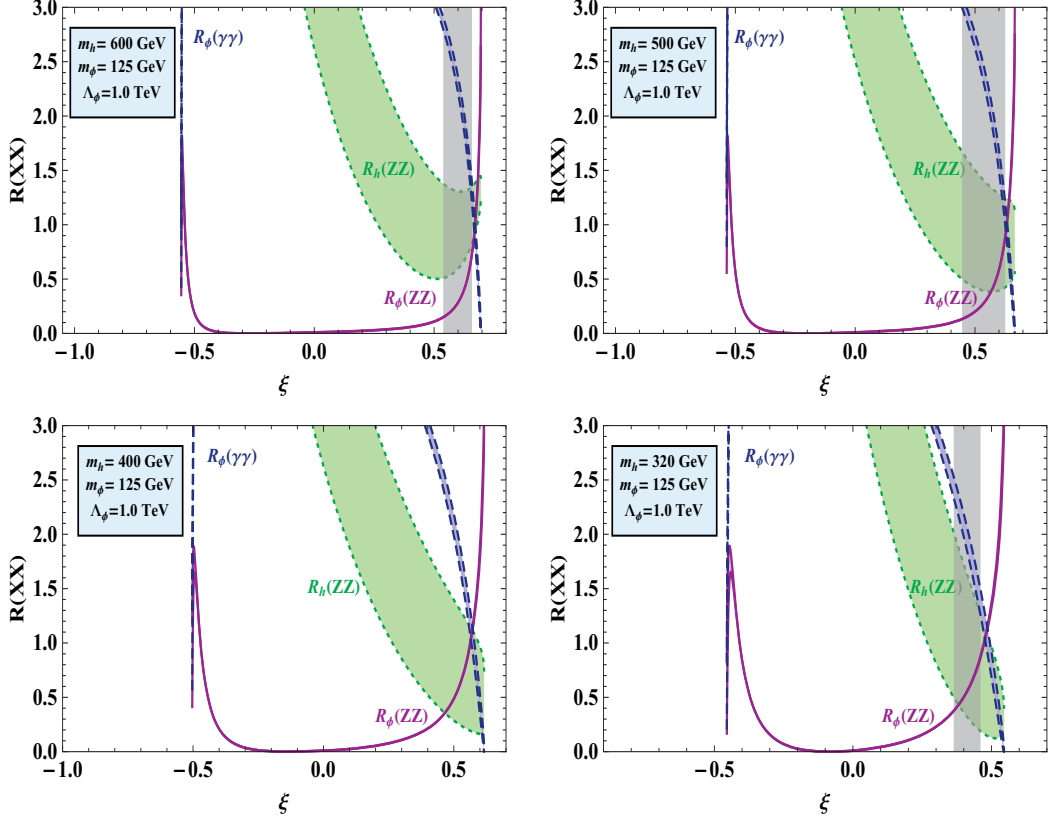


Figure 27: Ratio of discovery significances $R(XX) \sim \sigma/\sigma_{SM}$, defined in the text, for $m_\phi = 125$ GeV, $\Lambda_\phi = 1.0$ TeV and for different masses of h . The light green bands indicate the theoretical uncertainties in the ZZ signal. There is no change in these graphs if we include the EW corrected branching ratio to $\gamma\gamma$. We took $m_{\tau'} = 150$ GeV, precluding FCNC decays to fourth generation leptons. The vertical gray bands indicate the allowed parameter space for ξ .

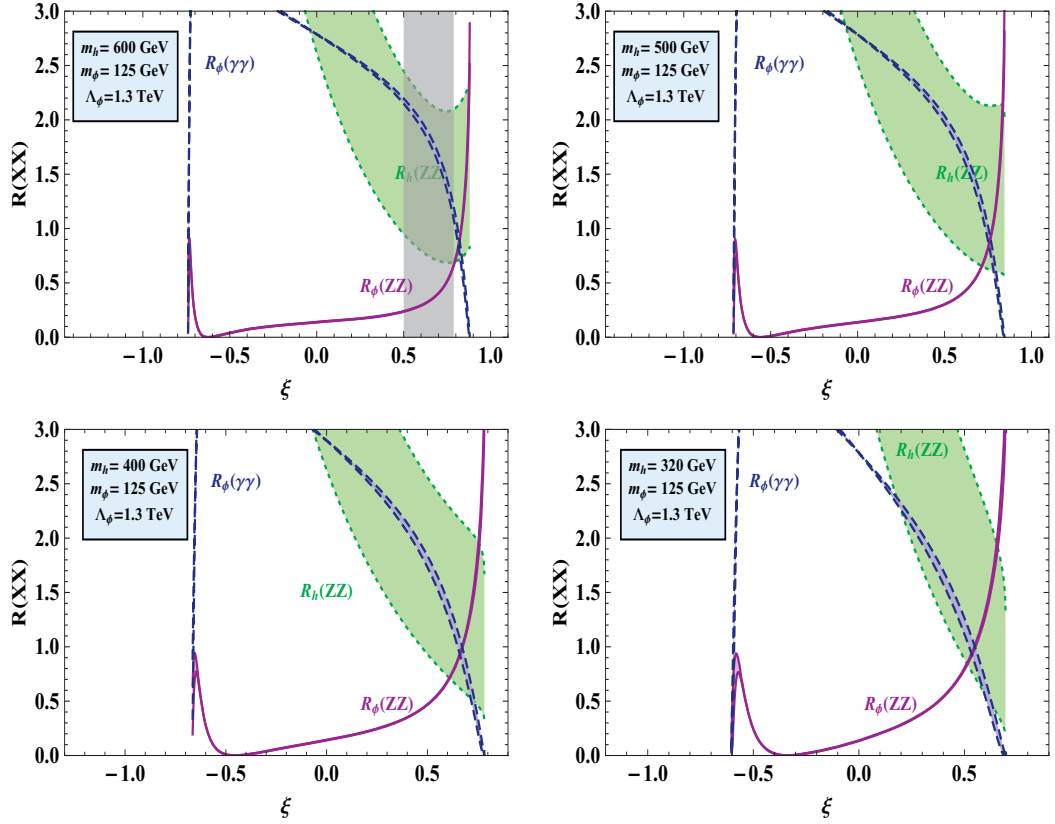


Figure 28: Same as Fig. 27, but for $\Lambda_\phi = 1.3$ TeV.

7.2 Flavor Changing Decays of the Higgs-Radion States in the Four Generation Model

Should the scalar discovered at the LHC be a Higgs-radion mixed state, its decay into two fermions will be different than for a SM Higgs boson, and further analysis at the LHC could differentiate the particles. In this section we present the branching ratios of the mixed Higgs-radion state into two fermions. We start by giving analytical formulas, as they have not appeared before, then show specific values for the flavor-conserving and the flavor-violating branching ratios, for the allowed points in the parameter space presented in the previous section. The branching ratios of the mixed

states ϕ and h into two fermions are given by:

$$\Gamma(\phi \rightarrow \bar{f}_i f_j) = \frac{S c m_i m_j}{8\pi m_\phi^3 v^2} \sqrt{m_\phi^4 + m_i^4 + m_j^4 - 2m_\phi^2 m_i^2 - 2m_\phi^2 m_j^2 - 2m_i^2 m_j^2} \\ \times \left(\left[(\tilde{c}_{ij})^2 + (\tilde{c}_{ji})^2 \right] (-m_\phi^2 + m_i^2 + m_j^2) + 4\Re[(\tilde{c}_{ij})(\tilde{c}_{ji})] m_i m_j \right), \quad (7.11)$$

$$\Gamma(h \rightarrow \bar{f}_i f_j) = \frac{S c m_i m_j}{8\pi m_h^3 v^2} \sqrt{m_h^4 + m_i^4 + m_j^4 - 2m_h^2 m_i^2 - 2m_h^2 m_j^2 - 2m_i^2 m_j^2} \\ \times \left(\left[(\tilde{d}_{ij})^2 + (\tilde{d}_{ji})^2 \right] (-m_h^2 + m_i^2 + m_j^2) + 4\Re[(\tilde{d}_{ij})(\tilde{d}_{ji})] m_i m_j \right) \quad (7.12)$$

Here S is a product of statistical factors $1/j!$ for each group of j identical particles in the final state. For flavor violating couplings, the particles in the final state are different, therefore, $S = 1$. The factor c is the color factor, for quarks $c = 3$, and for leptonic decays, $c = 1$.

The flavor violating couplings of the mixed states are defined as

$$\begin{aligned} \tilde{c}_{ij} &= c a_{ij} + a\gamma \tilde{a}_{ij}, \\ \tilde{d}_{ij} &= d a_{ij} + b\gamma \tilde{a}_{ij}, \end{aligned} \quad (7.13)$$

where the couplings a_{ij} and \tilde{a}_{ij} , of the original unmixed Higgs and radion, have been previously obtained in [174,181] in the case of three generations and in [107,108] with four generations. In the branching ratio calculations given in the Tables, we use the central values for a_{ij} s and \tilde{a}_{ij} s obtained in the numerical scans performed in the last references, and we choose a specific allowed value of ξ for each point studied in the parameter space.

We first present the branching ratios to FCNC decays for allowed parameter points from the previous section. We chose two different scenarios. In one $m_{\tau'} = 100$ GeV, thus a scalar of mass 125 GeV can have flavor-violating decays into $\tau\tau'$. These results are shown in Table 19. The FCNC decay branching ratios into $\tau\tau'$ can reach 5%. Overall, the effect is not measurable, however, should the mass of the τ' be close to its experimental limit 100 GeV, the situation could change drastically and the $BR(\phi \rightarrow \tau'\tau)$ can reach 50 %, suppressing all other decays.

$\Lambda(\text{TeV})$	ξ	$m(\text{GeV})$	$b'b$	tc	bs	$\tau'\tau$	$\mu\tau$	$\nu_\tau\nu_{\tau'}$
1.3	0.228	$m_\phi = 60$	-	-	9.53×10^{-5}	-	2.49×10^{-5}	-
		$m_h = 125$	-	-	5.51×10^{-4}	5.53×10^{-1}	1.52×10^{-4}	1.46×10^{-3}
1.3	-0.00866	$m_\phi = 124$	-	-	7.30×10^{-5}	4.67×10^{-2}	2.01×10^{-5}	7.76×10^{-4}
		$m_h = 120$	-	-	6.34×10^{-4}	4.74×10^{-1}	1.77×10^{-4}	1.48×10^{-3}
1.5	0.0221	$m_\phi = 120$	-	-	3.31×10^{-4}	2.20×10^{-1}	9.06×10^{-5}	1.46×10^{-3}
		$m_h = 124$	-	-	7.34×10^{-4}	7.19×10^{-1}	2.02×10^{-4}	1.76×10^{-3}
1.0	0.417	$m_\phi = 125$	-	-	7.47×10^{-5}	5.94×10^{-2}	2.05×10^{-5}	8.15×10^{-4}
		$m_h = 320$	-	1.53×10^{-4}	1.04×10^{-6}	7.84×10^{-3}	3.23×10^{-7}	9.28×10^{-6}
1.0	0.537	$m_\phi = 125$	-	-	4.21×10^{-5}	2.95×10^{-3}	1.16×10^{-5}	6.92×10^{-4}
		$m_h = 500$	1.27×10^{-2}	6.61×10^{-5}	2.93×10^{-7}	2.71×10^{-3}	9.83×10^{-8}	3.00×10^{-6}
1.0	0.601	$m_\phi = 125$	-	-	1.52×10^{-5}	7.29×10^{-3}	4.17×10^{-6}	5.42×10^{-4}
		$m_h = 600$	1.44×10^{-2}	4.84×10^{-5}	1.99×10^{-7}	1.89×10^{-3}	6.68×10^{-8}	2.02×10^{-6}

Table 19: The FCNC branching ratios of h and ϕ for allowed points in the parameter space. The fourth generation fermion masses are chosen as $m_{t'} = 400$ GeV, $m_{b'} = 350$ GeV, $m_{\tau'} = 100$ GeV, $m_{\nu_{\tau'}} = 90$ GeV.

In Table 20 we chose $m_{\tau'} = 150$ GeV, precluding FCNC decays of the lightest scalar into fourth generation leptons. As before, the Higgs-radion mixed state can decay into third and fourth generation neutrinos, but the branching ratios are not significant. For the other fourth generation fermions, we take throughout $m_{t'} = 400$ GeV, $m_{b'} = 350$ GeV, and $m_{\nu_{\tau'}} = 90$ GeV.

$\Lambda(\text{TeV})$	ξ	$m(\text{GeV})$	$b'b$	tc	bs	$\tau'\tau$	$\mu\tau$	$\nu_\tau\nu_{\tau'}$
1.0	0.0283	$m_\phi = 60$	-	-	1.08×10^{-5}	-	2.83×10^{-6}	-
		$m_h = 125$	-	-	1.05×10^{-3}	-	2.88×10^{-4}	3.00×10^{-3}
1.0	0.412	$m_\phi = 125$	-	-	7.60×10^{-5}	-	2.09×10^{-5}	8.52×10^{-4}
		$m_h = 320$	-	1.61×10^{-4}	1.10×10^{-6}	9.24×10^{-3}	3.40×10^{-7}	9.76×10^{-6}
1.0	0.565	$m_\phi = 125$	-	-	5.84×10^{-5}	-	1.61×10^{-5}	7.85×10^{-4}
		$m_h = 500$	1.26×10^{-2}	6.51×10^{-5}	2.90×10^{-7}	3.62×10^{-3}	9.72×10^{-8}	2.91×10^{-6}
1.0	0.644	$m_\phi = 125$	-	-	4.50×10^{-5}	-	1.24×10^{-5}	7.28×10^{-4}
		$m_h = 600$	1.42×10^{-2}	4.76×10^{-5}	1.96×10^{-7}	2.59×10^{-3}	6.57×10^{-8}	1.99×10^{-6}

Table 20: Same as Table 19, but for $m_{\tau'} = 150$ GeV.

We perform the same analysis, this time for the flavor-diagonal couplings, in Table 21 for $m_{\tau'} = 100$ GeV and in Table 22 for $m_{\tau'} = 150$ GeV. As no flavor-conserving decays into fourth generation fermions are possible, we compare the ratio of significance and

Yukawa couplings to the corresponding ones in the SM. The light scalar state (at 120 or 125 GeV) exhibits large enhancements for $b\bar{b}$ and $c\bar{c}$.

The enhancements in $b\bar{b}$ for the ϕ state are consistent with the Tevatron results $R(b\bar{b}) = 2.03_{-0.71}^{+0.73}$ [223], while the heavier scalars have correspondingly suppressed ratios of significance with respect to the SM. The former fact is quite unlike the case for SM4, where the branching ratio $\text{BR}(H \rightarrow b\bar{b})$ is 30% less than in the SM for $M_H \approx 125$ GeV [165–167]. The enhancements in the warped space model are inherited from the couplings of the bare Higgs boson to fermions, a_{ij} , given in [107]. The range of the flavor-conserving coefficients a_{ij} is large, and their values can accommodate the Tevatron findings (under most circumstances, they are in the same range, or only slightly reduced compared to the SM with 3 generations [181]). The final enhancements in the couplings of the physical states will give a clear indication for the warped space model. Because of this relative uncertainty in the fermion Yukawa couplings, we neglect higher order EW corrections to the couplings of the Higgs with vector bosons, in the presence of a fourth generation. Moreover these corrections have not been calculated out in the context of our scenario, in which the effects of heavy KK fermions should be included.

$\Lambda(\text{TeV})$	ξ	$m(\text{GeV})$	$\mathbf{R}(\text{bb})$	$\mathbf{R}(\text{cc})$	$\mathbf{R}(\text{tt})$	\mathbf{Y}_{tt}
1.5	0.0221	$m_\phi = 120$	2.05	2.13	-	0.496
		$m_h = 124$	0.563	0.557	-	0.880
1.0	0.421	$m_\phi = 125$	2.20	2.31	-	0.380
		$m_h = 320$	0.523	0.513	-	1.02
1.0	0.537	$m_\phi = 125$	1.81	1.93	-	0.317
		$m_h = 500$	0.532	0.521	0.556	1.19
1.0	0.601	$m_\phi = 125$	1.78	1.89	-	0.316
		$m_h = 600$	0.553	0.520	0.559	1.36

Table 21: Ratio of significance $R_{h(\phi)}(XX) = S(gg \rightarrow h(\phi) \rightarrow f\bar{f})/S(gg \rightarrow h_{SM} \rightarrow f\bar{f})$ for different parameter space. Last column are the Yukawa couplings for $h(\phi)$ to $t\bar{t}$. The fourth generation fermion masses are chosen as $m_{t'} = 400$ GeV, $m_{b'} = 350$ GeV, $m_{\tau'} = 100$ GeV, $m_{\nu_{\tau'}} = 90$ GeV.

$\Lambda(\text{TeV})$	ξ	$m(\text{GeV})$	$R(\text{bb})$	$R(\text{cc})$	$R(\text{tt})$	Y_{tt}
1.0	0.412	$m_\phi = 125$	2.45	2.59	-	0.374
		$m_h = 320$	0.586	0.575	-	1.01
1.0	0.565	$m_\phi = 125$	2.02	2.14	-	0.334
		$m_h = 500$	0.481	0.470	0.503	1.24
1.0	0.480	$m_\phi = 125$	1.48	1.59	-	0.602
		$m_h = 600$	0.636	0.625	0.661	0.819

Table 22: Same as Table 21, but for $m_{\tau'} = 150$ GeV.

7.3 Conclusions and Outlook

In this Chapter, we have investigated the phenomenology of the Higgs-radion mixed state with a fourth generation of quarks and leptons, in an attempt to explain the latest LHC data. We asked the question: if the scalar particle seen at the LHC is not the ordinary SM Higgs boson, but a mixed Higgs-radion state, could this state satisfy all the experimental constraints, even including the effects of a fourth generation? The four generations assumption in warped space models is of particular interest, as SM4, fails to reproduce the observed data to at least 95% confidence level. A fourth generation, which is severely restricted and perhaps even ruled out by the ATLAS and CMS data in SM4 could be resuscitated in warped space models. The answer to the question we posed is a cautious yes. That is, there exist regions of the parameter space where one of the mixed Higgs-radion states has mass of 125 GeV, and satisfies existing experimental constraints, while the other either has a mass of 120 GeV, thus fitting a CMS parameter point, or evades present collider bounds.

Higher order EW corrections to the couplings of Higgs to photons in SM4 show a substantial suppression. In our scenario, however the presence of heavy KK fermions should affect such calculations and so we decided to study the predictions both with and without these corrections whose effect is to close the parameter space for the case in which the observed scalar at the LHC is the mostly Higgs state h (leaving the ϕ possibility unaffected). With no corrections to $\gamma\gamma$, if the h state is the scalar observed at the LHC, the ϕ mass must be light. Parameter points with either $m_\phi = 60$ GeV,

which evade LEP restrictions, or $m_\phi = 120$ GeV, which fit the CMS data, are allowed for some range of the mixing parameter ξ . We analyzed these for both very light fourth generation charged leptons, $m_{\tau'} = 100$ GeV, or for heavier ones, $m_{\tau'} = 150$ GeV. The difference between these two masses is that the first case allows flavor-changing decays of the Higgs-radion state, which are large in this model and which modify the branching ratios to $\gamma\gamma$ and ZZ^* . All of these parameter points require the scale Λ_ϕ to be light, in the 1.0 – 1.3 TeV range, the exact values dependent on the rest of the parameters. For larger m_ϕ values, the branching ratio to ZZ increases beyond the LHC limits, and thus this parameter region is forbidden. This region of parameter space is very fragile. For $m_h = 124$ GeV, the point at $m_\phi = 120$ GeV shows signs of instability as the 4ℓ excess might be cancelled by $\gamma\gamma$, while its decay into $b\bar{b}$ appears to have increased. The signal for $m_\phi = 60$ GeV, while not ruled out by LEP data depends very sensitively on the values of $m_{\tau'}$ and Λ_ϕ .

If ϕ is the scalar observed at the LHC, the h state is most likely to be heavy. The exception is when $m_{\tau'} = 100$ GeV; for $m_h = 120$ GeV parameter points exist for $\Lambda_\phi = 1.0, 1.3,$ and 1.5 TeV. Regions where $m_h = 320, 400, 500$ and 600 GeV exist for some values of Λ_ϕ , which is still required to be in the 1.0 – 1.5 TeV range. These parameter regions seem quite robust and not dependent on whether τ' is heavy or light; however they could be ruled out within the next year at LHC as data for heavier scalars becomes available. To increase predictability of our scenario, we calculated the branching ratios of the allowed Higgs-radion states into fermions, both for flavor changing and flavor conserving channels (some of which are significantly enhanced with respect to the SM expectations). As more data on the scalar production and decay becomes available, these predictions can be compared with the experiment, specially noting the appearance of the interesting exotic FCNC decays.

In conclusion, we have achieved two goals in this part: first, we have shown that a scalar in a warped model with a fourth generation of fermions can be light *and* consistent with the LHC data, if the observed particle is a Higgs-radion mixed state. Second, the allowed parameter space is tightly constrained and expected to be confirmed or ruled out within a year by further analyses and/or higher luminosity at the LHC.

Chapter 8

CONCLUSION

The SM is a mathematically consistent renormalizable field theory of the elementary particles and their interactions. On July the 4th 2012, ATLAS and CMS experiments presented a preview of their preliminary results on the search for the Higgs Boson, the only missing element of the SM, and they announced a spin-zero bosonic resonance of mass 125 – 126 GeV a breakthrough sparking renewed interest in particle physics. The the discovery of the Higgs boson may even further substantiate the SM. However, the issue of whether or not this new finding is the Higgs boson predicted by the SM is still somewhat ambiguous, requiring the close examination of accumulating data over a longer period. All its accomplishments aside, the SM suffers from some drawbacks, which motivates supplementary searches at the LHC to look for new physics buried within the available results. In this thesis, we have introduced some of the extensions of the SM including LRSUSY and Warped Extra Dimensions with a Fourth Generation which may resolve some of the questions in particle physics that cannot be addressed in the SM, and investigate their scalar sectors.

We first analyzed the Higgs sector of a minimal left-right supersymmetric model where inclusion of the heavy Majorana neutrino Yukawa coupling insures a global minimum which is charge conserving, thus avoiding spontaneous R -parity breaking or the need to introduce higher dimensional terms. The Higgs sector contains four doubly-charged, six singly-charged, nine neutral scalar, and seven pseudoscalar fields. We have shown that, despite the existence of so many free parameters, most of the Higgs masses are sensitive to only few parameters, thus one can find a parameter space allowing to a light neutral flavor-conserving scalar Higgs boson as a counterpart to

the SM one, at least one light doubly-charged Higgs boson, which is interesting for phenomenology, and flavor-violating neutral Higgs bosons satisfying the constraints imposed by the experimental data from $\Delta F = 1, 2$ mixings. The masses of new gauge bosons, on the other hand, are predicted to be just outside of the accessible energies by LHC for the chosen parameter space. This analysis is important as a basis for a phenomenological study of signals from such a Higgs sector.

The warped extra dimensions including a fourth generation of fermions has been the second focus of the thesis. We present a comprehensive study of Higgs flavor-violating couplings introduced by the insertion of the higher dimensional operators in the model. In fact, the Higgs FCNCs become more pronounced with the addition of the fourth family of fermions due to their cumulative effects in flavor space. Both analytical and numerical results for the flavor violating couplings are calculated under the assumption that the three generation quark masses and mixing angles will be reproduced and by taking into consideration the unitarity of V_{CKM4} matrix to constrain the masses and mixings of the fourth generations, as well as and imposing the additional bounds from $\Delta F = 2$ mixings. The constraints are similar to those obtained in the scenario with three generations [181]. We briefly discussed the possibilities for the lepton sector as well, which is unfortunately complicated by the lack of a well-defined model of neutrino masses and mixings. We found that the effect of flavor-violating couplings contributing at the loop-level processes in the form $f_i \rightarrow f_j \gamma$ are negligible for quarks whereas might become more important and restrict the lepton flavor-violating couplings further that the numerical scan. FCNC decay channels including fourth generation of fermions as a decay product would provide a clear indication of the model. Moreover, in case that the fourth generation quarks and leptons are heavier than the Higgs boson, their decay into lighter quarks and Higgs bosons would be a promising channel for their discovery and identification.

In the same framework we have investigated the phenomenology of the couplings of the radion to fermions by giving analytical expressions in leading order together with our predictions on typical (and maximal) values for the radion couplings to heavy-heavy, light-light, and heavy-light quarks from a contour plot in a plane defined by the coefficients describing the quark localization with respect to TeV-brane, also confirmed by an extensive numerical scan. As in the case for the Higgs boson, restrictions are imposed on the couplings by tree-level FCNC contributions to

$\Delta F = 1, 2$ mixings. Further constraints are obtained by translating the most recent constraints on Higgs boson masses from ATLAS and CMS into combined radion mass-scale limits. Our analysis shows that, unlike the Higgs boson, there are minute differences between radion mass-scale limits in 3 and 4 generations, rendering them quite independent of the number of generations. In a complete decay plot, we include all branching ratios of the radion and show that for heavy radion FCNC, the most promising decay channels are the ones which include fourth generation leptons as one of the decay products. In addition the flavor-conserving radion decays into fourth generation leptons and neutrinos can be large and alter the dominant decay modes for a heavier radion to WW or ZZ gauge bosons and provide a distinguishing signal for the model. If a heavy Higgs-like state is discovered at the LHC with the usual “golden mode”, $pp \rightarrow h \rightarrow ZZ$, a width measurement could rule out a conventional Higgs boson. A careful study for different and/or exotic decay channels of that resonance might be the key to discover both a fourth generation of fermions and a warped extra dimension.

At last, we analyzed the phenomenology of the Higgs-radion mixed states in a warped extra dimensional scenario with an additional family of fermions where the gauge and matter fields are allowed to propagate in the bulk. Higher order EW corrections to the couplings of Higgs to two gluons and photons were also taken into account. However, since the presence of heavy KK fermions should affect Higgs to two photons calculations, we present our results both with and without these corrections. They affect the case in which the observed scalar at the LHC is the mostly Higgs state h , leaving the ϕ possibility unaffected. We have found out that there exist regions of the parameter space where one of the mixed Higgs-radion states satisfies the properties of the signal at 125 GeV, while the other either fits CMS or ATLAS parameter points, or evades the present collider bounds. To increase predictability of our scenario, we calculated the branching ratios of the allowed Higgs-radion states into fermions, both for flavor-changing and flavor-conserving channels. As more data on the scalar production and decay becomes available, these predictions can be compared with the experiment.

Now that a scalar spin-0 particle has been discovered, for the first time we might have access to electroweak symmetry breaking sector of the SM and to the mysteries it may reveal. As attention turns towards its couplings, it is important to test that the

observed boson is the SM Higgs boson or not. The preliminary results indicating an excess in $\gamma\gamma$, ZZ and WW decay channels are in agreement with the SM even though there may be a suggestion of BSM due to possible deviation in Higgs di-photon decay rates. In the experimental side, more accumulated data will be needed to determine if the excess is real or just due to a statistical fluctuation. Simultaneously, on the theoretical side, simultaneously, it is worth investigating which BSM can explain these deviations. In this thesis, we consider an extension of the Higgs sector in a minimal LRSUSY model, and warped extra dimensions with four generations which might be refuted or confirmed in the future experiments. Future work could be investigation of signals in Higgs production and decay modes at LHC for the LRSUSY model introduced.

The thesis is based on the following publications:

1. M. Frank and B. Korutlu, Higgs Bosons in a minimal R-parity conserving left-right supersymmetric model, *Phys. Rev. D* **83**, 073007 (2011).
2. M. Frank, B. Korutlu and M. Toharia, Higgs Phenomenology in Warped Extra-Dimensions with a 4th Generation, *Phys. Rev. D* **84**, 075009 (2011).
3. M. Frank, B. Korutlu and M. Toharia, Radion Phenomenology with 3 and 4 Generations, *Phys. Rev. D* **84**, 115020 (2011).
4. M. Frank, B. Korutlu and M. Toharia, Saving the fourth generation Higgs with radion mixing, *Phys. Rev. D* **85**, 115025 (2012).

Except for specific credits indicated throughout my thesis, everything else is my own work.

Bibliography

- [1] D. Binosi and L. Theussl. JaxoDraw: A Graphical user interface for drawing Feynman diagrams. *Comput.Phys.Commun.*, 161:76–86, 2004.
- [2] S. L. Glashow. Partial Symmetries of Weak Interactions. *Nucl.Phys.*, 22:579–588, 1961.
- [3] S. Weinberg. A Model of Leptons. *Phys.Rev.Lett.*, 19:1264–1266, 1967.
- [4] J. Glashow, S. L. Iliopoulos and L. Maiani. Weak Interactions with Lepton-Hadron Symmetry. *Phys.Rev.*, D2:1285–1292, 1970.
- [5] S. L. Glashow. Towards a Unified Theory: Threads in a Tapestry. *Rev.Mod.Phys.*, 52:539–543, 1980.
- [6] S. Weinberg. Conceptual Foundations of the Unified Theory of Weak and Electromagnetic Interactions. *Rev.Mod.Phys.*, 52:515–523, 1980.
- [7] A. Salam. Gauge Unification of Fundamental Forces. *Rev.Mod.Phys.*, 52:525–538, 1980.
- [8] H. Fritzsch and M. Gell-Mann. Current algebra: Quarks and what else? *eConf*, C720906V2:135–165, 1972.
- [9] G. Aad et al. Observation of a new particle in the search for the Standard Model Higgs boson with the ATLAS detector at the LHC. *Phys.Lett.*, B716:1–29, 2012.
- [10] S. Chatrchyan et al. Observation of a new boson at a mass of 125 GeV with the CMS experiment at the LHC. *Phys.Lett.*, B716:30–61, 2012.
- [11] F. Englert and R. Brout. Broken Symmetry and the Mass of Gauge Vector Mesons. *Phys. Rev. Lett.*, 13:321–323, Aug 1964.

- [12] P. W. Higgs. Broken Symmetries and the Masses of Gauge Bosons. *Phys. Rev. Lett.*, 13:508–509, Oct 1964.
- [13] G. S. Guralnik, C. R. Hagen, and T. W. B. Kibble. Global Conservation Laws and Massless Particles. *Phys. Rev. Lett.*, 13:585–587, Nov 1964.
- [14] H. Georgi and S. L. Glashow. Unity of All Elementary Particle Forces. *Phys.Rev.Lett.*, 32:438–441, 1974.
- [15] J. C. Pati and A. Salam. Lepton Number as the Fourth Color. *Phys.Rev.*, D10:275–289, 1974.
- [16] A. J. Buras, J. R. Ellis, M. K. Gaillard, and Dimitri V. Nanopoulos. Aspects of the Grand Unification of Strong, Weak and Electromagnetic Interactions. *Nucl.Phys.*, B135:66–92, 1978.
- [17] R. N. Mohapatra and J. C. Pati. Left-Right Gauge Symmetry and an Isoconjugate Model of CP Violation. *Phys.Rev.*, D11:566–571, 1975.
- [18] R. N. Mohapatra and J. C. Pati. A Natural Left-Right Symmetry. *Phys.Rev.*, D11:2558, 1975.
- [19] R. N. Mohapatra and G. Senjanovic. Neutrino Mass and Spontaneous Parity Violation. *Phys.Rev.Lett.*, 44:912, 1980.
- [20] J. Wess and B. Zumino. A Lagrangian Model Invariant Under Supergauge Transformations. *Phys.Lett.*, B49:52, 1974.
- [21] J. Wess and B. Zumino. Supergauge Transformations in Four-Dimensions. *Nucl.Phys.*, B70:39–50, 1974.
- [22] M. Cvetič and J. C. Pati. N=1 Supergravity Within the Minimal Left-Right Symmetric Model. *Phys.Lett.*, B135:57, 1984.
- [23] Y. J. Ahn. The Neutron Electric Dipole Moment in Left-Right Symmetric Low-Energy Supergravity. *Phys.Lett.*, B149:337–340, 1984.
- [24] R. M. Francis, M. Frank, and C. S. Kalman. Anomalous magnetic moment of the muon arising from the extensions of the supersymmetric standard model based on left-right symmetry. *Phys.Rev.*, D43:2369–2385, 1991.

- [25] K. Huitu, J. Maalampi, and M. Raidal. Slepton pair production in e^+e^- collision in supersymmetric left-right model. *Phys.Lett.*, B328:60–66, 1994.
- [26] K. Huitu, J. Maalampi, and M. Raidal. Supersymmetric left-right model and its tests in linear colliders. *Nucl.Phys.*, B420:449–467, 1994.
- [27] M. Frank and B. Korutlu. Higgs Bosons in a minimal R-parity conserving left-right supersymmetric model. *Phys.Rev.*, D83:073007, 2011.
- [28] P. H. Frampton, P. Q. Hung, and M. Sher. Quarks and leptons beyond the third generation. *Phys.Rept.*, 330:263, 2000.
- [29] B. Holdom, W. S. Hou, T. Hurth, M. L. Mangano, S. Sultansoy, et al. Four Statements about the Fourth Generation. *PMC Phys.*, A3:4, 2009.
- [30] M. B. Green and J. H. Schwarz. The Hexagon Gauge Anomaly in Type I Superstring Theory. *Nucl.Phys.*, B255:93–114, 1985.
- [31] N. Arkani-Hamed, S. Dimopoulos, and G. R. Dvali. The Hierarchy problem and new dimensions at a millimeter. *Phys.Lett.*, B429:263–272, 1998.
- [32] I. Antoniadis, N. Arkani-Hamed, S. Dimopoulos, and G. R. Dvali. New dimensions at a millimeter to a Fermi and superstrings at a TeV. *Phys.Lett.*, B436:257–263, 1998.
- [33] I. Antoniadis, S. Dimopoulos, and G. R. Dvali. Millimeter range forces in superstring theories with weak scale compactification. *Nucl.Phys.*, B516:70–82, 1998.
- [34] T. Appelquist, H-C. Cheng, and B. A. Dobrescu. Bounds on universal extra dimensions. *Phys.Rev.*, D64:035002, 2001.
- [35] T. Appelquist and H-U. Yee. Universal extra dimensions and the Higgs boson mass. *Phys.Rev.*, D67:055002, 2003.
- [36] J. Papavassiliou and A. Santamaria. Extra dimensions at the one loop level: Z to b anti-b and B anti-B mixing. *Phys.Rev.*, D63:016002, 2001.

- [37] A. J. Buras, M. Spranger, and A. Weiler. The Impact of universal extra dimensions on the unitarity triangle and rare K and B decays. *Nucl.Phys.*, B660:225–268, 2003.
- [38] K. R. Dienes, E. Dudas, and T. Gherghetta. Neutrino oscillations without neutrino masses or heavy mass scales: A Higher dimensional seesaw mechanism. *Nucl.Phys.*, B557:25, 1999.
- [39] Q-H. Cao, S. Gopalakrishna, and C. P. Yuan. Constraints on large extra dimensions with bulk neutrinos. *Phys.Rev.*, D69:115003, 2004.
- [40] L. Randall and R. Sundrum. A Large mass hierarchy from a small extra dimension. *Phys.Rev.Lett.*, 83:3370–3373, 1999. 9 pages, LaTeX Report-no: MIT-CTP-2860, PUPT-1860, BUHEP-99-9.
- [41] L. Randall and R. Sundrum. An Alternative to compactification. *Phys.Rev.Lett.*, 83:4690–4693, 1999.
- [42] K. S. Hirata et al. Constraints on neutrino oscillation parameters from the Kamiokande-II solar neutrino data. *Phys.Rev.Lett.*, 65:1301–1304, 1990.
- [43] K. S. Hirata et al. Observation of a small atmospheric muon-neutrino / electron-neutrino ratio in Kamiokande. *Phys.Lett.*, B280:146–152, 1992.
- [44] P. Minkowski. $\mu \rightarrow e\gamma$ at a Rate of One Out of 10^9 Muon Decays? *Phys.Lett.*, B67:421, 1977.
- [45] G. R. Farrar and P. Fayet. Phenomenology of the Production, Decay, and Detection of New Hadronic States Associated with Supersymmetry. *Phys.Lett.*, B76:575–579, 1978.
- [46] R. N. Mohapatra. New Contributions to Neutrinoless Double beta Decay in Supersymmetric Theories. *Phys.Rev.*, D34:3457–3461, 1986.
- [47] A. Font, L. E. Ibanez, and F. Quevedo. Does Proton Stability Imply the Existence of an Extra Z_0 ? *Phys.Lett.*, B228:79, 1989.
- [48] S. P. Martin. Some simple criteria for gauged R-parity. *Phys.Rev.*, D46:2769–2772, 1992.

- [49] R. N. Mohapatra and A. Rasin. A Supersymmetric solution to CP problems. *Phys.Rev.*, D54:5835–5844, 1996.
- [50] K. S. Babu, B. Dutta, and R. N. Mohapatra. Solving the strong CP and the SUSY phase problems with parity symmetry. *Phys.Rev.*, D65:016005, 2002.
- [51] G. S. Abrams, C. Adolphsen, R. Aleksan, J. P. Alexander, M. A. Allen, et al. Initial Measurements of Z Boson Resonance Parameters in e^+e^- Annihilation. *Phys.Rev.Lett.*, 63:724, 1989.
- [52] G. S. Abrams, C. Adolphsen, D. Averill, J. Ballam, B. C. Barish, et al. Measurements of Z Boson Resonance Parameters in e^+e^- Annihilation. *Phys.Rev.Lett.*, 63:2173, 1989.
- [53] B. Adeva et al. A Determination of the Properties of the Neutral Intermediate Vector Boson Z^0 . *Phys.Lett.*, B231:509, 1989.
- [54] D. Decamp et al. Determination of the Number of Light Neutrino Species. *Phys.Lett.*, B231:519, 1989.
- [55] M. Z. Akrawy et al. Measurement of the Z^0 Mass and Width with the OPAL Detector at LEP. *Phys.Lett.*, B231:530, 1989.
- [56] R. M. Barnett et al. Review of particle physics. Particle Data Group. *Phys.Rev.*, D54:1–720, 1996.
- [57] A. Soni. The '4th generation', B-CP anomalies and the LHC. hep-ph/0907.2057, 2009.
- [58] W-S. Hou. Source of CP Violation for the Baryon Asymmetry of the Universe. *Chin.J.Phys.*, 47:134, 2009.
- [59] W-S. Hou, Y-Y. Mao, and C-H. Shen. Leading Effect of CP Violation with Four Generations. *Phys.Rev.*, D82:036005, 2010.
- [60] W. J. Marciano, G. Valencia, and S. Willenbrock. Renormalization Group Improved Unitarity Bounds on the Higgs Boson and Top Quark Masses. *Phys.Rev.*, D40:1725, 1989.

- [61] V. A. Novikov, L. B. Okun, A. N. Rozanov, and M. I. Vysotsky. Mass of the Higgs versus fourth generation masses. *JETP Lett.*, 76:127–130, 2002.
- [62] J. M. Frere, A. N. Rozanov, and M. I. Vysotsky. Mass and decays of Brout-Englert-Higgs scalar with extra generations. *Phys.Atom.Nucl.*, 69:355–359, 2006.
- [63] H. Flacher, M. Goebel, J. Haller, A. Hocker, K. Monig, et al. Revisiting the Global Electroweak Fit of the Standard Model and Beyond with Gfitter. *Eur.Phys.J.*, C60:543–583, 2009.
- [64] P. Q. Hung. Minimal SU(5) resuscitated by longlived quarks and leptons. *Phys.Rev.Lett.*, 80:3000–3003, 1998.
- [65] W. D. Goldberger and M. B. Wise. Modulus stabilization with bulk fields. *Phys.Rev.Lett.*, 83:4922–4925, 1999.
- [66] W. D. Goldberger and M. B. Wise. Phenomenology of a stabilized modulus. *Phys.Lett.*, B475:275–279, 2000.
- [67] C. Csaki, M. Graesser, L. Randall, and J. Terning. Cosmology of brane models with radion stabilization. *Phys.Rev.*, D62:045015, 2000.
- [68] G. F. Giudice, R. Rattazzi, and J. D. Wells. Gravitational scalars from higher dimensional metrics and curvature Higgs mixing. *Nucl.Phys.*, B595:250–276, 2001.
- [69] T. Tanaka and X. Montes. Gravity in the brane world for two-branes model with stabilized modulus. *Nucl.Phys.*, B582:259–276, 2000.
- [70] C. Csaki, M. L. Graesser, and G. D. Kribs. Radion dynamics and electroweak physics. *Phys.Rev.*, D63:065002, 2001.
- [71] D. Dominici, B. Grzadkowski, J. F. Gunion, and M. Toharia. The Scalar sector of the Randall-Sundrum model. *Nucl.Phys.*, B671:243–292, 2003.
- [72] J. F. Gunion, M. Toharia, and J. D. Wells. Precision electroweak data and the mixed Radion-Higgs sector of warped extra dimensions. *Phys.Lett.*, B585:295–306, 2004.

- [73] K. Agashe, A. Delgado, M. J. May, and R. Sundrum. RS1, custodial isospin and precision tests. *JHEP*, 0308:050, 2003.
- [74] K. Agashe, G. Perez, and A. Soni. B-factory signals for a warped extra dimension. *Phys.Rev.Lett.*, 93:201804, 2004.
- [75] K. Agashe, G. Perez, and A. Soni. Collider Signals of Top Quark Flavor Violation from a Warped Extra Dimension. *Phys.Rev.*, D75:015002, 2007.
- [76] K. Agashe, A. E. Blechman, and F. Petriello. Probing the Randall-Sundrum geometric origin of flavor with lepton flavor violation. *Phys.Rev.*, D74:053011, 2006.
- [77] S. J. Huber and Q. Shafi. Neutrino oscillations and rare processes in models with a small extra dimension. *Phys.Lett.*, B512:365–372, 2001.
- [78] S. J. Huber and Q. Shafi. Majorana neutrinos in a warped 5-D standard model. *Phys.Lett.*, B544:295–306, 2002.
- [79] S. J. Huber and Q. Shafi. Seesaw mechanism in warped geometry. *Phys.Lett.*, B583:293–303, 2004.
- [80] T. Appelquist, B. A. Dobrescu, E. Ponton, and H-U. Yee. Neutrinos vis-a-vis the six-dimensional standard model. *Phys.Rev.*, D65:105019, 2002.
- [81] T. Gherghetta. Dirac neutrino masses with Planck scale lepton number violation. *Phys.Rev.Lett.*, 92:161601, 2004.
- [82] G. Moreau and J. I. Silva-Marcos. Neutrinos in warped extra dimensions. *JHEP*, 0601:048, 2006.
- [83] G. Moreau and J. I. Silva-Marcos. Flavor physics of the RS model with KK masses reachable at LHC. *JHEP*, 0603:090, 2006.
- [84] A. Aktas et al. Measurement of $F_2^{c\bar{c}}$ and $F_2^{b\bar{b}}$ at high Q^2 using the H1 vertex detector at HERA. *Eur.Phys.J.*, C40:349–359, 2005.
- [85] S. Chang, C. S. Kim, and M. Yamaguchi. Hierarchical mass structure of fermions in warped extra dimension. *Phys.Rev.*, D73:033002, 2006.

- [86] H. Davoudiasl, J. L. Hewett, and T. G. Rizzo. Bulk gauge fields in the Randall-Sundrum model. *Phys.Lett.*, B473:43–49, 2000.
- [87] A. Pomarol. Gauge bosons in a five-dimensional theory with localized gravity. *Phys.Lett.*, B486:153–157, 2000.
- [88] Y. Grossman and M. Neubert. Neutrino masses and mixings in nonfactorizable geometry. *Phys.Lett.*, B474:361–371, 2000.
- [89] T. Gherghetta and A. Pomarol. Bulk fields and supersymmetry in a slice of AdS. *Nucl.Phys.*, B586:141–162, 2000.
- [90] S. Chang, J. Hisano, H. Nakano, N. Okada, and M. Yamaguchi. Bulk standard model in the Randall-Sundrum background. *Phys.Rev.*, D62:084025, 2000.
- [91] K. Agashe, G. Perez, and A. Soni. Flavor structure of warped extra dimension models. *Phys.Rev.*, D71:016002, 2005.
- [92] K. Agashe, M. Papucci, G. Perez, and D. Pirjol. Next to minimal flavor violation. hep-ph/0509117, 2005.
- [93] C. Csaki, A. Falkowski, and A. Weiler. The Flavor of the Composite Pseudo-Goldstone Higgs. *JHEP*, 0809:008, 2008.
- [94] M. Blanke, A. J. Buras, B. Duling, S. Gori, and A. Weiler. $\Delta F=2$ Observables and Fine-Tuning in a Warped Extra Dimension with Custodial Protection. *JHEP*, 0903:001, 2009.
- [95] A. L. Fitzpatrick, G. Perez, and L. Randall. Flavor from Minimal Flavor Violation and a Viable Randall-Sundrum Model. *Phys.Rev.Lett.*, 100:171604, 2008.
- [96] S. Davidson, G. Isidori, and S. Uhlig. Solving the flavour problem with hierarchical fermion wave functions. *Phys.Lett.*, B663:73–79, 2008.
- [97] M. E. Albrecht, M. Blanke, A. J. Buras, B. Duling, and K. Gemmler. Electroweak and Flavour Structure of a Warped Extra Dimension with Custodial Protection. *JHEP*, 0909:064, 2009.

- [98] C. Csaki, A. Falkowski, and A. Weiler. A Simple Flavor Protection for RS. *Phys.Rev.*, D80:016001, 2009.
- [99] E. De Pree, G. Marshall, and M. Sher. The Fourth Generation t-prime in Extensions of the Standard Model. *Phys.Rev.*, D80:037301, 2009.
- [100] Z. Murdock, S. Nandi, and Z. Tavartkiladze. Perturbativity and a Fourth Generation in the MSSM. *Phys.Lett.*, B668:303–307, 2008.
- [101] A. Atre, G. Azuelos, M. Carena, T. Han, E. Ozcan, et al. Model-Independent Searches for New Quarks at the LHC. *JHEP*, 1108:080, 2011.
- [102] R. C. Cotta, K. T. K. Howe, J. L. Hewett, and T. G. Rizzo. Phenomenological minimal supersymmetric standard model dark matter searches on ice. *Phys.Rev.*, D85:035017, 2012.
- [103] R. Fok and G. D. Kribs. Four Generations, the Electroweak Phase Transition, and Supersymmetry. *Phys.Rev.*, D78:075023, 2008.
- [104] G. Burdman and L. Da Rold. Electroweak Symmetry Breaking from a Holographic Fourth Generation. *JHEP*, 0712:086, 2007.
- [105] G. Burdman, L. Da Rold, and R. D. Matheus. The Lepton Sector of a Fourth Generation. *Phys.Rev.*, D82:055015, 2010.
- [106] S. Bar-Shalom, G. Eilam, and A. Soni. Collider signals of a composite Higgs in the Standard Model with four generations. *Phys.Lett.*, B688:195–201, 2010.
- [107] M. Frank, B. Korutlu, and M. Toharia. Higgs Phenomenology in Warped Extra-Dimensions with a 4th Generation. *Phys.Rev.*, D84:075009, 2011.
- [108] M. Frank, B. Korutlu, and M. Toharia. Radion Phenomenology with 3 and 4 Generations. *Phys.Rev.*, D84:115020, 2011.
- [109] M. Frank, B. Korutlu, and M. Toharia. Saving the fourth generation Higgs with radion mixing. *Phys.Rev.*, D85:115025, 2012.
- [110] H-S. Lee, Z. Liu, and A. Soni. Neutrino dark matter candidate in fourth generation scenarios. *Phys.Lett.*, B704:30–35, 2011.

- [111] K. Agashe, K. Blum, S. J. Lee, and G. Perez. Astrophysical Implications of a Visible Dark Matter Sector from a Custodially Warped-GUT. *Phys.Rev.*, D81:075012, 2010.
- [112] M. Gell-Mann. Isotopic Spin and New Unstable Particles. *Phys.Rev.*, 92:833–834, 1953.
- [113] T. Nakano and K. Nishijima. Charge Independence for V-particles. *Prog.Theor.Phys.*, 10:581–582, 1953.
- [114] K. Nakamura et al. Review of particle physics. *J.Phys.G*, G37:075021, 2010.
- [115] E. Fermi. An attempt of a theory of beta radiation. 1. *Z.Phys.*, 88:161–177, 1934.
- [116] L. Wolfenstein. Parametrization of the Kobayashi-Maskawa Matrix. *Phys.Rev.Lett.*, 51:1945, 1983.
- [117] M. Bona et al. The 2004 UTfit collaboration report on the status of the unitarity triangle in the standard model. *JHEP*, 0507:028, 2005.
- [118] M. Bona et al. Model-independent constraints on $\Delta F=2$ operators and the scale of new physics. *JHEP*, 0803:049, 2008.
- [119] F. Abe et al. Observation of top quark production in proton anti-proton collisions. *Phys.Rev.Lett.*, 74:2626–2631, 1995.
- [120] S. Abachi et al. Observation of the top quark. *Phys.Rev.Lett.*, 74:2632–2637, 1995.
- [121] F. J. Hasert, H. Faissner, W. Krenz, J. Von Krough, D. Lanske, et al. Search for Elastic Muon-Neutrino Electron Scattering. *Phys.Lett.*, B46:121–124, 1973.
- [122] F. J. Hasert et al. Observation of Neutrino Like Interactions Without Muon Or Electron in the Gargamelle Neutrino Experiment. *Phys.Lett.*, B46:138–140, 1973.
- [123] D. Haidt. The discovery of the weak neutral currents. *CERN Cour.*, 44N8:21–24, 2004.

- [124] G. Arnison et al. Recent Results on Intermediate Vector Boson Properties at the CERN Super Proton Synchrotron Collider. *Phys.Lett.*, B166:484–490, 1986.
- [125] R. Ansari et al. Measurement of the Standard Model Parameters from a Study of W and Z Bosons. *Phys.Lett.*, B186:440–451, 1987.
- [126] R. Barate et al. Search for the standard model Higgs boson at LEP. *Phys.Lett.*, B565:61–75, 2003.
- [127] Combined CDF and D0 Upper Limits on Standard Model Higgs Boson Production with up to 8.6 fb^{-1} of Data. hep-ex:1107.5518, 2011.
- [128] T. D. Lee and C-N. Yang. Question of Parity Conservation in Weak Interactions. *Phys.Rev.*, 104:254–258, 1956.
- [129] C. S. Wu, E. Ambler, R. W. Hayward, D. D. Hoppes, and R. P. Hudson. Experimental Test of Parity Conservation in Beta Decay. *Phys.Rev.*, 105:1413–1414, 1957.
- [130] S. Chatrchyan et al. Search for a light charged Higgs boson in top quark decays in pp collisions at $\sqrt{s} = 7 \text{ TeV}$. *JHEP*, 1207:143, 2012.
- [131] ATLAS Collaboration et al. Search for a fermiophobic Higgs boson in the diphoton decay channel with the ATLAS detector. hep-ex/1205.0701, 2012.
- [132] G. Aad et al. Search for charged Higgs bosons decaying via $H^+ \rightarrow \text{tau nu}$ in top quark pair events using pp collision data at $\sqrt{s} = 7 \text{ TeV}$ with the ATLAS detector. *JHEP*, 1206:039, 2012.
- [133] P. Langacker. Bounds on Mixing Between Light and Heavy Gauge Bosons. *Phys.Rev.*, D30:2008, 1984.
- [134] P. Ramond. Dual Theory for Free Fermions. *Phys.Rev.*, D3:2415–2418, 1971.
- [135] A. Neveu and J. H. Schwarz. Factorizable dual model of pions. *Nucl.Phys.*, B31:86–112, 1971.
- [136] J-L. Gervais and B. Sakita. Field Theory Interpretation of Supergauges in dual Models. *Nucl.Phys.*, B34:632–639, 1971.

- [137] M. Kobayashi and T. Maskawa. CP Violation in the Renormalizable Theory of Weak Interaction. *Prog.Theor.Phys.*, 49:652–657, 1973.
- [138] J. H. Christenson, J. W. Cronin, V. L. Fitch, and R. Turlay. Evidence for the 2π Decay of the K_2^0 Meson. *Phys.Rev.Lett.*, 13:138–140, 1964.
- [139] G. Goldhaber, F. Pierre, G. S. Abrams, M. S. Alam, A. Boyarski, et al. Observation in e^+e^- Annihilation of a Narrow State at 1865-MeV/ c^2 Decaying to $K\pi$ and $K\pi\pi\pi$. *Phys.Rev.Lett.*, 37:255–259, 1976.
- [140] S. W. Herb, D. C. Hom, L. M. Lederman, J. C. Sens, H. D. Snyder, et al. Observation of a Dimuon Resonance at 9.5 GeV in 400 GeV Proton-Nucleus Collisions. *Phys.Rev.Lett.*, 39:252–255, 1977.
- [141] C. Berger et al. Observation of a Narrow Resonance Formed in e^+e^- Annihilation at 9.46-GeV. *Phys.Lett.*, B76:243–245, 1978.
- [142] C. S. Kim and A. S. Dighe. Tree FCNC and non-unitarity of CKM matrix. *Int.J.Mod.Phys.*, E16:1445–1461, 2007.
- [143] A. K. Alok, A. Dighe, and S. Ray. CP asymmetry in the decays $B \rightarrow (X(s), X(d))\mu^+\mu^-$ with four generations. *Phys.Rev.*, D79:034017, 2009.
- [144] A. K. Alok, A. Dighe, and D. London. Constraints on the Four-Generation Quark Mixing Matrix from a Fit to Flavor-Physics Data. *Phys.Rev.*, D83:073008, 2011.
- [145] W-S. Hou, M. Nagashima, and A. Soddu. Enhanced $K_L \rightarrow \pi^0\nu\bar{\nu}$ from direct CP violation in $B \rightarrow K\pi$ with four generations. *Phys.Rev.*, D72:115007, 2005.
- [146] W-S. Hou, M. Nagashima, and A. Soddu. Large time-dependent CP violation in B_s^0 system and finite $D^0 - \bar{D}^0$ mass difference in four generation standard model. *Phys.Rev.*, D76:016004, 2007.
- [147] A. Soni, A. K. Alok, A. Giri, R. Mohanta, and S. Nandi. The Fourth family: A Natural explanation for the observed pattern of anomalies in $B - CP$ asymmetries. *Phys.Lett.*, B683:302–305, 2010.

- [148] A. Soni, A. K. Alok, A. Giri, R. Mohanta, and S. Nandi. SM with four generations: Selected implications for rare B and K decays. *Phys.Rev.*, D82:033009, 2010.
- [149] A. J. Buras, B. Duling, T. Feldmann, T. Heidsieck, C. Promberger, et al. Patterns of Flavour Violation in the Presence of a Fourth Generation of Quarks and Leptons. *JHEP*, 1009:106, 2010.
- [150] W-S. Hou and C-Y. Ma. Flavor and CP Violation with Fourth Generations Revisited. *Phys.Rev.*, D82:036002, 2010.
- [151] O. Eberhardt, A. Lenz, and J. Rohrwild. Less space for a new family of fermions. *Phys.Rev.*, D82:095006, 2010.
- [152] M. Maltoni, V. A. Novikov, L. B. Okun, A. N. Rozanov, and M.I. Vysotsky. Extra quark lepton generations and precision measurements. *Phys.Lett.*, B476:107–115, 2000.
- [153] H-J. He, N. Polonsky, and S-f. Su. Extra families, Higgs spectrum and oblique corrections. *Phys.Rev.*, D64:053004, 2001.
- [154] N. J. Evans. Additional fermion families and precision electroweak data. *Phys.Lett.*, B340:81–85, 1994.
- [155] V. A. Novikov, L. B. Okun, A. N. Rozanov, and M. I. Vysotsky. Extra generations and discrepancies of electroweak precision data. *Phys.Lett.*, B529:111–116, 2002.
- [156] G. D. Kribs, T. Plehn, M. Spannowsky, and T. M. P. Tait. Four generations and Higgs physics. *Phys.Rev.*, D76:075016, 2007.
- [157] J. Erler and P. Langacker. Precision Constraints on Extra Fermion Generations. *Phys.Rev.Lett.*, 105:031801, 2010.
- [158] S. Chatrchyan et al. Search for heavy, top-like quark pair production in the dilepton final state in pp collisions at $\sqrt{s} = 7$ TeV. *Phys.Lett.*, B716:103–121, 2012.

- [159] S. Chatrchyan et al. Search for heavy bottom-like quarks in 4.9 inverse femtobarns of pp collisions at $\sqrt{s} = 7$ TeV. *JHEP*, 1205:123, 2012.
- [160] G. Aad et al. Search for down-type fourth generation quarks with the ATLAS detector in events with one lepton and hadronically decaying W bosons. *Phys.Rev.Lett.*, 109:032001, 2012.
- [161] G. Aad et al. Search for same-sign top-quark production and fourth-generation down-type quarks in pp collisions at $\sqrt{s} = 7$ TeV with the ATLAS detector. *JHEP*, 1204:069, 2012.
- [162] G. Aad et al. Limits on the production of the Standard Model Higgs Boson in pp collisions at $\sqrt{s} = 7$ TeV with the ATLAS detector. *Eur.Phys.J.*, C71:1728, 2011.
- [163] ATLAS Collaboration et. al. Update of the combination of higgs boson searches in pp collisions at $\sqrt{s} = 7$ tev with the atlas experiment at the lhc. Technical Report ATLAS-CONF-2011-135, CERN, Geneva, Sep 2011.
- [164] CMS Collaboration et. al. Combination of sm, sm4, fp higgs boson searches. Technical Report CMS-PAS-HIG-12-008, CERN, Geneva.
- [165] E. Kuflik, Y. Nir, and T. Volansky. Implications of Higgs Searches on the Four Generation Standard Model. 2012.
- [166] O. Eberhardt, G. Herbert, H. Lacker, A. Lenz, A. Menzel, et al. Joint analysis of Higgs decays and electroweak precision observables in the Standard Model with a sequential fourth generation. 2012.
- [167] A. Djouadi and A. Lenz. Sealing the fate of a fourth generation of fermions. *Phys.Lett.*, B715:310–314, 2012.
- [168] T. Aaltonen et al. Combined Tevatron upper limit on $gg \rightarrow H \rightarrow W^+W^-$ and constraints on the Higgs boson mass in fourth-generation fermion models. *Phys.Rev.*, D82:011102, 2010.
- [169] G. Passarino, C. Sturm, and S. Uccirati. Complete Electroweak Corrections to Higgs production in a Standard Model with four generations at the LHC. *Phys.Lett.*, B706:195–199, 2011.

- [170] S. Actis, G. Passarino, C. Sturm, and S. Uccirati. NNLO Computational Techniques: The Cases $H \rightarrow \gamma\gamma$ and $H \rightarrow gg$. *Nucl.Phys.*, B811:182–273, 2009.
- [171] S. Actis, G. Passarino, C. Sturm, and S. Uccirati. NLO Electroweak Corrections to Higgs Boson Production at Hadron Colliders. *Phys.Lett.*, B670:12–17, 2008.
- [172] A. Denner, S. Dittmaier, A. Muck, G. Passarino, M. Spira, et al. Higgs production and decay with a fourth Standard-Model-like fermion generation. *Eur.Phys.J.*, C72:1992, 2012.
- [173] S. J. Huber and Q. Shafi. Fermion masses, mixings and proton decay in a Randall-Sundrum model. *Phys.Lett.*, B498:256–262, 2001.
- [174] A. Azatov, M. Toharia, and L. Zhu. Radion Mediated Flavor Changing Neutral Currents. *Phys.Rev.*, D80:031701, 2009.
- [175] K. Agashe and R. Contino. Composite Higgs-Mediated FCNC. *Phys.Rev.*, D80:075016, 2009.
- [176] W. Buchmuller and D. Wyler. Effective Lagrangian Analysis of New Interactions and Flavor Conservation. *Nucl.Phys.*, B268:621, 1986.
- [177] F. del Aguila, M. Perez-Victoria, and J. Santiago. Effective description of quark mixing. *Phys.Lett.*, B492:98–106, 2000.
- [178] K. S. Babu and S. Nandi. Natural fermion mass hierarchy and new signals for the Higgs boson. *Phys.Rev.*, D62:033002, 2000.
- [179] G. F. Giudice and O. Lebedev. Higgs-dependent Yukawa couplings. *Phys.Lett.*, B665:79–85, 2008.
- [180] C. Csaki, C. Grojean, J. Hubisz, Y. Shirman, and J. Terning. Fermions on an interval: Quark and lepton masses without a Higgs. *Phys.Rev.*, D70:015012, 2004.
- [181] A. Azatov, M. Toharia, and L. Zhu. Higgs Mediated FCNC's in Warped Extra Dimensions. *Phys.Rev.*, D80:035016, 2009.

- [182] R. Kuchimanchi and R. N. Mohapatra. No parity violation without R-parity violation. *Phys.Rev.*, D48:4352–4360, 1993.
- [183] C. S. Aulakh, A. Melfo, and G. Senjanovic. Minimal supersymmetric left-right model. *Phys.Rev.*, D57:4174–4178, 1998.
- [184] Z. Chacko and R. N. Mohapatra. Supersymmetric left-right model and light doubly charged Higgs bosons and Higgsinos. *Phys.Rev.*, D58:015003, 1998.
- [185] K. S. Babu and R. N. Mohapatra. Minimal Supersymmetric Left-Right Model. *Phys.Lett.*, B668:404–409, 2008.
- [186] C. S. Aulakh, A. Melfo, A. Rasin, and G. Senjanovic. Supersymmetry and large scale left-right symmetry. *Phys.Rev.*, D58:115007, 1998.
- [187] K. Huitu and J. Maalampi. The Higgs sector of a supersymmetric left-right model. *Phys.Lett.*, B344:217–224, 1995.
- [188] M. E. Pospelov. FCNC in left-right symmetric theories and constraints on the right-handed scale. *Phys.Rev.*, D56:259–264, 1997.
- [189] M. Bona et al. Status of the unitarity triangle analysis. *PoS*, EPS-HEP2009:160, 2009.
- [190] A. J. Buras. Weak Hamiltonian, CP violation and rare decays. hep-ph/9806471:281–539, 1998.
- [191] A. J. Buras, S. Jager, and J. Urban. Master formulae for $\Delta F = 2$ NLO QCD factors in the standard model and beyond. *Nucl.Phys.*, B605:600–624, 2001.
- [192] T. Aaltonen et al. Combined CDF and D0 Upper Limits on Standard Model Higgs Boson Production with up to 8.2 fb^{-1} of Data. hep-ex/1103.3233, 2011.
- [193] S. Chatrchyan et al. Measurement of W^+W^- Production and Search for the Higgs Boson in pp Collisions at $\sqrt{s} = 7 \text{ TeV}$. *Phys.Lett.*, B699:25–47, 2011.
- [194] S. P. Martin and M. T. Vaughn. Two loop renormalization group equations for soft supersymmetry breaking couplings. *Phys.Rev.*, D50:2282, 1994.

- [195] N. Setzer and S. Spinner. One-loop RGEs for two left-right SUSY models. *Phys.Rev.*, D71:115010, 2005.
- [196] A. Ferrari, C. Collot, M-L. Andrieux, B. Belhorma, P. de Saintignon, et al. Sensitivity study for new gauge bosons and right-handed Majorana neutrinos in pp collisions at $s = 14$ -TeV. *Phys.Rev.*, D62:013001, 2000.
- [197] S. Casagrande, F. Goertz, U. Haisch, M. Neubert, and T. Pfoh. The Custodial Randall-Sundrum Model: From Precision Tests to Higgs Physics. *JHEP*, 1009:014, 2010.
- [198] A. Azatov, M. Toharia, and L. Zhu. Higgs Production from Gluon Fusion in Warped Extra Dimensions. *Phys.Rev.*, D82:056004, 2010.
- [199] S. Casagrande, F. Goertz, U. Haisch, M. Neubert, and T. Pfoh. Flavor Physics in the Randall-Sundrum Model: I. Theoretical Setup and Electroweak Precision Tests. *JHEP*, 0810:094, 2008.
- [200] T. P. Cheng and M. Sher. Mass Matrix Ansatz and Flavor Nonconservation in Models with Multiple Higgs Doublets. *Phys.Rev.*, D35:3484, 1987.
- [201] G. Perez and L. Randall. Natural Neutrino Masses and Mixings from Warped Geometry. *JHEP*, 0901:077, 2009.
- [202] K. Agashe. Relaxing Constraints from Lepton Flavor Violation in 5D Flavorful Theories. *Phys.Rev.*, D80:115020, 2009.
- [203] S. Nandi and A. Soni. Constraining the mixing matrix for Standard Model with four generations: time dependent and semi-leptonic CP asymmetries in B_d^0 , B_s and D^0 . *Phys.Rev.*, D83:114510, 2011.
- [204] C. Csaki, Y. Grossman, P. Tanedo, and Y. Tsai. Warped penguin diagrams. *Phys.Rev.*, D83:073002, 2011.
- [205] T. Hahn. Feynman Diagram Calculations with FeynArts, FormCalc, and LoopTools. *PoS*, ACAT2010:078, 2010.
- [206] S. Bar-Shalom, S. Nandi, and A. Soni. Two Higgs doublets with 4th generation fermions - models for TeV-scale compositeness. *Phys.Rev.*, D84:053009, 2011.

- [207] G. Eilam, J. L. Hewett, and A. Soni. Rare decays of the top quark in the standard and two Higgs doublet models. *Phys.Rev.*, D44:1473–1484, 1991.
- [208] J. F. Gunion. Ruling out a 4th generation using limits on hadron collider Higgs signals. hep-ph/1105.3965, 2011.
- [209] D. Benjamin. Combined CDF and D0 upper limits on $gg \rightarrow H \rightarrow W^+W^-$ and constraints on the Higgs boson mass in fourth-generation fermion models with up to 8.2 fb^{-1} of data. hep-ex/1108.3331, 2011.
- [210] L. M. Carpenter, A. Rajaraman, and D. Whiteson. Searches for Fourth Generation Charged Leptons. hep-ph/1010.1011, 2010.
- [211] K. Agashe, C. Csaki, C. Grojean, and M. Reece. The S-parameter in holographic technicolor models. *JHEP*, 0712:003, 2007.
- [212] D. Krohn, T. Liu, J. Shelton, and L-T. Wang. A Polarized View of the Top Asymmetry. *Phys.Rev.*, D84:074034, 2011.
- [213] M. Cacciari, S. Frixione, M. L. Mangano, P. Nason, and G. Ridolfi. Updated predictions for the total production cross sections of top and of heavier quark pairs at the Tevatron and at the LHC. *JHEP*, 0809:127, 2008.
- [214] D. Atwood, S. K. Gupta, and A. Soni. Detecting Fourth Generation Quarks at Hadron Colliders. *JHEP*, 1206:105, 2012.
- [215] C. Csaki, J. Hubisz, and S. J. Lee. Radion phenomenology in realistic warped space models. *Phys.Rev.*, D76:125015, 2007.
- [216] S. Bae, P. Ko, H. S. Lee, and J. Lee. Phenomenology of the radion in Randall-Sundrum scenario at colliders. *Phys.Lett.*, B487:299–305, 2000.
- [217] K-M. Cheung. Phenomenology of radion in Randall-Sundrum scenario. *Phys.Rev.*, D63:056007, 2001.
- [218] K. Huitu, S. Khalil, A. Moursy, S. K. Rai, and A. Sabanci. Radion Flavor Violation in Warped Extra Dimension. *Phys.Rev.*, D85:016005, 2012.

- [219] W. D. Goldberger, B. Grinstein, and W. Skiba. Distinguishing the Higgs boson from the dilaton at the Large Hadron Collider. *Phys.Rev.Lett.*, 100:111802, 2008.
- [220] H. Davoudiasl and E. Ponton. B-Decay Signatures of Warped Top-Condensation. *Phys.Lett.*, B680:247–250, 2009.
- [221] G. Aad et al. Combined search for the Standard Model Higgs boson using up to 4.9 fb⁻¹ of pp collision data at sqrt(s) = 7 TeV with the ATLAS detector at the LHC. *Phys.Lett.*, B710:49–66, 2012.
- [222] S. Chatrchyan et al. Combined results of searches for the standard model Higgs boson in pp collisions at sqrt(s) = 7 TeV. *Phys.Lett.*, B710:26–48, 2012.
- [223] Combined CDF and D0 Search for Standard Model Higgs Boson Production with up to 10.0 fb⁻¹ of Data. hep-ex/1203.3774, 2012.
- [224] G. Couture, C. Hamzaoui, S. S. Y. Lu, and M. Toharia. Patterns in the Fermion Mixing Matrix, a bottom-up approach. *Phys.Rev.*, D81:033010, 2010.

Appendix A

Notations and Conventions

We will specify the notations and conventions that we use throughout the thesis.

- **Indices:** $(i, j, k = 1, \dots, 3)$ are three-vector indices, $(\mu, \nu, \rho, \sigma = 1, \dots, 4)$ are Lorentz indices, and $(M, N, R, S = 1, \dots, 5)$ are 5D indices. For three-vectors we do not distinguish between upper and lower indices.
- **Units and Physical Constants:** $\hbar = c = 1$, implying that $E, p, m, \frac{1}{x}, \frac{1}{t}$ have energy units.
- **Flat Space-Time Metric Tensor:** We use the mostly minus convention such that

$$\eta_{\mu\nu} = \eta^{\mu\nu} = \begin{pmatrix} 1 & 0 & 0 & 0 \\ 0 & -1 & 0 & 0 \\ 0 & 0 & -1 & 0 \\ 0 & 0 & 0 & -1 \end{pmatrix}. \quad (\text{A-1})$$

- **Four-Vector Notation:**

Position Vector: $x^\mu = (t, \vec{x}), \quad x_\mu = (t, -\vec{x}),$

Momentum Vector: $p^\mu = (E, \vec{p}), \quad p_\mu = (E, -\vec{p}),$

Derivatives: $\partial^\mu = \frac{\partial}{\partial x^\mu} = \left(\frac{\partial}{\partial t}, \vec{\nabla} \right), \quad \partial_\mu = \frac{\partial}{\partial x_\mu} = \left(\frac{\partial}{\partial t}, -\vec{\nabla} \right),$

$$\square \equiv \partial_\mu \partial^\mu = \frac{\partial^2}{\partial t^2} - \vec{\nabla}^2.$$

- **Pauli Matrices:** The 2×2 Pauli matrices $\vec{\sigma} = (\sigma_1, \sigma_2, \sigma_3)$ (for internal

symmetries denoted by $\vec{\tau}$) are defined by

$$[\sigma_i, \sigma_j] = 2i\epsilon_{ijk}\sigma_k. \quad (\text{A-2})$$

A convenient representation satisfying eq. (A-2) is

$$\sigma_1 = \begin{pmatrix} 0 & 1 \\ 1 & 0 \end{pmatrix}, \quad \sigma_2 = \begin{pmatrix} 0 & -i \\ i & 0 \end{pmatrix}, \quad \sigma_3 = \begin{pmatrix} 1 & 0 \\ 0 & -1 \end{pmatrix}. \quad (\text{A-3})$$

A-1 Dirac Matrices and Spinors

The Dirac Matrices γ^μ are defined by

$$\{\gamma^\mu, \gamma^\nu\} = 2g^{\mu\nu}I, \quad (\text{A-4})$$

where I is an identity matrix. It is also useful to define

$$\sigma^{\mu\nu} = \frac{i}{2}[\gamma^\mu, \gamma^\nu], \quad \gamma^5 = \gamma_5 \equiv i\gamma^0\gamma^1\gamma^2\gamma^3. \quad (\text{A-5})$$

The γ^5 matrix enters for spin and chirality projections of fermions. In the following two subsections we will give two different representation of Dirac Matrices and spinors satisfying eq. (A-4). The projection operator are given as

$$P_L = \frac{1 - \gamma^5}{2} = \begin{pmatrix} I & 0 \\ 0 & 0 \end{pmatrix}, \quad P_R = \frac{1 + \gamma^5}{2} = \begin{pmatrix} 0 & 0 \\ 0 & I \end{pmatrix} \quad (\text{A-6})$$

Note also that $P_{L,R}^2 = P_{L,R}$, $P_L P_R = 0$, $P_{L,R}^\dagger = P_{L,R}$ and $P_{L,R}^T = P_{L,R}$.

A-1.1 Pauli-Dirac Representation

Pauli-Dirac Representation is useful for studying non-relativistic limit of an interaction.

- **Dirac Matrices:**

$$\gamma^0 = \begin{pmatrix} I & 0 \\ 0 & -I \end{pmatrix}, \quad \gamma^i = \begin{pmatrix} 0 & \sigma^i \\ -\sigma^i & 0 \end{pmatrix}, \quad \gamma^5 = \begin{pmatrix} 0 & I \\ I & 0 \end{pmatrix}, \quad (\text{A-7})$$

where I is the 2×2 identity matrix and σ^i are the Pauli matrices given in eq. (A-3)

$$\sigma^{0i} = i \begin{pmatrix} 0 & \sigma^i \\ \sigma^i & 0 \end{pmatrix}, \quad \sigma^{ij} = \epsilon^{ijk} \begin{pmatrix} \sigma^k & 0 \\ 0 & \sigma^k \end{pmatrix}. \quad (\text{A-8})$$

- **Fermion Fields:** Fermion fields and the adjoint fields are represented by four-component column vectors and four-component row vectors, respectively.

$$\begin{aligned}\psi &= \begin{pmatrix} \Psi_L \\ \Psi_R \end{pmatrix}, \\ \bar{\psi} &= \psi^\dagger \gamma^0 = \begin{pmatrix} \Psi_L^\dagger & \Psi_R^\dagger \end{pmatrix} \begin{pmatrix} I & 0 \\ 0 & -I \end{pmatrix} = \begin{pmatrix} \Psi_L^\dagger & -\Psi_R^\dagger \end{pmatrix},\end{aligned}\quad (\text{A-9})$$

where both $\Psi_{L,R}$ are 2×1 column vectors. For a fermion field one can define the left- (L) and right- (R) chiral projections as

$$\begin{aligned}\psi_L &= P_L \psi = \begin{pmatrix} I & 0 \\ 0 & 0 \end{pmatrix} \begin{pmatrix} \Psi_L \\ \Psi_R \end{pmatrix} = \begin{pmatrix} \Psi_L \\ 0 \end{pmatrix}, \\ \psi_R &= P_R \psi = \begin{pmatrix} 0 & 0 \\ 0 & I \end{pmatrix} \begin{pmatrix} \Psi_L \\ \Psi_R \end{pmatrix} = \begin{pmatrix} 0 \\ \Psi_R \end{pmatrix},\end{aligned}\quad (\text{A-10})$$

where ψ_L and ψ_R can be considered as independent degrees of freedom of ψ . Let us also define $\bar{\psi}_{L,R}$ as projection of $\bar{\psi}$

$$\begin{aligned}\bar{\psi}_L &= \psi_L^\dagger \gamma^0 = (P_L \psi)^\dagger \gamma^0 = \psi^\dagger P_L \gamma^0 = \psi^\dagger \gamma^0 P_R = \bar{\psi} P_R, \\ \bar{\psi}_R &= \bar{\psi} P_L.\end{aligned}\quad (\text{A-11})$$

- **Charge Conjugation:** Charge conjugation changes a particle into the corresponding antiparticle without affecting its spin or momenta. We will denote the antiparticles with a superscript c.

$$\begin{aligned}\psi^c &= C \bar{\psi}^T = C (\psi^\dagger \gamma^0)^T = C \gamma^{0T} \psi^{\dagger T}, \\ \bar{\psi}^c &= \psi^{c\dagger} \gamma^0 = (C \gamma^{0T} \psi^{\dagger T})^\dagger \gamma^0 = \psi^T \gamma^0 C^\dagger \gamma^0 = \psi^T C = -\psi^T C^{-1},\end{aligned}\quad (\text{A-12})$$

where

$$C = -C^{-1} = -C^\dagger = -C^T = i\gamma^2 \gamma^0 = \begin{pmatrix} 0 & -i\sigma^2 \\ -i\sigma^2 & 0 \end{pmatrix}.\quad (\text{A-13})$$

In explicit form we can write

$$\begin{aligned}\psi^c &= \begin{pmatrix} \Psi_L^c \\ \Psi_R^c \end{pmatrix} = \begin{pmatrix} 0 & -i\sigma^2 \\ -i\sigma^2 & 0 \end{pmatrix} \begin{pmatrix} I & 0 \\ 0 & -I \end{pmatrix} \begin{pmatrix} \Psi_L^* \\ \Psi_R^* \end{pmatrix} = \begin{pmatrix} i\sigma^2 \Psi_R^* \\ -i\sigma^2 \Psi_L^* \end{pmatrix}, \\ \bar{\psi}^c &= \begin{pmatrix} \Psi_L^T & \Psi_R^T \end{pmatrix} \begin{pmatrix} 0 & -i\sigma^2 \\ -i\sigma^2 & 0 \end{pmatrix} = \begin{pmatrix} -i\sigma^2 \Psi_R^T & -i\sigma^2 \Psi_L^T \end{pmatrix}.\end{aligned}\quad (\text{A-14})$$

The left- and right-chiral antiparticles are obtained as follows

$$\begin{aligned}\psi_L^c &= P_L \psi^c = P_L C \bar{\psi}^T = (\bar{\psi} C^T P_L)^T = (\bar{\psi} P_L C^T)^T = (\bar{\psi}_R C^T)^T = C \bar{\psi}_R^T, \\ \psi_R^c &= C \bar{\psi}_L^T,\end{aligned}\tag{A-15}$$

where we have used eqs. (A-4) and (A-11). Note that even though ψ_L and ψ_R can be considered as independent degrees of freedom for ψ , ψ_L^c and ψ_R^c , on the other hand are not independent. One can also write $\bar{\psi}_{L,R}^c$

$$\begin{aligned}\bar{\psi}_L^c &= \psi_L^{c\dagger} \gamma^0 = (P_L C \gamma^{0T} \psi^{\dagger T})^\dagger \gamma^0 = \psi^T P_R C = (P_R \psi)^T C = \psi_R^T C = -\psi_R^T C^{-1}, \\ \bar{\psi}_R^c &= -\psi_L^T C^{-1}.\end{aligned}\tag{A-16}$$

A-1.2 Chiral Representation

- **Dirac Matrices:**

$$\gamma^0 = \begin{pmatrix} 0 & I \\ I & 0 \end{pmatrix}, \quad \gamma^i = \begin{pmatrix} 0 & \sigma^i \\ -\sigma^i & 0 \end{pmatrix}, \quad \gamma^5 = \begin{pmatrix} -I & 0 \\ 0 & I \end{pmatrix},\tag{A-17}$$

and

$$\sigma^{0i} = i \begin{pmatrix} -\sigma^i & 0 \\ 0 & \sigma^i \end{pmatrix}, \quad \sigma^{ij} = \epsilon^{ijk} \begin{pmatrix} \sigma^k & 0 \\ 0 & \sigma^k \end{pmatrix}.\tag{A-18}$$

It is sometimes more convenient to rewrite the Dirac Matrices in chiral representation as

$$\gamma^\mu = \begin{pmatrix} 0 & \sigma^\mu \\ \bar{\sigma}^\mu & 0 \end{pmatrix},\tag{A-19}$$

where $\sigma^\mu \equiv (I, \vec{\sigma})$ and $\bar{\sigma}^\mu \equiv (I, -\vec{\sigma}) = \sigma_\mu$.

- **Fermion Fields:** Fermion fields and the adjoint fields are represented by two-component column vectors and two-component row vectors, respectively.

$$\begin{aligned}\Psi_L &\quad \text{and} \quad \Psi_R \\ \Psi_L^\dagger &\quad \text{and} \quad \Psi_R^\dagger\end{aligned}\tag{A-20}$$

- **Charge Conjugation:** Charge Conjugation change a particle into the corresponding antiparticle, without affecting its spin or momenta. We will denote the antiparticles with a superscript c.

$$C = -C^{-1} = -C^\dagger = -C^T = -i\gamma^2\gamma^0 = \begin{pmatrix} -i\sigma^2 & 0 \\ 0 & i\sigma^2 \end{pmatrix},\tag{A-21}$$

which gives

$$\psi^c = \begin{pmatrix} \Psi_L^c \\ \Psi_R^c \end{pmatrix} = \begin{pmatrix} -i\sigma^2 & 0 \\ 0 & i\sigma^2 \end{pmatrix} \begin{pmatrix} 0 & I \\ I & 0 \end{pmatrix} \begin{pmatrix} \Psi_L^* \\ \Psi_R^* \end{pmatrix} = \begin{pmatrix} -i\sigma^2 \Psi_R^* \\ i\sigma^2 \Psi_L^* \end{pmatrix}. \quad (\text{A-22})$$

In many cases it is convenient to work with $\Psi_{L,R}$ fields as it is conveniently done in QED and QCD. However, sometimes it is easier to work with left-chiral fields for both the particles and antiparticles that is Ψ_L and Ψ_L^c , or equivalently one can get rid of the subscript L and write Ψ and Ψ^c by keeping in mind that they are the left-chiral fermions. This is typically done when discussing the LRSM, SUSY, LRSUSY.

Appendix B

Gauge Group and Transformations

A group G is a set of elements g_1, g_2, \dots with a map $G \times G$ into G (called as the product operation for the group and denoted by $g_1 * g_2$) with the following properties

- **Associativity:** For each $g_{1,2} \in G$, $g_1 * g_2 = g_3$ with $g_3 \in G$ (closure) and $g_1 * (g_2 * g_3) = (g_1 * g_2) * g_3$ (associative).
- **Identity Element:** There exist an identity element $I \in G$ with $I * g = g * I = g$ for all $g \in G$.
- **Inverse:** For each $g \in G$ there is a unique inverse g^{-1} such that $g * g^{-1} = g^{-1} * g = I$.

According to the commutation relations of the group elements, we can classify the groups as:

- **Abelian group:** The group is commutative such that $[g_1, g_2] = 0$ for each $g_{1,2} \in G$.
- **Non-abelian group:** The group is non-commutative: $[g_1, g_2] \neq 0$ for any $g_{1,2} \in G$.

In Field theory, to describe continuous global and gauge transformations **Lie Groups** and algebras are used. A Lie group G is a continuous group for which the multiplication law can be defined in terms of its associated Lie algebra consisting N generators $T^i, i = 1, 2, \dots, N$, and their commutation rules

$$[T^i, T^j] = \sum_k i c_{ijk} T^k, \quad (\text{B-1})$$

where $c_{ijk} = -c_{jik}$ are the structure constants of G . Without the loss of generality, T^i can be assigned to be Hermitian which give rise to real structure constants. Below we will give some examples of the Lie Groups.

- **U(1) Group:** $G = U(1)$ is the simplest example of a Lie group. It is an abelian group with a single generator T . The elements of a $U(1)$ are 1×1 dimensional unitary matrices which can be represented as

$$U_G(\beta) = e^{-i\beta T}. \quad (\text{B-2})$$

There is a special case with $T = 1$ and group elements $U_G(\beta) \rightarrow e^{-i\beta}$ as well.

- **SU(2) Group:** $G = SU(2)$ is a non-abelian group with 3 generators and the structure constants are $c_{ijk} = \epsilon_{ijk}$. Its elements are 2×2 unitary matrices with the extra constraint that their determinant is unity. The generators are $L_i = \tau^i/2$ where $\tau_i = \sigma_i$ are the Pauli matrices given in eq. (A-3). The group elements are

$$U_G(\vec{\beta}) = e^{-i\vec{\beta} \cdot \frac{\vec{\tau}}{2}} = \cos \frac{\beta}{2} \mathbf{I} - i \sin \frac{\beta}{2} \hat{\beta} \cdot \vec{\tau}. \quad (\text{B-3})$$

- **SU(3) Group:** $G = SU(3)$ is a non-abelian group with 8 generators and the structure constants are $c_{ijk} = f_{ijk}$, $i, j, k = 1, \dots, 8$. Its elements are 3×3 unitary matrices with determinant one. The generators are $L_i^3 = \lambda_i/2$ where λ_i , $i = 1, \dots, 8$ are Gell-Mann Matrices given as

$$\begin{aligned} \lambda_1 &= \begin{pmatrix} 0 & 1 & 0 \\ 1 & 0 & 0 \\ 0 & 0 & 0 \end{pmatrix}, \quad \lambda_2 = \begin{pmatrix} 0 & -i & 0 \\ i & 0 & 0 \\ 0 & 0 & 0 \end{pmatrix}, \quad \lambda_3 = \begin{pmatrix} 1 & 0 & 0 \\ 0 & -1 & 0 \\ 0 & 0 & 0 \end{pmatrix}, \\ \lambda_4 &= \begin{pmatrix} 0 & 0 & 1 \\ 0 & 0 & 0 \\ 1 & 0 & 0 \end{pmatrix}, \quad \lambda_5 = \begin{pmatrix} 0 & 0 & -i \\ 0 & 0 & 0 \\ i & 0 & 0 \end{pmatrix}, \quad \lambda_6 = \begin{pmatrix} 0 & 0 & 0 \\ 0 & 0 & 1 \\ 0 & 1 & 0 \end{pmatrix}, \\ \lambda_7 &= \begin{pmatrix} 0 & 0 & 0 \\ 0 & 0 & -i \\ 0 & i & 0 \end{pmatrix}, \quad \lambda_8 = \frac{1}{\sqrt{3}} \begin{pmatrix} 1 & 0 & 0 \\ 0 & 1 & 0 \\ 0 & 0 & -2 \end{pmatrix}, \end{aligned} \quad (\text{B-4})$$

and the nonzero totally antisymmetric structure constants f_{ijk} are

$$\begin{aligned} f_{123} &= 1, \quad f_{147} = \frac{1}{2}, \quad f_{156} = -\frac{1}{2}, \quad f_{246} = \frac{1}{2}, \quad f_{257} = \frac{1}{2}, \\ f_{345} &= \frac{1}{2}, \quad f_{367} = -\frac{1}{2}, \quad f_{678} = \frac{\sqrt{3}}{2}. \end{aligned} \quad (\text{B-5})$$

The group elements are

$$U_G(\beta_i) = e^{-\frac{i}{2}\beta_i\lambda_i} = \cos\frac{\beta}{2}\mathbf{I} - i\sin\frac{\beta}{2}\hat{\beta}_i\lambda_i. \quad (\text{B-6})$$

In modern particle theories the underlying group of the theory consists some gauge transformations under which Lagrangian remains unchanged. This is called the gauge invariance and is the origin of the forces. The gauge transformations can be divided into two:

- **Global Gauge Transformations:** The global gauge transformation (GGT) represents an identical operation at all points in space-time and causes a simple shift in the phase of a fermion wave function as follows:

$$\psi \rightarrow e^{i\theta}\psi, \quad (\text{B-7})$$

where θ is a real number. Thus, GGT is just a statement of the fact that the laws of physics are independent of the choice of phase convention.

- **Local Gauge Transformations:** The LGT corresponds to choosing a convention to define the phase of the fermion wavefunction, which is different at different points in space-time. In other words, the matter fields will be transformed differently at each space-time point. The expression for is

$$\psi \rightarrow e^{iq\theta(x)}\psi, \quad (\text{B-8})$$

where θ is a function of $x = (\mathbf{x}, t)$. Therefore, one requires a redefinition of the derivative, which compares fields at different points in space-time.

The SM, based on the gauge invariance principle with gauge group $SU(3)_c \otimes SU(2)_L \otimes U(1)_Y$, can excellently describe the three out of four fundamental forces of nature introduced in Chapter 2 by making use of global and local gauge transformations.

Appendix C

Ricci Tensor and Brane Tensions

C-1 The Components of the Ricci Tensor

Let us first write the metric given in eq. (3.83) in component form:

$$\begin{aligned} g_{\mu\nu} &= e^{-2\sigma(\phi)}\eta_{\mu\nu}, & g_{55} &= -r^2, \\ g^{\mu\nu} &= e^{2\sigma(\phi)}\eta^{\mu\nu}, & g^{55} &= -r^{-2}. \end{aligned} \quad (\text{C-1})$$

Since the metric is diagonal we have $g_{\mu 5} = g_{5\mu} = g^{\mu 5} = g^{5\mu} = 0$. We will start our calculation by 4D component of the Ricci tensor, $R_{\mu\nu}$, which can be written as

$$R_{\mu\nu} = \Gamma_{\mu\nu,K}^K - \Gamma_{\mu K,\nu}^K - \Gamma_{\mu M}^K \Gamma_{\nu K}^M - \Gamma_{\mu\nu}^K \Gamma_{KM}^M, \quad (\text{C-2})$$

using the eq. (3.86). Let us analyze this term by term. The first term is derived as follows

$$\begin{aligned} \Gamma_{\mu\nu,K}^K &= \{g^{KL}\Gamma_{L\mu\nu}\}_{,K} \\ &= \frac{1}{2}\{g^{KL}[g_{L\mu,\nu} + g_{L\nu,\mu} - g_{\mu\nu,L}]\}_{,K} \\ &= \frac{1}{2}\{g^{K\rho}[g_{\rho\mu,\nu} + g_{\rho\nu,\mu} - g_{\mu\nu,\rho}] + g^{K5}[-g_{\mu\nu,5}]\}_{,K} \\ &= \frac{1}{2}\{g^{\xi\rho}[g_{\rho\mu,\nu} + g_{\rho\nu,\mu} - g_{\mu\nu,\rho}]\}_{,\xi} + \frac{1}{2}\{g^{55}[-g_{\mu\nu,5}]\}_{,5} \\ &= \frac{1}{2}\{(-r^{-2})(-e^{-2\sigma(\phi)}\eta_{\mu\nu})_{,5}\}_{,5} \\ &= \frac{1}{2r^2}\{(-2)\sigma'(\phi)e^{-2\sigma(\phi)}\eta_{\mu\nu}\}_{,5} \end{aligned}$$

$$\begin{aligned}
&= \frac{-1}{r^2} \{ \sigma''(\phi) e^{-2\sigma(\phi)} + \sigma'(\phi) (-2) \sigma'(\phi) e^{-2\sigma(\phi)} \} \eta_{\mu\nu} \\
&= \frac{e^{-2\sigma(\phi)}}{r^2} \{ -\sigma''(\phi) + 2[\sigma'(\phi)]^2 \} \eta_{\mu\nu}.
\end{aligned} \tag{C-3}$$

where we have used the fact that $\sigma = \sigma(\phi)$. Therefore, the derivative of it with respect to 4D space-time ($g_{\mu\nu,\rho}$) vanishes, whereas the derivative with respect to the 5th dimension ($g_{\mu\nu,5}$) survives. In addition, the size of the fifth dimension, r , is a constant, as a result, the derivatives $g_{55,K} = 0$. Keeping these information in mind, we will now calculate the second term in $R_{\mu\nu}$:

$$\begin{aligned}
\Gamma_{\mu K, \nu}^K &= \{ g^{KL} \Gamma_{L\mu K} \}_{, \nu} \\
&= \frac{1}{2} \{ g^{KL} [g_{L\mu, K} + g_{LK, \mu} - g_{\mu K, L}] \}_{, \nu} \\
&= \frac{1}{2} \{ g^{K\rho} [g_{\rho\mu, K} + g_{\rho K, \mu} - g_{\mu K, \rho}] + g^{K5} [g_{5K, \mu} - g_{\mu K, 5}] \}_{, \nu} \\
&= \frac{1}{2} \{ g^{\xi\rho} [g_{\rho\mu, \xi} + g_{\rho\xi, \mu} - g_{\mu\xi, \rho}] + g^{55} [g_{55, \mu}] \}_{, \nu} \\
&= 0,
\end{aligned} \tag{C-4}$$

The third term is calculated as

$$\begin{aligned}
\Gamma_{\mu M}^K \Gamma_{\nu K}^M &= g^{KL} \Gamma_{L\mu M} g^{MS} \Gamma_{S\nu K} \\
&= \frac{1}{2} g^{KL} [g_{L\mu, M} + g_{LM, \mu} - g_{\mu M, L}] \frac{1}{2} g^{MS} [g_{S\nu, K} + g_{SK, \nu} - g_{\nu K, S}] \\
&= \frac{1}{4} g^{K\rho} [g_{\rho\mu, M} + g_{\rho M, \mu} - g_{\mu M, \rho}] g^{MS} [g_{S\nu, K} + g_{SK, \nu} - g_{\nu K, S}] \\
&+ \frac{1}{4} g^{K5} [g_{5M, \mu} - g_{\mu M, 5}] g^{MS} [g_{S\nu, K} + g_{SK, \nu} - g_{\nu K, S}] \\
&= \frac{1}{4} g^{\xi\rho} [g_{\rho\mu, M} + g_{\rho M, \mu} - g_{\mu M, \rho}] g^{MS} [g_{S\nu, \xi} + g_{S\xi, \nu} - g_{\nu\xi, S}] \\
&+ \frac{1}{4} g^{55} [g_{5M, \mu} - g_{\mu M, 5}] g^{MS} [g_{S\nu, 5} + g_{S5, \nu}] \\
&= \frac{1}{4} g^{\xi\rho} [g_{\rho\mu, \alpha} + g_{\rho\alpha, \mu} - g_{\mu\alpha, \rho}] g^{\alpha S} [g_{S\nu, \xi} + g_{S\xi, \nu} - g_{\nu\xi, S}] \\
&+ \frac{1}{4} g^{55} [-g_{\mu\alpha, 5}] g^{\alpha S} [g_{S\nu, 5} + g_{S5, \nu}] + \frac{1}{4} g^{\xi\rho} [g_{\rho\mu, 5}] g^{5S} [g_{S\nu, \xi} + g_{S\xi, \nu} - g_{\nu\xi, S}] \\
&+ \frac{1}{4} g^{55} [g_{55, \mu}] g^{5S} [g_{S\nu, 5} + g_{S5, \nu}] \\
&= \frac{1}{4} g^{\xi\rho} [g_{\rho\mu, \alpha} + g_{\rho\alpha, \mu} - g_{\mu\alpha, \rho}] g^{\alpha\beta} [g_{\beta\nu, \xi} + g_{\beta\xi, \nu} - g_{\nu\xi, \beta}] \\
&+ \frac{1}{4} g^{55} [-g_{\mu\alpha, 5}] g^{\alpha\beta} [g_{\beta\nu, 5}] + \frac{1}{4} g^{\xi\rho} [g_{\rho\mu, 5}] g^{55} [-g_{\nu\xi, 5}] + \frac{1}{4} g^{55} [g_{55, \mu}] g^{55} [g_{55, \nu}]
\end{aligned}$$

$$\begin{aligned}
&= \frac{1}{4}g^{55}[-g_{\mu\alpha,5}]g^{\alpha\beta}[g_{\beta\nu,5}] + \frac{1}{4}g^{\xi\rho}[g_{\rho\mu,5}]g^{55}[-g_{\nu\xi,5}] \\
&= \frac{1}{4}(-r^{-2})[-(e^{-2\sigma(\phi)}\eta_{\mu\alpha})_{,5}]e^{2\sigma(\phi)}\eta^{\alpha\beta}(e^{-2\sigma(\phi)}\eta_{\beta\nu})_{,5} \\
&+ \frac{1}{4}e^{2\sigma(\phi)}\eta^{\xi\rho}(e^{-2\sigma(\phi)}\eta_{\rho\mu})_{,5}(-r^{-2})[-(e^{-2\sigma(\phi)}\eta_{\nu\xi})_{,5}] \\
&= \frac{1}{4r^2}(-2)\sigma'(\phi)e^{-2\sigma(\phi)}\eta_{\mu\alpha}e^{2\sigma(\phi)}\eta^{\alpha\beta}(-2)\sigma'(\phi)e^{-2\sigma(\phi)}\eta_{\beta\nu} \\
&+ \frac{1}{4r^2}e^{2\sigma(\phi)}\eta^{\xi\rho}(-2)\sigma'(\phi)e^{-2\sigma(\phi)}\eta_{\rho\mu}(-2)\sigma'(\phi)e^{-2\sigma(\phi)}\eta_{\nu\xi} \\
&= \frac{2e^{-2\sigma(\phi)}}{r^2}[\sigma'(\phi)]^2\eta_{\mu\nu}. \tag{C-5}
\end{aligned}$$

where we have used $\eta_{\mu\alpha}\eta^{\alpha\nu} = \eta_{\mu}^{\nu}$ and $\eta_{\alpha\beta}\eta^{\alpha\beta} = 4$ to simplify the result. There remains only the last term in $R_{\mu\nu}$ which one can simply obtain as

$$\begin{aligned}
\Gamma_{\mu\nu}^K\Gamma_{KM}^M &= g^{KL}\Gamma_{L\mu\nu}g^{MS}\Gamma_{SKM} \\
&= \frac{1}{2}g^{KL}[g_{L\mu,\nu} + g_{L\nu,\mu} - g_{\mu\nu,L}]\frac{1}{2}g^{MS}[g_{SK,M} + g_{SM,K} - g_{KM,S}] \\
&= \frac{1}{4}g^{K\rho}[g_{\rho\mu,\nu} + g_{\rho\nu,\mu} - g_{\mu\nu,\rho}]g^{MS}[g_{SK,M} + g_{SM,K} - g_{KM,S}] \\
&+ \frac{1}{4}g^{K5}[-g_{\mu\nu,5}]g^{MS}[g_{SK,M} + g_{SM,K} - g_{KM,S}] \\
&= \frac{1}{4}g^{\xi\rho}[g_{\rho\mu,\nu} + g_{\rho\nu,\mu} - g_{\mu\nu,\rho}]g^{MS}[g_{S\xi,M} + g_{SM,\xi} - g_{\xi M,S}] \\
&+ \frac{1}{4}g^{55}[-g_{\mu\nu,5}]g^{MS}[g_{S5,M} + g_{SM,5} - g_{5M,S}] \\
&= \frac{1}{4}g^{\xi\rho}[g_{\rho\mu,\nu} + g_{\rho\nu,\mu} - g_{\mu\nu,\rho}]g^{\alpha S}[g_{S\xi,\alpha} + g_{S\alpha,\xi} - g_{\xi\alpha,S}] \\
&+ \frac{1}{4}g^{55}[-g_{\mu\nu,5}]g^{\alpha S}[g_{S5,\alpha} + g_{S\alpha,5}] \\
&+ \frac{1}{4}g^{\xi\rho}[g_{\rho\mu,\nu} + g_{\rho\nu,\mu} - g_{\mu\nu,\rho}]g^{5S}[g_{S\xi,5} + g_{S5,\xi}] \\
&+ \frac{1}{4}g^{55}[-g_{\mu\nu,5}]g^{5S}[g_{S5,5} + g_{S5,5} - g_{55,S}] \\
&= \frac{1}{4}g^{\xi\rho}[g_{\rho\mu,\nu} + g_{\rho\nu,\mu} - g_{\mu\nu,\rho}]g^{\alpha\beta}[g_{\beta\xi,\alpha} + g_{\beta\alpha,\xi} - g_{\xi\alpha,\beta}] \\
&+ \frac{1}{4}g^{55}[-g_{\mu\nu,5}]g^{\alpha\beta}[g_{\beta\alpha,5}] + \frac{1}{4}g^{\xi\rho}[g_{\rho\mu,\nu} + g_{\rho\nu,\mu} - g_{\mu\nu,\rho}]g^{55}[g_{55,\xi}] \\
&+ \frac{1}{4}g^{55}[-g_{\mu\nu,5}]g^{55}[g_{55,5}] \\
&= \frac{1}{4}g^{55}[-g_{\mu\nu,5}]g^{\alpha\beta}[g_{\beta\alpha,5}] \\
&= \frac{1}{4}(-r^{-2})[-(e^{-2\sigma(\phi)}\eta_{\mu\nu})_{,5}]e^{2\sigma(\phi)}\eta^{\alpha\beta}(e^{-2\sigma(\phi)}\eta_{\beta\alpha})_{,5}
\end{aligned}$$

$$\begin{aligned}
&= \frac{1}{4r^2}(-2)\sigma'(\phi)e^{-2\sigma(\phi)}\eta_{\mu\nu}e^{2\sigma(\phi)}\eta^{\alpha\beta}(-2)\sigma'(\phi)e^{-2\sigma(\phi)}\eta_{\beta\alpha} \\
&= \frac{4e^{-2\sigma(\phi)}}{r^2}[\sigma'(\phi)]^2\eta_{\mu\nu},
\end{aligned} \tag{C-6}$$

Then, $R_{\mu\nu}$ reads

$$R_{\mu\nu} = \frac{e^{-2\sigma(\phi)}}{r^2}(4[\sigma'(\phi) - \sigma''(\phi)]^2)\eta_{\mu\nu}. \tag{C-7}$$

In the same way we will calculate R_{55} which is given as

$$R_{55} = \Gamma_{55,K}^K - \Gamma_{5K,5}^K - \Gamma_{5M}^K \Gamma_{5K}^M + \Gamma_{55}^K \Gamma_{KM}^M. \tag{C-8}$$

The first term in the curvature R_{55} is

$$\begin{aligned}
\Gamma_{55,K}^K &= \{g^{KL}\Gamma_{L55}\}_{,K} \\
&= \frac{1}{2}\{g^{KL}[g_{L5,5} + g_{L5,5} - g_{55,L}]\}_{,K} \\
&= \frac{1}{2}\{g^{K\rho}[-g_{55,\rho}] + g^{K5}[2g_{55,5} - g_{55,5}]\}_{,K} \\
&= \frac{1}{2}\{g^{\xi\rho}[-g_{55,\rho}]\}_{,\xi} + \frac{1}{2}\{g^{55}(g_{55,5})\}_{,5} \\
&= 0.
\end{aligned} \tag{C-9}$$

The second term is

$$\begin{aligned}
\Gamma_{5K,5}^K &= \{g^{KL}\Gamma_{L5K}\}_{,5} \\
&= \frac{1}{2}\{g^{KL}[g_{L5,K} + g_{LK,5} - g_{5K,L}]\}_{,5} \\
&= \frac{1}{2}\{g^{K\rho}[g_{\rho K,5} - g_{5K,\rho}] + g^{K5}[g_{55,K} + g_{5K,5} - g_{5K,5}]\}_{,5} \\
&= \frac{1}{2}\{g^{\xi\rho}[g_{\rho\xi,5}] + g^{55}[g_{55,5}]\}_{,5} \\
&= \frac{1}{2}\{e^{2\sigma(\phi)}\eta^{\xi\rho}(e^{-2\sigma(\phi)}\eta_{\rho\xi})\}_{,5,5} \\
&= \frac{1}{2}\{e^{2\sigma(\phi)}\eta^{\xi\rho}(-2)\sigma'(\phi)e^{-2\sigma(\phi)}\eta_{\rho\xi}\}_{,5} \\
&= -\{\eta^{\xi\rho}\eta_{\rho\xi}\sigma'(\phi)\}_{,5} \\
&= -4\sigma''(\phi).
\end{aligned} \tag{C-10}$$

Finally, the third and fourth terms are calculates as

$$\begin{aligned}
\Gamma_{5M}^K \Gamma_{5K}^M &= g^{KL} \Gamma_{L5M} g^{MS} \Gamma_{S5K} \\
&= \frac{1}{2} g^{KL} [g_{L5,M} + g_{LM,5} - g_{5M,L}] \frac{1}{2} g^{MS} [g_{S5,K} + g_{SK,5} - g_{5K,S}] \\
&= \frac{1}{4} g^{K\rho} [g_{\rho M,5} - g_{5M,\rho}] g^{MS} [g_{S5,K} + g_{SK,5} - g_{5K,S}] \\
&+ \frac{1}{4} g^{K5} [g_{55,M}] g^{MS} [g_{S5,K} + g_{SK,5} - g_{5K,S}] \\
&= \frac{1}{4} g^{\xi\rho} [g_{\rho M,5} - g_{5M,\rho}] g^{MS} [g_{S5,\xi} + g_{S\xi,5}] \\
&+ \frac{1}{4} g^{55} [g_{55,M}] g^{MS} [g_{S5,5} + g_{S5,5} - g_{55,S}] \\
&= \frac{1}{4} g^{\xi\rho} [g_{\rho\alpha,5}] g^{\alpha S} [g_{S5,\xi} + g_{S\xi,5} + \frac{1}{4} g^{55} [g_{55,\alpha}] g^{\alpha S} [2g_{S5,5} - g_{55,S}] \\
&+ \frac{1}{4} g^{\xi\rho} [g_{55,\rho}] g^{5S} [g_{S5,\xi} + g_{S\xi,5}] + \frac{1}{4} g^{55} [g_{55,M}] g^{5S} [2g_{S5,5} - g_{55,S}] \\
&= \frac{1}{4} g^{\xi\rho} [g_{\rho\alpha,5}] g^{\alpha\beta} [g_{\beta\xi,5}] + \frac{1}{4} g^{55} [g_{55,\alpha}] g^{\alpha\beta} [-g_{55,\beta}] \\
&+ \frac{1}{4} g^{\xi\rho} [-g_{55,\rho}] g^{55} [g_{55,\xi}] + \frac{1}{4} g^{55} [g_{55,5}] g^{55} [g_{55,5}] \\
&= \frac{1}{4} g^{\xi\rho} [g_{\rho\alpha,5}] g^{\alpha\beta} [g_{\beta\xi,5}] \\
&= \frac{1}{4} e^{2\sigma(\phi)} \eta^{\xi\rho} (e^{-2\sigma(\phi)} \eta_{\rho\alpha})_{,5} e^{2\sigma(\phi)} \eta^{\alpha\beta} (e^{-2\sigma(\phi)} \eta_{\beta\xi})_{,5} \\
&= \frac{1}{4} e^{2\sigma(\phi)} \eta^{\xi\rho} (-2) \sigma'(\phi) e^{-2\sigma(\phi)} \eta_{\rho\alpha} e^{2\sigma(\phi)} \eta^{\alpha\beta} (-2) \sigma'(\phi) e^{-2\sigma(\phi)} \eta_{\beta\xi} \\
&= 4[\sigma'(\phi)]^2, \tag{C-11}
\end{aligned}$$

and

$$\begin{aligned}
\Gamma_{55}^K \Gamma_{KM}^M &= g^{KL} \Gamma_{L55} g^{MS} \Gamma_{SKM} \\
&= \frac{1}{2} g^{KL} [g_{L5,5} + g_{L5,5} - g_{55,L}] \frac{1}{2} g^{MS} [g_{SK,M} + g_{SM,K} - g_{KM,S}] \\
&= \frac{1}{4} g^{K\rho} [-g_{55,\rho}] g^{MS} [g_{SK,M} + g_{SM,K} - g_{KM,S}] \\
&+ \frac{1}{4} g^{K5} [2g_{55,5} - g_{55,5}] g^{MS} [g_{SK,M} + g_{SM,K} - g_{KM,S}] \\
&= \frac{1}{4} g^{\xi\rho} [-g_{55,\rho}] g^{MS} [g_{S\xi,M} + g_{SM,\xi} - g_{\xi M,S}] \\
&+ \frac{1}{4} g^{55} [g_{55,5}] g^{MS} [g_{S5,M} + g_{SM,5} - g_{5M,S}]
\end{aligned}$$

$$\begin{aligned}
&= \frac{1}{4}g^{\xi\rho}[-g_{55,\rho}]g^{\alpha S}[g_{S\xi,\alpha} + g_{S\alpha,\xi} - g_{\xi\alpha,S}] + \frac{1}{4}g^{55}[g_{55,5}]g^{\alpha S}[g_{S5,\alpha} + g_{S\alpha,5}] \\
&+ \frac{1}{4}g^{\xi\rho}[-g_{55,\rho}]g^{5S}[g_{S\xi,5} + g_{S5,\xi}] + \frac{1}{4}g^{55}[g_{55,5}]g^{5S}[g_{S5,5} + g_{S5,5} - g_{55,S}] \\
&= \frac{1}{4}g^{\xi\rho}[-g_{55,\rho}]g^{\alpha\beta}[g_{\beta\xi,\alpha} + g_{\beta\alpha,\xi} - g_{\xi\alpha,\beta}] + \frac{1}{4}g^{55}[g_{55,5}]g^{\alpha\beta}[g_{\beta\alpha,5}] \\
&+ \frac{1}{4}g^{\xi\rho}[-g_{55,\rho}]g^{55}[g_{55,\xi}] + \frac{1}{4}g^{55}[g_{55,5}]g^{55}[g_{55,5}] \\
&= 0,
\end{aligned} \tag{C-12}$$

respectively. Substituting into eq. (C-8) we arrive at

$$R_{55} = 4(\sigma''(\phi) - [\sigma'(\phi)]^2). \tag{C-13}$$

The last component of the Ricci tensor is $R_{\mu 5}$. Note that it is symmetric tensor, thus $R_{\mu 5} = R_{5\mu}$. Let us calculate the curvature $R_{\mu 5}$ which one can write in terms of connection coefficients as

$$R_{\mu 5} = \Gamma_{\mu 5, K}^K - \Gamma_{\mu K, 5}^K - \Gamma_{\mu M}^K \Gamma_{5K}^M + \Gamma_{\mu 5}^K \Gamma_{KM}^M. \tag{C-14}$$

The first term is obtained as

$$\begin{aligned}
\Gamma_{\mu 5, K}^K &= \{g^{KL}\Gamma_{L\mu 5}\}_{,K} \\
&= \frac{1}{2}\{g^{KL}[g_{L\mu,5} + g_{L5,\mu}]\}_{,K} \\
&= \frac{1}{2}\{g^{K\rho}[g_{\rho\mu,5}] + g^{K5}[g_{55,\mu}]\}_{,K} \\
&= \frac{1}{2}\{g^{\xi\rho}[g_{\rho\mu,5}]\}_{,\xi} + \frac{1}{2}\{g^{55}(g_{55,\mu})\}_{,5} \\
&= 0.
\end{aligned} \tag{C-15}$$

The second term can be calculated as follows

$$\begin{aligned}
\Gamma_{\mu K, 5}^K &= \{g^{KL}\Gamma_{L\mu K}\}_{,5} \\
&= \frac{1}{2}\{g^{KL}[g_{L\mu,K} + g_{LK,\mu} - g_{\mu K,L}]\}_{,5} \\
&= \frac{1}{2}\{g^{K\rho}[g_{\rho\mu,K} + g_{\rho K,\mu} - g_{\mu K,\rho}] + g^{K5}[g_{5K,\mu} - g_{\mu K,5}]\}_{,5} \\
&= \frac{1}{2}\{g^{\xi\rho}[g_{\rho\mu,\xi} + g_{\rho\xi,\mu} - g_{\mu\xi,\rho}] + g^{55}[g_{55,\mu}]\}_{,5} \\
&= 0.
\end{aligned} \tag{C-16}$$

The third term is

$$\begin{aligned}
\Gamma_{\mu M}^K \Gamma_{5K}^M &= g^{KL} \Gamma_{L\mu M} g^{MS} \Gamma_{S5K} \\
&= \frac{1}{2} g^{KL} [g_{L\mu, M} + g_{LM, \mu} - g_{\mu M, L}] \frac{1}{2} g^{MS} [g_{S5, K} + g_{SK, 5} - g_{5K, S}] \\
&= \frac{1}{4} g^{K\rho} [g_{\rho\mu, M} + g_{\rho M, \mu} - g_{\mu M, \rho}] g^{MS} [g_{S5, K} + g_{SK, 5} - g_{5K, S}] \\
&+ \frac{1}{4} g^{K5} [g_{5M, \mu} - g_{\mu M, 5}] g^{MS} [g_{S5, K} + g_{SK, 5} - g_{5K, S}] \\
&= \frac{1}{4} g^{\xi\rho} [g_{\rho\mu, M} + g_{\rho M, \mu} - g_{\mu M, \rho}] g^{MS} [g_{S5, \xi} + g_{S\xi, 5}] \\
&+ \frac{1}{4} g^{55} [g_{5M, \mu} - g_{\mu M, 5}] g^{MS} [g_{S5, 5} + g_{S5, 5} - g_{55, S}] \\
&= \frac{1}{4} g^{\xi\rho} [g_{\rho\mu, \alpha} + g_{\rho\alpha, \mu} - g_{\mu\alpha, \rho}] g^{\alpha S} [g_{S5, \xi} + g_{S\xi, 5}] \\
&+ \frac{1}{4} g^{55} [-g_{\mu\alpha, 5}] g^{\alpha S} [2g_{S5, 5} - g_{55, S}] \\
&+ \frac{1}{4} g^{\xi\rho} [g_{\rho\mu, 5}] g^{5S} [g_{S5, \xi} + g_{S\xi, 5}] + \frac{1}{4} g^{55} [g_{55, \mu}] g^{5S} [2g_{S5, 5} - g_{55, S}] \\
&= \frac{1}{4} g^{\xi\rho} [g_{\rho\mu, \alpha} + g_{\rho\alpha, \mu} - g_{\mu\alpha, \rho}] g^{\alpha\beta} [g_{\beta\xi, 5}] + \frac{1}{4} g^{55} [-g_{\mu\alpha, 5}] g^{\alpha\beta} [-g_{55, \beta}] \\
&+ \frac{1}{4} g^{\xi\rho} [g_{\rho\mu, 5}] g^{55} [g_{55, \xi}] + \frac{1}{4} g^{55} [g_{55, \mu}] g^{55} [g_{55, 5}] \\
&= 0.
\end{aligned} \tag{C-17}$$

The last term is calculated as

$$\begin{aligned}
\Gamma_{\mu 5}^K \Gamma_{KM}^M &= g^{KL} \Gamma_{L\mu 5} g^{MS} \Gamma_{SKM} \\
&= \frac{1}{2} g^{KL} [g_{L\mu, 5} + g_{L5, \mu}] \frac{1}{2} g^{MS} [g_{SK, M} + g_{SM, K} - g_{KM, S}] \\
&= \frac{1}{4} g^{K\rho} [g_{\rho\mu, 5}] g^{MS} [g_{SK, M} + g_{SM, K} - g_{KM, S}] \\
&+ \frac{1}{4} g^{K5} [g_{55, \mu}] g^{MS} [g_{SK, M} + g_{SM, K} - g_{KM, S}] \\
&= \frac{1}{4} g^{\xi\rho} [g_{\rho\mu, 5}] g^{MS} [g_{S\xi, M} + g_{SM, \xi} - g_{\xi M, S}] \\
&+ \frac{1}{4} g^{55} [g_{55, \mu}] g^{MS} [g_{S5, M} + g_{SM, 5} - g_{5M, S}] \\
&= \frac{1}{4} g^{\xi\rho} [g_{\rho\mu, 5}] g^{\alpha S} [g_{S\xi, \alpha} + g_{S\alpha, \xi} - g_{\xi\alpha, S}] + \frac{1}{4} g^{55} [g_{55, \mu}] g^{\alpha S} [g_{S5, \alpha} + g_{S\alpha, 5}] \\
&+ \frac{1}{4} g^{\xi\rho} [g_{\rho\mu, 5}] g^{5S} [g_{S\xi, 5} + g_{S5, \xi}] + \frac{1}{4} g^{55} [g_{55, \mu}] g^{5S} [g_{S5, 5} + g_{S5, 5} - g_{55, S}]
\end{aligned}$$

$$\begin{aligned}
&= \frac{1}{4}g^{\xi\rho}[g_{\rho\mu,5}]g^{\alpha\beta}[g_{\beta\xi,\alpha} + g_{\beta\alpha,\xi} - g_{\xi\alpha,\beta}] + \frac{1}{4}g^{55}[g_{55,\mu}]g^{\alpha\beta}[g_{\beta\alpha,5}] \\
&+ \frac{1}{4}g^{\xi\rho}[g_{\rho\mu,5}]g^{55}[g_{55,\xi}] + \frac{1}{4}g^{55}[g_{55,\mu}]g^{55}[g_{55,5}] \\
&= 0.
\end{aligned} \tag{C-18}$$

Then, we can conclude

$$R_{\mu 5} = 0. \tag{C-19}$$

As one last step we will calculate Ricci Scalar as well

$$\begin{aligned}
R &= g^{MN}R_{MN} \\
&= g^{M\nu}R_{M\nu} + g^{M5}R_{M5} \\
&= g^{\mu\nu}R_{\mu\nu} + g^{55}R_{55} \\
&= e^{2\sigma(\phi)}\eta^{\mu\nu}\left\{\frac{e^{-2\sigma(\phi)}}{r^2}\left(4[\sigma'(\phi)]^2 - \sigma''(\phi)\right)\eta_{\mu\nu}\right\} - r^{-2}\left\{4\left(\sigma''(\phi) - [\sigma'(\phi)]^2\right)\right\} \\
&= \frac{4}{r^2}\left\{5[\sigma'(\phi)]^2 - 2\sigma''(\phi)\right\}.
\end{aligned} \tag{C-20}$$

C-2 Brane Tensions

Derivative of a function $f(x)$ in absolute value can be easily found by considering $|f(x)| = \sqrt{f(x)^2} = (f(x)^2)^{1/2}$. Utilizing the chain rule we get

$$\frac{d}{dx}|f(x)| = \frac{d}{dx}(f(x)^2)^{1/2} = \frac{1}{2}(f(x)^2)^{-1/2}2f(x)f'(x) = \frac{f(x)f'(x)}{|f(x)|}. \tag{C-21}$$

Recall from eq. (3.103) that $\sigma(\phi) = kr|\phi|$. The first derivative with respect to ϕ reads

$$\sigma'(\phi) = kr\frac{\phi}{|\phi|}. \tag{C-22}$$

By definition, $U(\phi) = \phi/|\phi|$ where $U(\phi)$ is the unit step function which can be written in terms of step functions as $U(\phi) = (\theta(\phi) - \theta(-\phi))$. The derivative of a step function is a delta function. The second derivative of $\sigma(\phi)$ then becomes,

$$\sigma''(\phi) = 2kr\left[\delta(\phi) - \delta(\phi - \pi)\right]. \tag{C-23}$$

Appendix D

Rotation and CKM4 Matrices in Warped Extra Dimensions with Four Generation

D-1 Rotation Matrices

Let \mathbf{A} be an $n \times n$ matrix, $[\mathbf{A}]_{ij}$ be its $\{ij\}$ first order minor¹ and $[\mathbf{A}]_{ij,\alpha\beta}$ represent the $\{ij, \alpha\beta\}$ second order minor² of \mathbf{A} . It is useful to record some basic properties of determinants which will be needed later

$$\det(a\mathbf{A}) = a^n \det(\mathbf{A}), \quad (\text{D-1})$$

where a is a constant, and \mathbf{B} being another $n \times n$ matrix

$$\det(\mathbf{AB}) = \det(\mathbf{A})\det(\mathbf{B}). \quad (\text{D-2})$$

In addition, the minor of the multiplication of two matrices is

$$[\mathbf{AB}]_{ij} = \sum_k [\mathbf{A}]_{ik} [\mathbf{B}]_{kj}. \quad (\text{D-3})$$

We will try to obtain quark masses in terms of f_i 's and 5D Yukawa couplings with the help of the basic properties of matrices summarized above. Let us start our calculation

¹The $\{ij\}$ first order minor of a matrix \mathbf{A} is the determinant of $(n-1) \times (n-1)$ submatrix which is obtained by removing i^{th} row and j^{th} column from \mathbf{A} .

²The $\{ij, \alpha\beta\}$ second order minor of a matrix \mathbf{A} is the determinant of $(n-2) \times (n-2)$ submatrix which is obtained by removing the rows i and α , and columns j and β from \mathbf{A} .

by the absolute value of the determinant of the up-type quarks mass matrix ($\mathbf{M}_{\mathbf{u}}$), previously defined in Chapter 5.1 in eq. (5.2). By using eqns. (D-1) and (D-2) it yields

$$\begin{aligned} \left| \det(\mathbf{M}_{\mathbf{u}}) \right| &= \left| v_4^4 \det(\mathbf{F}_{\mathbf{Q}}) \det(\mathbf{Y}_{\mathbf{u}}) \det(\mathbf{F}_{\mathbf{u}}) \right| \\ &= v_4^4 f_{Q_1} f_{Q_2} f_{Q_3} f_{Q_4} f_{u_1} f_{u_2} f_{u_3} f_{u_4} \left| \det(\mathbf{Y}_{\mathbf{u}}) \right|, \end{aligned} \quad (\text{D-4})$$

and also from eq. (5.3)

$$\det(\mathbf{M}_{\mathbf{u}}) = \det(\mathbf{U}_{\mathbf{Q}_{\mathbf{u}}}) \det(\mathbf{M}_{\mathbf{u}}^{\text{diag}}) \det(\mathbf{W}_{\mathbf{u}}^\dagger), \quad (\text{D-5})$$

where $\mathbf{U}_{\mathbf{Q}_{\mathbf{u}}}$ and $\mathbf{W}_{\mathbf{u}}$ are unitary transformation matrices. Therefore, $\det(\mathbf{U}_{\mathbf{Q}_{\mathbf{u}}}) = \det(\mathbf{W}_{\mathbf{u}}) = 1$. Then, one can simply write

$$\det(\mathbf{M}_{\mathbf{u}}) = \det(\mathbf{M}_{\mathbf{u}}^{\text{diag}}) = m_{t'} m_t m_c m_u. \quad (\text{D-6})$$

Combining the results of eqs. (D-4) and (D-6) we get

$$\prod_{i=1}^{i=4} m_i = m_{t'} m_t m_c m_u = v_4^4 f_{Q_1} f_{Q_2} f_{Q_3} f_{Q_4} f_{u_1} f_{u_2} f_{u_3} f_{u_4} \left| \det(\mathbf{Y}_{\mathbf{u}}) \right|. \quad (\text{D-7})$$

Here the absolute values are necessary to get rid of the phases in the Yukawa matrices. Now let us calculate the absolute value of the $\{11\}$ first minor of $\mathbf{M}_{\mathbf{u}}$. Using eqs. (D-1) and (D-3) it can be written as

$$\left| [\mathbf{M}_{\mathbf{u}}]_{11} \right| = \left| v_4^3 [\mathbf{F}_{\mathbf{Q}}]_{11} [\mathbf{Y}_{\mathbf{u}}]_{11} [\mathbf{F}_{\mathbf{u}}]_{11} \right| = v_4^3 f_{Q_2} f_{Q_3} f_{Q_4} f_{u_2} f_{u_3} f_{u_4} \left| [\mathbf{Y}_{\mathbf{u}}]_{11} \right|, \quad (\text{D-8})$$

where since $\mathbf{F}_{\mathbf{i}}$'s are diagonal matrices, they only admit principal minors $[\mathbf{F}_{\mathbf{i}}]_{kk}$. We can also write $[\mathbf{M}_{\mathbf{u}}]_{11}$ utilizing the other definition of the up-type quarks mass matrix given in eq. (5.3) as

$$[\mathbf{M}_{\mathbf{u}}]_{11} = [\mathbf{U}_{\mathbf{Q}_{\mathbf{u}}}]_{1k} [\mathbf{M}_{\mathbf{u}}^{\text{diag}}]_{kk} [\mathbf{W}_{\mathbf{u}}^\dagger]_{k1}. \quad (\text{D-9})$$

The largest contribution to $[\mathbf{M}_{\mathbf{u}}]_{11}$ happens when $k = 1$ giving

$$[\mathbf{M}_{\mathbf{u}}]_{11} = m_{t'} m_t m_c, \quad (\text{D-10})$$

since $[\mathbf{U}_{\mathbf{Q}_{\mathbf{u}}}]_{11} = [\mathbf{W}_{\mathbf{u}}^\dagger]_{11} = 1$. Therefore, to lowest order in the ratios of f_i 's we can write

$$\prod_{i=2}^{i=4} m_i = m_{t'} m_t m_c = v_4^3 f_{Q_2} f_{Q_3} f_{Q_4} f_{u_2} f_{u_3} f_{u_4} \left| [\mathbf{Y}_{\mathbf{u}}]_{11} \right|. \quad (\text{D-11})$$

We will follow the same procedure for the $\{11, 22\}$ second minor of \mathbf{M}_u as

$$\left| [\mathbf{M}_u]_{11,22} \right| = v_4^2 \left| [\mathbf{F}_u]_{11,22} [\mathbf{Y}_u]_{11,22} [\mathbf{F}_Q]_{11,22} \right| = v_4^2 f_{Q_3} f_{Q_4} f_{u_3} f_{u_4} \left| [\mathbf{Y}_u]_{11,22} \right|, \quad (\text{D-12})$$

and

$$[\mathbf{M}_u]_{11,22} = [\mathbf{U}_{Q_u}]_{11,2k} [\mathbf{M}_u^{\text{diag}}]_{11,kk} [\mathbf{W}_u^\dagger]_{11,k2}, \quad (\text{D-13})$$

which will have the largest contribution when $k = 2$, and since $[\mathbf{U}_{Q_u}]_{11,22} = [\mathbf{W}_u^\dagger]_{11,22} = 1$ we obtain

$$[\mathbf{M}_u]_{11,22} = m_{t'} m_t. \quad (\text{D-14})$$

Then, in leading order, we have

$$\prod_{i=3}^{i=4} m_i = m_{t'} m_t = v_4^2 f_{Q_3} f_{Q_4} f_{u_3} f_{u_4} \left| [\mathbf{Y}_u]_{11,22} \right|. \quad (\text{D-15})$$

We can therefore obtain the leading contributions to the up-type quark masses as

$$m_u = \frac{m_{t'} m_t m_c m_u}{m_{t'} m_t m_c} = v_4 f_{Q_1} f_{u_1} \frac{|\det(\mathbf{Y}_u)|}{|[\mathbf{Y}_u]_{11}|}, \quad (\text{D-16})$$

$$m_c = \frac{m_{t'} m_t m_c}{m_{t'} m_t} = v_4 f_{Q_2} f_{u_2} \frac{|[\mathbf{Y}_u]_{11}|}{|[\mathbf{Y}_u]_{11,22}|}, \quad (\text{D-17})$$

$$m_{t'} m_t = v_4^2 f_{Q_3} f_{Q_4} f_{u_3} f_{u_4} \left| [\mathbf{Y}_u]_{11,22} \right|. \quad (\text{D-18})$$

Recalling the definition of the down-type quarks mass matrix (\mathbf{M}_d) given in eq. (5.2), we can write

$$\prod_{i=1}^{i=4} m_i = m_{b'} m_b m_s m_d = v_4^4 f_{Q_1} f_{Q_2} f_{Q_3} f_{Q_4} f_{d_1} f_{d_2} f_{d_3} f_{d_4} \left| \det(\mathbf{Y}_d) \right|. \quad (\text{D-19})$$

To lowest order in ratios of f_i 's we have

$$\prod_{i=2}^{i=4} m_i = m_{b'} m_b m_s = v_4^3 f_{Q_2} f_{Q_3} f_{Q_4} f_{d_2} f_{d_3} f_{d_4} \left| [\mathbf{Y}_d]_{11} \right|, \quad (\text{D-20})$$

and

$$\prod_{i=3}^{i=4} m_i = m_{b'} m_b = v_4^2 f_{Q_3} f_{Q_4} f_{d_3} f_{d_4} \left| [\mathbf{Y}_d]_{11,22} \right|. \quad (\text{D-21})$$

Then, the leading contributions to the down quark masses are

$$m_d = \frac{m_{b'} m_b m_s m_d}{m_{b'} m_b m_s} = v_4 f_{Q_1} f_{d_1} \frac{|\det(\mathbf{Y}_d)|}{|[\mathbf{Y}_d]_{11}|}, \quad (\text{D-22})$$

$$m_s = \frac{m_{b'} m_b m_s}{m_{b'} m_b} = v_4 f_{Q_2} f_{d_2} \frac{|[\mathbf{Y}_d]_{11}|}{|[\mathbf{Y}_d]_{11,22}|}, \quad (\text{D-23})$$

$$m_{b'} m_b = v f_{Q_3} f_{d_3} f_{Q_4} f_{d_4} |[\mathbf{Y}_d]_{11,22}|. \quad (\text{D-24})$$

Since $f_{Q_3} \sim f_{Q_4}$ we must have that $\frac{f_{d_3}}{f_{d_4}} \sim \frac{m_b}{m_{b'}} \sim 10^{-2}$. Because of this, we can find also

$$m_{b'}^2 = v^2 f_{d_4}^2 (f_{Q_4}^2 |Y_{44}^d|^2 + f_{Q_3}^2 |Y_{34}^d|^2). \quad (\text{D-25})$$

One can form a diagonal matrix, $\hat{\mathbf{H}}$, with n eigenvalues, λ_i , via the unitary matrix, \mathbf{V} , from a hermitian $n \times n$ matrix \mathbf{H} as follows

$$\mathbf{V}^\dagger \mathbf{H} \mathbf{V} = \hat{\mathbf{H}}. \quad (\text{D-26})$$

A useful parametrization to find the entries of the unitary matrix, V , can be written as [224]

$$V_{ij} = (-1)^{i+j} \frac{[\mathbf{H} - \lambda_j \mathbf{I}]_{ji}}{\sqrt{[\mathbf{H} - \lambda_j \mathbf{I}]_{jj} \prod_{j \neq \alpha} (\lambda_\alpha - \lambda_j)}}. \quad (\text{D-27})$$

Note that this formula is exact and it is valid for any square hermitian matrix, \mathbf{H} . We will now follow the standard procedure to obtain a simple formulation for the rotation matrices \mathbf{U}_{Q_u} , \mathbf{U}_{Q_d} , \mathbf{W}_u and \mathbf{W}_d in an expansion of small ratios of f_i 's. Let $\mathbf{H}_u = \mathbf{M}_u \mathbf{M}_u^\dagger = \mathbf{U}_{Q_u} \mathbf{M}_u^{\text{diag}} \mathbf{W}_u^\dagger \mathbf{W}_u \mathbf{M}_u^{\text{diag}} \mathbf{U}_{Q_u}^\dagger$. Because \mathbf{W}_u is a hermitian matrix, we can write $\mathbf{H}_u = \mathbf{U}_{Q_u} (\mathbf{M}_u^{\text{diag}})^2 \mathbf{U}_{Q_u}^\dagger$. Multiplying this from left by $\mathbf{U}_{Q_u}^\dagger$ and from right by \mathbf{U}_{Q_u} , we get $\mathbf{U}_{Q_u}^\dagger \mathbf{H}_u \mathbf{U}_{Q_u} = (\mathbf{M}_u^{\text{diag}})^2$ which is the same form as in eq. (D-26) such that $\mathbf{V} = \mathbf{U}_{Q_u}$, and eigenvalues of \mathbf{H}_u (or the diagonal entries of $\hat{\mathbf{H}}_u$) are the squares of the physical masses of up-type quarks. Let us first concentrate on $\lambda_1 = m_u^2$.

$$V_{i1} = (-1)^{i+1} \frac{[\mathbf{H}_u - m_u^2 \mathbf{I}]_{1i}}{\sqrt{[\mathbf{H}_u - m_u^2 \mathbf{I}]_{11} (m_c^2 - m_u^2) (m_t^2 - m_u^2) (m_{b'}^2 - m_u^2)}}. \quad (\text{D-28})$$

Because of the hierarchical nature of this scenario, we know that to the lowest order in ratios of f 's, the minors of $(\mathbf{H}_u - m_u^2 \mathbf{I})$ not involving the first row or column, can be approximated by

$$[\mathbf{H}_u - m_u^2 \mathbf{I}]_{1i} \simeq [\mathbf{H}_u]_{1i}. \quad (\text{D-29})$$

Thus, we have

$$V_{i1} = (-1)^{i+1} \frac{[\mathbf{H}_u]_{1i}}{\sqrt{[\mathbf{H}_u]_{11} (m_c^2 - m_u^2)(m_t^2 - m_u^2)(m_{t'}^2 - m_u^2)}}. \quad (\text{D-30})$$

Using eq. (5.2) we can write \mathbf{H}_u as

$$\mathbf{H}_u = v_4^2 \mathbf{F}_Q \mathbf{Y}_u \mathbf{F}_u^2 \mathbf{Y}_u^\dagger \mathbf{F}_Q, \quad (\text{D-31})$$

where we have used $\mathbf{F}_{Q(u)} = \mathbf{F}_{Q(u)}^\dagger$ based on the fact that they are diagonal matrices with real entries. From eqs. (D-1) and (D-3), the $\{1i\}$ first minor of \mathbf{H}_u is

$$\begin{aligned} [\mathbf{H}_u]_{1i} &= [v_4^2 \mathbf{F}_Q]_{11} [\mathbf{Y}_u]_{1k} [\mathbf{F}_u^2]_{kk} [\mathbf{Y}_u^\dagger]_{ki} [\mathbf{F}_Q]_{ii} \\ &= v_4^6 [\mathbf{F}_Q]_{11} [\mathbf{Y}_u]_{1k} [\mathbf{F}_u^2]_{kk} [\mathbf{Y}_u^\dagger]_{ki} [\mathbf{F}_Q]_{ii}. \end{aligned} \quad (\text{D-32})$$

The largest contribution for $[\mathbf{H}_u]_{1i}$ will be when $k = 1$, giving

$$[\mathbf{H}_u]_{1i} = v_4^6 [\mathbf{F}_Q]_{11} [\mathbf{Y}_u]_{11} [\mathbf{F}_u^2]_{11} [\mathbf{Y}_u^\dagger]_{1i} [\mathbf{F}_Q]_{ii}, \quad (\text{D-33})$$

which can also be written as

$$\begin{aligned} [\mathbf{H}_u]_{1i} &= v_4^6 [\mathbf{F}_Q]_{11} [\mathbf{Y}_u]_{11} [\mathbf{F}_u^2]_{11} [\mathbf{Y}_u^\dagger]_{11} [\mathbf{F}_Q]_{11} \frac{[\mathbf{Y}_u^\dagger]_{1i} [\mathbf{F}_Q]_{ii}}{[\mathbf{Y}_u^\dagger]_{11} [\mathbf{F}_Q]_{11}} \\ &= [\mathbf{H}_u]_{11} \frac{[\mathbf{Y}_u^\dagger]_{1i} [\mathbf{F}_Q]_{ii}}{[\mathbf{Y}_u^\dagger]_{11} [\mathbf{F}_Q]_{11}}, \end{aligned} \quad (\text{D-34})$$

where $[\mathbf{H}_u]_{11}$ is

$$\begin{aligned} [\mathbf{H}_u]_{11} &= v_4^6 [\mathbf{F}_Q]_{11} [\mathbf{Y}_u]_{11} [\mathbf{F}_u^2]_{11} [\mathbf{Y}_u^\dagger]_{11} [\mathbf{F}_Q]_{11} \\ &= v_4^6 f_{Q_2}^2 f_{Q_3}^2 f_{Q_4}^2 f_{u_2}^2 f_{u_3}^2 f_{u_4}^2 \left| [\mathbf{Y}_u]_{11} \right|^2, \end{aligned} \quad (\text{D-35})$$

which if one compares with eq. (D-11), can simply conclude as $[\mathbf{H}_u]_{11} = (m_c m_t m_{t'})^2$. Moreover, the product $(m_c^2 - m_u^2)(m_t^2 - m_u^2)(m_{t'}^2 - m_u^2)$ can be approximated by $(m_c m_t m_{t'})^2$. We can put all this together and rewrite V_{i1} as

$$V_{i1} = (-1)^{i+1} \frac{[\mathbf{Y}_u^\dagger]_{1i} [\mathbf{F}_Q]_{ii}}{[\mathbf{Y}_u^\dagger]_{11} [\mathbf{F}_Q]_{11}} = (-1)^{i+1} \frac{[\mathbf{Y}_u]_{i1}^* [\mathbf{F}_Q]_{ii}}{[\mathbf{Y}_u]_{11}^* [\mathbf{F}_Q]_{11}}. \quad (\text{D-36})$$

Then we can simply write

$$\begin{aligned}
V_{11} &= (-1)^2 \frac{[\mathbf{Y}_{\mathbf{u}}]_{11}^* [\mathbf{F}_{\mathbf{Q}}]_{11}}{[\mathbf{Y}_{\mathbf{u}}]_{11}^* [\mathbf{F}_{\mathbf{Q}}]_{11}} = 1, \\
V_{21} &= (-1)^3 \frac{[\mathbf{Y}_{\mathbf{u}}]_{21}^* [\mathbf{F}_{\mathbf{Q}}]_{22}}{[\mathbf{Y}_{\mathbf{u}}]_{11}^* [\mathbf{F}_{\mathbf{Q}}]_{11}} = -\frac{[\mathbf{Y}_{\mathbf{u}}]_{21}^* f_{Q_1} f_{Q_3} f_{Q_4}}{[\mathbf{Y}_{\mathbf{u}}]_{11}^* f_{Q_2} f_{Q_3} f_{Q_4}} = -\frac{[\mathbf{Y}_{\mathbf{u}}]_{21}^* f_{Q_1}}{[\mathbf{Y}_{\mathbf{u}}]_{11}^* f_{Q_2}}, \\
V_{31} &= (-1)^4 \frac{[\mathbf{Y}_{\mathbf{u}}]_{31}^* [\mathbf{F}_{\mathbf{Q}}]_{33}}{[\mathbf{Y}_{\mathbf{u}}]_{11}^* [\mathbf{F}_{\mathbf{Q}}]_{11}} = \frac{[\mathbf{Y}_{\mathbf{u}}]_{31}^* f_{Q_1} f_{Q_2} f_{Q_4}}{[\mathbf{Y}_{\mathbf{u}}]_{11}^* f_{Q_2} f_{Q_3} f_{Q_4}} = \frac{[\mathbf{Y}_{\mathbf{u}}]_{31}^* f_{Q_1}}{[\mathbf{Y}_{\mathbf{u}}]_{11}^* f_{Q_3}}, \\
V_{41} &= (-1)^5 \frac{[\mathbf{Y}_{\mathbf{u}}]_{41}^* [\mathbf{F}_{\mathbf{Q}}]_{44}}{[\mathbf{Y}_{\mathbf{u}}]_{11}^* [\mathbf{F}_{\mathbf{Q}}]_{11}} = -\frac{[\mathbf{Y}_{\mathbf{u}}]_{41}^* f_{Q_1} f_{Q_2} f_{Q_3}}{[\mathbf{Y}_{\mathbf{u}}]_{11}^* f_{Q_2} f_{Q_3} f_{Q_4}} = -\frac{[\mathbf{Y}_{\mathbf{u}}]_{41}^* f_{Q_1}}{[\mathbf{Y}_{\mathbf{u}}]_{11}^* f_{Q_4}}. \quad (\text{D-37})
\end{aligned}$$

Let us follow the same procedure for the second eigen value $\lambda_2 = m_c$. Using the eq. (D-27) we can write

$$V_{i2} = (-1)^{i+2} \frac{[\mathbf{H}_{\mathbf{u}} - m_c \mathbf{I}]_{11,2i}}{\sqrt{[\mathbf{H}_{\mathbf{u}} - m_c \mathbf{I}]_{11,22} (m_t^2 - m_c^2) (m_{t'}^2 - m_c^2)}}. \quad (\text{D-38})$$

In leading order in f_i 's it is a good approximation to take

$$[\mathbf{H}_{\mathbf{u}} - m_c \mathbf{I}]_{11,2i} \simeq [\mathbf{H}_{\mathbf{u}}]_{11,2i}, \quad (\text{D-39})$$

which could be expanded as

$$\begin{aligned}
[\mathbf{H}_{\mathbf{u}}]_{11,2i} &= [v_4^2 \mathbf{F}_{\mathbf{Q}}]_{11,22} [\mathbf{Y}_{\mathbf{u}}]_{11,2k} [\mathbf{F}_{\mathbf{u}}^2]_{11,kk} [\mathbf{Y}_{\mathbf{u}}^\dagger]_{11,ki} [\mathbf{F}_{\mathbf{Q}}]_{11,ii} \\
&= v_4^4 [\mathbf{F}_{\mathbf{Q}}]_{11,22} [\mathbf{Y}_{\mathbf{u}}]_{11,2k} [\mathbf{F}_{\mathbf{u}}^2]_{11,kk} [\mathbf{Y}_{\mathbf{u}}^\dagger]_{11,ki} [\mathbf{F}_{\mathbf{Q}}]_{11,ii}. \quad (\text{D-40})
\end{aligned}$$

The largest contribution is when $k = 2$. Thus, we get

$$\begin{aligned}
[\mathbf{H}_{\mathbf{u}}]_{11,2i} &= [v_4^2 \mathbf{F}_{\mathbf{Q}}]_{11,22} [\mathbf{Y}_{\mathbf{u}}]_{11,22} [\mathbf{F}_{\mathbf{u}}^2]_{11,22} [\mathbf{Y}_{\mathbf{u}}^\dagger]_{11,2i} [\mathbf{F}_{\mathbf{Q}}]_{11,ii} \\
&= [\mathbf{H}_{\mathbf{u}}]_{11,22} \frac{[\mathbf{Y}_{\mathbf{u}}^\dagger]_{11,2i} [\mathbf{F}_{\mathbf{Q}}]_{11,ii}}{[\mathbf{Y}_{\mathbf{u}}^\dagger]_{11,22} [\mathbf{F}_{\mathbf{Q}}]_{11,22}} \quad (\text{D-41})
\end{aligned}$$

Let us calculate $[\mathbf{H}_{\mathbf{u}}]_{11,22}$ for the leading order.

$$\begin{aligned}
[\mathbf{H}_{\mathbf{u}}]_{11,22} &= v_4^4 [\mathbf{F}_{\mathbf{Q}}]_{11,22} [\mathbf{Y}_{\mathbf{u}}]_{11,2k} [\mathbf{F}_{\mathbf{u}}^2]_{11,kk} [\mathbf{Y}_{\mathbf{u}}^\dagger]_{11,k2} [\mathbf{F}_{\mathbf{Q}}]_{11,22} \\
&= v_4^4 f_{Q_3}^2 f_{Q_4}^2 f_{u_3}^2 f_{u_4}^2 \left| [\mathbf{Y}_{\mathbf{u}}]_{11,22} \right|^2 \\
&= m_t^2 m_{t'}^2 \left| [\mathbf{Y}_{\mathbf{u}}]_{11,22} \right|^2 \quad (\text{D-42})
\end{aligned}$$

In the same way we did for the calculation of V_{i1} , we can take the product $(m_t^2 - m_c^2)(m_{t'}^2 - m_c^2)$ approximately as $(m_t m_{t'})^2$. If we put everything together we obtain

$$V_{i2} = (-1)^{i+2} \frac{[\mathbf{Y}_{\mathbf{u}}^\dagger]_{11,2i} [\mathbf{F}_{\mathbf{Q}}]_{11,ii}}{[\mathbf{Y}_{\mathbf{u}}^\dagger]_{11,22} [\mathbf{F}_{\mathbf{Q}}]_{11,22}} = (-1)^{i+2} \frac{[\mathbf{Y}_{\mathbf{u}}]_{11,i2}^* [\mathbf{F}_{\mathbf{Q}}]_{11,ii}}{[\mathbf{Y}_{\mathbf{u}}]_{11,22}^* [\mathbf{F}_{\mathbf{Q}}]_{11,22}}. \quad (\text{D-43})$$

We can obtain the CKM entries V_{22} , V_{32} and V_{42} from eq. (D-43) as follows

$$\begin{aligned}
V_{22} &= (-1)^{2+2} \frac{[\mathbf{Y}_{\mathbf{u}}]_{11,22}^* [\mathbf{F}_{\mathbf{Q}}]_{11,22}}{[\mathbf{Y}_{\mathbf{u}}]_{11,22}^* [\mathbf{F}_{\mathbf{Q}}]_{11,22}} = 1, \\
V_{32} &= (-1)^{3+2} \frac{[\mathbf{Y}_{\mathbf{u}}]_{11,32}^* [\mathbf{F}_{\mathbf{Q}}]_{11,33}}{[\mathbf{Y}_{\mathbf{u}}]_{11,22}^* [\mathbf{F}_{\mathbf{Q}}]_{11,22}} = -\frac{[\mathbf{Y}_{\mathbf{u}}]_{11,32}^* f_{Q_2} f_{Q_4}}{[\mathbf{Y}_{\mathbf{u}}]_{11,22}^* f_{Q_3} f_{Q_4}} = -\frac{[\mathbf{Y}_{\mathbf{u}}]_{11,32}^* f_{Q_2}}{[\mathbf{Y}_{\mathbf{u}}]_{11,22}^* f_{Q_3}}, \\
V_{42} &= (-1)^{4+2} \frac{[\mathbf{Y}_{\mathbf{u}}]_{11,42}^* [\mathbf{F}_{\mathbf{Q}}]_{11,44}}{[\mathbf{Y}_{\mathbf{u}}]_{11,22}^* [\mathbf{F}_{\mathbf{Q}}]_{11,22}} = \frac{[\mathbf{Y}_{\mathbf{u}}]_{11,42}^* f_{Q_2} f_{Q_3}}{[\mathbf{Y}_{\mathbf{u}}]_{11,22}^* f_{Q_3} f_{Q_4}} = \frac{[\mathbf{Y}_{\mathbf{u}}]_{11,42}^* f_{Q_2}}{[\mathbf{Y}_{\mathbf{u}}]_{11,22}^* f_{Q_4}}.
\end{aligned} \tag{D-44}$$

Finally, for $\lambda_3 = m_t$

$$V_{i3} = (-1)^{i+3} \frac{[\mathbf{H}_{\mathbf{u}} - m_t \mathbf{I}]_{11,22,3i}}{\sqrt{[\mathbf{H}_{\mathbf{u}} - m_t \mathbf{I}]_{11,22,33} (m_{t'}^2 - m_t^2)}}. \tag{D-45}$$

Since the mass of top quark is high we cannot make an approximation as we did for the up and charm quarks when calculating V_{i1} and V_{i2} terms.

$$\begin{aligned}
[\mathbf{H}_{\mathbf{u}}]_{11,22,3i} &= [v_4^2 \mathbf{F}_{\mathbf{Q}}]_{11,22,33} [\mathbf{Y}_{\mathbf{u}}]_{11,22,3k} [\mathbf{F}_{\mathbf{u}}^2]_{11,22,kk} [\mathbf{Y}_{\mathbf{u}}^\dagger]_{11,22,ki} [\mathbf{F}_{\mathbf{Q}}]_{11,ii} \\
&= v_4^2 [\mathbf{F}_{\mathbf{Q}}]_{11,22,33} [\mathbf{Y}_{\mathbf{u}}]_{11,22,3k} [\mathbf{F}_{\mathbf{u}}^2]_{11,22,kk} [\mathbf{Y}_{\mathbf{u}}^\dagger]_{11,22,ki} [\mathbf{F}_{\mathbf{Q}}]_{11,22,ii} \\
&= v_4^2 f_{Q_4} [\mathbf{Y}_{\mathbf{u}}]_{11,22,33} [\mathbf{F}_{\mathbf{u}}^2]_{11,22,33} [\mathbf{Y}_{\mathbf{u}}^\dagger]_{11,22,3i} [\mathbf{F}_{\mathbf{Q}}]_{11,22,ii} \\
&+ v_4^2 f_{Q_4} [\mathbf{Y}_{\mathbf{u}}]_{11,22,34} [\mathbf{F}_{\mathbf{u}}^2]_{11,22,44} [\mathbf{Y}_{\mathbf{u}}^\dagger]_{11,22,4i} [\mathbf{F}_{\mathbf{Q}}]_{11,22,ii} \\
&= v_4^2 f_{Q_4} \left(Y_{44}^u f_{u_4}^2 [\mathbf{Y}_{\mathbf{u}}^\dagger]_{11,22,3i} + Y_{34}^u f_{u_3}^2 [\mathbf{Y}_{\mathbf{u}}^\dagger]_{11,22,4i} \right) [\mathbf{F}_{\mathbf{Q}}]_{11,22,ii} \\
&= v_4^2 f_{Q_4} \left(f_{u_4}^2 Y_{44}^u [\mathbf{Y}_{\mathbf{u}}]_{11,22,i3}^* + f_{u_3}^2 Y_{34}^u [\mathbf{Y}_{\mathbf{u}}]_{11,22,i4}^* \right) [\mathbf{F}_{\mathbf{Q}}]_{11,22,ii} \tag{D-46}
\end{aligned}$$

and $[\mathbf{H}_{\mathbf{u}}]_{11,22,33}$ can be calculated as

$$\begin{aligned}
[\mathbf{H}_{\mathbf{u}}]_{11,22,33} &= v_4^2 f_{Q_4}^2 \left(f_{u_4}^2 Y_{44}^u [\mathbf{Y}_{\mathbf{u}}]_{11,22,33}^* + f_{u_3}^2 Y_{34}^u [\mathbf{Y}_{\mathbf{u}}]_{11,22,34}^* \right) \\
&= v_4^2 f_{Q_4}^2 \left(f_{u_4}^2 |Y_{44}^u|^2 + f_{u_3}^2 |Y_{34}^u|^2 \right) \tag{D-47}
\end{aligned}$$

$$V_{i3} = (-1)^{i+3} \frac{v_4^2 f_{Q_4} \left(f_{u_4}^2 Y_{44}^u [\mathbf{Y}_{\mathbf{u}}]_{11,22,i3}^* + f_{u_3}^2 Y_{34}^u [\mathbf{Y}_{\mathbf{u}}]_{11,22,i4}^* \right) [\mathbf{F}_{\mathbf{Q}}]_{11,22,ii} - [m_t \mathbf{I}]_{11,22,3i}}{\sqrt{v_4^2 f_{Q_4}^2 \left(f_{u_4}^2 |Y_{44}^u|^2 + f_{u_3}^2 |Y_{34}^u|^2 \right) (m_{t'}^2 - m_t^2)}} \tag{D-48}$$

Then, the V_{33} and V_{43} entries are

$$\begin{aligned}
V_{33} &= (-1)^{3+3} \frac{v_4^2 f_{Q_4}^2 \left(f_{u_4}^2 |Y_{44}^u|^2 + f_{u_3}^2 |Y_{34}^u|^2 \right) - [m_t \mathbf{I}]_{11,22,33}}{\sqrt{v_4^2 f_{Q_4}^2 \left(f_{u_4}^2 |Y_{44}^u|^2 + f_{u_3}^2 |Y_{34}^u|^2 \right) (m_{t'}^2 - m_t^2)}} \\
&= \frac{v_4^2 f_{Q_4}^2 \left(f_{u_4}^2 |Y_{44}^u|^2 + f_{u_3}^2 |Y_{34}^u|^2 \right) - m_t}{\sqrt{v_4^2 f_{Q_4}^2 \left(f_{u_4}^2 |Y_{44}^u|^2 + f_{u_3}^2 |Y_{34}^u|^2 \right) (m_{t'}^2 - m_t^2)}}, \\
V_{43} &= (-1)^{4+3} \frac{v_4^2 f_{Q_4} \left(f_{u_4}^2 Y_{44}^u [\mathbf{Y}_{\mathbf{u}}]_{11,22,43}^* + f_{u_3}^2 Y_{34}^u [\mathbf{Y}_{\mathbf{u}}]_{11,22,44}^* \right) [\mathbf{F}_{\mathbf{Q}}]_{11,22,44} - [m_t \mathbf{I}]_{11,22,34}}{\sqrt{v_4^2 f_{Q_4}^2 \left(f_{u_4}^2 |Y_{44}^u|^2 + f_{u_3}^2 |Y_{34}^u|^2 \right) (m_{t'}^2 - m_t^2)}} \\
&= - \frac{v_4^2 f_{Q_3} f_{Q_4} \left(f_{u_4}^2 Y_{44}^u Y_{34}^{u*} + f_{u_3}^2 Y_{34}^u Y_{33}^{u*} \right)}{\sqrt{v_4^2 f_{Q_4}^2 \left(f_{u_4}^2 |Y_{44}^u|^2 + f_{u_3}^2 |Y_{34}^u|^2 \right) (m_{t'}^2 - m_t^2)}}. \tag{D-49}
\end{aligned}$$

The remaining elements are calculated by using the unitarity conditions $\mathbf{V}^\dagger \mathbf{V} = \mathbf{I}$. To find the V_{12} element for example we calculate $(\mathbf{V}^\dagger \mathbf{V})_{12}$ entry

$$\begin{aligned}
0 &= V_{11}^* V_{12} + V_{21}^* V_{22} + V_{31}^* V_{32} + V_{41}^* V_{42} \\
&= V_{12} + \frac{[\mathbf{Y}_{\mathbf{u}}]_{21} f_{Q_1}}{[\mathbf{Y}_{\mathbf{u}}]_{11} f_{Q_2}} - \frac{[\mathbf{Y}_{\mathbf{u}}]_{31} f_{Q_1}}{[\mathbf{Y}_{\mathbf{u}}]_{11} f_{Q_3}} \frac{[\mathbf{Y}_{\mathbf{u}}]_{11,32} f_{Q_2}}{[\mathbf{Y}_{\mathbf{u}}]_{11,22}^* f_{Q_3}} \\
&\quad - \frac{[\mathbf{Y}_{\mathbf{u}}]_{41} f_{Q_1}}{[\mathbf{Y}_{\mathbf{u}}]_{11} f_{Q_4}} \frac{[\mathbf{Y}_{\mathbf{u}}]_{11,42} f_{Q_2}}{[\mathbf{Y}_{\mathbf{u}}]_{11,22}^* f_{Q_4}}. \tag{D-50}
\end{aligned}$$

In leading order we can simply write V_{12} as

$$V_{12} = - \frac{[\mathbf{Y}_{\mathbf{u}}]_{21} f_{Q_1}}{[\mathbf{Y}_{\mathbf{u}}]_{11} f_{Q_2}}. \tag{D-51}$$

The V_{13} and V_{23} entries are obtained by simultaneously solving for the unitarity conditions $(\mathbf{V}^\dagger \mathbf{V})_{31} = 0$ and $(\mathbf{V}^\dagger \mathbf{V})_{32} = 0$ in leading order. We solve for V_{43} and V_{44} by assuming a sub-unitarity condition such that

$$\begin{pmatrix} V_{33}^* & V_{43}^* \\ V_{34}^* & V_{44}^* \end{pmatrix} \begin{pmatrix} V_{33} & V_{34} \\ V_{43} & V_{44} \end{pmatrix} = \begin{pmatrix} 1 & 0 \\ 0 & 1 \end{pmatrix}. \tag{D-52}$$

Finally, one can get the V_{14} and V_{24} entries by simultaneously solving for the unitarity conditions $(\mathbf{V}^\dagger \mathbf{V})_{41} = 0$ and $(\mathbf{V}^\dagger \mathbf{V})_{42} = 0$ in leading order. We summarize our results in eq. (5.5).

For the down sector, we follow the same procedure. Let $\mathbf{H}_d = \mathbf{M}_d \mathbf{M}_d^\dagger = \mathbf{U}_{Q_d} \mathbf{M}_d^{\text{diag}} \mathbf{W}_d^\dagger \mathbf{W}_d \mathbf{M}_d^{\text{diag}} \mathbf{U}_{Q_d}^\dagger = \mathbf{U}_{Q_d} (\mathbf{M}_d^{\text{diag}})^2 \mathbf{U}_{Q_d}^\dagger$. Multiplying this from left by $\mathbf{U}_{Q_d}^\dagger$ and from right by \mathbf{U}_{Q_d} , we get $\mathbf{U}_{Q_d}^\dagger \mathbf{H}_d \mathbf{U}_{Q_d} = (\mathbf{M}_d^{\text{diag}})^2$ which is the same form as in eq. (D-26) such that $\mathbf{V} = \mathbf{U}_{Q_d}$, and eigenvalues of \mathbf{H}_d (or the diagonal entries of $\hat{\mathbf{H}}_d$) are the squares of the physical masses of up-type quarks. The V_{i1} , V_{i2} entries of \mathbf{U}_{Q_d} , will be exactly in the same form as in \mathbf{U}_{Q_u} except the $\mathbf{Y}_u \rightarrow \mathbf{Y}_d$. For the elements V_{i3} we can make further approximation since as opposed to the top sector where m_t is not much smaller than m'_t in the bottom sector we have $m_b \ll m'_b$. Therefore, V_{33} and V_{43} can be approximated in leading order as

$$\begin{aligned}
V_{33} &= (-1)^{3+3} \frac{v_4^2 f_{Q_4}^2 \left(f_{d_4}^2 |Y_{44}^d|^2 + f_{d_3}^2 |Y_{34}^d|^2 \right)}{\sqrt{v_4^2 f_{Q_4}^2 \left(f_{d_4}^2 |Y_{44}^d|^2 + f_{d_3}^2 |Y_{34}^d|^2 \right)} m_{b'}^2} \simeq \frac{v_4 f_{Q_4} f_{d_4} |Y_{44}^d|}{m_{b'}}, \\
V_{43} &= -\frac{v_4^2 f_{Q_3} f_{Q_4} \left(f_{d_4}^2 Y_{44}^d Y_{34}^{d*} + f_{d_3}^2 Y_{34}^d Y_{33}^{d*} \right)}{\sqrt{v_4^2 f_{Q_4}^2 \left(f_{d_4}^2 |Y_{44}^d|^2 + f_{d_3}^2 |Y_{34}^d|^2 \right)} m_{b'}^2} \simeq \frac{v_4 f_{Q_3} f_{d_4} Y_{34}^{d*}}{m_{b'}} e^{i \arg(Y_{44}^d)}. \quad (\text{D-53})
\end{aligned}$$

The rotation matrices $\mathbf{W}_{u,d}$ can also be calculated in the same way except $\mathbf{H}_{u,d} = \mathbf{W}_{u,d} \mathbf{M}_{u,d}^{\text{diag}} \mathbf{U}_{Q_{u,d}}^\dagger \mathbf{U}_{Q_{u,d}} \mathbf{M}_{u,d}^{\text{diag}} \mathbf{W}_{u,d}^\dagger$.

D-2 Cabibbo-Kobayashi-Maskawa Matrix for Four Generations in Warped ExtraDimensions

We will use eq. (5.9) to obtain the V_{us} , V_{cb} , V_{ub} entries of CKM4 in warped extra dimensional scenario. Note that V in Appendix D-1 does not refer to entries of CKM matrix.

$$\begin{aligned}
V_{us} &= (\mathbf{U}_{Q_u}^\dagger \mathbf{U}_{Q_d})_{12} \\
&= \sum_{i=1}^4 (\mathbf{U}_{Q_u}^\dagger)_{1i} (\mathbf{U}_{Q_d})_{i2} \\
&= \sum_{i=1}^4 (\mathbf{U}_{Q_u})_{i1}^* (\mathbf{U}_{Q_d})_{i2} \\
&= U_{11}^{Q_u*} U_{12}^{Q_d} + U_{21}^{Q_u*} U_{22}^{Q_d} + U_{31}^{Q_u*} U_{32}^{Q_d} + U_{41}^{Q_u*} U_{42}^{Q_d}
\end{aligned}$$

$$\begin{aligned}
&= \frac{[\mathbf{Y}_d]_{21} f_{Q_1}}{[\mathbf{Y}_d]_{11} f_{Q_2}} - \frac{[\mathbf{Y}_u]_{21} f_{Q_1}}{[\mathbf{Y}_u]_{11} f_{Q_2}} - \frac{[\mathbf{Y}_u]_{31} f_{Q_1}}{[\mathbf{Y}_u]_{11} f_{Q_3}} \frac{[\mathbf{Y}_d]_{11,32}^* f_{Q_2}}{[\mathbf{Y}_d]_{11,22}^* f_{Q_3}} \\
&\quad - \frac{[\mathbf{Y}_u]_{41} f_{Q_1}}{[\mathbf{Y}_u]_{11} f_{Q_4}} \frac{[\mathbf{Y}_d]_{11,42}^* f_{Q_2}}{[\mathbf{Y}_d]_{11,22}^* f_{Q_4}} \\
&\simeq \frac{f_{Q_1}}{f_{Q_2}} \left(\frac{[\mathbf{Y}_d]_{21}}{[\mathbf{Y}_d]_{11}} - \frac{[\mathbf{Y}_u]_{21}}{[\mathbf{Y}_u]_{11}} \right). \tag{D-54}
\end{aligned}$$

$$\begin{aligned}
V_{cb} &= (\mathbf{U}_{\mathbf{Q}_u}^\dagger \mathbf{U}_{\mathbf{Q}_d})_{23} \\
&= \sum_{i=1}^4 (\mathbf{U}_{\mathbf{Q}_u}^\dagger)_{2i} (\mathbf{U}_{\mathbf{Q}_d})_{i3} \\
&= \sum_{i=1}^4 (\mathbf{U}_{\mathbf{Q}_u})_{i2}^* (\mathbf{U}_{\mathbf{Q}_d})_{i3} \\
&= U_{12}^{Q_u*} U_{13}^{Q_d} + U_{22}^{Q_u*} U_{23}^{Q_d} + U_{32}^{Q_u*} U_{33}^{Q_d} + U_{42}^{Q_u*} U_{43}^{Q_d} \\
&= \frac{[\mathbf{Y}_u]_{21}^* f_{Q_1}}{[\mathbf{Y}_u]_{11}^* f_{Q_2}} \left(c_{Q_d} \frac{f_{Q_1}}{f_{Q_3}} \frac{[\mathbf{Y}_d]_{21,32}}{[\mathbf{Y}_d]_{11,22}} + s_{Q_d}^* \frac{f_{Q_1}}{f_{Q_4}} \frac{[\mathbf{Y}_d]_{21,42}}{[\mathbf{Y}_d]_{11,22}} \right) \\
&\quad + c_{Q_d} \frac{f_{Q_2}}{f_{Q_3}} \left(\frac{[\mathbf{Y}_d]_{11,32}}{[\mathbf{Y}_d]_{11,22}} - \frac{[\mathbf{Y}_u]_{11,32}}{[\mathbf{Y}_u]_{11,22}} \right) + s_{Q_d}^* \frac{f_{Q_2}}{f_{Q_4}} \left(\frac{[\mathbf{Y}_d]_{11,42}}{[\mathbf{Y}_d]_{11,22}} - \frac{[\mathbf{Y}_u]_{11,42}}{[\mathbf{Y}_u]_{11,22}} \right) \\
&\simeq c_{Q_d} \frac{f_{Q_2}}{f_{Q_3}} \left(\frac{[\mathbf{Y}_d]_{11,32}}{[\mathbf{Y}_d]_{11,22}} - \frac{[\mathbf{Y}_u]_{11,32}}{[\mathbf{Y}_u]_{11,22}} \right) + s_{Q_d}^* \frac{f_{Q_2}}{f_{Q_4}} \left(\frac{[\mathbf{Y}_d]_{11,42}}{[\mathbf{Y}_d]_{11,22}} - \frac{[\mathbf{Y}_u]_{11,42}}{[\mathbf{Y}_u]_{11,22}} \right) \tag{D-55}
\end{aligned}$$

$$\begin{aligned}
V_{ub} &= (\mathbf{U}_{\mathbf{Q}_u}^\dagger \mathbf{U}_{\mathbf{Q}_d})_{13} \\
&= \sum_{i=1}^4 (\mathbf{U}_{\mathbf{Q}_u}^\dagger)_{1i} (\mathbf{U}_{\mathbf{Q}_d})_{i3} \\
&= \sum_{i=1}^4 (\mathbf{U}_{\mathbf{Q}_u})_{i1}^* (\mathbf{U}_{\mathbf{Q}_d})_{i3} \\
&= U_{11}^{Q_u*} U_{13}^{Q_d} + U_{21}^{Q_u*} U_{23}^{Q_d} + U_{31}^{Q_u*} U_{33}^{Q_d} + U_{41}^{Q_u*} U_{43}^{Q_d} \\
&= c_{Q_d} \frac{f_{Q_1}}{f_{Q_3}} \frac{[\mathbf{Y}_d]_{21,32}}{[\mathbf{Y}_d]_{11,22}} + s_{Q_d}^* \frac{f_{Q_1}}{f_{Q_4}} \frac{[\mathbf{Y}_d]_{21,42}}{[\mathbf{Y}_d]_{11,22}} \\
&\quad - \frac{[\mathbf{Y}_u]_{21} f_{Q_1}}{[\mathbf{Y}_u]_{11} f_{Q_2}} \left(c_{Q_d} \frac{f_{Q_2}}{f_{Q_3}} \frac{[\mathbf{Y}_d]_{11,32}}{[\mathbf{Y}_d]_{11,22}} + s_{Q_d}^* \frac{f_{Q_2}}{f_{Q_4}} \frac{[\mathbf{Y}_d]_{11,42}}{[\mathbf{Y}_d]_{11,22}} \right) \\
&\quad + c_{Q_d} \frac{f_{Q_1}}{f_{Q_3}} \frac{[\mathbf{Y}_u]_{31}}{[\mathbf{Y}_u]_{11}} + s_{Q_d}^* \frac{f_{Q_1}}{f_{Q_4}} \frac{[\mathbf{Y}_u]_{41}}{[\mathbf{Y}_u]_{11}} \\
&= c_{Q_d} \frac{f_{Q_1}}{f_{Q_3}} \left(\frac{[\mathbf{Y}_u]_{31}}{[\mathbf{Y}_u]_{11}} + \frac{[\mathbf{Y}_d]_{21,32}}{[\mathbf{Y}_d]_{11,22}} - \frac{[\mathbf{Y}_u]_{21}}{[\mathbf{Y}_u]_{11}} \frac{[\mathbf{Y}_d]_{11,32}}{[\mathbf{Y}_d]_{11,22}} \right) \\
&\quad + s_{Q_d}^* \frac{f_{Q_1}}{f_{Q_4}} \left(\frac{[\mathbf{Y}_u]_{41}}{[\mathbf{Y}_u]_{11}} + \frac{[\mathbf{Y}_d]_{21,42}}{[\mathbf{Y}_d]_{11,22}} - \frac{[\mathbf{Y}_u]_{21}}{[\mathbf{Y}_u]_{11}} \frac{[\mathbf{Y}_d]_{11,42}}{[\mathbf{Y}_d]_{11,22}} \right). \tag{D-56}
\end{aligned}$$

Appendix E

Feynman Rules in Warped Extra Dimensions with Four Generation

In this Appendix, we will summarize the Feynman rules for the scalar sector of warped extra dimensional scenarios with fourth generation including Higgs (h_0), radion (ϕ_0), and higgs-radion mixed states (h) and (ϕ). Φ being any of the scalars mentioned above, the only two body decays that occur at tree level for those scalars are $\Phi \rightarrow f_i \bar{f}_j$ (f stands for fermion) or $\Phi \rightarrow VV$ (V represents vector bosons). The decays $\Phi \rightarrow \gamma\gamma$ or $\Phi \rightarrow gg$ arise in loop level by allowing either gauge bosons and/or fermions in the loops. Here we will give the effective couplings of scalars to two photons or gluons. Let us first summarize the F functions appearing in these effective couplings which are represented by $F_{1/2}$ when the particle in the loop is a spin-1/2 and F_1 for spin-1 particles.

$$\begin{aligned} F_{1/2}(\tau_i) &= -2\tau_i [1 + (1 - \tau_i)f(\tau_i)], \\ F_1(\tau_i) &= 2 + 3\tau_i + 3\tau_i(2 - \tau_i)f(\tau_i), \end{aligned} \tag{E-1}$$

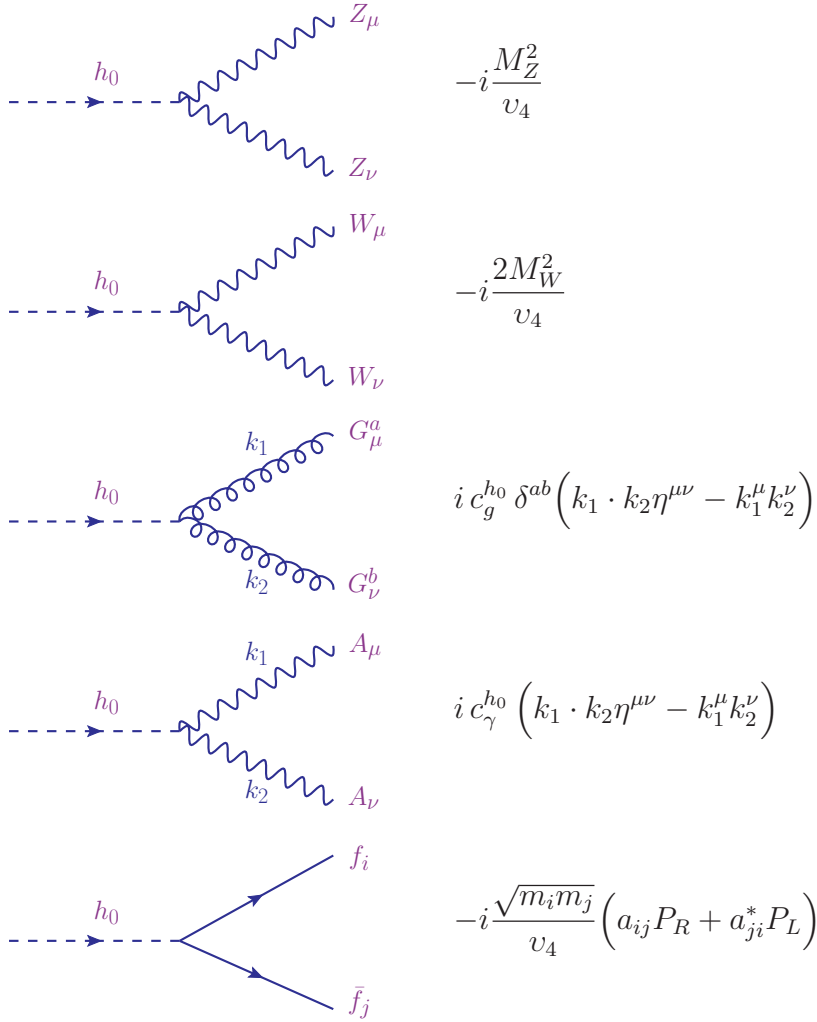
where $\tau_i = 4m_i^2/m_\Phi^2$

$$f(\tau_i) = \begin{cases} \left[\sin^{-1} \left(\sqrt{1/\tau_i} \right) \right]^2, & \text{if } \tau_i \geq 1, \\ -\frac{1}{4} [\ln(\eta_+/\eta_-) - i\pi]^2, & \text{if } \tau_i < 1, \end{cases} \tag{E-2}$$

where

$$\eta_\pm = (1 \pm \sqrt{1 - \tau_i}). \tag{E-3}$$

E-1 Feynman Rules for the Higgs Field



$$-i \frac{M_Z^2}{v_4}$$

$$-i \frac{2M_W^2}{v_4}$$

$$i c_g^{h_0} \delta^{ab} \left(k_1 \cdot k_2 \eta^{\mu\nu} - k_1^\mu k_2^\nu \right)$$

$$i c_\gamma^{h_0} \left(k_1 \cdot k_2 \eta^{\mu\nu} - k_1^\mu k_2^\nu \right)$$

$$-i \frac{\sqrt{m_i m_j}}{v_4} \left(a_{ij} P_R + a_{ji}^* P_L \right)$$

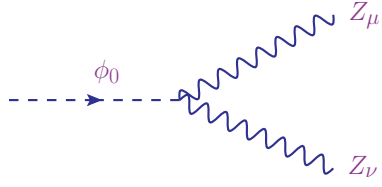
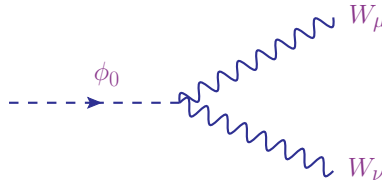
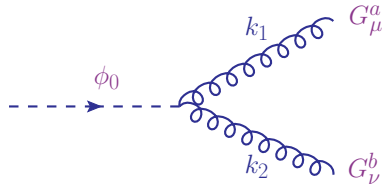
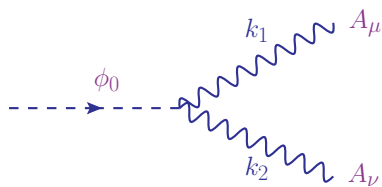
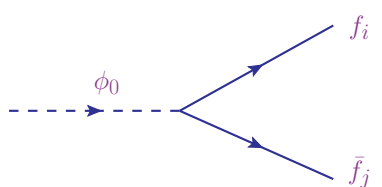
where

$$\begin{aligned}
 c_g^{h_0} &= -\frac{\alpha_s}{4\pi v_4} \left[\sum_i F_{1/2}(\tau_i) \right], \\
 c_\gamma^{h_0} &= -\frac{\alpha}{2\pi v_4} \left[\sum_i e_i^2 N_c^i F_i(\tau_i) \right],
 \end{aligned} \tag{E-4}$$

where N_{c_i} is the color multiplicity (3 for quarks as they have three different colors and 1 for leptons) and e_i is the electric charge in units of e of the particle i .

E-2 Feynman Rules for the Radion Field

In general, the radion couplings are similar to Higgs couplings in that they are proportional to the mass of the particles it couples with.

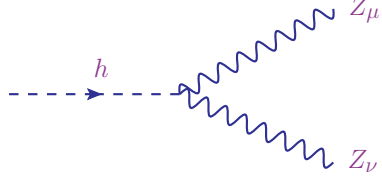
	$-i \frac{M_Z^2}{\Lambda} \left[1 - \frac{3 \ln\left(\frac{\sqrt{6}M_{Pl}}{\Lambda}\right) M_Z^2}{\Lambda^2} \right]$
	$-i \frac{2M_W^2}{\Lambda} \left[1 - \frac{3 \ln\left(\frac{\sqrt{6}M_{Pl}}{\Lambda}\right) M_W^2}{\Lambda^2} \right]$
	$i c_g^{\phi_0} \delta^{ab} \left(k_1 \cdot k_2 \eta^{\mu\nu} - k_1^\mu k_2^\nu \right)$
	$i c_\gamma^{\phi_0} \left(k_1 \cdot k_2 \eta^{\mu\nu} - k_1^\mu k_2^\nu \right)$
	$-i \frac{\sqrt{m_i m_j}}{v_4} \left(\tilde{a}_{ij} P_R + \tilde{a}_{ji}^* P_L \right)$

where

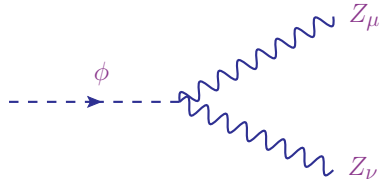
$$\begin{aligned}
c_g^{\phi_0} &= -\frac{\alpha_s}{4\pi\Lambda} \left[\sum_i F_{1/2}(\tau_i) - 2 \left(b'_3 + \frac{2\pi}{\alpha_s \ln\left(\frac{\sqrt{6}M_{Pl}}{\Lambda}\right)} \right) \right], \\
c_\gamma^{\phi_0} &= -\frac{\alpha}{2\pi\Lambda} \left[\sum_i e_i^2 N_e^i F_i(\tau_i) - \left(b'_2 + b'_Y + \frac{2\pi}{\alpha \ln\left(\frac{\sqrt{6}M_{Pl}}{\Lambda}\right)} \right) \right], \quad (E-5)
\end{aligned}$$

where b'_3, b'_2 and b'_Y are the coefficients of the beta functions of the $SU(3)_c$, $SU(2)_L$ and $U(1)_Y$ groups respectively, in the presence of 4 generations of quarks and leptons. The coefficients are $b'_3 = 18/3$ and $b'_2 + b'_Y = -65/9$.

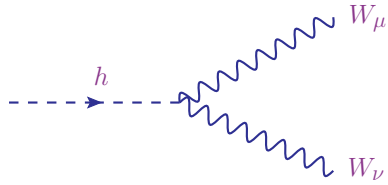
E-3 Feynman Rules for Higgs-Radion Mixed States



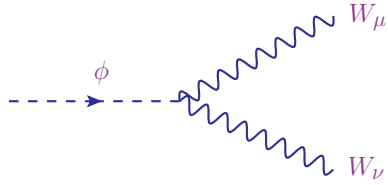
$$-i \frac{M_Z^2}{v_4} \left[d + b\gamma \left(1 - \frac{3 \ln\left(\frac{\sqrt{6}M_{Pl}}{\Lambda}\right) M_Z^2}{\Lambda^2} \right) \right]$$



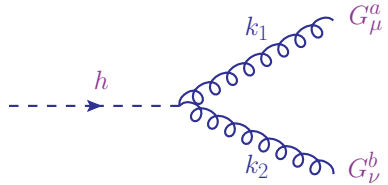
$$-i \frac{M_Z^2}{v_4} \left[c + a\gamma \left(1 - \frac{3 \ln\left(\frac{\sqrt{6}M_{Pl}}{\Lambda}\right) M_Z^2}{\Lambda^2} \right) \right]$$



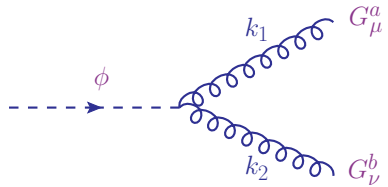
$$-i \frac{2M_W^2}{v_4} \left[d + b\gamma \left(1 - \frac{3 \ln\left(\frac{\sqrt{6}M_{Pl}}{\Lambda}\right) M_W^2}{\Lambda^2} \right) \right]$$



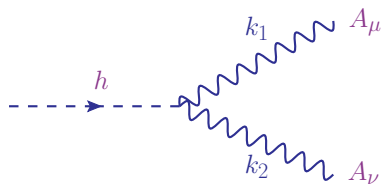
$$-i \frac{2M_W^2}{v_4} \left[c + a\gamma \left(1 - \frac{3 \ln\left(\frac{\sqrt{6}M_{Pl}}{\Lambda}\right) M_W^2}{\Lambda^2} \right) \right]$$



$$i c_g^h \delta^{ab} \left(k_1 \cdot k_2 \eta^{\mu\nu} - k_1^\mu k_2^\nu \right)$$



$$i c_g^\phi \delta^{ab} \left(k_1 \cdot k_2 \eta^{\mu\nu} - k_1^\mu k_2^\nu \right)$$



$$i c_\gamma^h \left(k_1 \cdot k_2 \eta^{\mu\nu} - k_1^\mu k_2^\nu \right)$$

$$i c_\gamma^\phi \left(k_1 \cdot k_2 \eta^{\mu\nu} - k_1^\mu k_2^\nu \right)$$

$$-i \frac{\sqrt{m_i m_j}}{v_4} \left[\left(a_{ij} P_R + a_{ji}^* P_L \right) d + \left(\tilde{a}_{ij} P_R + \tilde{a}_{ji}^* P_L \right) b \gamma \right]$$

$$-i \frac{\sqrt{m_i m_j}}{v_4} \left[\left(a_{ij} P_R + a_{ji}^* P_L \right) a + \left(\tilde{a}_{ij} P_R + \tilde{a}_{ji}^* P_L \right) c \gamma \right]$$

$$c_g^{h,\phi}(max) = -\frac{\alpha_s}{4\pi v} \left[g_g^{h,\phi}(max) \sum_i F_{1/2}(\tau_i) - 2 \left(b'_3 + \frac{2\pi}{\alpha_s \ln(\frac{\sqrt{6} M_{Pl}}{\Lambda_\phi})} \right) g^{h,\phi} \right],$$

$$c_g^{h,\phi}(min) = -\frac{\alpha_s}{4\pi v} \left[g_g^{h,\phi}(min) \sum_i F_{1/2}(\tau_i) - 2 \left(b'_3 + \frac{2\pi}{\alpha_s \ln(\frac{\sqrt{6} M_{Pl}}{\Lambda_\phi})} \right) g^{h,\phi} \right],$$

$$c_\gamma^{h,\phi}(max) = -\frac{\alpha}{2\pi v} \left[g_\gamma^{h,\phi}(max) \sum_i e_c^2 N_c^i F_i(\tau_i) - \left(b'_2 + b'_Y + \frac{2\pi}{\alpha \ln(\frac{\sqrt{6} M_{Pl}}{\Lambda_\phi})} \right) g^{h,\phi} \right],$$

$$c_\gamma^{h,\phi}(min) = -\frac{\alpha}{2\pi v} \left[g_\gamma^{h,\phi}(min) \sum_i e_c^2 N_c^i F_i(\tau_i) - \left(b'_2 + b'_Y + \frac{2\pi}{\alpha \ln(\frac{\sqrt{6} M_{Pl}}{\Lambda_\phi})} \right) g^{h,\phi} \right]. \quad (\text{E-6})$$

Here $g_g^{h,\phi}$ values appearing in the effective vertex of Higgs or radion to gluon coupling have some uncertainties due to the heavy Kaluza-Klein fermions in the loop. We assume an additional correction to the h_0 couplings squared to massless gauge bosons of $\pm 20\%$ for gluons and these maximum and minimum values can be written in explicit form as follows

$$g_g^\phi(max) = a\gamma + c\sqrt{(1 + \delta_{EW}^4)}(1.20),$$

$$g_g^h(max) = b\gamma + d\sqrt{(1 + \delta_{EW}^4)}(1.20),$$

$$g_g^\phi(min) = a\gamma + c\sqrt{(1 + \delta_{EW}^4)}(0.80),$$

$$g_g^h(min) = b\gamma + d\sqrt{(1 + \delta_{EW}^4)}(0.80),$$

$$g^\phi = a\gamma, \quad (\text{E-7})$$

and for photon we have $\pm 10\%$ uncertainty yielding

$$\begin{aligned}
g_\gamma^\phi(max) &= a\gamma + c\sqrt{(1.10)(1 + \bar{\delta}_{EW}^4)(1 + \delta_{THU})}, \\
g_\gamma^h(max) &= b\gamma + d\sqrt{(1.10)(1 + \bar{\delta}_{EW}^4)(1 + \delta_{THU})}, \\
g_\gamma^\phi(min) &= a\gamma + c\sqrt{(0.90)(1 + \bar{\delta}_{EW}^4)(1 - \delta_{THU})}, \\
g_\gamma^h(min) &= b\gamma + d\sqrt{(0.90)(1 + \bar{\delta}_{EW}^4)(1 - \delta_{THU})}, \\
g^h &= b\gamma.
\end{aligned}
\tag{E-8}$$

Note that while the bare Higgs (h_0) couplings are corrected by $(1 + \delta_{EW}^4)$, there is no such correction for the bare radion (ϕ_0) couplings. The reason is that the latter are dominated by the trace anomaly, and so higher order loop effects are much smaller. We have also included the corrections to the $h_0 \rightarrow \gamma\gamma$ coupling due to loop effects [172]. A note of caution is warranted with these corrections. The authors show that the NLO EW corrections are of the same order as the LO estimate, and negative, due to the strong cancellation between the W and fermion loops with four generations. This might be indicative of a non-perturbative regime, and the authors rely on an estimation of the higher-order corrections, without any certainty that the perturbation series converges. Moreover, in our scenario, heavy Kaluza-Klein fermions are known to affect $h_0 \rightarrow \gamma\gamma$ at lowest order [197, 198]. See Tables 11 and 12 for the numerical values taken for δ_{EW} , $\bar{\delta}_{EW}$ and δ_{THU} .